DEVELOPMENT OF ROBUST BUILDING ENERGY DEMAND-SIDE CONTROL STRATEGY UNDER UNCERTAINTY

A Dissertation
Presented to
The Academic Faculty

by

Sean Hay Kim

In Partial Fulfillment
of the Requirements for the Degree
Doctor of Philosophy in the
College of Architecture

Georgia Institute of Technology
August 2011

DEVELOPMENT OF ROBUST BUILDING ENERGY DEMAND-SIDE CONTROL STRATEGY UNDER UNCERTAINTY

Approved by:

Professor. Godfried Augenbroe, Advisor
College of Architecture
Georgia Institute of Technology

Dr. Sheldon M. Jeter
School of Mechanical Engineering
Georgia Institute of Technology

Dr. Christiaan Paredis
School of Mechanical Engineering
Georgia Institute of Technology

Dr. Jason Brown
College of Architecture
Georgia Institute of Technology

Dr. Chellury Ram Sastry
Senior Engineer
Pacific Northwest National Laboratory

Date Approved: April 1st, 2011

This Ph.D. thesis I dedicate
To the
Memory of my mother, Young Hee Kim

ACKNOWLEDGEMENTS

I would like to especially thank advisor Professor Godfried Augenbroe, Dr. Ellen Do and Dr. Mark Gross for giving me an opportunity of Ph.D. study. Without them, I would not have today's glorious moment.

I appreciate my committee members. Dr. Sastry helped me initiate this dissertation while working for Siemens. From Dr. Paredis I learnt about researcher's attitude and how to tackle a research problem. Dr. Jeter showed me generous gratitude. Finally I thank Dr. Brown for his endeavor to improve the quality of my dissertation till the last stage.

Also I appreciate my advisor in Yonsei University, Dr. Byung Seon Kim. He encouraged me to start Ph.D. study, and has given me good advices whenever needed.

I thank all of my friends and colleagues during Ph.D. years, Dr. Huafen Hu, Sang Hoon, Yeon Sook, Atefe, Paola, Ji Hyun, Zhengwei, Fei and Yuming, Dr. Jae Min Lee, Dong Hoon, Ho Young, Hong Gab, Sang Min, Hae Youn, Jin Sol, Chan Kyu, So Myung, Jimin, Ji Sun, Sue, Dr. Cheol Soo Park and my cousin Jung Ju.

I deeply appreciate my best friend, Dr. Viraj Srivastava, for his unlimited support and care whenever I'm in troubles emotionally and intellectually. I owe a completion of this dissertation to him. I thank my father, brother and father-in-law who show their patience for a long time.

Lastly I dedicate this dissertation to Ju Hyun who devotes himself for me despite all the hardship and Yoon Jin who enabled me to forget endless loneliness by staying with me at the toughest moment.

TABLE OF CONTENTS

LIST OF TABLES

LIST OF FIGURES

SUMMARY

The potential of carbon emission regulations applied to an individual building will encourage building owners to purchase utility-provided green power or to employ onsite renewable energy generation. As both cases are based on intermittent renewable energy sources, demand side control is a fundamental precondition for maximizing the effectiveness of using renewable energy sources. Such control leads to a reduction in peak demand and/or in energy demand variability, therefore, such reduction in the demand profile eventually enhances the efficiency of an erratic supply of renewable energy.

The combined operation of active thermal energy storage and passive building thermal mass has shown substantial improvement in demand-side control performance when compared to current state-of-the-art demand-side control measures. Specifically, "model-based" optimal control for this operation has the potential to significantly increase performance and bring economic advantages. However, due to the uncertainty in certain operating conditions in the field its control effectiveness could be diminished and/or seriously damaged, which results in poor performance.

This dissertation pursues improvements of current demand-side controls under uncertainty by proposing a robust supervisory demand-side control strategy that is designed to be immune from uncertainty and perform consistently under uncertain conditions.

Uniqueness and superiority of the proposed robust demand-side controls are found as below:

a. It is developed based on fundamental studies about uncertainty and a systematic approach to uncertainty analysis.

b. It reduces variability of performance under varied conditions, and thus avoids the worst case scenario.

c. It is reactive in cases of critical "discrepancies" observed caused by the unpredictable uncertainty that typically scenario uncertainty imposes, and thus it increases control efficiency. This is obtainable by means of i) multi-source composition of weather forecasts including both historical archive and online sources and ii) adaptive Multiple model-based controls (MMC) to mitigate detrimental impacts of varying scenario uncertainties.

The proposed robust demand-side control strategy verifies its outstanding demand-side control performance in varied and non-indigenous conditions compared to the existing control strategies including deterministic optimal controls. This result reemphasizes importance of the demand-side control for a building in the global carbon economy. It also demonstrates a capability of risk management of the proposed robust demand-side controls in highly uncertain situations, which eventually attains the maximum benefit in both theoretical and practical perspectives.

MOTIVATING QUESTIONS

Main motivation of this research is the question:

"How can we improve performance of demand-side control strategies under uncertain conditions?"

Sub-motivating questions with a short answer are:

a. Why is demand-side control necessary?

Demand-side control is a fundamental precondition to reduce the Carbon footprint of a building. Such control reduces net energy demand and energy demand variability, and therefore enhances the effectiveness of an erratic supply of renewable energy sources.

b. Why does uncertainty become a critical assumption for the demand-side control?

"Model-based" predictive control of active (i.e. mechanical system) and passive (i.e. building thermal mass) thermal energy storage has shown a substantial improvement of the demand-side control performance when compared with current state-of-the-art demand control measures.

However, due to the uncertainty in certain operating conditions in the field, its control effectiveness could be diminished and/or seriously damaged; hence resulting in poor performance. This research proposes a robust supervisory demand-side control strategy that is designed to be immune to uncertainty.

d. What are characteristics of uncertainty, and how do we perform uncertainty analysis?

Predicting uncertainty as accurate as possible is the most fundamental resolution and critical prerequisite for the demand-side controls. This is, however, almost not feasible since uncertainty holds characteristics that are both “random” (e.g., unpredictable) and “imprecise” (e.g., lack of knowledge). And different dimensions of uncertainties initiate issues such as whether uncertainties are identifiable, whether and/or how strongly they influence performance of the demand-side controls, how feasible to capture and represent them, how they can be associated with development process of the demand-side controls and how to make the demand-side control robust against uncertainties.

By these reasons, a fundamental investigation of uncertainty and identifying a systemic approach of uncertainty analysis with respect to the robust control solution development process are very required.

e. What are required characteristics of robust demand control strategy, and how is it developed?

Robust demand control strategy should take into account relevant uncertainty sources, in particular those related to building load predictions, since demand-side control measures could be more vulnerable to uncertainty in building load prediction. Then uncertainty sources are described and quantified in the functional models of simulation tools and optimization procedures. An employment of Systems Modeling Language (SysML) offers a systemized and complete line of the process from initial problem framing to seamless and faster deployment to model uncertainties. Finally performance of the robust demand control strategy should be evaluated under dynamic conditions with respect to the very fundamental goals of the demand-side controls.

f. Why does the robust control strategy perform better than the one composed through the deterministic process?

A robust solution is exhaustive and stable with minimal loss in varied situations; thereby, it will avoid the worst case scenario. Whereas, a deterministic solution may underperform in non-indigenous situations other than for which it was designed.

g. How can we further enhance performance of robust demand side control strategies?

Robust controls reduce variability of performance under varied conditions, and will avoid the worst case scenario. However one of criticisms is that robust controls could be overly conservative in "good" and "best" scenarios in deciding demand-side control portfolios. Therefore robust demand-side controls have to be reactive in cases of critical "discrepancies" observed caused by the unpredictable uncertainty, and thus it should increase control efficiency.

Thereby it needs to alleviate impacts of the unpredictable uncertainty that typically scenario uncertainty (such as a combination of building usage scenarios and weather conditions) imposes. This is obtainable by means of i) multi-source composition of weather forecasts including both historical archive and online sources and ii) adaptive Multiple model-based controls (MMC) to mitigate detrimental impacts of varying scenario uncertainties.

CHAPTER 1

INTRODUCTION

1.1 Carbon footprint initiative and renewable energy sources

Buildings account for 38% of Carbon emissions in the United States, more than the transportation or industry sectors (USGBC 2007). Over the next 25 years, Carbon emissions from U.S. commercial buildings are projected to grow faster than other types of buildings – 1.8% a year through 2030 (USGBC 2007).

Figure 1.1 Projected CO2 emission increase rate of U.S. commercial buildings (USGBC 2007)

Administrative approaches such as Carbon cap-and-trading and Carbon tax to retard global carbon emissions by means of economic incentives (or disincentives) have been adopted worldwide. In United States building industry, Carbon tax on household in Boulder, CO in 2006 was the first time in the nation that a municipal government has imposed an energy tax on its residents (City of Boulder, 2006).

Such economic initiatives will encourage building owners to reduce the building's Carbon foot print. Their typical immediate reactions would be an introduction of renewable energy sources that do not consume fossil fuel. Renewable energy sources that can be applied at the individual building level typically can be provided through i) purchasing the grid-provided green energy, or ii) onsite small-scaled renewable energy.

1.1.1 The grid-provided green energy

Green energy includes natural energetic processes that can be harnessed with little pollution; geothermal power, wind power, small-scale hydropower, solar energy, biomass power, tidal power, and wave power fall under this category (Wikipedia 2010). Most of them require large scale generation stations.

In several countries including the U.S., electricity retailing arrangements make it possible for consumers to purchase green power from either utility or green power providers who are able to run large scale generators. By participating in a green power program incorporating various funding and premium options a consumer may have an impact on promoting and expanding use of green energy. However, if such monetary options are not economically viable for an individual consumer, for example the Dutch government exempts green power from pollution taxes (Born 2001), consumers might not choose the green energy, which is more expensive than other power.

In the United States, one of the main issues with purchasing green energy through the grid is current centralized infrastructure, such as hydropower plants and wind turbine farms. The major barriers associated to the centralized infrastructure are environmental, land and capital constraints. These constraints are elaborated as i) the limited number of potential sites to install renewable generation facilities since abundant renewable sources must be guaranteed, e.g. hydro-generation exemplified at (Baird 1993) and ii) a failure to obtain planning permission and required expenditure, e.g. the UK's failure case for the year 2000 (Department of Trade and Industry 2000).

Another restriction is that, due to the large amount of space that renewable resources require, the centralized infrastructure is often located in remote areas where there is a lower energy demand. Current infrastructure would make transporting this energy to high demand areas, such as urban centers, highly inefficient and in some cases impossible. Opponents of the current U.S. electrical grid have also advocated for

decentralizing the grid. They support their claims by that i) reducing the amount of energy lost in transmission would increase the efficiency and ii) many types of renewable energy systems are locally available.

1.1.2 Onsite small-scale renewable energy

Choosing onsite small-scale renewable energy systems would be able to compensate for political, economical and technical issues of grid-provided green energy. Such systems are ideally suited for building integration. There are some benefits of using onsite renewable energy generations for a building, including:

a. Onsite power generations would reduce the energy losses due to transmission.

b. Many U.S. states offer incentives to offset the cost of installation of a local renewable energy system. Once the system is paid for, the owner of a renewable energy system will be producing their own renewable electricity for essentially no cost and can sell the excess to the local utility at a profit.

c. Aside from generating electricity, onsite renewable systems can be directly integrated with building heating and cooling. Then it offers the potential to reduce conventional natural gas and petroleum-fueled heat bills are feasible. Examples of those applications include micro-CHP, geothermal heat pump and solar heating.

However, several issues need to be resolved in order to make onsite renewable power generation more feasible.

a. The intermittent nature of renewable power results in highly unpredictable power flows. A direct building to grid connection having a significant amount of power intermittency can jeopardize power stability (Jenkins, Allan et al. 2000).

b. Such embedded generation would considerably alter building distribution networks. Penetration of renewable energy would transform current passive networks

(i.e., one directional supply to the load) into active networks where the relative magnitude of the generation and the load determine the direction of power flows.

c. Embedded generation accompanied with voltage disturbance and harmonic distortion of voltage waveforms may degrade power quality (Jenkins, Allan et al. 2000, Thomas 1996)

An urgent and vital resolution for those issues is demand-side management. Although other merits of demand-side management will be introduced in the next section, the greatest advantage concerned with the above issues is that demand-side management enhances the effectiveness of renewable energy supply.

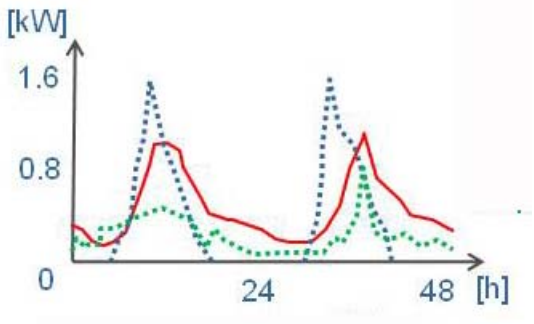

Figure 1.2 A example of the mismatch between the demand (red solid) and the supplies (blue dotted for the PV and green dotted for the wind turbine) (Born 2001) of a building for two days

As Figure 1.2 illustrates, the supply profile does not always coincide with the demand profile. During the period when supply exceeds demand, the delta supply (i.e., the difference between the supply and the demand) could be discarded. Vice versa when demand exceeds supply, importing grid power is required.

Two control options, either installing a battery to accumulate energy or shaping the demand profile, will improve the effectiveness. In both cases, forecasting the demand of a building and the supply from renewable resources is inevitable.

Priority should be placed on the demand side. The most effective way to reduce Carbon emissions and slow global warming is through conservation efforts, i.e.,

minimizing the net demand rather than increasing the supply. In addition, supply from renewable sources that are available for buildings with the least marginal cost (e.g., solar, wind, geothermal power generation) is drastically sporadic than the demand, thus the demand-side management becomes more doable.

Demand-side management pursues matching the two profiles in frequency and magnitude. Thus it will alleviate a number of issues caused from mismatches as mentioned above, for instance, power stability will be enhanced. An inventory of the power surplus and deficiency will be under control such that this can be used as a basis for technical decision-making regarding unit commitment, spinning reserve, control reserve, fuel scheduling and maintenance outages to control power quality (Oldbach 1994).

The next section will review objectives and fundamental methods of demand-side management.

1.2 Demand-side management

Demand-side management is a strategy which employs measures to alter the system load profile. As Figure 1.3 illustrates, the primary objective of demand-side management is to modify the demand profile to reduce variability and net demand, as large variations in the demand limit efficiency of the supply infrastructure.

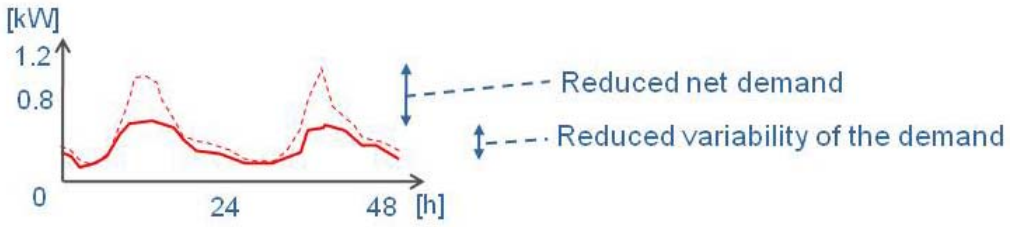

Figure 1.3 Two primary objectives of the demand-side management

The Energy Information Administration (2000) reported the four technical goals used in modifying the demand profile as:

a. Load shedding: to reduce the net demand during both on-peak and off-peak periods

b. Peak clipping: to reduce the on-peak demand

c. Load shaping: to alter the demand profile to meet certain performance criteria

d. Load building: to store power during off-peak in order to use it during on-peak

A number of works in the literatures have supported demand-side management with respect to system efficiency and life, cost effectiveness, and sustainability. Their main arguments are summarized as below:

- Sporadic peaks in a system demand profile are problematic to utilities (Born 2001). In order to generate sufficient power during these short periods, an operational plant is required to run at full load or an additional peaking plant is required to be turn on. Neither of these options, however, is favorable: regularly cycling plant operation to full load reduces both plant life and efficiency, also does irregular turning on/off operation of peaking plant. Smoothing out the demand profile would reduce the frequency of those operations.

- Demand-side management could contain the growth of demand thereby deferring or even canceling the need to expand supply capacity (Busch and Eto 1996). This is particularly significant when additional transmission and distribution capacity expenditure is avoided.

- The soothed local on-peak demand offers a steadier base demand for the grid, thus the reserve margin at the grid level decreases when their individual local contributions are aggregated. Lower consumption of current fossil fuel, increased

efficiency by reducing the energy lost in transmission, and thus reduced Carbon emissions are anticipated. It would also reduce the amount of power lines that will need to be constructed to keep up with growing demand.

As various types of demand-side measures are found in the literature (Walawalkar 2004), demand-side management can be applied in different ways in many domains where its application can eventually result in altering the system load curve (for example, when the utility is subject to a variable utility rate structure, enhancement of energy distribution system technologies or adopting energy efficiency policies).

This study emphasizes the role of the demand-side management in enhanced building technology, and this study is interested in technical measures such as thermal energy distribution, heat storage, and control systems in terms of increasing energy efficiency (i.e., reducing the net demand) and/or peak load reduction potentials (i.e., reshaping the demand profile).

Among current state-of-the-art measures, outstanding demand control performance of thermal storage inventories has been reported in many studies (Drees and Brauns 1996; Henze et al. 1997; Braun 1990; Braun, Montgomery et al. 2001; Henze, Felsmann et al. 2004). In particular, utility cost savings and on-peak demand reductions are proven to be substantial through the combined operation of both “passive” building thermal capacitance and “active” mechanical thermal energy storage systems (TES) compared to results had via theses techniques individually.

1.3 Demand-side controls via thermal energy storage

A number of technologies to enhance demand-side management performance of thermal energy inventories are found. Some of those include design innovation, increased

sizing or refined architecture of mechanical systems, which can be mainly referred as improvements in capacity and function of the hardware.

However this study aims at demonstrating that an improved control strategy with simple and ordinary hardware in the given architecture would enhance performance. Two business and engineering claims support this goal:

a. Building owners prefer low cost improvement measures, therefore, an enhanced control strategy without extra capital cost is favored over installing new expensive systems with an improved efficiency, and
b. Energy efficiency of HVAC&R system components has improved considerably over the past 20 years, yet effective building operation is often lacking (Henze, Felsmann et al. 2004)

All four technical goals of the demand-side management explain all of the outstanding features of the combined operation of both building thermal capacitance and mechanical thermal energy storage systems (TES).

A general operation is that both measures store "cooling" or "heating" energy when utility cost is relatively low (i.e., Load building) and take advantage of it when utility cost is relatively expensive (i.e., Peak clipping). A discharge of the stored energy is controllable such that the release profile can be manipulated to meet certain control goals (i.e. Load shaping). Load shedding is not always ensured, but a well-devised demand-limiting feature of building thermal capacitance reduces the net demand (Lee and Braun 2008). This operation assigns control flow of both thermal energy storage inventories as follows.

a. Control of the passive building thermal capacitance uses pre-cooling of building mass. This shifts the on-peak cooling load toward the off-peak period (i.e., load shifting). It also manipulates the set-point temperature trajectory during on-peak periods such that it prevents an abrupt rise of on-peak cooling

load, and also diminishes the net on-peak cooling load (i.e., demand limiting). For both cases, changing a trajectory of the set point temperature of the zone controls cooling capability of the passive building thermal mass.

b. Control of the active TES modulates a charge/discharge rate of the chilled medium, altering the system load curve of cooling plants.
c. These control parameters are typically written in a supervisory control strategy (Ellis, Torcellini et al. 2007).

1.4 Model-based supervisory control of thermal energy storage inventory

This section emphasizes two control terms, “supervisory” and “model”. Figure 1.4 introduces a definition of supervisory control in the context of control functions generally used in HVAC&R systems. Control settings of local controllers might be optimal and energy or cost efficient for certain subsystems. However performance of the entire system may not be optimal and efficient. With this handicap of local control, supervisory control seeks to minimize or maximize an objective function by systemically selecting values of variables within the allowed ranges. Therefore its objectives often include the minimum energy input or operating cost of the entire system. Compared to local control, supervisory control considers the system level characteristics and interactions among all components and their associated values. Thus supervisory control determines the optimal solutions in terms of i) operation mode, ii) operation sequence and iii) set-points of individual components. Apparently control of both thermal energy storage inventories fall under supervisory controls since their control variables which are written as set-points are operation sequences of devices.

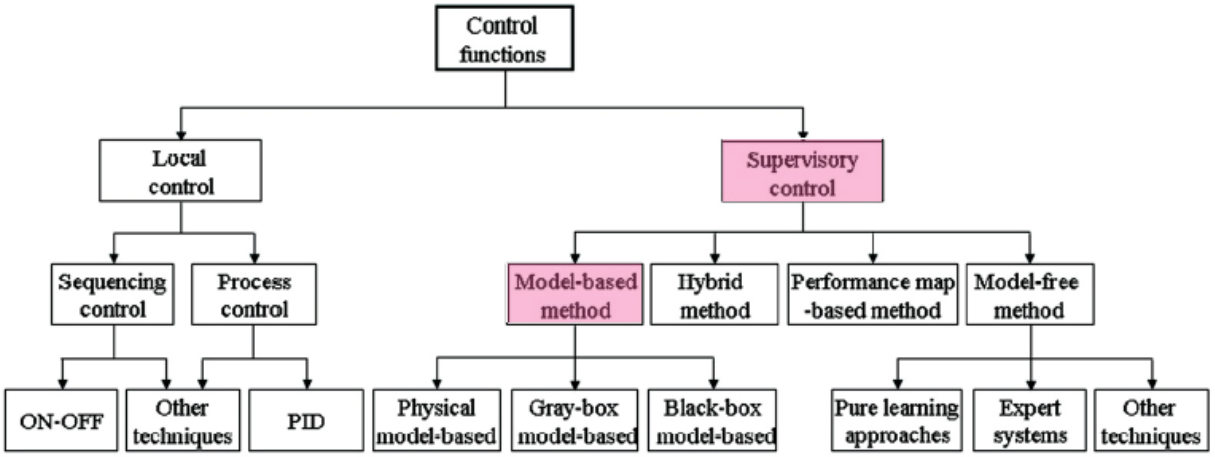

Figure 1.4 Classification schematic of control functions in HVAC&R systems (Wang and Ma 2008)

Controls for the systems with and without energy storage are significantly different. The control related to systems without storage is a result of a quasi-steady, single-point optimization, while the optimization related to systems with storage is the dynamic optimization determining a trajectory of set-points (Wang and Ma 2008). This dynamic optimization is only feasible when system and control models are available. This argument is supported in that predictive controls of thermal storage inventories are known to be more effective than other rule-based control strategies (Henze 2004).

This argument is supported again by a general statement for model-based predictive controls by Gwerder and Tödtli (2005). They identified that feed-forward capability of the model-based controls significantly enhances control performance when:

a. The controlled system has distinctive storage properties, i.e., when the system has enough thermal capacity allowing pre-cooling / preheating to be effective.
b. There are ranges for the controlled variables instead of single set points, allowing flexibility in control operations.
c. Future ranges for the controlled variables (i.e., a range of the allowed set-point variation) and future disturbances of the controlled system are known or can be estimated allowing pre-cooling / preheating energy requirements to be computed.

d. Costs for control actions are time dependent and/or depend on variables that are known or can be estimated in advance.
e. Future costs for control actions are known or can be estimated.

1.5 Uncertainty in building and HVAC&R controls

Model-based control is grounded on "predictability". Thus uncertainty is an unavoidable dilemma when the performance of model-based control is evaluated. Most studies on model-based controls, including those based on a deterministic approach, also consider uncertainty as a critical assumption.

Despite a fear of deterministic model-based control strategies underperforming in practice, there are only a few papers that relate uncertainty issues to the optimization controls of HVAC&R systems (Jiang, Reddy et al. 2007). Some studies use sensitivity analysis to test their robustness. However, uncertainty is a source of poor performance of deterministic optimal control is used as an example to highlight a potential risk due to uncertainty.

1.5.1 Uncertainty may cause a poor performance of the deterministic optimal control

Jiang and Reddy (2007) developed a methodology for dynamic scheduling and optimal control of complex primary HVAC&R plants, composed of various cooling plants. This study included a sensitivity analysis of the developed operating strategy on the practical degree of model-inherent uncertainty, load-prediction uncertainty, and control uncertainty. Under practical uncertainty conditions of (ε_m, 0.05), model-inherent uncertainty and load prediction uncertainty seem to have little effect (CV-STD being

around 2%) on the overall operating cost of the hybrid cooling plant with optimal deterministic operating strategy.

However, when model-based control strategies are developed for applications in which control performance critically depends on accuracy of predictability such as systems mentioned by Gwerder and Tödtli (2005), model-inherent uncertainty and load prediction uncertainty can cause seriously poor performance.

Simeng and Henze (2004) developed an optimal control using both thermal storage inventories in a deterministic situation where occupancy and lighting level happened to be underestimated. The unexpected level of internal heat gains causes serious risks. Serious side effects were found such as i) its passive control feature is lost (Figure 1.5), ii) load shifting may not be achievable as much as expected (Figure 1.6), and iii) on-peak system demand increases since pre-cooling did not work out. Despite these issues, since their purpose was to alarm a potential risky situation (i.e., "how to avoid" approach rather than "how to protect and breakthrough"), they emphasized the importance of simulation parameter calibration.

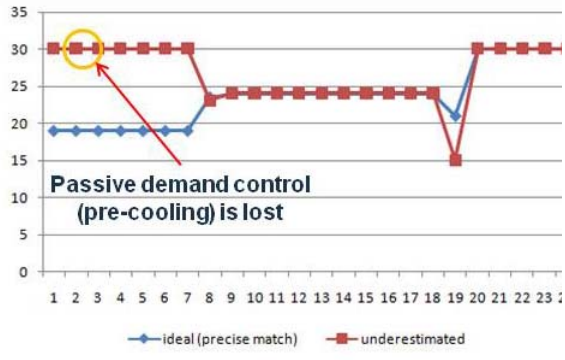

Figure 1.5 Pre-cooling of the building is lost due to the underestimated occupancy

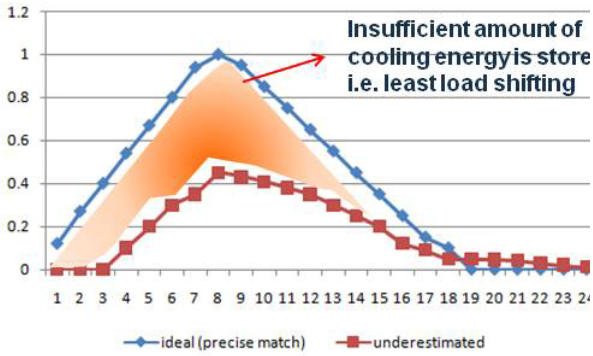

Figure 1.6 Insufficient amount of the cooling energy is stored in the Ice storage due to the underestimated occupancy

1.6 Research problems and motivations

I have reviewed literature related to uncertainty and optimal controls extensively. Reviews and analyses from the literature motivate the following research questions, and also have initiated aspects to enhance the performance of demand-side control strategies under uncertainty.

Research problems are grouped into three categories: requirements for further studies about uncertainty, requirements for better performance of demand-side controls and requirements for the development methodology of robust demand-side controls.

1.6.1 Uncertainty in building load prediction requires more attention for better control performances

Some studies have concluded that optimal controls of HVAC&R plants based on deterministic analysis are fairly robust on uncertainties on building load prediction (Olson 1987; Henze and Krati 1999; Jiang, Reddy et al. 2007).

In this study, however, uncertainties in building loads will be non-trivial factors in deriving the optimal demand-side control strategy since the magnitude and variations of building loads impose a strong influence on control decisions for passive building thermal mass. (e.g., the pre-cooling and the demand limiting set-point trajectory control). Results of existing studies for control of the passive thermal storage support this argument in that level of cost savings and the resulting set-point temperature trajectories are highly dependent on the building description (e.g., degree of building mass capacitance), HVAC descriptions, occupancy schedules, utility stricture and weather (Henze et al., 2008). Consequently, an operation of the active TES will also depend on the uncertainty inherited from the building load controlled by the passive building thermal mass.

Control performance of the energy supply plant is also highly dependent on uncertainty in building load prediction as the energy supply depends on the building load. When "storage" takes a large portion of the supply control (e.g., battery to store renewable energy) problems can arise, for instance, i) an early depletion of the stored energy due to unexpected higher loads, ii) an excessive storage due to unexpected lower loads or iii) supply profile under-matching or over-matching to demand profile (i.e., building loads) would decrease efficiency of energy supply control.

Sources of external prediction uncertainty (i.e., weather condition and building usage scenario) are known to have the most impact on the building load among all other uncertainty sources. Their sporadic nature has often led the research community to set a pre-fixed single scenario assumption for easier analysis. However, this practice should be re-examined, since the uncertainty in building load prediction may cause more detrimental impacts on control performance than they thought.

1.6.2 A fundamental study of uncertainty with respect to the development of robust demand-side controls is required

Some existing research proposing model-based optimal controls have assumed that either i) pre-fixed deterministic conditions are justified for the purpose of engineering efficiency (e.g., an assumption of single nominal condition) or ii) uncertainty issues can be somehow, or have been already, cleared by internal robust mechanisms of their engineering measures (e.g., artificial neural network based controllers are able to take care of all conditions).

Therefore, if a critical disparity between the predicted and the actual performance is found, they often recommend "calibration" of model parameters. This type of solution, in fact, would reflect their conception that uncertainty is an "error" or a "fault" that should be eliminated. However, this can be a misunderstanding in the case of calibrating

single component: i) the calibration uncertainty still exists after standard calibration (e.g., ASHRAE Guideline 14) and ii) calibration itself is an ideal situation. Not all parameters can be calibrated. Not all building and system components can afford calibrations. If model parameters that are recommended for calibration that are not practically feasible, degradation of performance is unavoidable. In other word, those model parameters are not accurate and precise enough for model-based optimal controls.

In case of calibrating multiple components via system identification, data available from HVAC systems for model calibration are not typically from the range of operation (Buswell and Wright 2004). This means that iii) if the calibrated model is used out of the calibration range, it may behave in an unexpected manner.

These three cases imply that calibrations are necessary, yet "being calibrated" does not mean that there is no (or negligible) uncertainty when the model-based optimal controls are actually used.

Due to these characteristics of uncertainty, uncertainty should first be properly defined. Then uncertainties have to be classified, thus capturing the pertinent uncertainties of which impacts may not be compensated by calibrations, should be prioritized. And then corresponding solutions need to be devised. The above mentioned external prediction uncertainty would be a typical example of this case.

A fundamental study of uncertainty will support this work. Because the goal of this study is the development of a systemic approach to deal with uncertainty with respect to robust control solution development process, such a process is required.

1.6.3 Proactive robust demand-side controls are necessary beyond a sensitivity analysis

Uncertainty issues related to optimal supervisory control of HVAC&R systems have been addressed in only a few papers. Moreover most of them are based on

sensitivity analysis (Jiang, Reddy et al. 2007). Sensitivity analysis is one of many uncertainty analysis methods, but is a "reactive" approach to assessing the impacts of uncertainty on the optimization result without providing a controlling mechanism. Thus, those studies often end with raising a warning when dealing with sensitive factors to develop models.

Not many studies have overcome issues of uncertainty by employing a comprehensive uncertainty study and suggesting constructive optimal controls under uncertainty. There is a strong need for suggesting a proactive approach that yields a robust demand-side control solution that is less sensitive to uncertainty.

1.6.4 A demand-side control strategy should meet its basic and core objectives

The objective of most existing demand-side controls is to make the operating cost as small as possible under a few of varied utility rate scenarios. Under some conditions, its cost function holds the lowest value. However, it is often found that at the same time the demand-side control does not reduce the on-peak load as much as it should, nor reduce variations. This can be attributed to failure in predicting the building load and/or a too weak weight effect of the utility rate premium that undermines actual value of the load shifting. For example, if the COP of the TES chiller is lower than the COP of the base chiller, the optimizer may choose cheaper control decisions. Thus very undesirable situations may happen, such as the base chiller serves a large portion of on-peak loads instead of charging the TES. Hence load shifting and consequent peak clipping may not be made effectively.

Many existing studies of developing a model-based control strategy use the operating cost as their optimization target, such that a criterion of evaluating and comparing the resulting performance is also operating cost. This practice could raise a claim that excessively strong weight of the utility rate premium might veil or compensate

for a degraded energy saving efficiency due to uncertainty. An explicit clarification for demand-side control objectives in the optimization algorithm would clear off this suspicion. Then evaluation criteria should reflect multiple aspects mandated by multi-dimensional goals of the demand-side controls.

First of all it should be emphasized again that a fundamental objective of demand-side control is foremost in reducing the net power consumption and increasing the effectiveness of using renewable energy sources in order to minimize carbon emission.

1.6.5 A robust and adaptive demand control solution needs to be researched

A concept of robust control is that an optimal control increases its feasibility under varied and uncertain conditions while prevention of the worst case scenario by reducing the sensitivity in optimization principles. Robust control, however, is often criticized for being overly conservative even in generic scenarios and thus could decrease control efficiency.

In demand-side controls, most of worst case scenarios are mainly attributed to a failure in accurately predicting the building load. This type of failure is typically due to unpredictable uncertainty in building load prediction. Examples of such unpredictable uncertainty include:

a. The presence of less or more occupants than the estimated occupancy schedule.
b. An abrupt increase or decrease of solar radiation (e.g., caused by cloud movement) that cannot be known from the historical data.
c. Increase of outdoor ambient air temperature that results in a higher utility rate in a Real-time pricing (RTP).
d. Actual operation range of the physical system is wider than the “training” operation range used during calibration of model parameters.

e. Occupants' requests to adjust their thermal environment resulting in unpredictable cooling loads.

As notion of the unpredictable uncertainty implies, predicting this uncertainty is theoretically and practically not feasible. All disturbances cannot be accurately forecasted and exact compensation is not possible. For such unpredictable uncertainty, it is more important to take a quick and effective reaction to reduce performance losses than an effort to predict them accurately. In other word, robust predictive control strategy needs to be adaptive, taking into account observations of current conditions in the building, and reacting appropriately.

1.6.6 A domain-specific, systemic procedure is required to develop robust demand-side control strategies

While general robust model-predictive control (MPC) problems mainly deal with parameter uncertainty of the model (Section 3.1), robust demand-side supervisory controls for building and systems deal with different dimensions and types of uncertainties. These uncertainties inherently require setting up a domain-specific procedure that covers as broadly as framing problem statements, and as detailed as choosing optimization algorithms.

Moreover the demand-side control of thermal energy storage developed using associated building and system component models naturally requires a series of building energy simulations (BES). They are computational processes that de-facto BES tools or custom made applications (e.g., Matlab) run. Therefore quantification methods of uncertainty depend on the simulation environment, in other words tool-specific.

Although quantification methods may vary per tool, describing uncertainty in the model typically would not differ since types of demand-side control measures decide sources of uncertainty (i.e., architecture-specific). Thereby a systemic method to describe

uncertainty per uncertainty source is attainable when architecture model of the demand-side controls is defined.

In summary, development of robust demand-side controls for building and HVAC&R systems should take a domain-specific approach due to its domain-specific uncertainty sources. Additionally this approach should still follow a systemic procedure for describing uncertainties.

1.6.7 A platform for standard and fast implementation of developing the robust demand-side controls and its deployment is required

Incorporating uncertainty is a data-driven process, thus the quality and volume of uncertainty data lead to difficulties in developing the robust control strategy. A systemic approach of uncertainty analysis and development process could alleviate an issue with the quality of the data. However an issue with a large volume of data and resulting prolonged processing time would hinder widespread applications of the robust controls, particularly in the building automation industry where feasibility and fast turn-around are virtues.

A platform that takes advantages of i) existing de-facto simulation tools with an affluent model library that reduces a painfully long model development time, ii) de-facto CASE (computer-aided software engineering) tools for an easier and faster analysis and iii) introducing the model-based system engineering (MBE) to standardize the modeling process and iv) an advanced computing environment such as cloud computing would suggest a solution for this issue.

1.7 Goals of the research

Encouraged by the requirements described in section 1.6, this research pursues improvement of current demand-side controls by proposing a robust and adaptive supervisory demand-side control strategy that is designed to maintain stability and near-nominal system performance under uncertain conditions. Specific objectives are:

1. To emphasize the importance of uncertainty analysis in developing robust demand-side control strategies that operate in buildings with both passive and active systems
   - 1.1 To study the performance of current demand-side controls under uncertainty
   - 1.2 To identify critical uncertainty sources affecting control performance and to examine the causality between uncertainty and demand-side control performance
   - 1.3 To propose a systematic approach to uncertainty analysis within building simulation models to develop robust demand-side control strategies

2. To improve the performance of a robust demand-side control strategy under uncertainty
   - 2.1 To propose a constructive development methodology that yields a robust demand-side control solution that maintains stability under uncertain conditions
   - 2.2 To enhance control effectiveness by means of mitigating the impact of the unpredictable uncertainty
   - 2.3 To enhance control efficiency by means of increasing adaptability in cases of critical “disparity”
   - 2.4 To demonstrate a model-based platform for standard and fast development and evaluation of the proposed robust demand-side control solutions

1.8 Research approach and outlines

This thesis will follow a step-by-step approach as the goals of the research dictate. The next list introduces how this thesis will proceed and each stage accompanied with the corresponding chapters. A brief introduction and explanation for each chapter follows after.

Stage 1: Background survey and identification of the research problem (Chapter 1)

Stage 2: Develop a robust demand-side supervisory control strategy based on fundamentals of uncertainty and its demonstration (Chapter 2, 3, 4 and 6)

Stage 3: Improve performance of the developed robust demand-side control strategy and its demonstration (Chapter 5 and 7)

State 4: Discussions and research expansions (Chapter 8)

The thesis is composed of motivating questions and eight chapters:

Motivating questions

: Refreshing research questions that capture main ideas of the thesis

Chapter 1 Introduction to the demand-side control and uncertainty

: Background of the study, detailed research questions and agenda of the thesis

Chapter 2 Fundamentals of uncertainty for robust model-based demand-side controls

: Definition, dimensions and sources of uncertainty and their classification in a matrix frame

Chapter 3 Modeling uncertainty for robust model-based predictive controls

: Introduction to classic robust Model-predictive Control (MPC) and its projection to the robust supervisory MPC for building and HVAC&R systems. A domain-specific interpretation about describing and quantifying uncertainty follows.

Chapter 4 Development of a robust supervisory demand-side control strategy

: Introduction to two representative demand-side control measures and a step-by-step methodology to develop the robust supervisory demand-side control strategy

Chapter 5 Using the NDFD weather forecast for model-based control applications

: The first improvement method to mitigate unpredictable uncertainty caused from the single sourced and historical archive based weather forecast by means of including the online weather forecast

Chapter 6 Case study

: A case study and performance verifications of the robust demand-side control against legacy control strategies including the deterministic optimal control

Chapter 7 Multiple model-based control strategy for robust and adaptive supervisory demand-side controls

: The second improvement method by means of Multiple model-based controls (MMC) to mitigate detrimental impacts caused by varying scenario uncertainty and its performance verifications against the static single model-based robust controls and the deterministic optimal controls

Chapter 8 Discussion and remark

: Summary of contributions, discussion about future work and further applicability

CHAPTER 2

FUNDAMENTALS OF UNCERTAINTY FOR ROBUST DEMAND-SIDE CONTROLS

2.1 Introduction

Uncertainty analysis is an increasing requirement for evaluating building energy performance and developing robust demand-side controls; thus uncertainty needs to be defined and systemically characterized. Although terminology and typology of uncertainty in general have been proposed, there is no domain specific approach to investigate fundamentals of uncertainty in the building and system energy performance domain.

Therefore this study attempts to arrange the general terminology and typology of uncertainty, and to search for their applications in engineering decision-making support, in particular for developing robust demand-side controls. At the last this study delivers a heuristic tool to classify uncertainties, such that the relevant uncertainty sources can be recognized, prioritized and characterized.

2.2 Definition of uncertainty

Among a number of contributions in the literature (Funtowicz and Ravetz 1990; Van Asselt 2002; Van der Sluis 1997; Environmental resources 1985; Alcamo and Batnicki 1987; Beck 1987; Hodges 1987; Morgan and Henrion 1990; Rowe 1994; Shrader-Frechette 1996; Davis and Hillestad 2000; Van Asselt 2000), Walker et al. (2003) provides a theoretical framework for systemic uncertainty analysis in model-based

decision support. They defined uncertainty as any deviation from the unachievable ideal of completely deterministic knowledge of the relevant system. This general statement suggests that uncertainty needs to be defined with respect to its literal antonym "certainty". This is restated in Nikolaidis's definition (2005) that uncertainty is defined indirectly from the definition of certainty while certainty is defined as the condition of knowing everything necessary to choose the course of actions whose outcome is most preferred.

Augenbaugh (2006) defined uncertainty as being the gap between certainty and the decision-makers' "present state of information" (Figure 2.1). This study adopts Augenbaugh's definition (2006) for uncertainty in engineering problem considering its relevancy to the problem statement of this study.

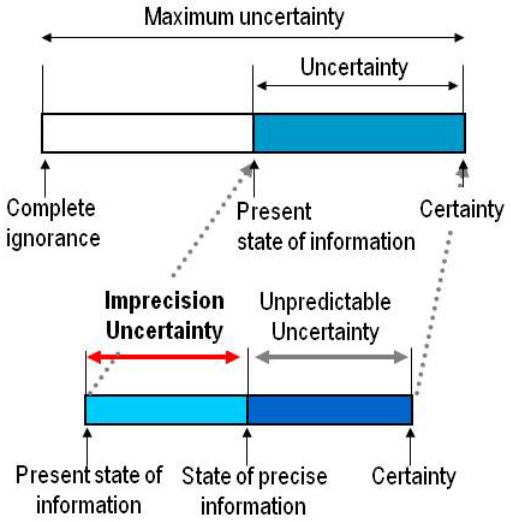

Figure 2.1 Characteristics of uncertainty (Nikolaidis 2005)

According to Augenbaugh's statement, "state of precise information" indicates the state that the decision maker has all information about the use of model, i.e., the distribution type and statistical parameters are known perfectly.

However, knowing all information about the model does not mean that there is no uncertainty, i.e., certainty, in the decision-making problem since a specific occasion originating from the unpredictable part may or may not happen.

As shown in Figure 2.1, the gap between the present state of information and the state of precise information is defined as "imprecision uncertainty". The remainder, "unpredictable uncertainty" accounts for the gap between a state of precise information and certainty.

It should be noted that an interpretation of unpredictable uncertainty in this study is that things can be knowable but currently it is not practically possible to know. For example, future weather information is necessary to estimate energy consumption of a building (i.e., present state of information). The weather model can be estimated by analyzing historical data, such that a pattern of future weather state can be formulated (e.g., TMY2 or BIN). Parameters of the weather pattern (e.g. mean, curve fits, variance etc.) can be known, however, yet not perfectly known, i.e., imprecision uncertainty exists. Meanwhile a sudden blizzard that may occur in the season, but it is not known when it will exactly happen, thus unpredictable uncertainty exists.

2.3 Dimension of uncertainty

Walker et al. (2003) noted that it is important to distinguish between the modelers' view of uncertainty and the decision makers' (or policy makers') view of uncertainty. Two have fundamentally distinct perspectives and therein require different analysis approaches: The modeler's view focuses on the accumulated uncertainties associated with the outcomes of the model and the robustness of conclusions of the decision support exercise, while the policy maker's views focuses on how to value the outcomes in the context of their goals and (possibly conflicting) objectives, priorities, and interests.

In this study, engineering decision-making problems specifically refers to decision support of demand-side control strategies. Robust control decisions should be made in the context that uncertainties exist in building and system behavior, environment,

energy policy and market status that are manifested into power cost, and eventually these uncertainties need to be modeled in computational simulations. Therefore this study more focuses on the first view on uncertainty, i.e., uncertainty analysis providing information to support control strategy decisions.

There is consensus in the uncertainty literature that different dimensions of uncertainty have influences on model-based decision makings (Walker et al., 2003).

a. The nature of uncertainty: whether the uncertainty is due to the imperfection of our knowledge or is due to the inherent variability of the phenomena being described (Section 2.4)
b. The level of uncertainty: where the uncertainty manifests itself along the spectrum between deterministic knowledge (i.e., determinism) and total ignorance (Section 2.5)
c. The location of uncertainty: where the uncertainty manifest itself within the model complex (Section 2.6)

It should be noted that these three dimensions are used to confine the uncertainty within which this study is interested. In the following section, each dimension of uncertainty will be further detailed.

2.4 Nature of uncertainty

Nature of uncertainty is closely related to the definition of uncertainty used in engineering decision-making problems. Recall its definition; a distinction of dual natures of uncertainty is a branch-off from the state at which the decision-maker knows perfectly the decision-making problem (aforementioned "state of precise information") (Figure 2.1): uncertainty has sporadic characteristics in nature (called "unpredictable") as well as

indefinite characteristics caused by lack of pertinent knowledge to make an engineering decision (called “imprecise”).

An ideal objective of uncertainty analysis would be to get rid of the uncertainty. However in practice this cannot be achievable, rather uncertainty could be mitigated at best to reduce undesired impacts. Mitigating uncertainty takes two different approaches due to its dual nature.

Refining a model can be interpreted as an attempt to mitigate its imprecision uncertainty. Therein by extension from the definition of being “precise” (Merriam-Webster 1993), imprecision is defined as not being exactly or sharply defined or stated. This is what needs to be captured in the engineering problem addressed in this study. If more information is available, i.e., parameters of the model of imprecision uncertainty become sharply defined, and the present state of information moves towards the state of precise information, the imprecision uncertainty reduces. This will, in fact, reduce total uncertainty of the decision-making problem (Figure 2.2).

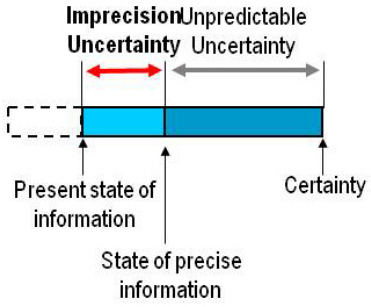

Figure 2.2 Reduced imprecision uncertainty by means of refining a model

Sources of unpredictable uncertainty, relevant to this study include the inherent randomness of nature and human behavior (non-rational or deviations of standard patterns) (Van Asselt 2002 and 2000). Removing unpredictable uncertainty, hence, may not be feasible with the given information. At a current stage where we only know what

happened before, predicting when a sporadic event will manifest itself in the future is almost impossible.

However, if certain inferences enable expecting a future (random) event within a (rough) boundary then at least part of them can be transferred into imprecision uncertainty, thereby unpredictable uncertainty can be mitigated. In an engineering problem, a future event often can be estimated by an extended analysis propagated from a larger system that motivates a movement of the current system. For instance, a hurricane strikes Miami today in the middle of the Atlantic hurricane season. If it typically takes 1-2 days for the hurricane to reach Pensacola, then at least a certain (higher than usual) probability of heavy rain in Pensacola can be anticipated, so Pensacola residents may have to prepare for heavy rain tomorrow or the day after.

2.5 Level of uncertainty

Level of uncertainty takes a different perspective over the maximum uncertainty dealt when the uncertainty is defined. An entire spectrum of the maximum uncertainty ranges from the complete ignorance to the completely precise knowledge, i.e., determinism, at the other end (Figure 2.3).

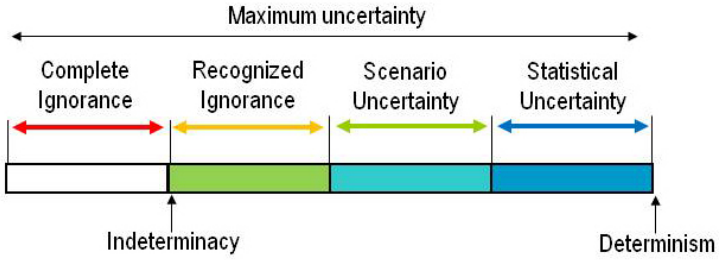

Figure 2.3 The progressive transition between complete ignorance and determinism (Walker et al., 2003)

An idea that the uncertainty transits phases depending on the degree of knowledge is useful to match a "tackling" approach to the level of uncertainty to reduce the undesired impacts. For instance, in an analogy from Lewis and Clark tour planning (Schlesinger 1996) they acknowledged that many alternative courses of action and forks in the road will appear, but their precise character and timing cannot be anticipated. Therefore very uncertain situations call for robust plans (which will succeed in a variety of situations) or adaptive plans (which can be easily modified to fit the situations encountered). The level of uncertainty and ignorance should be accounted for as the basis for decisions to act or not act.

Walker et al. (2003) suggested four levels of uncertainty as illustrated in Figure 2.3 and they are briefly introduced as followings.

2.5.1 Complete ignorance

This term refers to the deep level of uncertainty that we do not even know that what we don't know. Therefore this is hardly dealt in uncertainty analysis.

2.5.2 Recognized ignorance

This is fundamental uncertainty about the mechanism and functional relationships being studied (Walker et al. 2003). The definition implies that at this phase statistical description or a scientific basis for developing scenarios is still weak. Neither research nor further development can provide sufficient knowledge about the mechanism, i.e., we know an uncertain thing exists, but we don't know anything about it. This is called "indeterminacy" in Figure 2.3, which is a branching point from complete ignorance.

Quantifying recognized ignorance for an analysis purpose is still not so feasible; therefore it will not be considered for this study.

2.5.3 Scenario uncertainty

Scenarios are used to deal with uncertainty related to the external environment of a system (usually its future environment) and its effects on the system (Van der Heijden 1996). Hence a scenario means a likely description of how the system and/or its key driving forces may develop in the future, i.e., what might happen instead of what will happen. This notion about "being likely in the future" distinguishes scenario uncertainty from statistical uncertainty that will be explained next.

Scenario uncertainty indicates a range of possible model outcomes, but the driving force leading to these outcomes is not clearly distinguishable or these outcomes form a wide range of discrete possibilities. Therefore when scenario uncertainty is around, it may not be possible to formulate the probability of any one particular outcome occurring like a statistical description.

According to Walker et al. (2003), scenario uncertainty can manifest itself, and be eventually quantifiable, in three ways:

a. As a range in the outcomes of an analysis due to different underlying assumptions;
b. As uncertainty about which changes and developments (e.g., in driving forces or in system characteristics) are relevant for the outcomes of interests, or
c. As uncertainty about the level of these relevant changes.

2.5.4 Statistical uncertainty

Statistical uncertainty is any uncertainty that can be described in statistical terms. It is distinguished from scenario uncertainty when a change of the model outcomes occurs from a consistent continuum of the aggregated outcomes, which is expressed stochastically as a result of research and scientific reasoning.

Statistical uncertainty is referred in two typical use cases i) when describing the functional relationships in the given model assuming that statistical terms are able to

represent the phenomenon being simulated and ii) when the data used to calibrate the model are representative of configurations where the model will be applied. The most obvious examples of statistical uncertainty, therefore, are measurement errors and sampling errors.

2.6 Location of uncertainty

Location of uncertainty refers to where uncertainty presents itself within the entire model complex and process. Describing a location in the model will depend on the system model in question. Therein a description of the location should be characterized in order to offer more understandings on which location would affect the outcome of the model. As a generic guideline, Walker et al. (2003) suggested four locations in the whole model complex.

2.6.1 Context

Context refers to the reasoning behind the choice of boundaries of the system (Walker et al., 2003). The model context is typically determined in the problem framing stage and thus it clarifies the issues to be addressed and the choice of the outcomes to be evaluated.

Thus once the context uncertainty is introduced, ambiguity in the problem formulation may lead to the wrong question being answered. That is why it is important to involve all stakeholders and experts from the very beginning of the process of defining what the issue is. It is also crucial to set up a roll-back process if context uncertainty causes critical issues after the decision-making process has already been in the progress.

2.6.2 Model uncertainty

Model uncertainty is related to both the conceptual model and the computer (simulation) model. The conceptual model refers to the inputs/outputs/parameters and their relationships (i.e., assumptions, functions, equations, algorithms) to describe the real system and its context located within the decision-making problem boundary. Model uncertainty is thus further divided into model structure uncertainty (uncertainty about the relationship within the model) and model technical uncertainty (uncertainty from the computer implementation of the model).

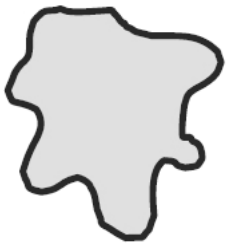

Figure 2.4 Context

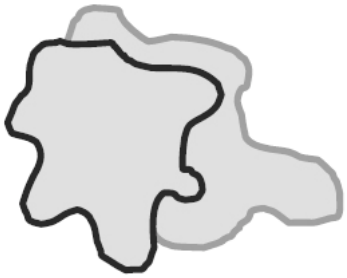

Figure 2.5 Context uncertainty introduces ambiguity in the definition of the boundary of the system (Walker et al., 2003)

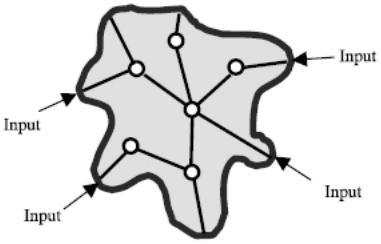

Figure 2.6 Model structure

Figure 2.7 Model structure uncertainty introduces different interpretations of the dominant relationship within the system (Walker et al., 2003)

Figure 2.4 to Figure 2.7 schematically describes the fundamental difference between the context uncertainty and the model structure uncertainty with respect to their definitions.

2.6.3 Inputs

Inputs are associated with the data describing the base system and the external driving forces that have an influence on the system and its performance. Two typical

input locations where uncertainty is located include external driving forces and system data.

Uncertainty about the external force produces changes within the system (the relevant scenario variables and decision variables) and the magnitude of those variables. A critical feature of this uncertainty is that it is one of dominant factors leading to model structure uncertainty (Walker et al., 2003). Uncertainty about the system data produces changes of relevant features of the base system and its behavior. It is typically originated by a lack of knowledge of the properties of the base system and deficiencies in describing the variability of system data.

2.6.4 Parameters

Parameters are constant in the model, and are invariant within the chosen context and scenario (Walker et al., 2003). There are four types of parameters in the model.

a. Exact parameter, e.g., mathematical constant π
b. Fixed parameter that is determined by previous investigations and considered exact, e.g., the acceleration of gravity
c. A priori chosen parameter that is chosen to be fixed to a certain invariant value based on a priori knowledge due to a difficulty of calibrations
d. Calibrated parameter that is typically chosen by means of comparisons of model outcomes for historical data archives and the measured data regarding the same input

This study will consider only calibrated parameter uncertainty since other three parameter uncertainties can be considered somehow "determined" from past similar practices of the uncertainty analysis in question.

2.7 The uncertainty matrix

A matrix is compiled as a heuristic tool to classify uncertainties by three dimensions as shown in Table 2.1. This matrix provides a tool that enables analysts to envision a systematic and graphical overview such that the essential features of uncertainty are identified, in particular in relation to the use of models for decision support of robust design and control of building and HVAC&R systems. It should be noted that the uncertainties located in a particular part of the matrix can belong to other parts, however a priority is given to a part that has the greatest effects on the outcomes of the model.

Table 2.1 Uncertainty matrix

Location		Level		Nature	
		Statistical uncertainty	Scenario uncertainty	Imprecision uncertainty	Unpredictable uncertainty
Context					
Model	Model structure				
	Computer model				
Inputs	External driving forces				
	System data				
Parameters	Calibrated parameter				

Application of this matrix constitutes a handy but comprehensive inventory of the nature, level, and location of uncertainties. Results of "characterizing" uncertainties will benefit several tasks in general engineering decision making process as below:

a. As heuristics during pre-uncertainty analysis phase (e.g., problem framing, a choice of the system boundary, model structuring)
b. As a checklist during uncertainty analysis (e.g., sensitivity analysis, co-variance analysis, design of experiments)
c. As a prioritization list of policies or tasks in order to prevent the unwanted results due to critical uncertainties in advance

d. As a performance check criteria during development of robust control mechanisms considering various uncertainties being present

For developing supervisory robust demand-side controls of a building and HVAC&R system, this matrix will guide what types of control strategies should be developed for each type of uncertainty. It also will provide a clue on what scientific basis and technical methods can support each control strategy.

To do so, the first task is to identify sources of uncertainties for developing supervisory robust demand-side controls and to characterize them according to the suggested uncertainty matrix.

2.8 Sources of uncertainty for developing supervisory robust demand-side controls

In the process of designing and operating building and HVAC&R systems, sources of uncertainties can be classified into three categories (Pistikopoulos and Ierapetritou 1995, Jiang and Reddy 2007).

a. Model-inherent uncertainty: the uncertainty of the various building and system component models, which is caused by inaccurate or incomplete data in the analytic model and/or lack of a perfect regression fit in the response model
b. Process-inherent uncertainty: the range due to randomness and bias within which the control and process variables can be dispersed
c. External prediction uncertainty: the unpredictable discrepancy in estimating the driving forces located outside the system, mainly weather, building usage and demand and supply status of energy typically manifested as utility rates in the energy market

2.8.1 Model-inherent uncertainty

The model-inherent uncertainty has four sub-types of uncertainties: specification uncertainty, uncertainty in model realism, uncertainty in scope of model and boundary conditions, interpretation uncertainty due to different model resolutions and lastly simulation algorithm and numerical uncertainty. Each uncertainty source will be explained in following sections.

2.8.1.1 Specification uncertainty

Design specifications do not completely represent all relevant physical properties and installations. For example, instead of specifying material properties, a type of material can be provided with an uncertainty that it may not match the exact property. Moreover deviations from the design specifications during the installation process may cause this type of uncertainty. Aged material and its transformed property due to changed physical conditions (e.g., overheat, condensation), thus may not comply with its design specification.

There are four sub- groups of specification uncertainty sources in building and system descriptions: building material properties, thermal zone properties, built environment & external environment and power efficiency and degradation of HVAC&R systems. As types of their sub-sources are case-specific, a complete list of sub-sources can be found in a case study of the Acme building in section 6.5.

Appendix B introduces literature that the reported locations of sub-uncertainty sources, the degree of uncertainty (i.e., range of variations), a theoretical/empirical basis to identify uncertainty sources, and representation of uncertainty sources (e.g., probability distribution). From Table 2.2 to Table 2.5 summarizes some of this information.

a. Uncertainties in building material properties (M)

Table 2.2 Detailed uncertainty sources in building material properties and their probability distributions

Sources	Detailed sources	Probability dist.
{Wall,Roof,Floor}::Material:: Thermophysical properties	Conductivity	Gaussian
	Density	Gaussian
	Specific heat capacity	Gaussian
Ceiling ::Material:: Thermophysical properties	Resistance	Gaussian
Window ::Glazing:: Thermophysical properties	U_value	Gaussian
ExtWall ::Material:: Thermophysical properties	Solar Absorptance	Gaussian
ExtRoof::Material:: Thermophysical properties	Solar Absorptance	Gaussian

b. Uncertainties in thermal zone properties (Z)

Table 2.3 Detailed uncertainty sources in thermal zone properties and their probability distributions

Sources	Detailed sources	Probability dist.
Zone::Thermophysical properties	Thermal capacitance	Gaussian
Zone::Infiltration properties	Infiltration air change rate	Gaussian

c. Uncertainties in built environment & external environment (E)

Table 2.4 Detailed uncertainty sources in built and external environment and their probability distributions

Sources	Detailed sources	Probability dist.
Environment:: Heat transfer properties	External convective heat transfer coefficient	Uniform
	Internal convective heat transfer coefficient	Uniform
Environment::Wind properties	Wind reduction factor constant K	Gaussian
	Wind reduction factor exponent α	Gaussian
Environment:: Ground properties	Ground albedo	Uniform
Environment::Soil:: Thermophysical properties	Conductivity	Uniform
	Density	Uniform
	Specific heat capacity	Uniform

d. Uncertainties in power efficiency and degradation of HVAC&R systems (S)

Table 2.5 Detailed uncertainty sources in power efficiency and degradation of HVAC&R systems and their probability distributions

Sources	Detailed sources	Probability dist.
Fan coil unit (FCU) ::Design specification	Electricity consumption tolerance	Uniform
Primary chiller::Design specification	Degradation coefficient	Uniform
Thermal energy storage (TES) chiller::Design specification	Degradation coefficient	Uniform
Cooling tower:: Design specification	Fan efficiency	Uniform
Thermal energy storage (TES) :: Design specification	Surface loss coefficient	Uniform
	Additional thermal conductivity	Uniform
Pump:: Design specification	Pump efficiency	Uniform
Pipe:: Design specification	Heat loss coefficient	Uniform

2.8.1.2 Model realism

A component class represents a unitary system or a composite system assembled with sub-modules. Both systems can be modeled analytically or empirically. For empirical models, modeling assumptions and simplifications of a complex physical process (e.g., implementing polynomial behavior using a linear function) during the

development introduces a gap between model representation and reality. Analytical models repeatedly introduce the model-inherent uncertainty previously observed at its sub-component level.

A typical example of uncertainty in model realism is that i) the performance curve that the degree of uncertainties (e.g., NMB , CV-RMSE) is able to transform and ii) boundary of system performance that varies by different operation regimes of a non-linear system (Lee and Lee 2008; He, Cai et al. 2005). In the latter case, a compositional modeling approach consisting of multiple sub-models for different operation regimes can be an alternative modeling approach. Refer to (He, Cai et al. 2005) for more details.

2.8.1.3 Scope of model and boundary conditions

Developing whole building and HVAC&R model is often avoided due to its higher development cost. Instead partial HVAC&R and control models can be developed for a specific simulation task. Therefore boundary conditions of partial models are usually prescribed by users, rather than by thermophysical results of heat transfer and mass transfer between elements. Poorly defined boundary conditions (e.g., a room model surrounded by all boundary walls having the same temperature condition, significant thermal coupling with the ground, or the building load being assumed to be fixed) may impair the accuracy of simulation or cause unexpected simulation results.

In particular setting the building load as a boundary condition is problematic, given that occupancy level and weather conditions are considered critical in developing supervisory control strategies due to their high impact on the building load (Simeng and Henze 2004; Henze, Biffar et al. 2008; Florita and Henze 2009). As a compromise, some trials to simulate their imprecise characteristics such as introducing noises are reported. However without building and system models over which those uncertainties propagate and then bring about a synergy effect, the control performance of the developed control strategies with this approach could be in question.

2.8.1.4 Model resolution

Required details of the system model (i.e., resolution) depend upon given simulation tasks. A finer or coarser model resolution than the required level of model resolution adequate to the given task may introduce interpretation uncertainty. To avoid this, a selection of correct model resolution appropriate for the simulation task during developing descriptive models (Section 3.4.5.1) is a critical step.

For instance, in testing control performance of a given chiller controller using simulation (Figure 2.8), two cases of system and control models are feasible. In case A, primitive equipment level control variables (e.g., compressor motor speed) decide the chiller output. In case B, set point temperature of the chilled water leaving the chiller decides the chiller output. A controller of the control model in case A sends an "electronic signal" to modulate pumps and valves, whereas supervisory controls of the control model in case B send a "data bit" containing the set point temperature for chilled water. In this example, it is demonstrated that case A and case B operate at different resolutions: equipment actuation level vs. performance value level.

Resolution of control command (equipment actuation level vs. set point value level) sent out from the given controller should be dependent on resolution of the chiller model. If both resolutions are not equivalent, conversion logic to connect the model and controller have to intervene. This conversion logic (perhaps based on another model or function) may introduce further model-inherent uncertainty if the logic is too simple or if it is based on irrational assumptions.

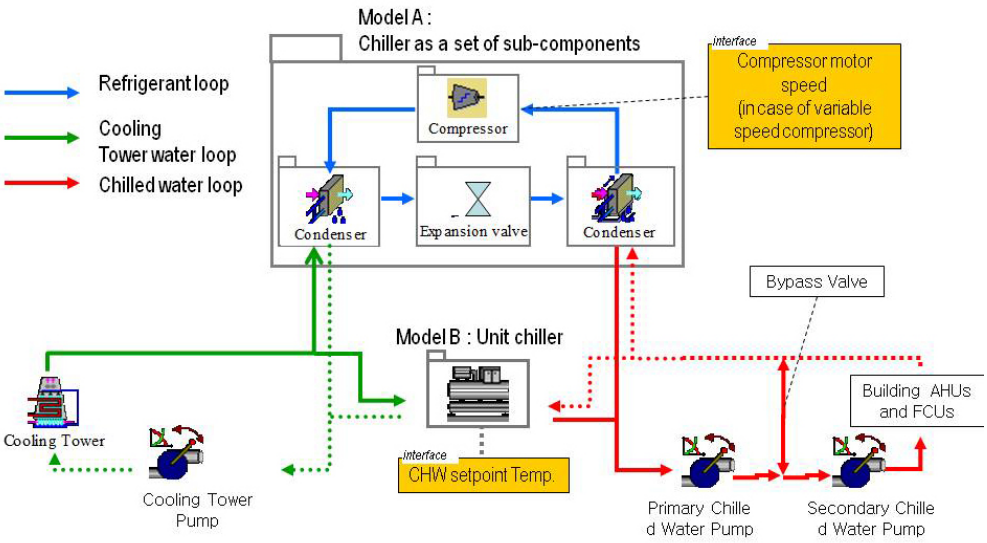

Figure 2.8 Chiller models with two resolutions

2.8.1.5 Simulation algorithm and numerical uncertainty

A selection of an inappropriate simulation algorithm for analyzing heat and mass transfer phenomena introduces uncertainty that can avoided if a suitable simulation algorithm is used. Furthermore numerical errors can be introduced while discretizing the model.

Uncertainty inherited from numerical calculation of simulation is probably the most familiar in engineering design, but possibly the least significant (Aughenbaugh 2006). If appropriate algorithms, discretizations and time steps are chosen, this uncertainty can be minimized.

2.8.2 Process-inherent uncertainty

Process-inherent uncertainty that can be observed in developing robust demand-side controls for building and systems primarily includes hysteresis in sensor reading, unknown characteristics of controllers and measurement and installation errors. Each source of the process-inherent uncertainty will be explained next.

2.8.2.1 Hysteresis in sensor reading

A system with hysteresis may have any number of states and responses depending on loading or unloading paths. In order to predict outputs of a system with hysteresis, however, one must look at the path that the system response followed before it reaches its current value.

Figure 2.9 shows an example of the hysteresis of thermocouples in reading temperature variations. Temperature readings when temperature rises and when temperature drops follw shifted trajectories toward opposite direction with respect to the actual temperature variation. Hysteresis is a property of the sensor that is specified in the sensor data sheet. Hysteresis of a well-calibrated sensor is typically within ±2-3% of the output without hysteresis (i.e., calibration uncertainty).

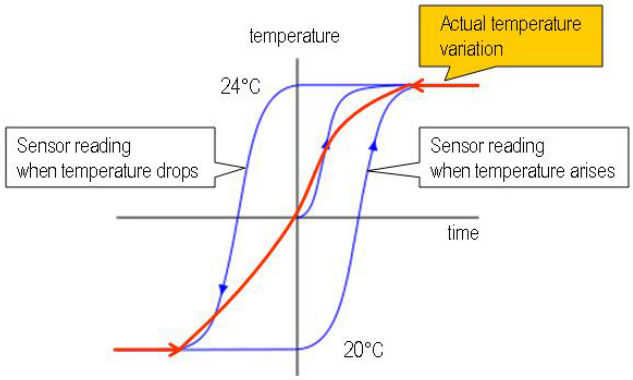

Figure 2.9 An example of hysteresis in thermocouples

2.8.2.2 Unknown characteristics of controllers

Control logic is usually implemented by hardware level feedback controllers in which set-point tracking response will generally be imperfect due to actuator constraints and un-modeled time-varying behavior, nonlinearities and disturbances (i.e., noise). To protect mechanical devices (i.e., actuators and controlled equipment) from an integral windup and resulting control degradation or malfunctioning caused by these atypical

occurrences, a dead band is implemented in the control logic. The dead band itself is used for protection purposes, but it could also introduce uncertainty.

Figure 2.10 and 2.11 describe uncertain controller behavior caused by dead bands. Dead band is a region of allowable deviation of the measured variable around the set-point where the controller is inactive. It is a common actuator constraint to prevent repeated activation-deactivation cycles (called hunting) in proportional control systems (Johnson 2002). It introduces a deviation from the desired value (i.e., set point); for instance, supply air temperature of the terminal unit is supposed to be 20°C as the set point indicates, but actual supply temperature could be in the range between 19 or 21°C.

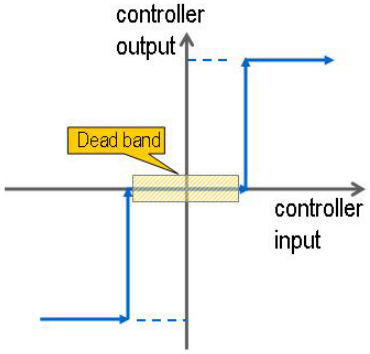

Figure 2.10 An example of dead band in thermostat

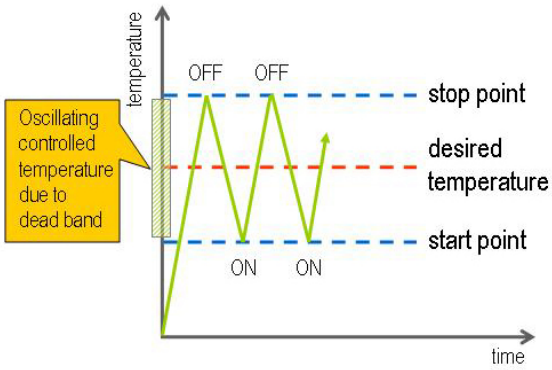

Figure 2.11Controlled temperature variation due to dead band

2.8.2.3 Measurement and installation errors

Energy management control system (EMCS) consists of complex and heterogeneous monitoring and control devices, the installation and measurement of which can introduce uncertainties. Related uncertainty sources include bias and precision errors in sensor reading, signal conditioning, amplification, and data acquisition. However, measurement uncertainty can be combined into calibration uncertainty (Huang 1999), and solved by the proper calibration of devices.

Three process-inherent uncertainties eventually come to calibration uncertainty. It should be noted that uncertainty sources in this study focuses on properly working devices and equipment. In other words, a malfunction due to a failure of testing and validation should be regarded as a problem rather than uncertainty.

Generally speaking calibration uncertainty exists in a "port" (i.e. connector) between devices. A port in building systems can be a flow port (e.g., fluid, energy) or a non-flow port (e.g., signal). Table 2.6 lists typical types of ports used in building and HVAC&R system models and associated sources of calibration uncertainty.

Table 2.6 Detailed calibration uncertainty sources and their probability distributions

Sources	Detailed sources	Probability dist.
Airflow properties	Airflow rate	Uniform
	Temperature	Uniform
Water flow properties	Water flow rate	Uniform
	Temperature	Uniform
Power properties	Real power	Uniform
Sensor properties	Hysteresis	Uniform

2.8.3 External prediction uncertainty

External prediction uncertainty originates from occasions when predictions of weather conditions, building usage scenarios, and utility rates used for the BES differ from the actual observation. The next sections illustrate causes and factors of external prediction uncertainty.

2.8.3.1 Weather condition

Accuracy of short-term prediction (typically 24 hr or less) of ambient weather conditions is crucial to the success of control technologies for building system operations (Henze, Felsmann et al. 2004). In particular when renewable energy sources or thermal storage are involved, an accurate control decision is made on the basis of predictions of

short-term heat gains and loads that are highly dependent on weather conditions. Although short-term prediction methods for outside air temperature have been extensively studied, reliable prediction methods for solar radiation are yet to be established (Zhang and Hanby 2007).

One primary reason for difficulties in obtaining an accurate weather forecast is that the inherent sporadic characteristics cannot be forecast from long-term averaged past values (e.g., TMY2). Concerning short-term forecast, using an on-line weather forecast could be a method to reduce degree of the unpredictable uncertainty. Zhang and Hanby (2007) compared actual observations and three on-line weather forecasts of short-term solar scale distributions. Figure 2.12 and 2.13 show that on-line weather forecasts are close to an actual observation with a small variation within each source. They applied the data fusion technique to obtain a synthetic profile from all investigated on-line weather forecasts to increase reliability. This result implies an important finding that the weather forecast can be treated as a combinational effect of multiple weather profiles.

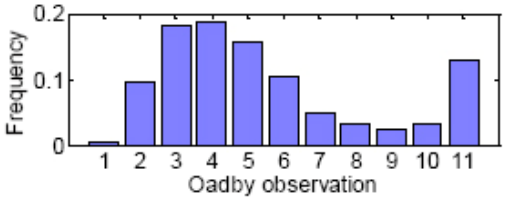

Figure 2.12 Distribution of the solar scales observed (Zhang and Hanby 2007)

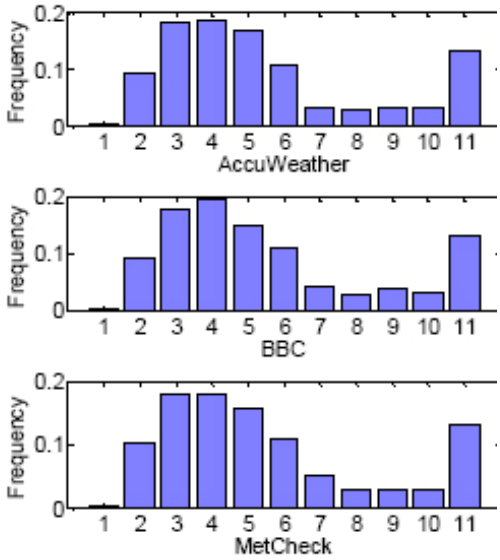

Figure 2.13Distribution of the solar scales predicted by three on-line weather forecasts (Zhang and Hanby 2007)

Table 2.7 lists up the most prevalent weather variables of the short-term weather forecast for the control reported in the relevant studies (Ren and Wright 2002; Florita and Henze 2009) and their tentative probability distribution.

Table 2.7 Detailed uncertainty sources of weather and their probabilty distribution

Sources	Detailed sources
Environment::Weather	Ambient temperature
	Global horizontal solar radiation
	Relative humidity

2.8.3.2 Building usage scenario

The influence of occupancy on the building can be broken down into several means of interaction (Figure 2.14). Human beings emit heat and pollutants (e.g. CO2). Occupants interact with the building system to enhance their personal comfort, thus they heat, cool, ventilate their environment. They also adjust the lighting level for visual comfort (e.g., artificial lighting or blind). Occupants operate electrical appliances which is another heat source. Occupancy is therefore central to the prediction model of building usage scenario.

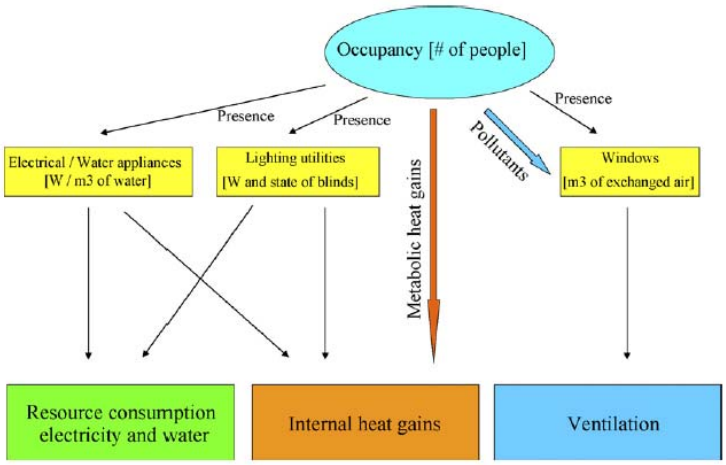

Figure 2.14 Occupancy interactions to building thermal physics (Page, Robinson et al., 2008)

Currently the most common way of including occupancy within simulations is a "diversity profile" (Abushakra et al. 2001). The diversity profile provides annual profiles of occupancy and heat gain, per building type and per hour/day/week. The weakness of this method lies in the repetition of one or possibly two profiles, and the fact that the resulting profile presents the behavior of all occupants in the building (Page, Robinson et al. 2008).

This simplification may overlook various patterns of individual occupant behavior, since it incorporates an average behavior (e.g., sedentary in an office all the time), and may neglect temporal variations and atypical behavior. Thereby random fluctuations (or even very different profile curves) in heat gain, energy consumption, and amount of ventilation may be emergent sources of unpredictable uncertainty as the simulation proceeds.

Mahdavi and Pröglhöf (2009) have observed uncertainty in occupancy (Figure 2.15 and 2.16). Five different offices in the same building have shown considerably different occupancy patterns with unique profiles. This finding indicates that to achieve increased control effectiveness, occupancy must be treated as multiple profiles and the imprecise uncertainty of each profile (i.e., fluctuations) should be considered. This is reinforced by the fact that different profiles of internal heat gain scenarios may cause very different control decisions due to its large sensitivity on building.

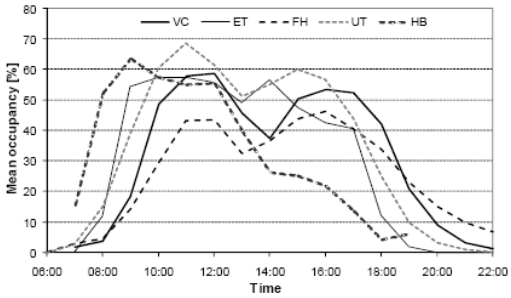

Figure 2.15 Mean occupancy level in different offices of a building (Mahdavi and Pröglhöf 2009)

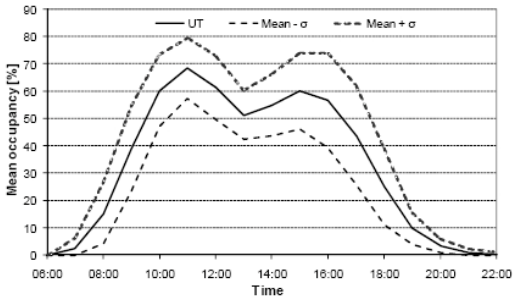

Figure 2.16 Mean occupancy level with fluctuations (±σ) (Mahdavi and Pröglhöf 2009)

Table 2.8 lists up associated sub-variables as sources of building usage scenario uncertainty and their tentative probability distribution for each profile.

Table 2.8 Detailed uncertainty sources of building usage and their probabilty distributions

Sources	**Detailed sources**	**Probability dist.**
Occupant::Heat gain	Sensible heat gain	Gaussian
	Latent heat gain	Gaussian
Occupant::Ventilation requirement	Fresh air flow rate	Gaussian
Lighting: Heat gain	Sensible heat gain	Gaussian
Equipment: Heat gain	Sensible heat gain	Gaussian

2.8.3.3 Uncertainty in utility rate

Decisions of demand-side control strategies are very sensitive to utility rates since they aim to reduce demand during higher operating cost periods (i.e., peak demand) meanwhile maintaining the same or better thermal performance of control strategies.

A utility rate reflects both community (or national) energy policy, and energy supply and demand in the utility market. Utility providers offer diverse rate structures (so called tariff) to meet the different needs of customers. Typically three tariff options are offered in the U.S. electricity companies; time of use (TOU) pricing, demand charges and real-time pricing (RTP). Table 2.9 illustrates their features and advantages/disadvantages.

Table 2.9 Three utility structures and their features

	Features	Advantages	Disadvantages
Time-of-use (TOU)	Fixed on-peak and off-peak rates	• The simplest • Beneficial to certain energy patterns	• Irregular demand pattern may cause unexpected expensive cost
Demand charge	Base charge plus a charge at the greatest amount of power used in 15-minute intervals during a billing cycle, i.e., once in a month	• Pay at prices based on the amount a customer needs while taking advantage of lower base charge	• A failure in managing demand patterns may cause the cost to increase dramatically
Real-time pricing (RTP)	The cost of electricity at the time is determined by customers in community. Ideally based on the marginal cost*. Announced a day-ahead or an hour-ahead.	• Since it reduces the variance of the grid level demands, it is known as the greenest in terms of environmental effects (Holland and Mansur 2007)	• Typically constant for 1 hour but can vary dramatically next hours, thus highly uncertain

* Defined as the most expensive unit that has to be operated to meet the electricity demand

As their features explain, demand charge and real-time pricing options have utility rate uncertainty. Although the cost that will be levied under two options may not be precisely known before the actual event occurs, driving forces to cause the potential highest rate can be known ahead by means of analyzing charging mechanism of each. Demand charge is levied at the greatest power demand in a billing period, typically a month. This fact implies that demand charge is likely to take place in case of the monthly-highest-cooling-load scenario, which is typically at an occasion with a combination of monthly maximum temperature and maximum internal heat gains.

In the meantime typical RTP rates are dependent on the time. Sun, Temple et al. (2006) have developed the time-varying RTP model that depends on the time of day and the maximum temperature for the day such as in Figure 2.17.

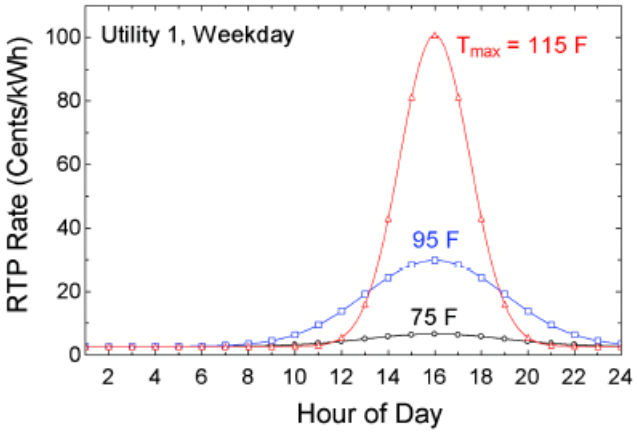

Figure 2.17 Typical RTP profile depends on the daily max temperature (Sun, Temple et al. 2006)

It is often the case that the utility company offers two options for commercial buildings: i) TOU as a base charge plus demand charge and ii) RTP. Uncertainty sources in this study will limit its scope to utility rate uncertainty in the TOU plus demand charge as a first target since it is relatively simpler for the analysis purpose. Therefore analyzing utility rate uncertainty in the RTP will be a task of future work.

2.9 Characterizing uncertainty sources and conclusion

According to the definitions of the three dimensions of uncertainty, uncertainty sources identified in section 2.8 are characterized as shown in Table 2.10. This matrix enables one to identify, articulate, and prioritize critical uncertainties, which is a crucial step for more adequate acknowledgement and treatment of uncertainty for uncertainty analysis, and eventually for developing robust demand-side controls. Also this matrix shows how those uncertainty sources can be understood and interpreted when developing robust demand-side controls. Use of this matrix has two main benefits as below.

- It enables one to draw a boundary on the scope of uncertainty analysis practically feasible for developing robust supervisory controls. In many cases uncertainties

located in i) the context of a problem compilation and ii) the system model are already designated to appear when an architecture of simulation models and simulation tools are chosen. Knowing that such heuristic uncertainties can be prevented through clear guidelines, normative procedures or use of standard tools in the process of model preparation and development, identifying heuristic uncertainties via this matrix works as a pre-informative guide when choosing system boundaries and modeling methods for the simulation model. Eventually physical uncertainties located in inputs and parameters become the primary quantifiable uncertainty sources that make technical uncertainty analyses feasible.

- The matrix offers i) a technical basis on which physical uncertainties located in inputs and parameters are represented and ii) a quantification method and an appropriate control strategy depending on characteristics of the physical uncertainty.

  According to the characterization of uncertainty sources shown in Table 2.10, physical uncertainty sources are largely divided into statistical uncertainty and scenario uncertainty in terms of level of uncertainty. Coincidentally this division corresponds to the division between imprecision uncertainty and unpredictable uncertainty. This study will focus on further developing a technical embodiment and description of two groups of physical uncertainties in chapter 3. For convenience, they will be nominated as statistical uncertainty and scenario uncertainty, respectively.

Table 2.10 Characterizing uncertainty sources of developing robust demand-side controls according to three dimensions of uncertainty

Location		Level		Nature	
		Statistical uncertainty	Scenario uncertainty	Imprecision uncertainty	Unpredictable uncertainty
Context			• Scope of model and boundary conditions	• Scope of model and boundary conditions	
Model	Model structure	• Model resolution • Model realism	• Model realism	• Model resolution • Model realism	
	Computer model	• Simulation algorithm and numerical uncertainty		• Simulation algorithm and numerical uncertainty	
Inputs	External driving forces		• Weather • Building usage • Utility rate structure	• Weather • Building usage	• Weather • Building usage • Utility rate structure
	System data	• Specification uncertainty		• Specification uncertainty	
Parameters	Calibrated parameter	• Hysteresis in sensor reading • Unknown characteristics of controllers • Measurement and installation errors		• Hysteresis in sensor reading • Unknown characteristics of controllers • Measurement and installation errors	

CHAPTER 3

MODELING UNCERTAINTY FOR ROBUST MODEL-BASED PREDICTIVE CONTROLS (MPC)

3.1 Deterministic model-based controls under uncertainty

As discussed in section 1.5, the current practice of an optimal deterministic model-based predictive control (MPC) may not perform as designed when it operates outside the indigenous circumstance in which the optimal MPC is cultivated. From the design to operational stages, incomplete knowledge and the inherent random characteristics of uncertainty are identified as reasons for this underperformance.

The existence of uncertainty motivates transforming conventional "deterministic" MPC into "stochastic" MPC. Finding a solution for stochastic MPC remains challenging, yet is of obvious practical importance.

In mathematical and control theory existing solutions have mostly developed the optimization algorithm under uncertainty (Dantzig 1955; Tintner 1955; Charnes and Cooper 1959).

In domain of supervisory control strategies for building and HVAC&R systems, several approaches that deal with optimization in control algorithms under uncertainty have been suggested: sensitivity analysis, stochastic linear programming (Gero and Dudnik 1978) and robust optimization (Mulvey and Vanderbei 1995). In domain of local controls for HVAC&R system, a robust control technique, H-infinity loop-shaping[1]

---

[1] This technique minimizes the sensitivity of a system over its frequency spectrum, and this guarantees that the system will not greatly deviate from the expected trajectories when disturbances interrupt the system. The H∞ norm is the maximum singular value of the function over that space. This can be interpreted as a maximum gain in any direction and at any frequency (Green and Limebeer 1995).

(Underwood 2000), can be regarded as the most important development. Except for sensitivity analyses that assess the impact of uncertainty without a controlling mechanism, the other methods pursue a system that is less sensitive to model data or disturbances than deterministic optimization programming is.

This study will use stochastic programming and robust optimization in particular due to their applicability to optimization algorithms for building and HVAC&R supervisory control. However, similar to the existing approaches dealing with uncertainty in this domain, stochastic linear programming and robust optimization still need to be supplemented with a method for screening relevant uncertainty sources and prioritizing them (an objective of uncertainty characterization and uncertainty analysis), and a method for describing and quantifying significant uncertainties in their proper location within a system model.

As fundamentals of uncertainty for robust demand-side control was investigated in chapter 2, this chapter will investigate a method of modeling uncertainty for a robust supervisory model-based predictive control (MPC) strategy for building and HVAC&R controls. These methods of modeling uncertainty will borrow mechanisms and mathematical formulations of the robust optimization and general robust MPC in control theory while fortifying their deficiencies by taking into account the characteristics of uncertainty in building and HVAC&R controls.

For more comprehensive and easier understanding, section 3.2 will compare classical robust MPC strategy in control theory with mechanisms of deterministic MPC strategies. Then section 3.3 will investigate prerequisites and references to model uncertainty for building and HVAC&R controls.

3.2 Mathematical definition of robust MPC in control theory

This section reviews basic concepts of deterministic MPC as compared to those of the robust MPC. In the literature, MPC is almost always formulated in state space

(Bemporad and Morari 1999). Thus concepts of the robust MPC can also be expressed in state space notation for comparison, which should be concise and clear enough to contrast fundamental differences between the deterministic and robust MPC.

3.2.1 The MPC formulation

The dynamics of the MPC can be described by the following linear discrete-time difference equations:

$$x(t+1) = Ax(t) + Bu(t) \qquad x(0) = x_0 \qquad (3.1)$$
$$y(t) = Cx(t)$$

where $x(t) \in R^n$, $u(t) \in R^m$, and $y(t) \in R^p$ denote the state, the control input, and the system output, respectively. Let $x(t+k|t)$ denote the prediction obtained by iterating the control model k times from the current state x(t). A series of optimum values during the control horizon is typically obtained through the following open-loop optimization problem:

$$\min_{U \triangleq \{u(t+k|t)\}_{k=t}^{t+Hc-1}} J(U, x(t)) \qquad (3.2)$$

$$J(U, x(t)) = x(H_p)P_0x^T(H_p) + \sum_{k=0}^{H_p-1} x(t+k|t)Qx(t+k|t) + \sum_{k=0}^{H_c-1} u(t+k|t)Ru(t+k|t)$$

where H_p and H_c denote the length of the prediction horizon and the length of the control horizon, respectively ($H_c \leq H_p$). Equation (3.2) should be subject to several constraints: $u(t+k|t) \leq G_1$ and $E_2x(t+k|t) + F_2u(t+k|t) \leq G_2$.

3.2.2 The robust MPC formulation

While the MPC algorithm assumes that the system to be controlled and the model used for prediction and optimization are the same, to describe the robust MPC problem, this hypothesis has to be relaxed and new assumptions are introduced: i) the true system s∈S, where S is a family of systems, and/or ii) uncertainty input W enters the system. A notion of "uncertainty" W introduces a concept of "being robust" into the MPC. A robust MPC problem for the system s is then described as follows:

$$x(t+1) = Ax(t) + Bu(t) + Hw(t) \qquad x(0) = x_0 \qquad (3.3)$$
$$y(t) = Cx(t) + Kw(t)$$

where w(t) ∈ W.

The system is referred to as having robust stability, if the respective property is guaranteed for all possible s∈S, and w(t) ∈W. As indicated, an appropriate description of uncertainty W in the context of S is a key factor that makes the robust MPC performs *robustly*. However previous studies have not rigorously determined the exact relationship between the uncertainty input set W and the covered set S (Bemporad and Morari 1999). However they suggested three types of model uncertainty describing that can be appropriately used in conjunction with the robust MPC problem. These three description types are summarized below:

a. Impulse or step-response of the model

Model uncertainty can be described as the range intervals over which the coefficients of the impulse- and/or step-responses vary. For example, the simplest SISO (single-input single-output) model s with an impulse-response is described as

$$y(t) = \sum_{k=0}^{N} h(t)u(t-k) \qquad S = \{ s : h_t^- \le h(t) \le h_t^+ \}, \qquad t = 0, \dots, N \qquad (3.4)$$

where $[h_t^- \; h_t^+]$ are given intervals.

b. Structured feedback uncertainty

The uncertainty can be included in the feedback loop of the model, so the noise or convolution term is introduced to the robust MPC problem, such that Equation (3.3) transforms to

$$x(t+1) = Ax(t) + Bu(t) + B_p p(t) \qquad x(0) = x_0 \qquad (3.5)$$
$$y(t) = Cx(t)$$
$$q(t) = C_q x(t) + D_{qu} u(t)$$

where $p(t) = \Delta\,(\,q(t)\,)$, and Δ is a memoryless time-varying matrix or a convolution operator that is located outside of the feedback loop.

c. Multi-system G and polytopic uncertainty

This type refers to a description in which the model uncertainty is parameterized by a finite list of possible systems:

$$G \in \{\, g_1, \dots, g_n\} \qquad (3.6)$$

Then the set of models G is described as

$$x(t+1) = A(t)x(t) + B(t)u(t) \qquad x(0) = x_0 \qquad (3.7)$$
$$y(t) = Cx(t) \qquad [A(t)\ B(t)] \in \mathrm{G}$$

Although problem formulations for robust MPC are based on strong supporting mathematical theory, since they originate from the development of local as opposed to supervisory controllers, a direct application of these concepts and theories to robust supervisory MPC for building and HVAC&R systems requires development in different hierarchical levels.

Alternatively this study implies an analogy that borrows concepts of robust MPC, particularly the description of uncertainty, and then it applies this implication to an

appropriate place in the development framework of the robust supervisory MPC for building and HVAC&R systems.

3.3 Modeling uncertainty for the robust supervisory MPC for building and HVAC&R systems

Compared to local control, supervisory control allows a consideration of the system level characteristics and interactions among all components and their associated variables (Wang and Ma 2008). Therefore supervisory control carries out a portfolio of control strategies dictating the operating sequence of equipment and set point profiles that are typically given to the local controller.

As supervisory control aims for the minimum energy input or the minimum operating cost at the building complex level, the supervisory control should consider "external force" variables outside the controlled system as well as process variables inside the control system.

If the external force causes or/and augments load (viz., an effort to maintain the designated state), the supervisory control also needs to properly describe both building and HVAC&R systems as delaying, delivering and distributing the externally originated load to local controllers. This process propagates uncertainty to very bottom mechanical level of the hierarchy of the control systems.

These difficulties in properly describing such systems and propagating uncertainty ask control system developers to think about several prerequisites before major development of the robust supervisory control. Four requirements are indentified as:

a. To describe uncertainty appropriate to the schema of the control model
b. To describe uncertainty appropriate to the resolution of the control model
c. To choose an objective function of the robust MPC

d. To deal with an increased volume of computation caused due to describing uncertainty

3.3.1 To describe uncertainty appropriate to the schema of the control model

Among three uncertainty sources as described in section 2.8, the process-inherent uncertainty has the closest description to the uncertainty description of the classic robust MPC. It is because process controllers that mechanically and electronically control HVAC&R equipment use algorithms that are typically built based on classical control theories. However, to describe two other sources of uncertainties (i.e., the model-inherent and external prediction uncertainties) requires more attention since the scope of these two uncertainties is beyond the assumptions that a typical process controller hold.

Model-inherent uncertainty is concerned with the building components and the whole system, and the properties and assumptions of those components. If a component model "outputs" via a certain process under uncertainty, the model-inherent uncertainty can be described in a similar fashion as in describing the process-inherent uncertainty. But if a system or a building component "behaves" differently from as designed such as under specification uncertainty, one method of describing this uncertainty results in multiple systems that are varied from a true system g, i.e Multi-system G (section 3.2.2). Then the robust supervisory MPC should find its robust solutions feasible for multi-system G. This will be further illustrated in section 3.7.1 about Latin hypercube sampling.

External prediction uncertainty is characterized as i) random variations and ii) a range of discrete profiles in external prediction variables. Because of the latter feature of external prediction variables, it is reasonable to treat external prediction uncertainty as scenario uncertainty (section 2.5). Thus describing external prediction uncertainty refers to subjecting the system g (or multi-system G) to multiple scenarios. Since a scenario is

time-dependent, it should be described in an objective function of the optimization algorithm. Then the robust supervisory MPC should find a solution feasible under all these scenarios. This will be further illustrated in section 3.7.2 about scenario robust optimization.

As shown above different sources of uncertainty need different descriptions for robust supervisory MPC. An "origin" of uncertainty determines a proper location to describe uncertainties in the context of building, system and controller models. Therefore i) identifying uncertainty sources relevant to given problems, ii) characterizing them according to uncertainty analysis framework (as suggested in chapter 2), and iii) describing each uncertainty by means of choosing the right location in the schema of the control model should be desired steps for describing uncertainty for the robust supervisory MPC.

3.3.2 To describe uncertainty appropriate to the resolution of the control model [2]

Choosing the right positioning is a starting point of a well-structured process for describing uncertainty. Then "how" and "how well" to describe uncertainty are the details of the given problem. Here "well" can be interpreted as "effectively" and "efficiently".

Firstly, "how to describe the uncertainty" is paraphrased into two procedures in later stages of modeling uncertainty: "how to mathematically represent the uncertainty" and "how to analytically or statistically quantify uncertainty". As numerous studies have

---

[2] The uncertainty due to improper model resolution, one of the model-inherent uncertainty sources discussed in chapter 2, emphasizes am importance of choosing a right model resolution appropriate to the simulation purpose. However here this issue emphasizes that the resolution of describing uncertainty should be equivalent to the given model resolution.

addressed this issue, relevant literature will be thoroughly reviewed and discussed in section 3.5 and 3.7.

A more important point is that describing uncertainty should fit the resolution of the control model. In other words, if it is described at finer level than the model resolution, issues of control instability and computational load could degrade control performance (i.e., lower efficiency). If it is described at coarser level, issues of unrealistic uncertainty boundary could arise (i.e., lower effectiveness).

This study pursues a systemized way to describe uncertainty matched to the resolution of the robust supervisory MPC framework that will be developed to support model-based system engineering (MBSE) supports. This will be discussed in section 3.4 and 3.6.

3.3.3 To choose an objective function of the robust supervisory MPC

According to Bemporad and Morari (1999), two strategies to choose an objective function of the optimization are possible when formulating robust MPC: i) to define a nominal model $\hat{g}$ and nominal uncertainty $\hat{w}$, and then to optimize nominal performance (Equation 3.8), or ii) to solve the min-max problem to optimize robust performance (Equation 3.9). Mathematical formulations are as follows, respectively.

$$\hat{U} = \arg \min_{U \triangleq \{u(t+k|t)\}_{k=t}^{t+Hc-1}} J(U, x(t), \hat{g}, \hat{w}(t)) \tag{3.8}$$

$$\hat{\mathrm{U}} = \arg \min_{\mathrm{U}} \max_{\substack{s \in \mathrm{S} \\ \{w(k+t)\}_{k=0}^{Hc-1} \subseteq \mathrm{W}}} J(U, x(t), G, W) \tag{3.9}$$

Although the latter approach leans more toward a concept of being “robust”, its two drawbacks are known as i) more complex and larger computation than the former approach has and ii) resulting control solutions could be excessively conservative.

Knowing that the robust supervisory MPC solution pursues better performance over all uncertain spaces G and W, and given the two drawbacks of the latter approach, the former nominal approach would be more suitable for this study.

Additionally i) the perspective about distinguishing uncertainty and risk (Samson, Reneke et al. 2009) and ii) the performance aspect of supervisory controls (e.g., the least on-peak demand vs. the maximum use of renewable energy) can result in many variations of objective functions. Section 4.4.5 will review how a stakeholder can define his/her needs for demand-side controls with respect to their risk preference and what types of performance index can suit stakeholders' needs.

3.3.4 To deal with an increased volume of computation caused due to describing uncertainty

The robust supervisory MPC considers a large space of systems and building components. Describing uncertainty not only increases complexity of the system, but also increases the computational expense to achieve a robust solution. When scenarios and the multi-system G are involved, the computational expense grows proportionally to the number of their combinations.

Classical robust MPC is also overwhelmed by increased computation needed to handle uncertainty terms. Computationally efficient optimization algorithms (Kothare, Balakrishnan et al. 1996; Bemporad and Mosca 1998) have been proposed as solutions for this. However these are typically for analytical calculations. When a control problem involves an extensive number of occasions, parallel computation power becomes a more effective solution.

This study introduces a cloud computing environment and the use of middleware that enables massive parallel computing. It is known that jobs requiring a high volume of computations such as optimization or Monte-Carlo analysis would achieve benefits from both. Although cloud computing environments became popular in a wide range of

industries, yet its application has not been reported in the domain of building and system energy performance analysis.

3.4 Modeling uncertainty within building energy simulation (BES) models

Use of building energy simulation (BES) tools is considered to be a valid approach for developing supervisory control strategies and has demonstrated substantial accomplishments (Braun, Mitchell et al. 1987; Henze and Krarti 2005; Coffey, Haghighat et al. 2010). It is expected to be an adequate framework for the development of robust control strategies as well, as building energy simulation tools are able to capture important logical and physical characteristics of components and their behavior. These characteristics are realized in the mechanism programmed in BES tools. Therefore it is a useful framework to describe uncertainty that impinges almost every building and system components, and networks of those elements.

It is known that only physical and mathematical uncertainty sources (i.e., located in the inputs and parameters) can be quantified in the BES model. Heuristic uncertainty sources (i.e., located in the context and system model) are possible origins of such physical uncertainty sources. For instance, non-equivalent model resolution between components requires an extra mapping component, such that reduced degree of "information" (from finer resolution to coarser resolution) is quantified as a loss of "data" sets in the mapping component.

Previous practice, however, has disregarded this relationship between two groups of uncertainty sources while developing BES models. Indeed there is no objective ground for that this mapping component is really necessary. In fact it should have not been modeled in such ways. In other words, it is necessary to prevent such heuristic uncertainty sources in advance. A more urgent point is to set an "identifier" to recognize the possibility of such logical uncertainty sources in simulation models.

A set of the structured information that defines requirements, relations, rules and semantics of necessary components that strictly fulfill simulation objectives would work as this identifier. This set of the structured information also suggests an appropriate representation of a component in the network topology of the BES model according to its significance and relevance to the simulation objective. Thus if one finds less integrity in this set of the structured information, possible logical uncertainty sources can be identified.

Therefore modeling uncertainty has to be viewed from both logical and numerical perspectives. Typically three software architecture models of the BES tool take part of these two perspectives. This will be further discussed in next sections in the general software engineering context.

3.4.1 Software architecture of BES tools

The software architecture of a typical BES tool follows that of a generic computing system. Focusing on the use of simulation tools, it includes three relevant models: the concurrency/process view, the data view and the mathematical functional view.

An information model is a representation of concepts, relationships, constraints, rules and operations to specify “data semantics” for building simulation. It can provide sharable, stable, and organized structure of information requirements for the domain context (Lee 1999).

A data model is an abstract model that describes how data is represented and accessed in actual simulation code. While the information model formalizes the description of a problem domain without constraining how that description is mapped to an actual implementation in simulation tool, the mapping of the information model to simulation code is defined as “data modeling”. Most BES tools have a similar program structure due to common components necessary for thermo-physical simulations.

However, each BES tool has its own version of data model, i.e. is tool-specific, despite the fact that they are based on the similar (or even the same) information model. Consequently methods of quantifying uncertainty vary by individual BES tool.

A mathematical model is a series of mathematical formulas, e.g., differential algebraic equations (DAE), employed to solve the described systems. These formulas use the data prepared in data model to produce the solution. In this study, the algorithm includes a set of heat transfer/mass transfer equations, numerical solution methods and optimization algorithms.

3.4.2 TRNSYS and its extensions

TRNSYS (Klein, Duffie et al. 1976) is chosen as the thermodynamic BES tool of this study. It is a transient building and system simulation tool employing modular structure. This tool offers a strong system library of thermal and electrical energy systems based on either derivative model or algebraic model. As dynamic compositions using base library components and user-defined modules are fully supported, it has been applied mainly in simulations of solar thermal/photovoltaic systems, renewable energy systems, cogeneration, fuel cells and other innovative systems.

The modular structure[3] of TRNSYS enables a flexibility and scalability, and thus interrupting process and development of custom simulations can be easily performed compared to other packaged BES tools (e.g., EnergyPlus). Additionally its seamless interoperability with other simulation tools (e.g., CONTAM, Fluent) and generic mathematic programming tools (e.g., Matlab, Simulink) is a unique feature. This

---

[3] As of 2010, most tools that offer this capability are yet at research phase in building and HVAC&R domain (e.g., BCVTB of Lawrence Berkeley National Laboratory), such that affluent model libraries and their industry application examples are very required for further spreads among field developers.

facilitates the quantification of all uncertainties in this study while providing enough detail and an easy implementation.

In addition, interventions between simulation tools and optimization engines are often required to quantify certain types of uncertainties. A common way of connecting them is to use an external driver that an optimization tool (e.g., GenOpt) provides or that is coded by users themselves (e.g., Matlab). The former method is limited because deeper level of customizations is necessary for quantifying uncertainties such as scenario uncertainty, while the latter method is not easily implementable for quick deploy. In this case, a computer-aided-engineering (CAE) tool that supports design automation such as Design of experiments (DOE) can be a good alternative to extend capabilities of TRNSYS. This study provides an application of CAE tools in section 4.11.

3.4.3 How uncertainty is modeled in the software architecture of a simulation tool

The effects of uncertainty of various sources can be fully captured and quantified when they are analyzed in the three software architecture models of a building simulation tool. The information model is a front-end where modeling uncertainty starts.

The information model can describe the topology[4] of uncertainty sources. Then the topology and instantiated values are numerically expressed in data models of simulation tools. While behaviors and properties of an uncertainty may be encapsulated in an information model that can be shared by different simulation tools, quantifying uncertainty relies on how the data model of an individual simulation tool numerically implements the data according to its tool-specific proprietary set-ups and programs. For instance, in the information model, "uncertainty in convective heat transfer between surfaces and air" is one of heat transfer properties of a zone (e.g.,

---

[4] Topology is defined as mechanism of connectivity or adjacency of uncertainty sources that determines spatial relationships in an information model.

Zone::Surface::Convective heat transfer coefficient). Some simulation tools allow declaring the internal convective heat transfer coefficient in a comprehensive manner for generic surfaces. However, TRNSYS declares internal heat transfer coefficients separately depending on its applicable surface types (e.g. Zone::Ceiling::Convective heat transfer coefficient).

Uncertainties inscribed in mathematical models are mainly about simulation algorithm and numerical uncertainty. Algorithms and discretization methods are typically selected during the configuration of simulation environment. However, in many cases, few options are available and tuning them is not allowed to general users. Hence, quantifying uncertainties in mathematical models will not be discussed in this study.

3.4.4 Model-based systems engineering to support modeling uncertainty

It has been known that the unified modeling language (UML) is a standardized general-purpose information modeling language to support graphical modeling of software-centric systems. However, it is unlikely that a single UML will be able to model in sufficient detail a large number of system aspects addressed by domain-specific models such as uncertainty analysis (Paredis and Johnson 2008). Also it is not fully equipped with the functionality to interpret the information model, combine it with tool-specific simulation information and generate simulation codes at the level of data and mathematical model required by domain-specific simulation language.

The systems modeling language (SysML) standard in model-based system engineering (Fisher 1998), would take on those roles, and thus a resulting composite of system models written in SysML would constitute a well-formatted BES model that can be readily available for performance-based designs and quantitative analysis.

Model-based systems engineering (MBSE) is the formalized application of modeling to support system requirements, design, analysis, verification and validation activities beginning in the conceptual design phase and continuing throughout

development and later life cycle phases (INCOSE 2004). SysML offers two noteworthy improvements over UML, specifically relevant to model uncertainty. They include (SysML Forum 2009 and Paredis, Bernard et al. 2010):

a. Two new diagrams, i.e., requirement and parametric diagrams, expands the scope of system models. The former can be used to capture text requirements in the model, and enable them to be linked to other parts of the model, such that it provides unambiguous traceability between the requirement and system design. The latter provides the bridge between the system descriptive model in SysML and other simulation and engineering analysis models (i.e., data and mathematical model), and thus enables the performance analysis that supports uncertainty analysis.

b. In parametric diagrams of SysML, the syntax and semantics of the behavioral descriptions are left open to be integrated with other simulation and analysis tools. The expressive constructs of SysML model management support an execution of behavioral descriptions by means of implementing models, view and viewpoints to facilitate the integration.

Concerning the heuristic uncertainty, recall that heuristic uncertainties can be prevented through clear guidelines, normative procedures or use of standard tools in the process of model preparation and development (Section 2.9). Using SysML to construct BES models apparently helps to eliminate ambiguities when defining the system requirements, system boundary, model structure and model resolution. Therefore use of SysML is expected to alleviate a majority of issues caused from heuristic uncertainty.

Using SysML in order to describe uncertainty and quantify uncertainty requires integration between SysML and BES tools. The integration inherently involves a standardized bi-directional transformation between descriptive models in the SysML and

analysis models in the BES. The next section will discuss transformation requirements, transformation processes and specifications broadly from a general engineering aspect and closely from an aspect of describing uncertainty focusing the four requirements described in section 3.3.

3.4.5 Transformation requirements and specifications for integrating SysML with BES tools

This study conforms to a general framework of transformation in SysML-Modelica (Paredis et al., 2010). Modelica (Modelica Association 2010) is chosen as an analysis model for this framework, whereas this study chooses TRNSYS for an analysis model.

As Figure 3.1 depicts, the transformation starts from specifying an extension to SysML called the SysML4TRNSYS profile that represents the most common constructs of TRNSYS components. This profile allows SysML to express the relevant concepts of TRNSYS and thus enables the mapping between SysML and TRNSYS. The SysML-TRNSYS mapping is then specified between the SysML4TRNSYS profile constructs and the TRSNSYS constructs as captured in the TRNSYS meta-model. Framing the SysML4TRNSYS profile simplifies the transformation to TRNSYS and leverages model the reuse of existing TRNSYS model libraries for users' convenience. The user can create the system model that he/she would like to analyze using a SysML modeling tool. The user then selects particular subsystems to be analyzed by TRNSYS and applies the SysML4TRNSYS profile to create an analytical representation of that subsystem (i.e., SysML4TRNSYS AnalyticalModel). Meanwhile the SysML model tool needs to include such profiles. The AnalyticalModel expressed in the SysML4TRNSYS profile is then transformed to a TRNSYS model that will be executed by the TRNSYS simulation solver.

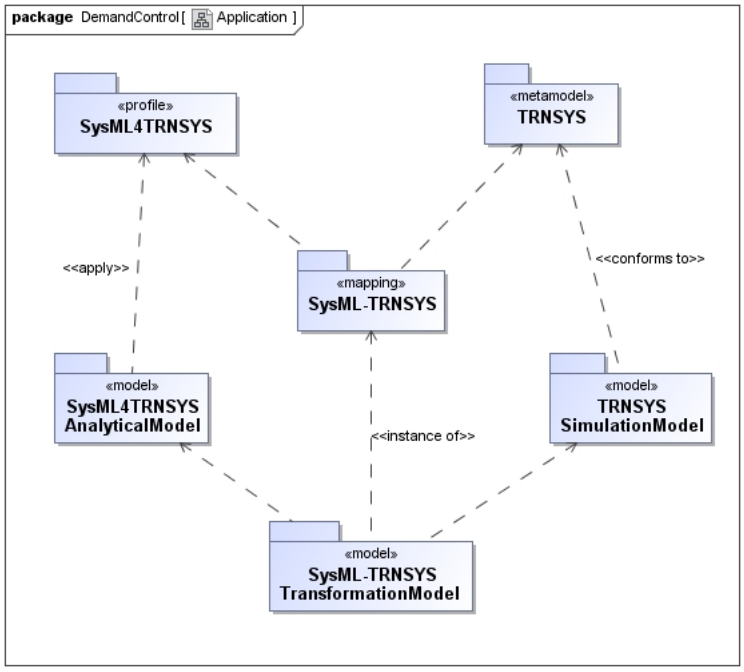

Figure 3.1 The SysML-TRNSYS transformation modified from (Paredis et al.,2010)

The SysML-TRNSYS transformation specification elicits conceptual requirements and processes of the mapping between TRNSYS and SysML. However implementing the SysML-TRNSYS transformation requires another layer of a set of models represents the transformation specification. This implementation models also follow the general framework suggested by (Paredis et al., 2010). In addition, it focuses on technical specifications of modeling uncertainty for an engineering application of building energy performance assessments.

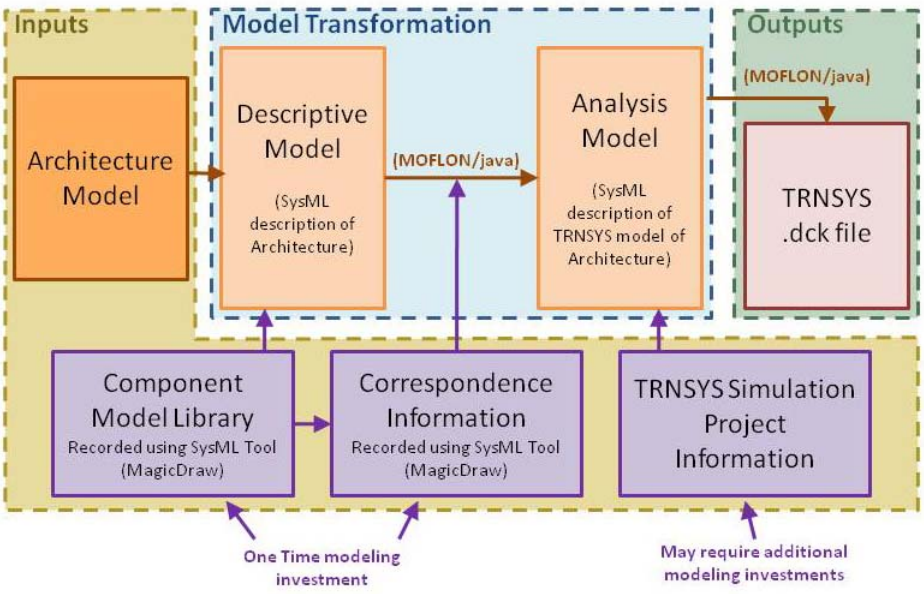

Figure 3.2 Implementation of the SysML-TRNSYS transformation (Lee 2010)

Figure 3.2 illustrates the implementation process of the model transformation from an architecture model to corresponding TRNSYS simulation code. Here the architecture model is high-level and conceptual and thus it contains a set of devices and connections between them schematically. Details of primary sub-models and constituent information will be introduced next.

3.4.5.1 Descriptive model

A descriptive model is a SysML description of the architecture model. To represent the descriptive model, internal block diagrams (IBD) in conjunction with block definition diagrams (BDD) are used to express system structural decompositions and interconnections between their parts (called blocks).

In the descriptive model, all devices (i.e. blocks) are connected via “port”. Typically two kinds of ports are described: flow Ports and standard Ports. The standard ports are geared towards service-based interactions by representing the interfaces provided or required by a particular block. The flow ports describe interaction points

through which input and/or output of items such as data, material, or energy flow in and out of a block (Paredis and Johnson 2008). For interactions occurring in BES, flow ports could be further detailed as either signals (for actuation and reaction quantities) or energy/mass (for flow and non-flow quantities).

Definitions and usages of "port" in the descriptive model support the claim that the model resolution that supervisory controls require corresponds to that of the descriptive model (Section 1.4), because supervisory control determines its control strategies in terms of i) operation mode, ii) operation sequence and iii) control set-points of individual components. These three types of supervisory control variables prescribe which flow ports will be used and how much of the interaction should be modeled.

As an example, Figure 3.3 illustrates a descriptive model to develop supervisory robust demand-side controls chosen for the case study (Chapter 5). All devices or components are connected via ports. When a port connects two devices, a specific part property in one device is connected to a corresponding part property in the other device while they share the same type (i.e., interface) indicating types of port. Notations of causal inputs and outputs in ports are currently missing. However, this issue has been already submitted requesting the modification of causality specification of SysML standards (Paredis et al., 2010).

While many parameters characterize a device, only the parameters of devices relevant to describing uncertainty for this study are chosen and displayed as part properties. For instance, Figure 3.4 and 3.5 depict SysML models of a fan coil unit, pump, interior zone and its supervisory controls. There are many other part properties and value types that characterize the relation and behavior of an FCU and its controls. However, only a part property called "electricPowerConsumptionTolerance" that specifies an allowed varying uncertainty range of power consumption of a FCU is selected and displayed for the purpose of describing uncertainty. Representation and

quantification of uncertainty within descriptive models will be further explained in section 3.5.1.

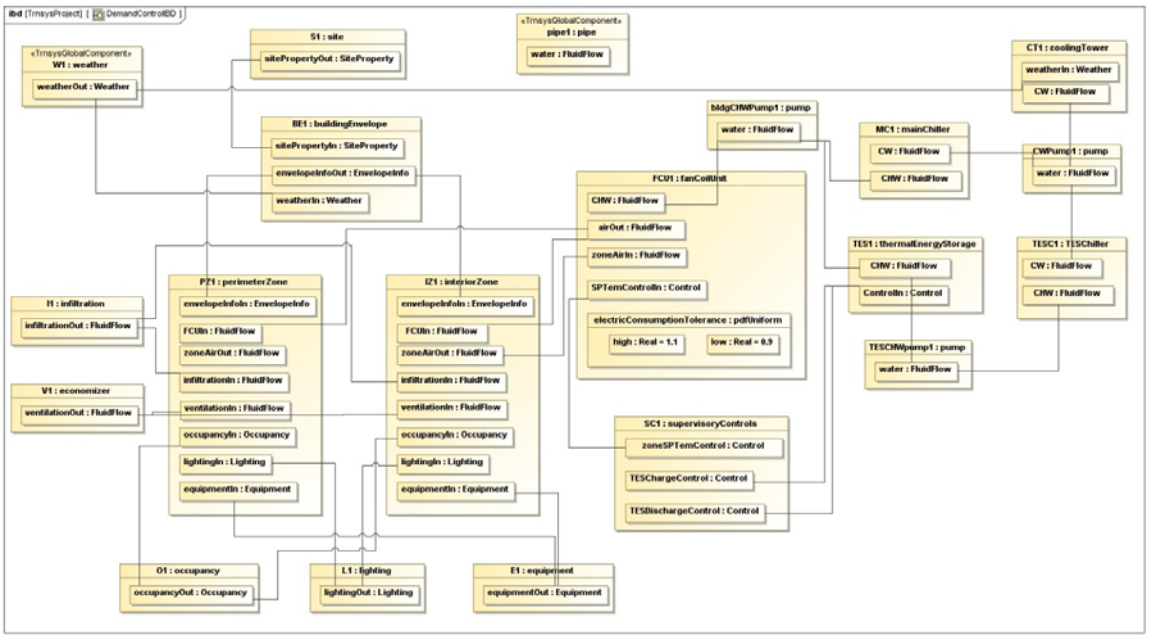

Figure 3.3 The descriptive model of supervisory robust demand-side controls for the case study of the Acme building

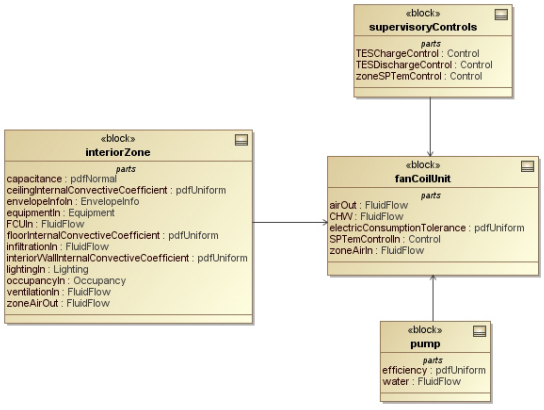

Figure 3.4 The Block definition diagram (BDD) for fan coil unit and controls

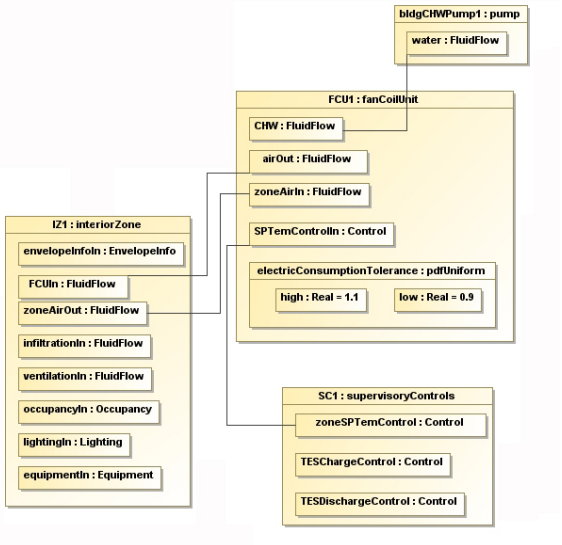

Figure 3.5 The Internal block diagram (IBD) for fan coil unit and controls

3.4.5.2 Analysis model

An analysis model is a SysML description of the TRNSYS simulation model of the architecture model, which is developed via compositions of TRNSYS components and equations defined in the component model library as the correspondence information directs. This unitary module of compositions thus corresponds to a device and its behavior as in defined in the descriptive model.

The analysis model resides in memory buffer of computers collecting all of the information, such as architecture-specific instance parameter values of devices, which are required to build a TRNSYS simulation model. Once all information is collected, it is written in neutral files (e.g., XMI) and eventually converted into a TRNSYS simulation code, i.e., a dck file. In this process third party tools such as Java or MOFLON interpret the information and compile data streams.

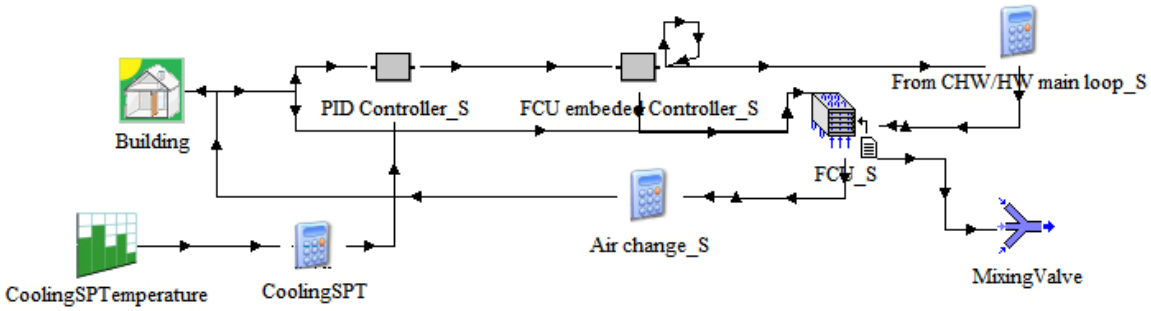

Figure 3.6 Visualization of an analysis model for a FCU1 and its control

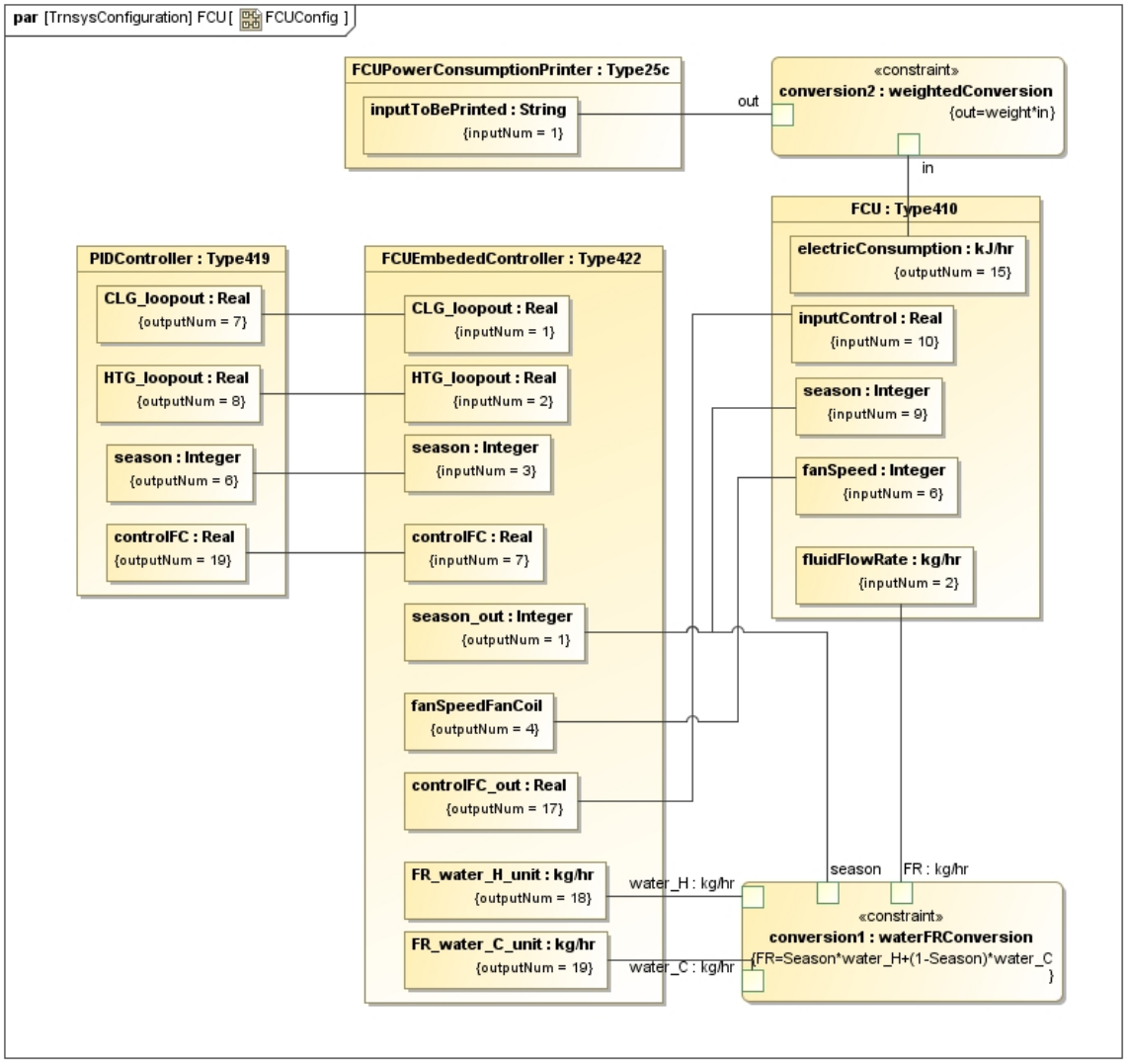

Figure 3.7 Configuration of an FCU having corresponding TRNSYS components and equations

Figure 3.6 illustrates an analysis model for FCU1 and its controls that expresses the same behavior and relations as FCU1 in the descriptive model (Figure 3.4 and 3.5). One can notice apparent differences such as that FCU1 in the descriptive model is a single block whereas FCU1 in the analysis model contains multiple TRNSYS components (e.g. PID controller, embedded controller, FCU, equations and peripheral devices) as depicted in the configuration of an FCU (Figure 3.7).

This difference originates from different usages and purposes between the descriptive model and the analysis model. While the descriptive model describes control flows for supervisory controls, the analysis model describes control flows for local controls. For instance, the supervisory controls set a zone set-point temperature and it is delivered to the FCU (FCU1 and SC1 in the descriptive model, Figure 3.5). Then the FCU modulates its fan speed (FCU::fanSpeed in the analysis model, Figure 3.7) to meet the given set-point temperature of a zone where the FCU is located. In a closer detail, the PID controller sends actuation signals to FCU embedded controller according to the given fan speed. Then the FCU embedded controller modulates the degree of valve opening to control flow rate of chilled water.

This cascading control flow from supervisory controls to local controls is closely related to the uncertainty in model resolution (section 2.8.1.4), thus whether model resolution uncertainty is introduced can be clearly identified when one develops constructs an association between a component in the descriptive model and corresponding sub-components in the analysis model (i.e., correspondence information).

3.4.5.3 Correspondence information

Correspondence information explicitly defines how to transform the descriptive model into the analysis model. Therefore the correspondence information should be aware of the structural configurations of both the descriptive model and the analysis model. In details it requires the following from each model:

- Definitions of properties (mainly part and value) of blocks in the descriptive model with their default values
- Definitions of variables (mainly parameter and input) of TRNSYS components with their default values

- Correspondences defining associations between the properties of blocks in the descriptive model and the variables of TRNSYS components
- Conversion logic that defines correspondences if the correspondence is not based on one-to-one mapping

While the analysis model (Figure 3.7) shows how an FCU in the descriptive model can be composed of a configuration of TRNSYS components and equations, the correspondence information (Figure 3.8) illustrates how each port of an FCU in the descriptive model (e.g. airOut, CHW, SPTemControlIn and zoneAirIn) can be mapped to correspondence variables of the TRNSYS components. In particular, a constraint "getUniformMean1" in the bottom of Figure 3.8 is an example of the conversion logic (in the above 4th bullet point) that decides a value of "weight" that is multiplied to the power consumption of FCU with the basis of its uncertain range.

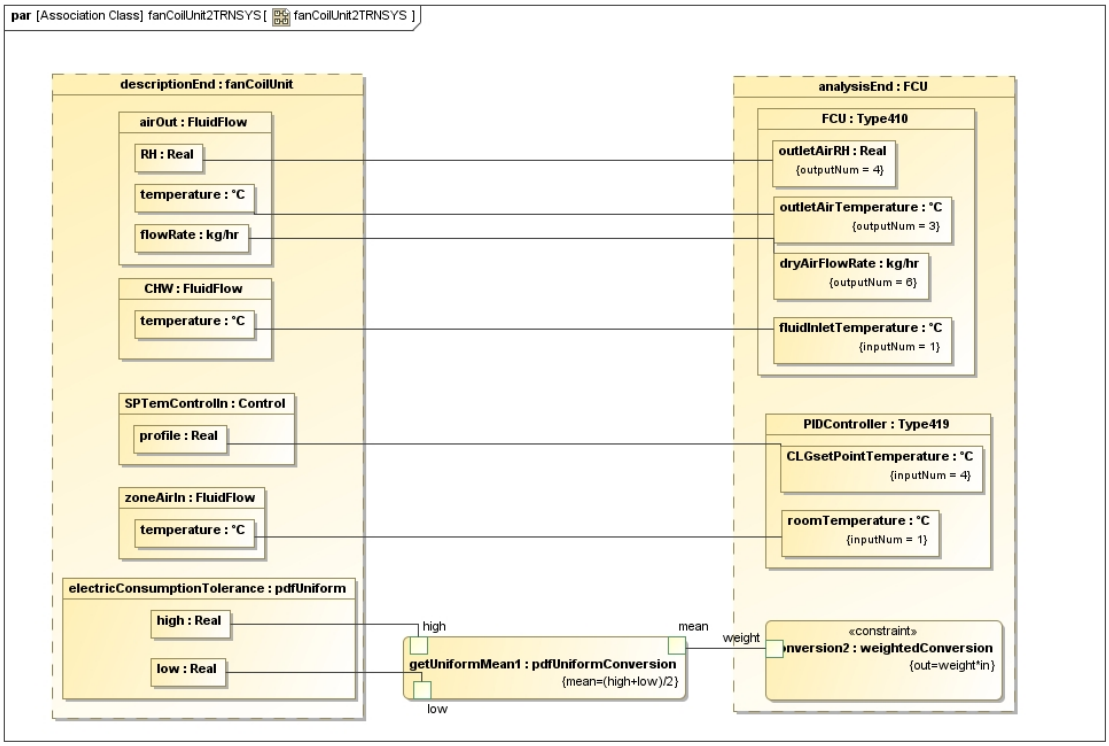

Figure 3.8 The correspondence rule mapping a FCU and TRNSYS configuration of a FCU

3.4.5.4 Component model library and TRNSYS simulation project information

A set of TRNSYS component models is reusable and can be used to develop more devices. Also, devices in the descriptive model can be reused to develop more architecture models. Those TRNSYS component models and descriptive components can be defined and stored in model libraries of a SysML modeling tool, e.g., MagicDraw. Initially building up such library requires some effort, but this is typically a onetime investment.

TRNSYS simulation project information contains the general information needed to set up a simulation environment. This typically includes time step, simulation time, types of solver and algorithm, tolerance and logging options.

3.5 Representation of uncertainty

This section discusses how to describe and quantify physical uncertainty within the BES model, assuming that the issues by heuristic uncertainties are taken care of during system boundary and modeling method definition.

The representation of uncertainty must convey a well-defined operational definition of its metric in a well-defined mathematical format (Aughenbaugh 2006). Here an operational definition can be interpreted as a measured quantity under a given problem. Uncertainty in the measured quantity should have a variable range since they cannot be determined precisely.

One fulfilling method for representing uncertainty, and the most common method as well is the probability theory. As well as its widespread use in engineering design, a large number of building and HVAC&R simulation studies choose probabilistic representations in the mathematical modeling of uncertainty (Macdonald 2002).

The next sections introduce representations of physical uncertainties classified according to their two groupings: statistical uncertainty and scenario uncertainty (Section 2.9).

3.5.1 Probability density function (pdf) that represents statistical uncertainty

A probability distribution function (pdf) is often used to mathematically represent uncertainty. Macdonald (2002) reviewed a few types of pdfs that are commonly used in uncertainty studies in the domain of building and HVAC&R simulation. Four frequently referred pdfs include:

a. Uniform distribution (Figure 3.10) as an example

$$f(x) = \begin{cases} \frac{1}{b-a} & \text{for } a \le x \le b, \\ 0 & \text{for } x < a \text{ or } x > b \end{cases} \tag{3.10}$$

b. Normal distribution (Figure 3.9) as an example

$$f(x) = \frac{1}{\sqrt{2\pi\sigma^2}} e^{-\frac{(x-\mu)^2}{2\sigma^2}}, \tag{3.11}$$

c. Triangular distribution

$$f(x|a,b,c) = \begin{cases} \frac{2(x-a)}{(b-a)(c-a)} & \text{for } a \le x \le c \\ \frac{2(b-x)}{(b-a)(b-c)} & \text{for } c \le x \le b \\ 0 & \text{otherwise} \end{cases} \tag{3.12}$$

d. Log-normal distribution

$$f_X(x;\mu,\sigma) = \frac{1}{x\sigma\sqrt{2\pi}} e^{-\frac{(\ln x-\mu)^2}{2\sigma^2}}, \quad x > 0 \tag{3.13}$$

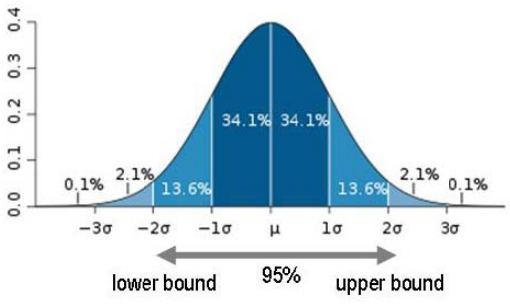

Figure 3.9 95% of normal distribution

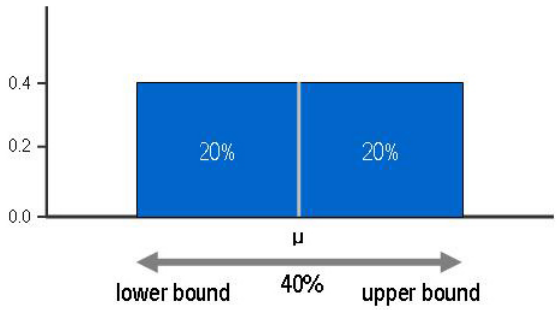

Figure 3.10 40% of uniform distribution

Unfortunately, it is not feasible to suggest a comprehensive guideline to pick one (prior) pdf that is suitable for a specific uncertainty source, because probability representation needs to account for both imprecise and unpredictable uncertainty. There

is no way to distinguish which characteristics of uncertainty leads to the resultant probability distribution. This means that even though the number of samples increases, the impact of unpredictable uncertainty may get weaker over the probability distribution using large samples. Therefore there is no chance that initially fixed distribution type transforms to another one, which assumed to be closer to a true distribution.

It seems to be more reasonable to set an imprecise definition of a pdf when it is initially chosen, for example $0.3 \leq P(a \leq X \leq b) \leq 0.4$, instead of $P(a \leq X \leq b) = 0.35$. This drawback of existing probability representation of uncertainty results in a formulization of imprecise probabilities (Walley 1991). A solution and its application for generic engineering design are fully illustrated in (Aughenbaugh 2006). Thereby this study follows existing literature with respect to a selection of a pdf for statistical uncertainty source.

3.5.2 Probability mass function (pmf) that represents scenario uncertainty

Impacts by scenario uncertainty primarily originate from weather and building usage scenario, due to their larger sensitivity on building energy and thermal performance (de Wit 2002, de Wilde and Rafiq et al. 2008, Hyun and Park et al. 2008).

Like other uncertainty sources, scenario uncertainty also has both imprecise and unpredictable characteristics. Its imprecision uncertainty seems to be resolvable, for example, as in Henze's finding that very simple short-term weather prediction models are able to accomplish the theoretical potential of optimal control strategy of both thermal inventories (i.e., a complex weather prediction model is not necessary) (Henze et al. 2004). Unfortunately, however, the unpredictable characteristic could be more problematic than we thought, and may be an imminent and urgent issue in the endeavor to enhance the performance of robust controls.

Although unpredictable uncertainty cannot be avoided, the detrimental impacts of unpredictable uncertainty can be mitigated by incorporating more data sources. Introducing streams of possible data to represent scenario uncertainty causes the imprecision uncertainty increase while unpredictable uncertainty decreases. Figure 3.11 illustrates a schematic of this concept. The maximum uncertainty would not change, but imprecision uncertainty will replace the portion of the alleviated unpredictable uncertainty.

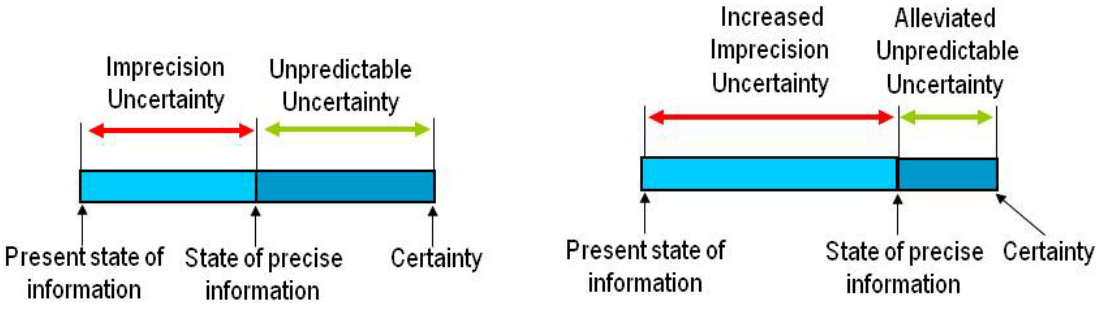

Figure 3.11 Adding more data sources of scenario uncertainty is able to alleviate unpredictable characteristic. However, its imprecision characteristic is extended.

Representing scenario uncertainty is conceptually similar to representing other imprecise uncertainty (e.g., probabilistic measures such as mean and deviation), but it is different in that it is composed of discretely distinguished and multiple series of events. If mathematically defined, it is a three-dimentional vector (Figure 3.12), whose third axis indicates different types of data series (i.e., multiple profiles of ambient temperatures that vary with time). Since a series of events is independent, it is more appropriate to represent them with a set of individual time-series profiles. Probability mass function (pmf) then describes a probability that certain discrete time-series profiles will occur. For example, a set of scenarios Σ has a pmf in which probabilities of three occurring scenarios $\{\varsigma_1, \varsigma_2, \varsigma_3\}$ as illustrated in Equation (3.14-1) and (3.14-2).

$$f_{\Sigma}(x) = \Pr(\Sigma = x) = \Pr(\{\, s \in S : \Sigma(s) = x \,\}) \qquad \Sigma : S \to R \qquad (3.14\text{-}1)$$

$$f_{\Sigma}(x) = \begin{Bmatrix} 0.25 & x \in \{\varsigma_1\} \\ 0.5 & x \in \{\varsigma_2\} \\ 0.25 & x \in \{\varsigma_3\} \end{Bmatrix} \qquad \Sigma \in \{\varsigma_1, \dots, \varsigma_n\} \qquad (3.14\text{-}2)$$

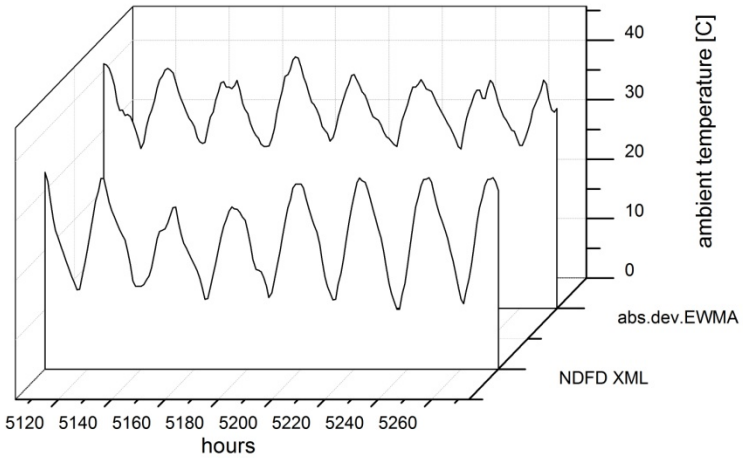

Figure 3.12 Representing scenario uncertainty with two weather profiles (NDFD XML and abs.dev.EWMA from chapter 5)

3.6 Describing uncertainty within the BES model

In chapter 2, physical uncertainty sources for developing robust supervisory demand-side controls are identified. They are mainly divided into statistical uncertainty and scenario uncertainty. This section focuses on describing physical uncertainties in a right position and a right way within the BES models, primarily considering quantifications.

Also uncertainties located in the context of a problem compilation and the system model, i.e., heuristic uncertainty, will be specially treated as an attention-requiring informative guide when choosing system boundary and modeling method for the simulation model.

3.6.1 Indentifying heuristic uncertainty in the problem context and model structure

Recall that the heuristic uncertainty, located in the context of a problem compilation and the model structure will appear when architecture models and simulation tools are chosen for a given simulation scope and objectives. This implies that when an analyst generates architecture models and then he/she designs corresponding descriptive models and device configurations (Section 3.4), she/he would need to answer for the following questions in order to recognize whether heuristic uncertainty could be present.

- Do you clearly understand the issues to be addressed and their possible solutions according to simulation objective?
- Did you choose simulation scope, boundary conditions and scenarios that are adequately framed for the simulation objective?
- Is the mechanism of the chosen simulation model able to deliver solutions to meet the simulation objective?
- Are the model structure and model resolution sufficient to resolve issues and to result in meaningful solutions?
- Or won't the model structure and model resolution be overly detailed so that the simulation takes outrageous time and resources?
- When two components with different resolutions are put together, won't proxy components (i.e., to level off resolutions) introduce new interpretation uncertainty that does not exist in reality?
- Regardless of a component model realized analytically or empirically, is uncertainty introduced by this component model within a reasonable and reliable range?

If any unnecessary ambiguity is found when answering the above questions, one must reexamine their decisions (and decision variables) about problem framing and architecture selection.

3.6.2 Describing statistical uncertainty

Based on the previous analysis (Section 2.8 and 2.9), major locations of statistical uncertainty are classified into “system data” and “calibrated parameters”. Statistical uncertainty residing in the system data can be described with a pdf and corresponding probabilistic measures that are prescribed in the *part properties of a device* in the descriptive model. Statistical uncertainty residing in the calibrated parameters can be described with the probabilistic description as well, but that is prescribed in part *properties of a port* in the descriptive model.

As an example, Figure 3.13 illustrates two distinct examples of describing statistical uncertainty in the system data (as in the part property of a device) and in the calibrated parameters (as in the part property of a port). Electric consumption of an FCU, capacitance of an interior zone and efficiency of a pump are identified as primary uncertainty sources for energy performance (Section 2.8.1.1). These uncertainties can be represented by means of a pdf (e.g. uniform distribution or normal distribution), thus parametric values for such probabilistic measures (e.g. mean, bottom/ceiling) are prescribed in part properties of each device.

Only two ports (“airOut” from FCU1 to IZ1 and “zoneAirOut” from IZ1 to FCU1) are displayed in order to focus on describing calibration uncertainty. A role of port “airOut” is to deliver the conditioned air from an FCU to a space (e.g., an interior zone), and the range of air flow rate is within [90%, 110%] of the nominal flow rate (Section 2.8.2 and Appendix B). The amount of air to be conditioned is delivered to an FCU via port “zoneAirOut”. A thermocouple embedded in the FCU has a hysteresis ranging as [97%, 103%] of its nominal reading (Section 2.8.2 and Appendix B). Since these two ports are causal, describing uncertainty must be done only in one side.

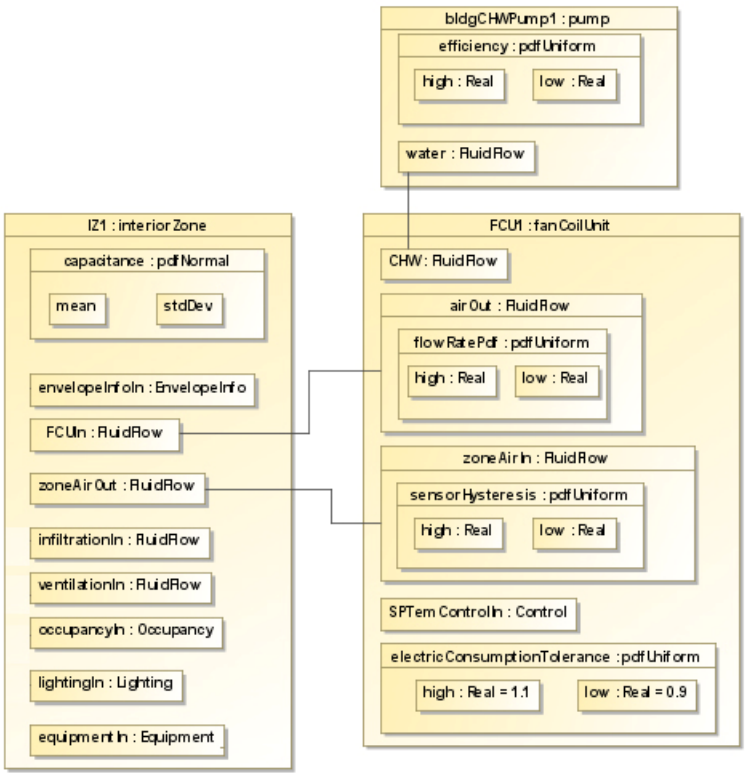

Figure 3.13 Descriptive models of FCU1, IZ1 and bldgCHWPump1 emphasizing on part properties of airOut and zoneAirIn ports

3.6.3 Describing scenario uncertainty

Sources that cause scenario uncertainty are largely classified into i) number of occupants specified in the building usage scenario as an origin of different internal heat gain levels and ii) different types of short-term weather predictions. Due to their strong impacts on building thermal physics and interactions with HVAC&R systems, components containing directly relevant profiles (e.g., weather, occupancy, lighting and equipment), scenario-dependent building components (e.g., ventilation, infiltration) and HVAC&R system devices (e.g. thermal energy storage or air handling unit) may need to be chosen appropriately depending on the chosen scenario. If models of such building components and HVAC&R system devices are robustly designed and thus behave stably

regardless of varying scenarios (i.e., with negligible model realism uncertainty), then they may not need to be replaced.

SysML offers a capability to describe scenario uncertainty and to support different architectures upon changing scenarios. One can lay-out multiple scenarios and the related requirements by means of explicitly expressing them in the Activity diagram as featured in Figure 3.14. Therein a specific scenario (e.g., weather profile #1 and medium occupancy: W1MO) can be drawn as illustrated in Figure 3.15. Figure 3.16 shows one possible descriptive model of the case study in the scenario W1MO. It should be noted that supervisory controls (SC1) would have different control strategies upon scenarios. This issue will be more discussed in Chapter 7.

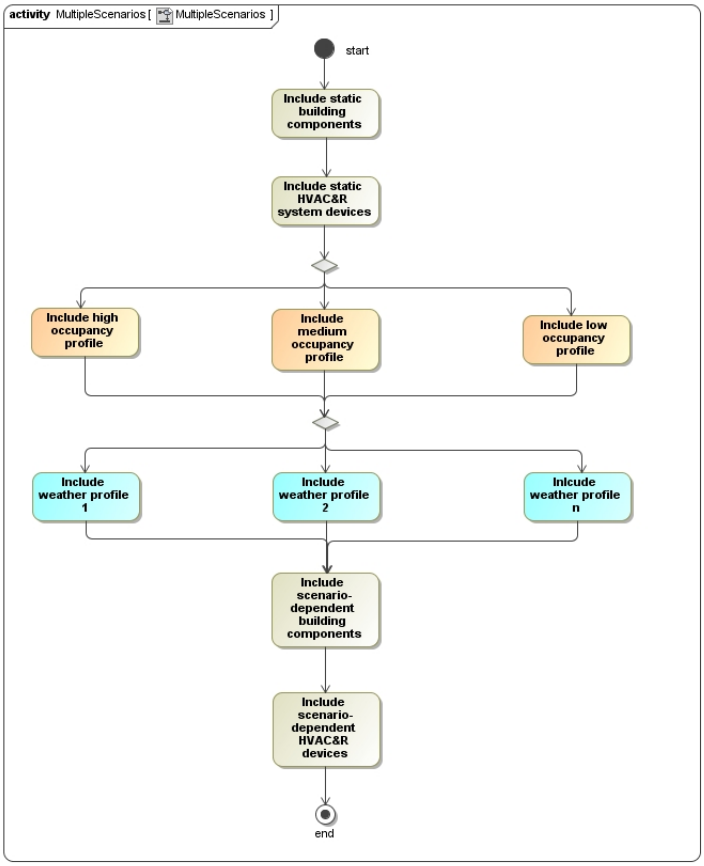

Figure 3.14 Activity diagram to generate specific scenario

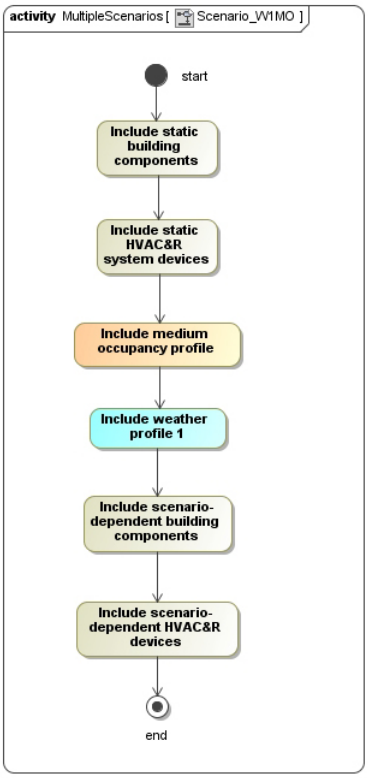

Figure 3.15 Activity diagram of the scenario W1MO

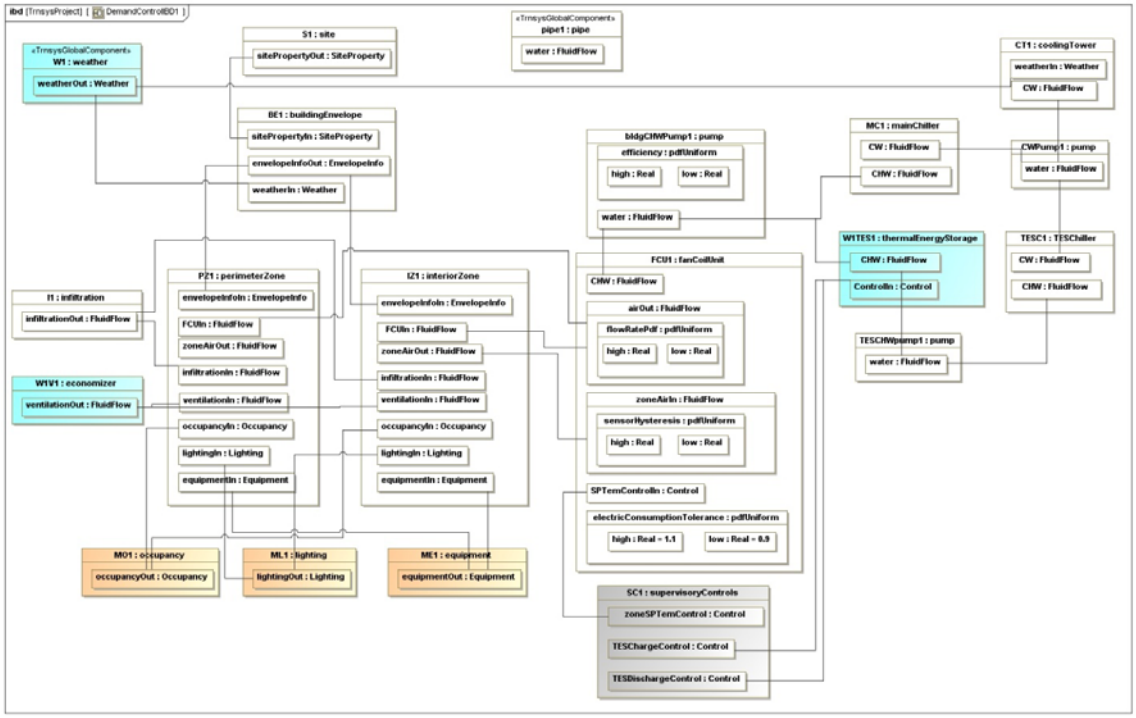

Figure 3.16 The descriptive model having the same architecture with Figure 3.3 in the scenario W1MO

3.7 Quantification of uncertainty

Section 3.6 discusses methods of describing uncertainty with respect to BES models. The architecture and descriptive models contain the information describing uncertainty. Quantifying uncertainty, however, requires another dimension when describing uncertainty needs to be implemented. In general quantification methods of uncertainty is related to how they will be represented in the analysis models of the BES. This section therein firstly discusses choosing an adequate general procedure to quantify uncertainty.

A general robust MPC problem defines three methods to describe uncertainty (Section 3.2.2). Recall that: they include i) uncertainty in system input, ii) system feed-back uncertainty, and iii) Multi-system G and polytopic uncertainty. Describing uncertainty in such general framework can be adopted and implemented as a general rule for quantifying uncertainty for robust supervisory MPC. However since a general rule

can easily make exceptions when it is applied in a specific problem, concerns and constraints about quantifying uncertainty particularly for the BES are as follows.

a. Among three methods of describing uncertainty for general robust controls, quantifying uncertainty in the system input is often effective only when certain preconditions and constraints met (Bemporad and Morari 1999). Thus only two other quantification approaches (structured feedback uncertainty and Multi-system G and Polytopic uncertainty) will be chosen in this study.
b. Quantification of uncertainty depends on types and sources of uncertainty, and so it should follow principles of how uncertainty is defined and described as characterizations of uncertainties that the uncertainty matrix guides (Section 2.9)
c. Since a statistical sampling approach is used to evaluate the system model during optimization (refer to section 4.4.2.6), a quantification process should be seamless with a statistical sampling approach.

These three constraints imply that there should not be a simple and flat case to declare that, for instance uncertainty "A" should be quantified in "α" way. Instead of this "typing" way of quantification, a set of general quantification rules by which the chosen BES tool and associated tools (such as CASE tools) can quantify uncertainty more comprehensively for characteristics of the uncertainty and more easily for implementations should be more applicable. This leads to three general quantification methods as below. Figure 3.17 depicts a procedure of quantifying uncertainty in TRNSYS simulation model and associated uncertainty quantification tools.

a. Statistical sampling (via Latin Hypercube Sampling) to quantify specification uncertainty

b. Scenario robust optimization (via ModelCenter®) to quantify scenario uncertainty

c. Bias and random noise filters attached to the system output (via TRSNSY components) to quantify calibration uncertainty

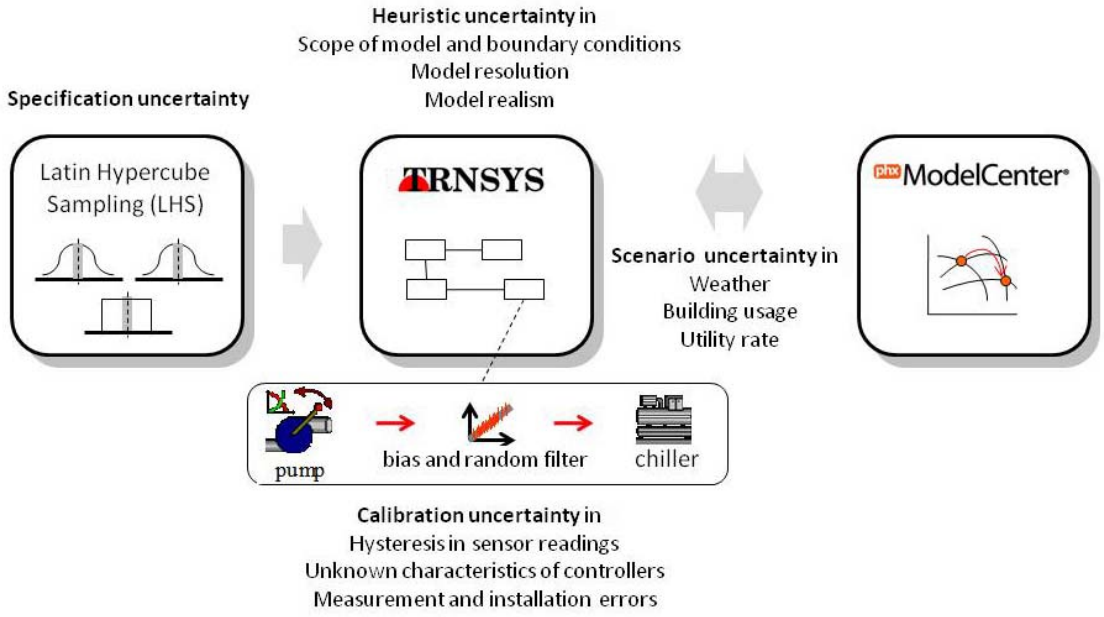

Figure 3.17 A procedure of quantifying uncertainty in the TRNSYS simulation model and associated uncertainty quantification tools

3.7.1 Latin hypercube sampling (LHS) to quantify specification uncertainty

One distinguished feature of the specification uncertainty is that it matches Multi-system G and polytopic uncertainty defined in the general robust MPC problem. This fact indicates that there will be varied versions of true system g when this uncertainty is quantified. This relationship is conceptualized in Equation (3.15).

$$G \in \{g_1, \ldots, g_n\} \tag{3.15}$$

A statistical sampling of the associated uncertain specification parameters is an effective method to represent multiple versions of true system g. A statistical sampling

method chosen in this study is the Latin Hypercube Sampling (LHS), which is a variant of the Monte Carlo techniques (Wyss and Jorgensen 1998). The way this sampling works is that the range of probable values for each uncertain parameter is divided into ordered segments of equal probability. Thus the whole parameter space that consists of all uncertain parameters is partitioned into cells with equal probability. And the LHS samples are in an efficient manner in that each parameter is sampled once from each of its possible segments.

LHS is commonly used to reduce the number of runs necessary for a standard Monte-Carlo simulation to achieve a reasonably accurate random distribution (Vose 1996). Typically 4k/3, where k is the number of input parameters, is recommended for the minimum number of samplings (Iman and Helton 1985). Instead of such fixed finite number of samples, however, this study will use a method to choose the number of samples that can ensure a quality distribution of samples. This will be described in section 4.4.2.5.

3.7.2 Scenario robust optimization to quantify scenario uncertainty

Scenario robust optimization shares the same concept on scenario-based descriptions of problem data in the robust goal programming. When parameters are known or effective only within the certain bounds that one scenario specifies, the fact that probability distributions governing the data are known or can be estimated becomes applicable. A goal of the scenario-robust optimization is then to find a solution that is feasible for all the possible data realized in potentially feasible and significant scenarios. Then it generates a series of solutions that are progressively less sensitive to any realization of the model data from a set of scenarios with minimal loss.

3.7.2.1 Mathematical formulation of the scenario robust optimization

To emphasize the relation between model data (i.e. variables) and uncertainty under different scenarios, the general robust control problem (Equation 3.3) can be paraphrased as

Minimize $\sigma(x, u_1, \dots, u_\sigma) + \omega p(w_1, \dots, w_\sigma)$ (3.16)

Subject to : $Ax = b$

$B_\varsigma x + C_\varsigma u_\varsigma + w_\varsigma = e_\varsigma$ For all $\varsigma \in \Sigma$

where A,b,B,C and e are constant.

a. Scenario ς

A set of scenarios Σ is introduced. Probability that a scenario ς occurs is defined p_ς and $\sum_{\varsigma=1}^{\Sigma} p_\varsigma = 1$. Set of realizations for the coefficients of the control constraints $\{ B_\varsigma, C_\varsigma, e_\varsigma \}$ is associated with each scenario ς.

b. Design variable x and control variable u

Design variables are static and free of noise in their inputs, and control variables are subject to vary such that their dynamics influence the performance of the system. Correlation between these two components defines an appropriate model of the system in an optimization problem. Robust values of control variables depend both on the uncertainty imposed over the control variable and the pre-specified design variable.

$x \in R^n$, denotes a design variable whose value is not conditioned on the uncertain factors that exist in the problem. Design variables cannot be adjusted once a specific realization of the data is observed. Equation (3.16) illustrates this relation.

$u \in R^n$, denotes a control variable whose value is subject to adjustment when uncertain factors (w) are observed in the problem.

c. Optimization objective σ and penalty p

In the scenario robust optimization, the general objective function $c^T x + d^T u$ (c and d are constant) becomes a random variable taking the value $c^T x + d_\varsigma^T u_\varsigma$ with probability p_ς. Hence, the aggregated objectives are no longer single choice. To apply this, for example, we can use the mean value $\sigma(x,u) = \sum_{\varsigma\in\Sigma} p_\varsigma(c^T x + d_\varsigma^T u_\varsigma)$. The second term $p(w_1, , w_\varsigma)$ is a feasibility penalty function. It is used to penalize violations of the control constraints under some scenarios.

To explain significances of optimization objective σ and penalty p in the scenario robust optimization problem, two robustness terms should be characterized. These features make themselves differentiated from general optimization problems and traditional stochastic linear problems (Mulvey and Vanderbei 1995).

Solution robust: The optimal solution of the linear programming will be robust with respect to optimality, if it remains **close** to optimal for any realization of the scenario $\varsigma\in\Sigma$. This is usually formulated as optimization objective in stochastic linear optimization problems. The first term (σ) measures this robustness. When there is only one scenario, this corresponds to optimization objective in general deterministic optimization problems.

Model robust: The solution is robust with respect to feasibility, if it remains **almost feasible** for any realization of the scenario $\varsigma\in\Sigma$. Control variables are no longer constant for each scenario. Thus a vector of control variables $\{u_1, \dots , u_\varsigma\}$ for each scenario $\varsigma\in\Sigma$, and hence a set $\{w_1, \dots , w_\varsigma\}$ of uncertainty vectors that measure the infeasibility allowed in the control constraints under scenario ς are introduced into the scenario-robust optimization problem. The penalty term (p) is a measure of this robustness. The weight (ω) is used to derive a tradeoff solution for model robustness.

3.7.3 Implementation of quantifying specification and scenario uncertainty within the TRNSYS model

Quantification of both specification uncertainty and scenario uncertainty results in n x m instances of simulation models where a set of system model $G \in \{g_1, \ldots, g_n\}$ and a set of scenarios $\Sigma \in \{\varsigma_1, \ldots, \varsigma_m\}$. Quantification of these permutations is doable, but cumbersome in terms of management, if only mundane simulation and optimization tools have to be used. It is because these permutations typically involve a parallel expansion of simulations due to an increased volume of data. In addition to that, scenario uncertainty should be quantified in an objective function of the optimization that is typically beyond scope of the simulation model. Thus a "middleware" approach between the simulation model and the optimization engine becomes indispensible.

A role of middleware in engineering designs is to support process integration and design automation, thus it manages all processes of simulation experiments [5]and specifically facilitates a connection between the simulation model and the optimization solver. Since these experiments basically require a high volume and horizontally extended computations for running many instances of the entire simulation model, e.g., optimization, the middleware should well equip with management capability for high volume data and the resulting side-processes and analysis. Hence it is a sound engineering approach to utilize the middleware for quantifying both specification uncertainty and scenario uncertainty. This study chooses ModelCenter® to run robust optimizations, details of which will be introduced in section 4.4.3.

A procedure of quantifying uncertainty in the above permutations using ModelCenter® is briefly summarized as three steps:

---

[5] Several relevant exemplary experiments include trade studies, Design-of-experiment (DOE), Response surface modeling (RSM) and etc.

a. For a set of simulation model G^{ς} each of which takes one scenario ς, n x m instances of system model G^{ς} are prepared.

$$G^{\varsigma} \in \{ g_1^{\varsigma}, \dots, g_n^{\varsigma} \} \qquad \text{For all } \varsigma \in \Sigma \text{ , i.e., } \Sigma \in \{ \varsigma_1, \dots, \varsigma_m \} \qquad (3.17)$$

b. G^{ς} is described in ModelCenter and a vector of control variables commonly shared among all instances are assigned to individual simulation model g^{ς}.

c. An objection function shared by all simulation models is defined according to a principle of the scenario robust optimization.

3.7.4 Bias and random modulation filters of TRNSYS to quantify calibration uncertainty

Bias and random modulation filters imitate a signal of a system response or output that is within an uncertain range. They can be applied to sensors (e.g. to quantify a hysteresis) and controllers (e.g. to quantify a dead-band) as well as system components.

According to ASHRAE Guideline 14 (ASHRAE 2002), simulation models are declared to be calibrated if they produce normalized mean bias error (NMB) within ±10% and root mean square error (CV-RMSE) within ±30% when using hourly data. Likewise ASHRAE Guideline 14 that stipulates calibration accuracy in terms of NMB and CV-RMSE, a signal varying within a bounded range can be represented as biased and/or random. Modulation filters, therefore, can be built as the same way that replicates NMB and CV-RMSE in TRNSYS as Figure 3.18 and 3.19 depict.

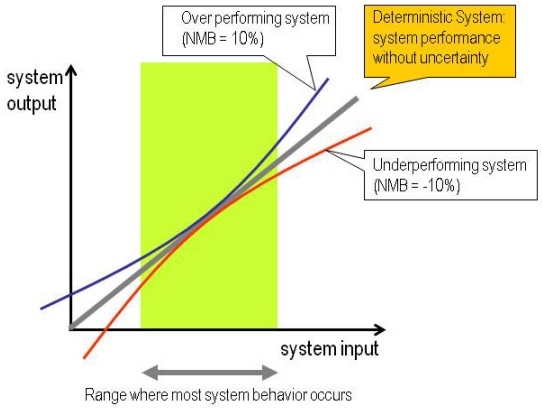

Figure 3.18 Biased system output

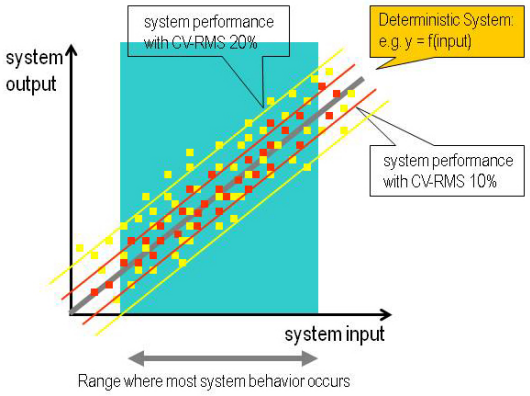

Figure3.19 Random system output

For instance Figure 3.19 illustrates behavior of a random filter attached to airflow output of a FCU and thermocouple. “Randomness” can be adjusted by changing tolerance. It should be noted that this range must be reasonably large, not to bring about control or simulation stability issues. If so, for example a modulation filter having range of ±20% attached to an air output of FCU causes a failure of simulation due to diverging solutions, the LHS could replace the modulation filter as an alternative quantification approach.

3.8 Summary and conclusions

This chapter proposes a new methodology to model uncertainty within functional models of software architecture of the building energy simulation (BES). Distinguished features of this methodology from the conventional methodology include:

a. Description and quantification of uncertainty for robust supervisory controls should fulfill definition and behavior of uncertainties. From a perspective of implementation of modeling uncertainty, this methodology suggests locating them at appropriate levels & structure of BES tools and associated uncertainty quantification tools in order to make this goal feasible.

b. Employment of SysML and SysML-TRNSY transformation framework offers a systemized and complete line of the process from initial problem framing to seamless and faster deployment to model uncertainty for various domain-specific needs such as uncertainty analysis.

CHAPTER 4

DEVELOPMENT OF A ROBUST SUPERVISORY DEMAND-SIDE CONTROL STRATEGY

4.1 Introduction and motivations

While chapter 2 and 3 discuss about the robust MPC and modeling uncertainty, respectively, this chapter takes its focus back to a development of robust "supervisory demand-side" control strategy. This chapter emphasizes:

a. Investigations of demand-side control measures, and their applicability and controllability in the context of the robust supervisory demand-side control
b. A general methodology to develop robust supervisory demand-side control strategy as a final deliverable of this study

Energy storage is a stable and effective demand-side control measure. Two representative methods for controlling energy storage include i) passive building thermal mass controls and ii) active mechanical Thermal energy storage (TES) controls. This chapter reviews the existing modeling and control approaches of those two measures, which are featured in the deterministic MPC frame. After that it will suggest customized and enhanced approaches that consider "uncertainty" for the development of robust supervisory demand-side controls using those two energy storage measures.

A relaxed assumption for uncertainty employed in robust control poses conceptually and structurally different development approaches from the conventional deterministic optimal controls (section 3.2.2). This chapter introduces a general step-by-step procedure with the accompanying technical issues and their resolution.

4.2 Passive demand side control based on the building thermal mass control

4.2.1 Building thermal mass control by modulating set-point temperature trajectories

In many commercial buildings, structural mass embodies a substantial thermal storage capacitance that can be harnessed to reduce operating costs with utility rate incentives. Achievable objectives of the demand-side controls via building thermal mass include i) flattening load by means of pre-cooling and ii) reduced power demand, i.e., load shedding. In general, building thermal mass control is attainted by manipulating the zone air temperature set-point. Thus building operators can employ the supervisory control strategy to shift cooling-related thermal loads to inexpensive off-peak hours, while keeping monthly electrical demand limited and sufficiently flat.

There is a long history of studies about thermal mass controls. Several significant works that enhance designs of thermal mass control models are summarized below.

4.2.2 Existing studies of building thermal mass controls

Several simulation and experimental studies (Braun 1990; Ruud, Mitchell et al. 1990; Conniff 1991) have shown that a pre-cooling control strategy can result in operating cost savings due to peak demand reduction. Morris, Braun et al. (1994) proposed a detailed modeling approach which involving optimizing 24 independent variables for hourly set-point temperature. Keeney and Braun (1996) approximated the optimal solution using only two variables. Recently Henze, Brandemuehl et al. (2007) used building modes defined by the on-set period of utility peak hours and occupancy schedule. They showed that a three building mode case is only slightly suboptimal compared to the 24 hour based full building mode solution.

Braun and Lee (2006 and 2008) developed an optimal demand-limiting strategy using an exponential trajectory of the zone set-point temperature based on a first-order analytical model. They proved its superior demand-limiting performance over conventional linear-rising and step-rising trajectories.

4.2.3 Design of building thermal mass control models

The set-point temperature critically contributes to occupants' thermal comfort. Also, a change of the set-point temperature can sensitively change the building thermal load, which eventually largely impacts the operating cost. Therefore building thermal mass control via set-point temperature modulation has different characteristics at different times of the day depending on occupancy, and a possibility of reducing building load.

An optimization problem in building thermal mass controls via set-point temperature is proved to be solved effectively by means of a basic direct search optimization algorithm with boundary constraints, between upper and lower zone temperatures. In this case, however, since an optimization process involves a huge number of function calls, simplifying the optimization problem is desirable.

Instead of having N slots of set-point temperature (i.e. $N = 24/\Delta t$) per day, a combination of set-point temperature profiles per significant control mode in the context of the time-of-use (TOU) plan would reduce the complexity of the control problem.

4.2.4 Building control modes

Four significant building control modes are identified based on occupancy schedule and peak hours defined by the utility rate difference (i.e. TOU). For a typical weekday, four modes include:

a. Unoccupied and off-peak (mode 1)

b. Occupied and off-peak (mode 2)

c. Occupied and on-peak (mode 3)

d. Unoccupied and on-peak (mode 4)

Since diverse TOU rate plans are available from utility providers, a combination of the above control modes relies on the selected TOU plan. Figure 4.1 depicts a typical combination.

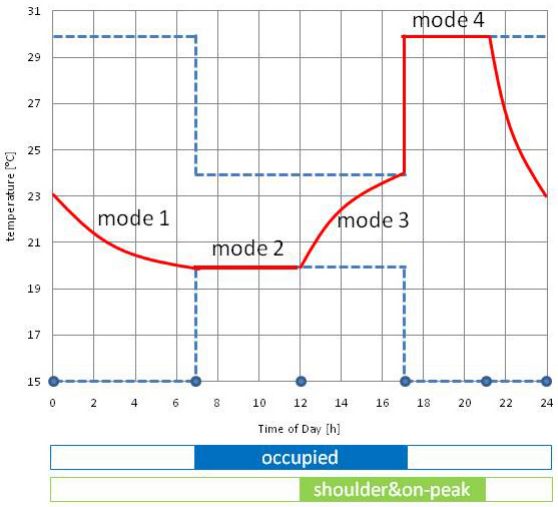

Figure 4.1 An example of a combination of building control modes having different thermal roles

Summarized from existing practices, the first two modes (mode 1 and mode 2) are pre-cooling phases before the on-peak period. At mode 2, pre-cooling temperature cannot be lower than the bottom of the comfort temperature limit as it may not secure thermal comfort for occupants. Typically a demand-limiting control strategy (Section 4.2.5) is applied at mode 3, which pursues a lower and more even cooling load while ensuring thermal comfort. Mode 4 is a phase where the set-point temperature must float up as there is no need for air-conditioning the unoccupied space given the higher utility rate.

A control strategy for each mode can be prefixed according to its role and thermal interactions with the prior and post modes. In spite of such complications, guided optimization simplifies the optimization problem for set-point temperature trajectories for

each mode while meeting the same objective as well as providing a sufficient degrees-of-freedom for optimization. Optimization using (semi) preset analytical guides is a common and sound approach, and is more efficient than optimization based on exhaustive searches. Guided optimization typically pursues a near-optimal strategy initiated with preset constraints and setup parameters.

Appropriate guided optimization approaches for each mode are suggested for this study. They include:

a. Exponentially decreasing set-point pre-cooling (EDPC) for mode 1,
b. Constant set-point pre-cooling for mode 2,
c. Demand-limiting set-point release (DMR) (Lee and Braun 2006) for mode 3 and
d. Constant set-point release for mode 4

Analytical functions involved in the DMR and the EDPC will be explained first, and descriptions on the constant set-point pre-cooling and constant set-point release will follow.

4.2.5 Demand-limiting set-point release (DMR) for mode3

Using a controlled release of the stored thermal energy allows the flattening of demand during on-peak period by adjusting the set-point temperature along an exponential trajectory from the pre-cooling temperature (T_{pc}) up to the upper comfort bound (T_{up}). Lee and Braun (2006) developed this analytical model (Equation 4.1) based on a first-order response model assuming constant thermal loads during on-peak period. A release of thermal energy is dependent on a discharge time constant τ, thus τ becomes a control variable at mode 3.

$$\frac{T_u - T_{pc}}{T_{up} - T_{pc}} = \frac{1 - \exp(-\frac{t}{\tau})}{1 - \exp(-\frac{t_{mode3}}{\tau})} \tag{4.1}$$

where T_u , T_{pc} , T_{up} denote the set-point temperature, the pre-cooling temperature at mode 2 and the upper comfort bound temperature, respectively (blue dotted in Figure 4.1). t denotes the time measured from the start of mode 3 while t_{mode3} is the duration of mode 3.

4.2.6 Exponentially decreasing set-point pre-cooling (EDPC) for mode1

The analytical formulation of the DMR provides the basis for developing exponentially decreasing set-point pre-cooling (EDPC) since the same control principle can be applied to pre-cool the thermal mass during mode 1. It is motivated by the fact that a typical step-down set-point temperature assignment results in a spike of cooling load (Figure 4.2) when it abruptly drops to the pre-cooling temperature. However the EDPC smoothes the cooling load profile as shown in Figure 4.3.

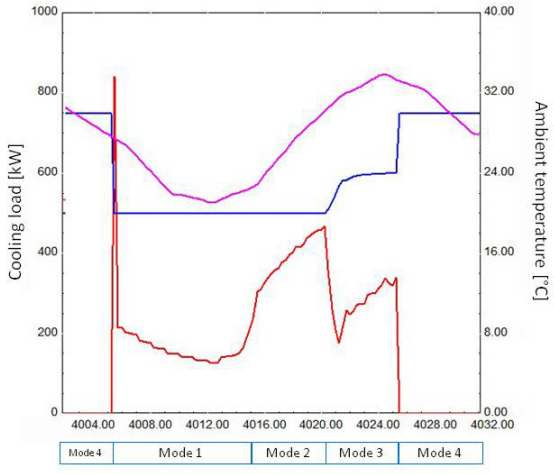

Figure 4.2 A step-down set-point temperature (the blue solid) results in a spike of cooling load (the red solid) when starting pre-cooling

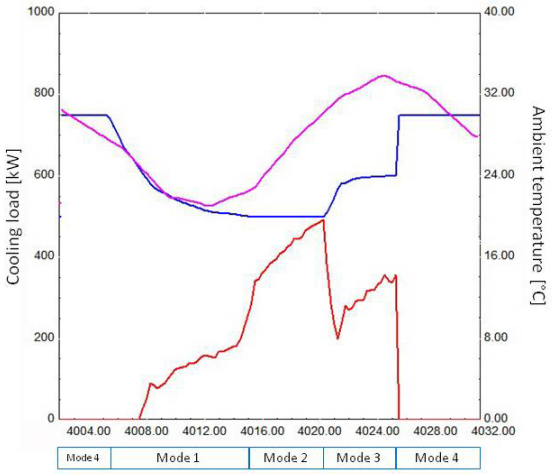

Figure 4.3 The EDPC at mode 1 smoothes the pre-cooling load profile (the red solid). The purple line indicates the ambient temperature.

The typical step-down set-point temperature assignment is not desired since i) it results in a sudden coil load to mechanical plants since it suddenly breaks up their thermal inertia as shown in Figure 4.2 and ii) thus a full amount of the initial cooling potential may not be stored in the thermal mass. Since a gradual "stack-up" of the cooling potential makes the thermal mass hold more cooling effect, a step-down set-point temperature assignment eventually results in a lower efficiency when the stored cooling effect is released.

An analytical model of the EDPD has been formulated via taking the inverse of the DMR as described in Equation (4.2) and (4.3):

$$\frac{T_u - T_{pc}}{T_{release} - T_{pc}} = \frac{\exp(-\frac{t}{\tau}) - \exp(-\frac{t_{mode1}}{\tau})}{1 - \exp(-\frac{t_{mode1}}{\tau})} \tag{4.2}$$

$$T_{bottom.mode1} \leq T_{pc} \; and \; T_{release} \leq T_{ceiling.mode1} \tag{4.3}$$

Here the same denotes of the demand-limiting set-point release are used. Additionally $T_{bottom.mode1}$ and $T_{ceiling.mode1}$ denotes the bottom and the ceiling temperature constraints at mode 1, respectively. $T_{release}$ is defined as the release temperature at mode 4 and T_{pc} is defined as the pre-cooling temperature at mode 2. Also it should be noted that the identical time constant τ of the DMR is used since the same building thermal mass of the DMR is involved, i.e. the same thermal characteristics.

4.2.7 Constant set-point pre-cooling for mode 2 and constant set-point release for mode 4

Sensitivity analysis of the optimal building thermal mass control (Henze, Brandemuehl et al. 2007) reported that i) the longer on-peak period, the greater the degree of pre-cooling is necessary, thus resulting in the more cost-savings and ii) a

favorable ratio of the cooling potential inventory in the building mass to the daily cumulative cooling load leads to the largest savings via pre-cooling. These two observations imply that both the optimal duration of pre-cooling and the pre-cooling temperature depends on the daily cumulated cooling load and other thermal factors.

Along with the constant pre-cooling set-point temperature T_{pc} during mode 2, therefore, one more optimization variable ($t_{pc.start}$) is introduced to give another degree-of-freedom for optimizing the pre-cooling duration. $t_{pc.start}$ denotes the start time of pre-cooling which must be earlier or the same time with the time when the mode 2 starts (i.e., $t_{pc.start} \leq t_{mode2.start}$). If $t_{pc.start}$ starts sooner, the cooling potnetial stored in the thermal mass is held longer. Then the constant set-point pre-cooling at mode 2 will "hold-back" the stored cooling potnetial toward mode 3.

At mode 4 as air-conditioning the unoccupied space is not necessary the set-point temperature must be released to $T_{release}$.

4.3 Active demand-side control based on thermal energy storage (TES) controls

Figure 4.4 illustrates the operation of chilled water storage, i.e., thermal energy storage (TES), a mechanical storage system provides an opportunity to reduce the operating cost of cooling plants by storing cooling potential when power cost is cheaper (i.e., load shifting). Ice storage and chilled water storage are popular technologies; however other cooling media can be applied.

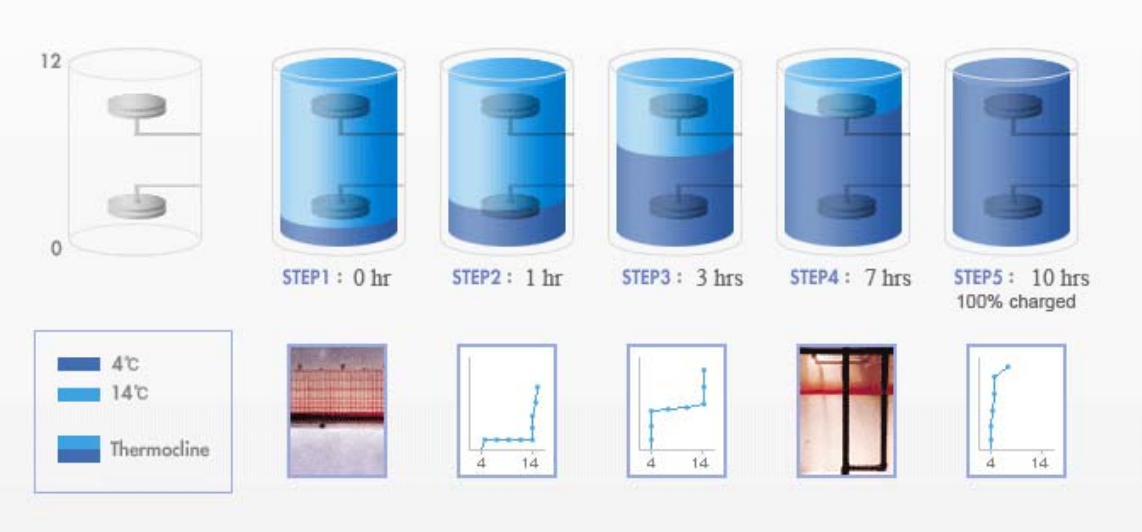

Figure 4.4 Operation of the chilled water TES

Since the principle of operation is similar for each cooling media, a common control strategy can be applied. There are distinct three types of conventional TES control strategies: chiller priority control, storage priority control, and (near) optimal control. The first two are rule-based control strategies while the last is developed based on a typical supervisory MPC problem. Therefore an investigation of the (deterministic) optimal control for the TES will suggest a clue of how a control model for TES should be designed for robust MPC. First of all, two heuristic TES controls are reviewed.

4.3.1 Chiller priority control

Chiller-priority control is the most common strategy employed for TES. With this strategy, the chiller operates to meet the building load if the cooling capacity is sufficient. If the chiller capacity is not enough, then TES becomes active to meet the difference. Recharging TES begins at the earliest possible time after the end of on-peak period, which is the time the building is unoccupied. The chiller operates at maximum capacity and completely recharges the TES.

The primary advantage of the chiller-priority control is simplicity. There is no need for load measurements or forecasting, and also there is no concern of running out of storage if the TES is sized properly. The least risk is anticipated, yet only relatively small operating cost savings are expected.

4.3.2 Storage priority control

Storage priority control aims at fully discharging the available storage capacity during on-peak period. The main chiller is base loaded during on-peak hours and operates at reduced capacity in parallel with the storage so that at the end of on-peak period, the stored cooling energy is almost depleted.

The main advantage of the storage-priority control is the largest possible demand shifting resulting in the largest operation cost savings. This is attained by restricting the main chiller not to operate at full capacity at any point during on-peak hours. Therefore the main disadvantage is a risk of running out of the stored cooling energy immaturely.

4.3.3 Optimal controls and its existing studies

The greater cost-saving benefit, yet higher risks due to uncertainty in load forecasting with storage-priority control motivates the development of optimal control. As implied, a general objective of (deterministic) optimal control is to obtain the least operating cost through forecasting and optimization. To do this, a flexible control strategy concordant with the building's highly dynamic environment (e.g., weather conditions, cooling loads and utility plans) needs to be devised. A few important existing studies are highlighted to illustrate their approaches to accomplish this need.

Henze and his group (1997, 1999, 2003, 2005, 2007, and 2008) have fertilized and deepened a great level of knowledge and detail for model-based optimal control.

Within a dynamic environment, model-based optimal control strategy minimizes the total electricity cost that combines energy cost (TOU) and demand charges. Dynamic environment includes uncertainties in weather, building loads and utility rate plans. To account for such variability, prediction models for those three factors are also developed. Uncertainty models for those three factors are used to test the robustness of the model-based optimal control. They concluded that their solution shows outstanding control performance compared to conventional control strategies, even when one hour-ahead real time pricing (RTP) is chosen.

Braun (2007) developed a simple supervisory algorithm that provides near-optimal control of the cool storage systems with RTP rates and evaluated its performance in relation to both optimal control and a conventional strategy. In contrast with optimal MPC, the near-optimal control switches operations between storage priority control and chiller priority control, based upon economics and availability of storage. His strategy prevents the premature depletion of storage through load forecasting. Compared to the optimal MPC, merits of the near-optimal control strategy include relatively low-cost measurement, very little plant-specific information, computational simplicity and satisfaction of the building cooling requirement.

There are common requirements and control measures for supervisory MPCs of the TES that many existing studies refer to. This study takes an advantage of the existing methods, and then improves them to suit them in the robust MPC framework.

4.3.4 Design of TES control models

To achieve an active demand-side control using the TES, two chillers are typically necessary: one is the main chiller serving the building cooling load and the other is the dedicated TES chiller that only serves to charge for the TES. Thus the TES chiller works only during TES charging. This independent and separated chiller architecture

design gives two benefits: i) the reduced on-peak load via operating the TES offers a chance to reduce size of the main chiller, ands extending the optimal operation time of the main chiller, leading to the reduced operation cost, ii) A change of design of system architecture becomes easier, in particular when TES is in a retrofit option.

Since the TES serves the building thermal load only during a limited period, the main chiller serves the rest of the load. The main chiller also could be used as a back-up chiller if the cooling capacity of TES is not sufficient. Figure 4.5 depicts this relationship. Here, $CAP_{main.chiller}$, $CAP_{TES.chiller}$ and CAP_{TES} denote the rate capacities of each plant, respectively. $\dot{Q}_{main.chiller}$, $\dot{Q}_{TEScharge}$ and $\dot{Q}_{TESdischarge}$ denote the thermal loads between plants.

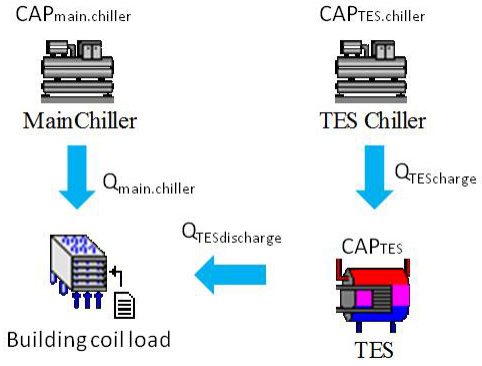

Figure 4.5 Cooling load is served by main chiller and TES

The principle of operating TES for demand-side control is simple: to spare the chilled (or iced) medium in the TES during the least expensive period of the day and to release it during the most expensive period of the day. Therefore control variables include i) the charging flow rate from the TES chiller to the TES and ii) the discharging flow rate from the TES to the building load at time step k, symbolized as C_k^u and D_k^u, respectively. And they are subject to own constraints:

$$0 \leq C_k^u \leq C_{max} \quad (4.4)$$

$$0 \leq D_k^u \leq D_{max} \quad (4.5)$$

where C_{max} and D_{max} denote the maximum charging and discharging flow rates set by physical system constraints, respectively. Charge and discharge rates depend on the available thermal energy storage inventory and the current cooling load. The available energy inventory of the TES at time step k (x_k) is then described as follows.

$$x_{k+1} = x_k + C_k^u \Delta t \quad (4.6)$$

$$x_{k+1} = x_k - D_k^u \Delta t \quad (4.7)$$

$$x_{min} \leq \frac{x_k}{x_{full}} \leq x_{max} \quad (4.8)$$

where x_{full} denotes the maximum volume of the chilled medium that meets the capacity of the TES (CAP_{TES}); x_{min} and x_{max} stand for the minimum % and maximum % of the state-of-charge, respectively. When the state-of-charge approaches to the bottom, a mixing effect accelerates a loss of cooling capacity of the TES. Thus x_{min} is usually set to 10-15%.

4.4 Development of a robust model-based demand side control strategy

A general methodology to develop a robust supervisory demand-side control strategy is introduced in this section. Based on the fundamental study on uncertainty (Chapter 2), investigations about modeling uncertainty within the BES model (Chapter 3) for robust controls, and control models of two demand-side control measures (Section 4.2 and 4.3) this section introduces a step-by-step procedure for the general methodology.

The proposed development methodology that accounts for uncertainty and randomness through simulations and stochastic analysis borrows its concept from robust design optimization (RDO), a probabilistic design analysis and design optimization methodology (McAllister and Simpson, 2003). Thus the motivations and goals that the RDO pursues are firstly reviewed.

4.4.1 Robust design optimization as a baseline methodology

Distinguishing feature of robust design optimization is the use of probability criteria to evaluate the technical system quality. Robust design optimization includes a stochastic problem statement and methods to solve optimization problems. It has common goals that can be generally applied in any robust optimization problem (Egorov, Kretinin et al. 2002). These goals are reorganized and modified to meet the need in the building and HVAC&R control domain as follows:

a. To identify a mechanism of the system that maintains the mean value of the performance under uncertain design, construction and operational conditions of the system;

b. To identify a mechanism of the system that minimizes the variability of the performance under uncertain conditions of the system;

c. To provide the best probability to ensure the preset constraints;

d. To provide the best overall performance over the entire operating ranges of the system;

e. To provide the best overall performance over various external scenarios around the system

A set of standard procedures to develop a general methodology for the RDO is suggested by (Egorov, Kretinin et al. 2002). This is customized to suit the needs of robust supervisory demand-side controls and step of the procedure are presented in section 4.2.

4.4.2 Steps of developing a robust supervisory demand-side control strategy

The development methodology for robust supervisory demand side control is summarized with following steps and individual details are discussed in following sections.

Step 1: State and frame out the problem

Step 2: Identify external prediction scenarios

Step 3: Select stochastic criteria of the performance indicator

Step 4: Identify the main uncertainties affecting the system and their bounds

Step 5: During development of the simulation models, model and quantify uncertainties within the simulation models and supporting tools

Step 6: Perform a sensitivity analysis in order to ease the problem structure and to reduce the computation expenses

Step 7: Design control models and choose adequate control horizons for each control model

Step 8: Formulate cost function and select stochastic optimization method

These steps from 1 to 8 streamline the entire process for developing robust controls. The next steps that are not mentioned in the above standard procedure primarily deal with implementation and deployment for developing the robust control. Their potential issues and solutions that take advantage of advanced computing environment such as computer-aided software engineering (CASE) tools, middleware and cloud computing are envisioned in section 4.4.10 and 4.4.11.

4.4.3 Step 1: State and frame out the problem

Problem statement and framing refers to a prerequisite and preparation step before an actual development of robust supervisory demand-side controls starts. A set of sub-tasks and further details are listed up in the below.

- Set an objective of the demand-side controls. Recall that projects in demand-side controls typically pursue i) a reduced net system load, ii) a reduced (or shifted) on-peak energy demand and/or iii) shaping the demand curve to meet a certain purpose (Section 1.2). This will be a guideline to select performance indices in step 3.

- Survey on site, building and system descriptions, existing operation strategies, building usage scenarios and the other required information to develop simulation models.
- Set a scope of the building and HVAC&R systems and their sub-systems to be controlled.
- Set a scope of control architecture and control variables, keeping in mind that all information for developing control models should consist of all relevant sub-system models, causality and information/data flow. And they should correspond to the actual system architecture that is sufficiently implementable in simulations.
- Acquire the available informative resources that could help enhancing quality of input data such as external information service provider (ISP), weather stations, national databases, and SmartGrid.
- Select simulation tools, i.e., de-facto tools or new development.
- Develop SysML component model libraries and SysML-TRNSY transformation framework.

4.4.4 Step 2: Identify external prediction scenarios

As scenario uncertainty poses critical influences on energy performance of a building, it is very significant to involve many and more realistic scenarios to ensure high control performance in actual field conditions. However it is not easy to achieve this goal primarily for that external scenarios are strongly handled by unpredictable uncertainty. In addition, complex external scenario models may impose more imprecise uncertainties. Also as it will be introduced next, not all scenarios need to be included.

Knowing this limitation, a purpose of this step is to suggest a method in order to at least reasonably assess feasible and implementable scenarios fitted in the robust

controls. A general approach suggested by EPA (1992, 2000), which is specialized for risk and uncertainty analysis, can be characterized as to "purge" and then "compile".

A general guideline for purging non-required scenarios for uncertainty analysis includes: i) scenarios that have very little possibility of happening, ii) scenarios that are likely to result in trivial amount of changes in system response, and iii) scenarios that have inadequate information to perform evaluations. A step of compilation after purging starts with setting up conventional and clear scenarios called "baseline" scenarios. "Alternative" scenarios based on different assumptions or observations should be added to comprehend scenario uncertainty.

a. Building usage scenario

If occupancy level and non-thermal loads have been monitored for long enough periods, the accumulated data could provide a reasonable baseline. If not, a standard occupancy profile and corresponding non-thermal load should be used as a baseline. In addition to that, separated profiles with the lower level (e.g., -20%) or higher level (e.g., +20%) can be added for complementing the baseline scenario. In this case, a probability that each scenario occurs should be specified in order to represent its scenario uncertainty as described in section 3.5.2. It is noted that unless a probability of the occurrence of a scenario is calculated from the historical archive, this process could be inherently arbitrary or depends on heuristics.

b. Weather scenario

As will be described in the literature review of chapter 5, a number of well-performing weather forecast models have been developed. Presence of such well-performing forecast models implies "multiplicity" of the weather scenario, thus a decision should be a choice of the most relevant combinations of weather forecast models. This will be further explained in chapter 5.

c. Utility rate structure

As described in section 2.8.3.3, demand charges at peak power consumptions are assessed depending on weather conditions and energy characteristics of the built environment, and the real-time pricing (RTP) depends on time and the maximum temperature of the day. Even in the same utility plan, therefore, the resulting operation costs will vary with the chosen set of weather scenarios and building usage scenarios; therefore utility rate structure depends on the previous two scenarios.

4.4.5 Step 3: Select stochastic criteria of the performance indicator

Let's denote $PI = J(U, x(t), G, W)$ where J is a cost function of the robust MPC. When solving robust optimization problems, uncertainty terms G and W make the performance index PI stochastic. Thus it is necessary to use probabilistic optimization criteria, $\widetilde{PI}(\hat{U})$, where $\hat{U}$ is a robust control solution to maximize or minimize $\widetilde{PI}(\hat{U})$. Various probabilistic criteria have been developed for general robust optimization problems. In this study, we discuss a few (potentially necessary) probabilistic criteria that could be standard forms with respect to developing robust controls.

a. $\widetilde{PI}(\hat{U}) = E\{J(U, x(t), G, W)\}$ (Expected mean of the performance value)

e.g., Expected mean of cooling load

b. $\widetilde{PI}(\hat{U}) = \sigma\{J(U, x(t), G, W)\}$ (Magnitude of the performance value deviation)

e.g., Deviation of the cooling load from the mean value

c. $\widetilde{PI}(\hat{U}) = Pr\{J(U, x(t), G, W) \leq PI_{preset}\}$ (Probability that the performance value is not worse than the given limit)

e.g., Pr(cooling load ≤ 1500KWh)

d. $Pr\left\{J(U,x(t),G,W) \leq \widetilde{PI}(\widehat{U})\right\} \geq Pr_{preset}$ (Performance value ensured with the probability is not less than the given value)

e.g., The probability that hourly cooling load is less than 300KWh is at least 80% over all occasions

A combination or stand-alone use of the performance indices 3 and/or 4 has been used for risk management criteria. The context about a risk attitude of stakeholders, detailed discussions and applications can be found at (Samson, Reneke et al. 2009) and (Hu 2009).

4.4.4.1 Performance indices to evaluate the robust demand-side controls

As shown above, each criterion reflects different robust aspects of the project. These aspects should match the goal of the demand-side control. To achieve this goal, the first and most fundamental step should be to reduce the power demand.

a. Mean daily power consumption

This is the most basic and bold indicator of the demand-side control. The least mean daily power consumption (Equation 4.9) satisfies the most fundamental need of the demand-side controls.

However, cases that the demand side control results in the least mean daily power consumption but unsatisfactory mean on-peak power consumption are often observed. Thus it is recommended to use additional performance criteria to evaluate multiple spects of the performance of the demand-side control.

$$\tilde{P}_{daily} = E\{P_{daily}(U_{opt}, x(t), G, W)\} = \int_{daily} P(U_{opt}, x(t), g, w) dF(g, w) \qquad (4.9)$$

b. Mean on-peak power consumption and Deviation of the on-peak power consumption

$\tilde{P}_{onpeak}$ indicates that how much of the on-peak power can be reduced or shifted by the demand-side control strategy (Equation 4.10). $\tilde{V}_{onpeak}$ indicates that how much of the potential momentum of the on-peak power is reduced (Equation 4.11). The latter can be used as a penalty term for optimization.

$$\tilde{P}_{onpeak} = E\{P_{onpeak}(U_{opt}, x(t), G, W)\} = \int_{onpeak} P(U_{opt}, x(t), g, w) dF(g, w) \tag{4.10}$$

$$\tilde{V}_{onpeak} = \sigma\{P_{onpeak}(U_{opt}, x(t), G, W)\} = \int_{onpeak} \{P(U_{opt}, x(t), g, w) - \tilde{P}_{onpeak}\}^2 dF(g, w) \tag{4.11}$$

Although the least on-peak power consumption is one of the final goal of the demand side controls (i.e., load shifting), an excessively increased off-peak power consumption to store more cooling energy during off-peak hours, as an adversary return of pushing on the least on-peak power consumption, should be avoided.

A balance between the on-peak and off-peak power consumption should be reserved. Therefore the "value" of the on-peak power consumption with respect to the off-peak power consumption should be assessed. The most useful and popular scale to weigh this value should depend on the market price, in other word, the utility rate.

In general the following performance index, the mean operating cost (i.e., the power consumption multiplied by utility rate) signifies an assessed (monetary) value the on-peak power consumption with respect to the off-peak power consumption.

c. Mean daily operating cost and Deviation of the operating cost

The operating cost is calculated by adding the net power demand plus the power consumed for load shifting, and then the sum is multiplied with the utility rate. This is obviously the most interesting performance indicator for financial stakeholders.

Along with this investment and cost aspect, it makes a balance between the on-peak power consumption and the off-peak power consumed for load shifting during the optimization, eventually in order to not result in unreasonably high off-peak power consumption compared to when the optimizer aims at only the least mean on-peak power consumption. Therefore it is suitable that this performance indicator is also used as an objective function of the optimization. This will be further discussed in section 4.4.10.

$$\tilde{C}_{total} = E\{C_{total}(U_{opt}, x(t), G, W)\} = \int_{daily} C(U_{opt}, x(t), g, w) dF(g, w) \tag{4.12}$$

$$\widetilde{CV}_{total} = \sigma\{C_{total}(U_{opt}, x(t), G, W)\} = \int_{daily} \{C(U_{opt}, x(t), g, w) - \tilde{C}_{total}\}^2 dF(g, w) \tag{4.13}$$

The above mentioned three types of performance indices belong to two basic objectives of the demand-side control; i) to reduce the net demand and ii) load shifting. Other performance criteria to meet the load shaping objective of the demand-side controls could be formulated too. However those performance indices are only necessary to appear on the table when new aspects originated from different environments and contexts need them. For instance, if an on-site renewable power generation is employed such as photovoltaic, matching the power demand profile to fit for the power supply profile is certainly a goal of the demand-side controls. This discussion is not included in the scope of this study, so it will be more discussed in the future tasks.

4.4.6 Step 4: Identify the main uncertainties affecting the system and their bounds

Sources of uncertainty during developing demand-side controls are surveyed and characterized according to the three dimensions in chapter 2. Thus the detail will not be repeated here.

4.4.7 Step 5: During development of the simulation models, model and quantify uncertainties within the simulation models and supporting tools

While developing simulation models based on the surveyed building and system descriptions, the identified uncertainties should be modeled within the simulation model and supporting uncertainty quantification tools. The method to describe and quantify uncertainty has been rigorously reviewed and analyzed in chapter 3, thus the detail will not be repeated here.

4.4.8 Step 6: Perform a sensitivity analysis in order to ease the problem structure and to reduce the computation expenses

When the statistical sampling approach to quantify specification uncertainty is used (e.g., LHS) , the robust optimization could take at least a few times of computation since the optimizer needs to evaluate all samples of the quantified uncertain parameters. Not all uncertain parameters are crucial to determine a robust control solution. Filtering out non-dominant uncertain parameters with respect to the performance of the robust controls will simplify the control model and reduce unnecessary computation expense.

Specifically when quantifying the specification uncertainty, the number of samples directly handles a volume of computation. Since a goal of statistical sampling is to simulate the true distribution F, more efficient way would be to build it with less number of samples. Two statistical methods to achieve this will be introduced.

4.4.8.1 Parameter screening

In a number of previous studies (de Wit 2001; Moon 2005; Hyun and Park 2006; Hu 2009), the elementary effect method suggested by Morris (1991) has shown efficient results in identifying dominant parameters. This method simply calculates an average of derivative of a parameter over the space in which all uncertain factors vary, thus a set of critical uncertain parameters that substantially contributes is chosen according to its rank.

In the elementary effect method, Y denotes the system model with k independent uncertain parameters $X_i(i = 1,..k)$. The parameter space Ψ_i $(=[\underline{\psi_i}, \overline{\psi_i}])$ is discretized into a p-level grid and X_i will vary across p levels. For a given scalar value of $\hat{X}$, the elementary effect of the i^{th} uncertain parameter is defined as in Equation (4.14).

$$EE_i = \frac{Y(X_1, \dots, X_i + \Delta, \dots, X_k) - Y(X_1, \dots, X_i, \dots, X_k)}{\Delta} \qquad (4.14)$$

where Δ denotes a value in $\left\{\frac{1}{p-1}, \dots, 1 - \frac{1}{p-1}\right\}$, p denotes the number of levels, and X denotes a subset of uncertain parameters.

The distribution of elementary effect by X_i (denoted by $f(x_i)$) can be calculated via r number of sampling, and r is defined in Equation (4.15),

$$r = p^{k-1}(p - \Delta(p-1)) \qquad (4.15)$$

The distribution $f(x_i)$ then has μ_i (mean) and σ_i (standard deviation), here μ_i indicates the overall influence of the input X_i on the output EE_i and σ_i estimates the degree of how $f(x_i)$ is dependent on the values of other inputs X (except X_i).

Campolongo, Cariboni et al. (2007) proposed μ_i^* to avoid problematic cases where positive and negative EE_i cancel each other, and thus μ_i^* is defined as the mean of the distribution of the absolute values of the elementary effect, as described in Equation (4.16),

$$\mu_i^* = \frac{1}{r}\sum_{j=1}^{r} |EE_i^j| \quad (4.16)$$

Therefore μ_i*will be used as a rank criterion for parameter screening. Examples will be illustrated on case studies.

A choice of dominant uncertain parameters depends on their ranks. However a choice of the lowest ranked parameter should depend on a combined contribution of the parameters above the lowest ranked one. The lowest ranked parameter can be chosen by heuristics from the rank list, while the combined contribution of the chosen parameters can be verified via comparing i) a variance of the chosen parameters and ii) a variance of the remainders with respect to a variance of the parameter space Ψ. This should be an iterative procedure, if the combined contribution of the chosen parameters cannot meet certain coverage (e.g. 95% of variance of the parameter space Ψ). Readers can find a detailed example from (de Wit 2000) and (Hu 2009).

4.4.8.2 Coefficient of variation (CV) to choose the sampling number to quantify specification uncertainty

Ideally the larger sampling number is the closer to the true distribution F of the parameter space Ψ. However it is more important to find a small sampling number, but that ensures a reasonable accuracy level. A classic way to evaluate the accuracy level of sampling is the coefficient of variation (CV) suggested by Billiton (1994), as described in Equation (4.17),

$$CV = \frac{\sigma}{E[J(U,G,W)]} \quad (4.17)$$

where $E[J(U,G,W)]$ is the expected mean of the system performance, and σ is its standard deviation.

Equation (4.17) indicates that either larger expected mean or smaller variation can enhance the sampling accuracy. Obviously this can be obtained by means of a large number of samplings, thus both metrics will be closer to the true value. However, a critical number of samples after which CV converges should be chosen. This study selects 0.05 of CV as the convergence criterion according to suggestions by (Hu 2009) and (Billiton 1994).

4.4.9 Step 7: Design control models and choose adequate control horizons for each control model

Control models of the passive building thermal mass and the active TES controls were thoroughly investigated previously (Section 4.2 and 4.3), thus this will not be restated in the section.

As shown in designing control models for two demand-side control measures, presetting building control modes greatly reduces the complexity of an optimization problem. The robust control solution for each control mode should be developed for a certain period ahead, which consists of several future control modes. It is called planning horizon (pH). During planning horizon, the thermal state at the last time step of the previous execution horizon becomes an initial state, and then new external information such as weather forecasts and building usage scenarios is introduced. A robust control strategy for the planning horizon is formulated based on all these information. The resulting robust control solution vector can be descritized, and saved as a time-series (e.g. every 15min or 30min). Then the planned robust control strategies are executed for an execution horizon eH. This cyclic process is well depicted in the Figure 4.6.

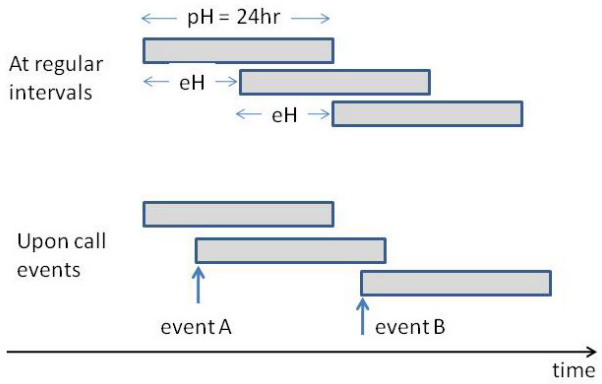

Figure 4.6 Different triggering options of the planned control strategy

As length of the planning horizon becomes extended, uncertainty in external and internal future events becomes more fatal to performance of robust control strategies. Hence there is a trade-off to choose a right planning horizon: apparently a shorter planning horizon containing less uncertainty would work out better, however, it should be long enough to fully account for thermo-dynamic transitions of the building systems to be controlled. For instance, a series of studies by Henze's group (Henze, Felsmann et al. 2004; Henze, Kalz et al. 2005; Henze, Biffar et al. 2008) suggested a 24 hour of planning horizon for model-based control applications in which building mass is involved.

As illustrated in Figure 4.6, the planned control strategy can be executed periodically at regular intervals (Henze 2004), or upon occurrences of significant events (Mahdavi 2001). For the first case, choosing the preset length of the execution horizon would depend on a specific control application. The shorter the execution horizon is, the closer to a real-time application the control solution is. It is because more frequent executions introduce more frequent updates of the current system states and external information, thus it becomes closer to real-time.

However, it should be noted that even with a shorter execution horizon, the planning horizon still need to be long enough. That is because an executed control strategy is always the first part of the optimized result over the entire planning horizon,

i.e. eH ≤ pH, thus the executed control strategy could be unlikely the true optimum if the planning horizon is not long enough to fully capture thermodynamics of the system.

4.4.10 Step 8: Formulate cost function and select stochastic optimization method

4.4.10.1 Formulation of the objective function

Although choosing multiple performance indices to evaluate a variety of performance aspects of the demand side controls is allowed in step3, only single statement should be chosen for the objective function of the optimization. In general operating cost is regarded as an adequate criteria for an objective function of the demand-side controls as it contains both on-peak and off-peak power consumption terms (to represent power demands) and their relative weights (to represent preferences of different types of the power demands), which are typically utility rate differences. Therefore the objective function pursues minimizing such operating cost, and can be formulated as follow:

$$\min_{\widehat{U}} E\{\, J(U, G, W)\,\} \tag{4.18}$$

$$J = \sum_{k=1}^{N} P_{ek}{}^{\varsigma} r_{ek}{}^{\varsigma} \Delta t + \sum_{k=1}^{N} P_{gk}{}^{\varsigma} r_{gk}{}^{\varsigma} + \max_{1\le k\le N}(P_{ek}{}^{\varsigma}) * r_{dN}{}^{\varsigma}$$

For all $\varsigma \in \Sigma$ (4.19)

where Δt is the time interval, and it is typically equal to the time window over which demand charges are levied; N is the number of the time steps in a billing period; r_{ek} is the cost per unit of electrical energy with the time step k ($/kWh); P_{ek} is the total electrical power of the HVAC&R system in the time step k; P_{gk} is the total gas usage in the time step k (therm); r_{gk} is the cost per unit of natural gas usage ($/therm); and r_{dN} is the cost per unit of the max electrical demand over the billing period ($/kW).

This formulation would satisfy overall performance requirements of the demand-side controls. The optimization seeks for a vector of the robust control strategy $\widehat{U}$ that minimizes the mean operating cost over the billing period (e.g. daily or monthly). It is likely to find relatively low on-peak and off-peak power consumption as well; hence it satisfies performance requirements such as reduced net demand, load shifting or both.

Also when renewable power generation is employed, P_{ek} and P_g represents the net power consumptions, i.e. the power demand by equipments minus the power supply by renewable systems. Then under this objective function the optimizer will try to fit both the demand pattern and the supply pattern to each other via varying a control vector U. This effort will eventually result in a higher synchronicity of two profiles in terms of frequency and magnitude, thus it pursues the better load shaping.

It should be noted that optimization is subject to a series of constraints of both control vector U and other variables defined in the system G. In current formulation, balancing weight factor between the on-peak and the off-peak power consumption is confined by the given TOU utility rate; however the balancing weight factor can be altered in order to meet stakeholders' further needs for different balance ratios. For instance, the current utility incentive for off-peak power consumption is too weak, i.e., relatively expensive power rate during off-peak, thus a degree of the load shifting is under satisfaction. Then the weight for the off-peak power consumption can be adjusted as smaller. Since this modification fairly depends on stakeholders' subjective judgments rather than the current market price, it should be taken very carefully not in order to result in unrealistic solutions.

4.4.10.2 Sample average approximation (SAA) with Monte Carlo

Kleywegt and Shaprio (2000) have shown that an analytical trial to solve a stochastic optimization problem (even with the simplest objective function) explicitly

depends on knowledge of the probability distributions of all uncertain factors W. In practice the corresponding cdf F(·) is never known exactly, and thus could be approximated or estimated though sampling method (e.g. Monte Carlo) at best.

According to them, there are several advantages of using the sample average approximation (SAA): i) an occurrence of samples have an equal probability, and ii) no extra sampling effort for stochastic optimization, and iii) samples are independent and identically distributed (i.i.d.).

By restating criteria of the objective function, the SAA using the Monte Carlo facilitates solving a stochastic optimization problem. The chosen objective function, i.e., to minimize the expected mean of operating cost (Equation 4.18) is written as,

$$\widehat{U} = \arg\min_{U_{opt}} E\{C_{op}(U_{opt}, G, W)\} = \arg\min_{U_{opt}} \int_{total} C_{op}(U_{opt}, g, w) dF(g, w) \quad (4.20)$$

When Equation (4.20) is descritized by N uncertainty sets { (g_1,w_1), …., (g_N, w_N) }, the expected mean becomes:

$$E\{C_{op}(U_{opt}, G, W)\} \equiv \frac{1}{N}\sum_{i=1}^{N} C_{op_i}(U_{opt}, g_i, w_i) \quad (4.21)$$

Ideally the larger N is, the closer the solution $\widehat{U_{opt}}$ to the true solution U_{opt} is. A choice of N was discussed in step 6 (Section 4.4.8). Therefore the robust optimization problem can be restated as:

$$\widehat{U_{opt}} = \arg\min_{U_{opt}} E\{C_{op}(U_{opt}, G, W)\} \equiv \arg\min_{U_{opt}} \frac{1}{N}\sum_{i=1}^{N} C_{op_i}(U_{opt}, g_i, w_i) \quad (4.22)$$

Equation (4.22) can be solved in two ways: i) native form to evaluate the objective function exhaustively and ii) response surface model approach (Box and Wilson 1951). The native form includes all N instances of uncertainty sets { (g_1,w_1), ….,

(g_N, w_N) }, and then the optimizer evaluates all N instances at each iteration, thus this approach is more suitable for the case when the number of uncertainty sets N is manageable.

In many cases, however, the number of uncertainty sets N may not be enough manageable for the optimizer to evaluate all N instances at each iteration. One way of alleviating this burden is by constructing approximation models, known as response surface models or surrogate models. The approximation model mimics the behavior of the true model as closely as possible as illustrated in Figure 4.7 while being computationally cheaper during evaluation. It is constructed purely by the data-driven relationships between inputs and outputs, thus it is often called black-box modeling.

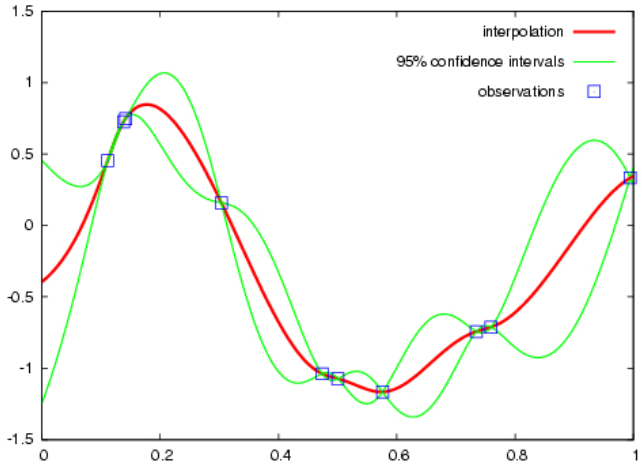

Figure 4.7 An example of the response surface model called Kriging. The Kriging interpolates the observed data points to estimate the value of the unknown real-value function.

In optimization based on the surface response model, an initial model is constructed through simulations by initial samples. Then this model is searched by optimization algorithm. If new locations that can make the surface model closer to the true model during finding the optimum, these locations can be added as new samples, and then the updated model is constructed. This process is iterated until the optimizer finds "good enough" solutions. One drawback is that depending on type of the surface model and complexity of the problem, thus the process may converge on a local optimum than

the global optimum, or neither local nor global optimum. Detailed information can be found at (Jones 2001) and (Gorissen, Couckuyt et al. 2010) that provide a review on theories of the surface response model and a software framework facilitating wider applications in a variety of engineering domains, respectively.

4.4.11 A future step I: implementation of robust supervisory demand-side controls in the energy management system (EMS)

This study limits its scope to the development of the robust supervisory demand-side control strategy, thus this study will not discuss about physical implementation of the control platform. However a broader perspective of implementation to deliver the resulting control strategy to the Energy management system (EMS) can be envisioned as shown in Figure 4.8.

All basic information needed such as current building and system responses (that becomes thermal history), current control states, weather forecasts & real time weather conditions, and grid/supply configuration are monitored and delivered to the EMS. The EMS carries on only necessary information and stored them in its local repository. The EMS calls the robust supervisory control platform at the designed planning horizon intervals, while it hands over the required information to the platform. The platform generates robust control strategies discretized as a time-series data and it is delivered to the EMS for an execution.

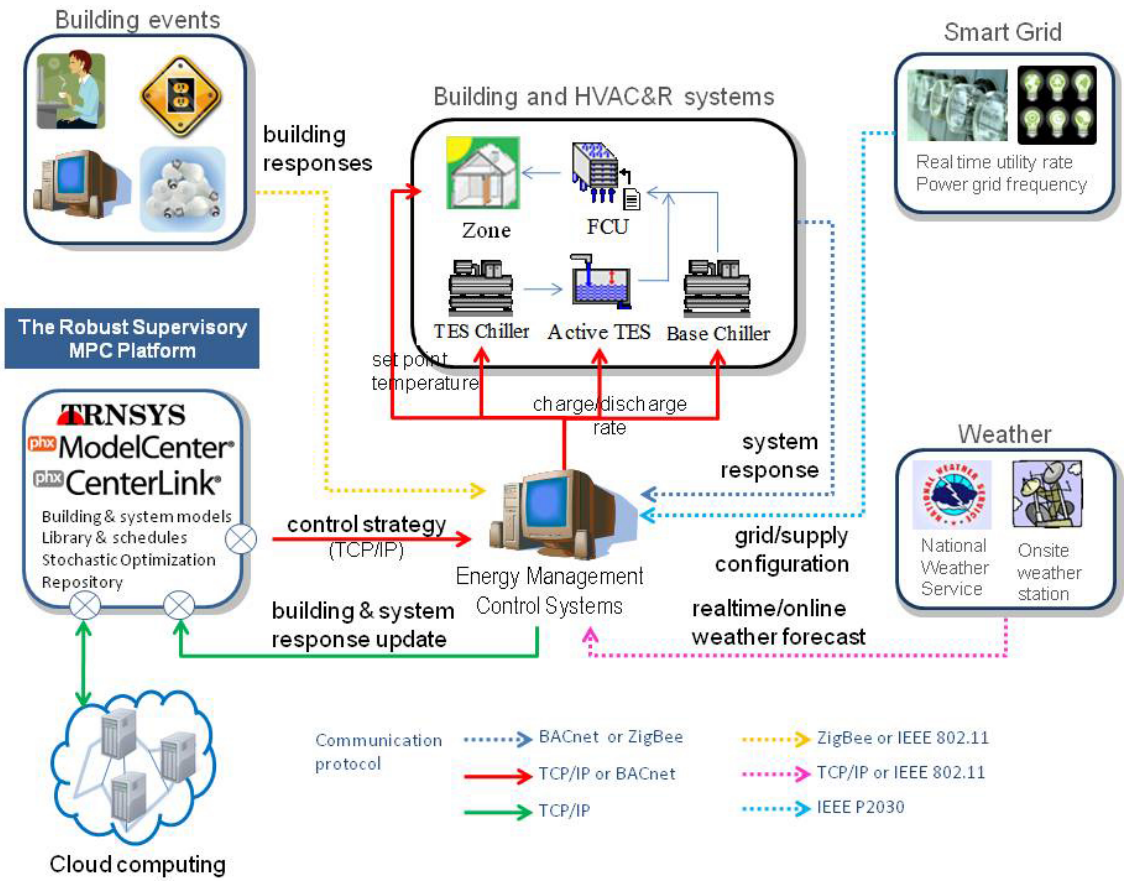

Figure 4.8 The robust supervisory MPC platform hands in control strategies to the EMS while obtaining necessary information from the EMS

4.4.12 A future step II: cloud computing and use of middleware as a deployment environment

For online control applications, supervisory control strategy should be developed and/or selected applicable to a wide operating range of building HVAC systems, while still satisfying the requirements and constraints of practical applications, i.e., control robustness, control accuracy, control efficiency, computational cost and memory demand, etc. (Wang and Ma 20008).

In order to meet such requirements of the supervisory controls, one concern that people would mind considering robust supervisory controls as a practical control application is computational cost. As uncertainties are explicitly incorporated into

control problems, meeting convergence criteria during optimization requires an extensive number of evaluations, thus it could make computation exceptionally complex.

In particular the proposed robust supervisory control for building and HVAC&R systems uses the SAA as a stochastic optimization method. As an accuracy of approximation improves with larger number of samples, a combination of samples (N) and scenarios (Ω) increases its computation complexity up to O(N x Ω).

However this is an increase in computation volume, solutions of which can be relatively easily and quickly achievable with multi-volume and simultaneous computing powers; therefore deploying the development of robust supervisory controls on cloud computing environment will alleviate this computational burden.

It should be noted again that since this study limits its scope to the development of the robust supervisory controls, parts of the deployment process presented in section 4.4.12, in particular deployment procedure to link the SysML-TRNSYS model transformation with the ModelCenter, are included in order to introduce concepts of implementation. However, strong technical backgrounds and feasibility still underlie.

4.4.12.1 Cloud computing environment

Cloud computing is network-based computing, whereby shared resource, software, and information are provided to computers and other devices on demand, like the electricity grid (Gartner.com 2010). It has been attractive more recently with an advance of high-speed bandwidth of the Internet due to its economics (less capital expenditure) and maintenance (serviced by the third-party provider). As of 2011 Amazon Web Service (AWS) gains its popularity in the market.

An interesting feature of the cloud computing for this study includes “grid computing”. This is a distributed and parallel computing environment where a virtual, yet voluminously powered computing frame is composed of a cluster of networked

computers in order to perform large tasks. Grid computing simultaneously applies the resources of many computers in a network to tackle a single point problem, usually to solve a scientific or technical problem that requires a great number of computer processing cycles or access to large amounts of data.

A notion of "supercomputing" have been referred in building simulation society (e.g., CFD-ES binding), in particular CFD analysis. Grid computing is, however, a type of parallel computing where multiple machines are tied in a network, whereas in the supercomputing multiple processors are connected through a bus, thus it accelerates faster serial computations. Therefore the grid computing is well-suited to applications in which multiple parallel computations can take place independently, without the need to communicate intermediate results between processors. If a problem can be adequately parallelized, a "thin" layer of "grid" infrastructure can allow conventional and standalone programs by running on multiple machines, given a different part of the same problem (WikiPedia 2010). Examples of those problems apparently include optimization and statistical samplings.

4.4.12.2 Middleware: ModelCenter and CenterLink

Grids are often constructed with the aid of general-purpose grid software libraries known as a type of the middleware. As described in Figure 4.10, the middleware is seen as a layer between the hardware and the software. It manages multiple applications running on one or more machines to interact. Particularly in general simulations the middleware provides a set of software services that is necessary to support "federation" to coordinate their operations and data exchange during a runtime execution, viz. Run-time infrastructure (Figure 4.9).

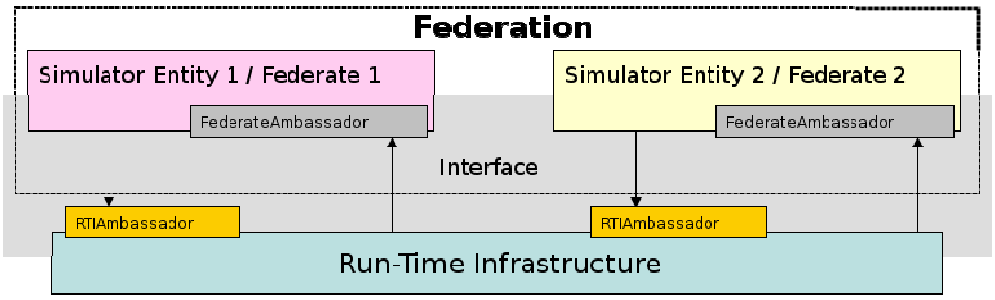

Figure 4.9 Multiple TRNSYS simulations can run on the RTI, thus their integrities are ensured (Wikipedia 2010)

In the robust MPC framework, roles of the middleware are classified into i) central system for parallel computing described as the above and ii) CAE (computer aided engineering) analysis, examples of which include parametric evaluations, design of experiments (DOE), response surface modeling (RSM) and optimizations. Two functionalities must be well-integrated at different levels of interoperability problems. Apparently these requirements may not be efficiently fulfilled by existing hand-coded programming practices, therefore a suite of commercial software, ModelCenter® and CenterLink® (Phoenix Integration 2010), is chosen for this study.

Figure 4.10 well describes high level architecture of this suite and roles of each component (Pheonix Integration 2010).

a. Registry of computing resources: CenterLink maintains a cluster of computers available for the parallel computing

b. Parallel computing execution management: ModelCenter performs CAE analysis and submits the request to CenterLink using its published SOAP API. CenterLink then redirects the request from ModelCenter to its load balancing services running on a cluster

c. Management of CAE analysis results: A standard SQL database is used to store the engineering analysis results in a central location. A large amount of data can be archived in the database thus the data is readily available for use wherever needed.

d. Progress monitor and control: CenterLink makes available the status of CAE analysis executions through web services so that users can monitor, suspend, restart, and stop the process through web browsers.

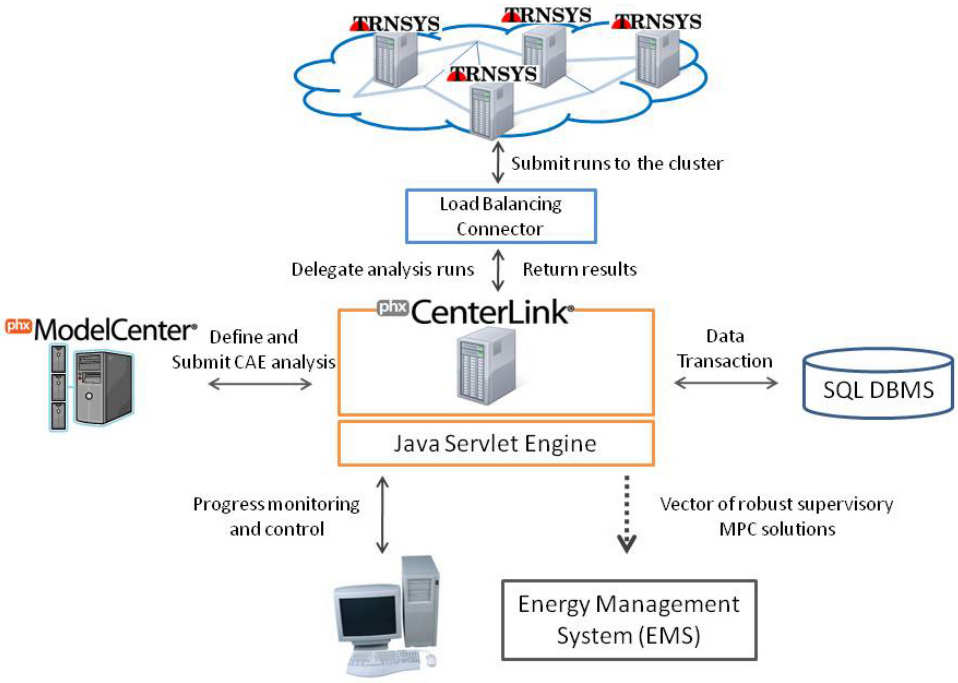

Figure 4.10 Grid computing architecture for the robust MPC framework

4.4.12.3 Deployment of the SysML-TRNYS model transformation using ModelCenter®

Generating multiple scenarios and multiple instances of a simulation model for each scenario and managing resultant highly bulky volume of data in a consistent fashion is cumbersome. As indicated, ModelCenter® would alleviate this management burden. By taking advantages of meta-CASE tool such as MOFLON (Weisemoller, Klar et al. 2009) and Java it is able to make use of intermediate information of the SysML-TRNSYS transformation in order to automatically generate ModelCenter QuickWrap and pxc files as well as TRNSYS simulation codes for more seamless and faster deployment.

Figure 4.11 briefly illustrates a deployment procedure to link the SysML-TRNSYS transformation with ModelCenter. ModelCenter QuickWrap file is a wrapper to bridge between the information of TRNSYS simulation models (including a scenario)

and ModelCenter model. ModelCenter model (i.e., pxc) supports CAE analyses such as optimization and trade study (Figure 4.12), thus it contains QuickWrap(s) and handles multiple scenarios and the global information such as commonly shared variables and weights of each scenario.

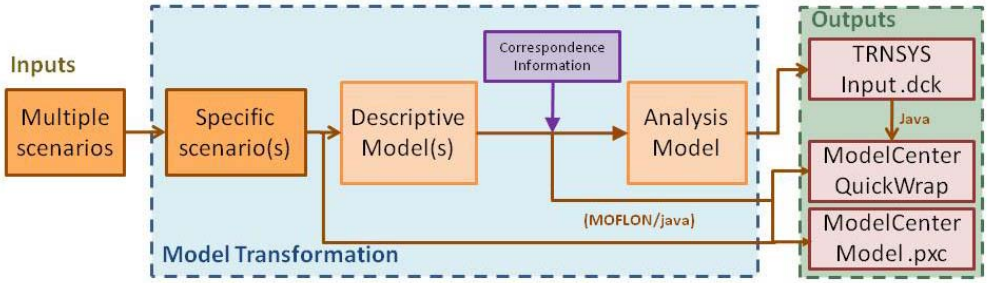

Figure 4.11 Deployment procedure to link the SysML-TRNSYS model transformation with the ModelCenter

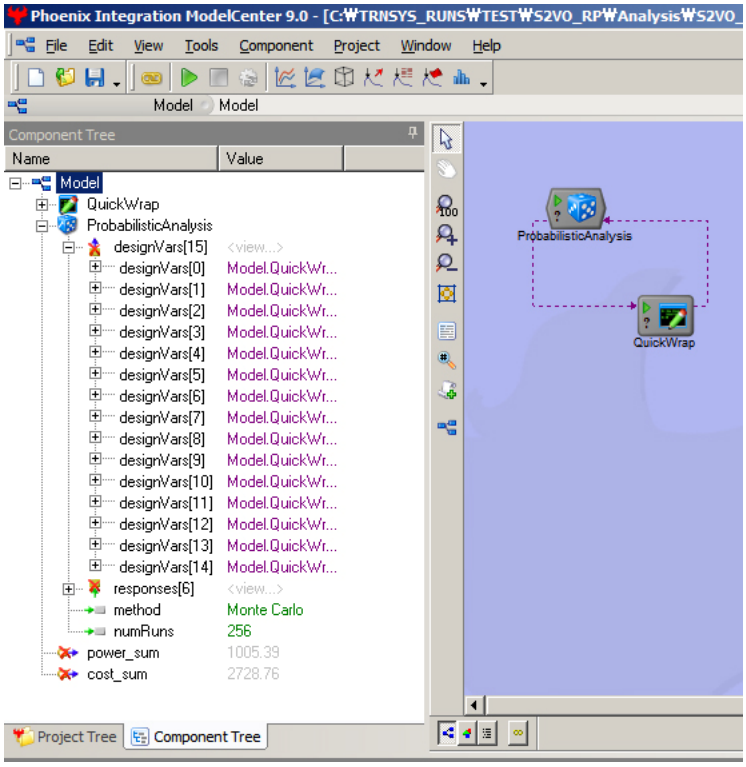

Figure 4.12 A snapshot of the ModelCenter model (.pxc) for probabilistic analyses

4.4.12.4 Performance tests of the grid computing

Computation speed using the grid computing is compared with that of the serial computing.

An optimization problem with genetic algorithm that takes 4 minutes and 30 seconds to evaluate one population in one generation is taken as an example. Since four populations are devised into four nodes and three generations are computed for each population according to setups of the genetic algorithm, a series of optimization problems in serial computing 54 minutes. However CenterLink finishes the optimization within 17 minutes, which corresponds to speed-up ratio 3.18. This is a similar performance measurement with examples shown by the vendor (a similar optimization task ends up with speed-up ratio 3.64) (Pheonix Integration 2005).

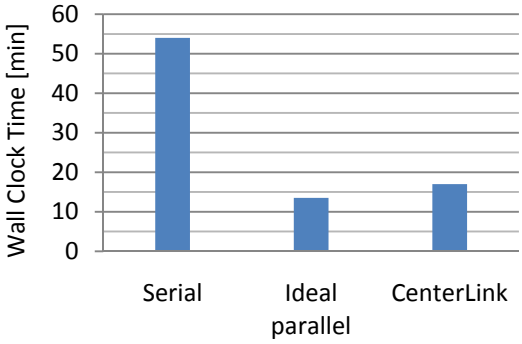

Figure 4.13 Benchmarks between serial and grid runs

4.5 Summary

This chapter focuses on developing robust demand-side controls for building and HVAC&R systems. Control models for passive building mass and active TES, and their applicability considered in the context of the robust MPC are firstly investigated. Additionally a new general methodology to develop a robust supervisory demand-side control strategy is proposed.

The proposed general methodology, however, still lacks of including multiple weather scenarios, an important source of the scenario uncertainty. Hence chapter 5 will introduce a new source for the short-term weather forecast based on the National Digital Forecast Database, and will show how a combination of multiple weather forecast sources will contribute on better performance of the robust demand-side controls.

Then chapter 6 will introduce a case study with an office building in order to demonstrate how the robust supervisory demand-side control strategy can be developed according the suggested framework, and its outstanding demand-side control performance compared with other legacy control strategies.

CHAPTER 5

USING THE NDFD WEATHER FORECAST FOR MODEL-BASED CONTROL APPLICATIONS

5.1 Introduction

A cornucopia of recent information technology (IT) has advanced control systems of commercial buildings. Before 1980, almost all HVAC controls installed in large commercial buildings in North America were pneumatic (Martin, Federspiel et al. 2002). These pneumatic controls were not able to directly control the actuator and suffered from the bias introduced by the dynamic properties of pneumatic machinery. The advent of direct digital control (DDC) systems replaced the pneumatic controls and hard-wired systems by means of signal communication technology, for example, valves controlled via microprocessors dictated by embedded or external control logic. Here, the building automation system controls the HVAC actuator directly. Features enabled by the DDC support the integration of HVAC&R system subcomponents, i.e. sensors and monitors are integrated under a systemic (e.g. hierarchical or distributed) process and supervisory controls.

With this rapid evolution in the hardware of the building control systems, new paradigms of control software solutions have been devised with a focus on sub-system integration. Current researches in applications of model-based controls for heating and cooling of buildings have demonstrated enhanced performances in energy saving, cost saving, thermal comfort and healthy indoor environment

The success of model-based control is dependent on the information used to construct and exercise the model. Thus, uncertainty inside and outside of the model is an inevitable issue in model-based control. In particular, the uncertainty caused from short-

term (24 hours or less) weather prediction is one of the dominant sources of uncertainty because of:

a. Its direct influence on energy consumption, and
b. Its sporadic characteristics.

Recognizing the importance of the weather, many studies have strived to suggest short-term weather forecast methods and models, which are often based on historical records of weather parameters that are observed by the weather station at a building. However, it is the author's conclusion based on literature reviews that forecasting the weather has not been sufficiently addressed from the viewpoint of uncertainty.

Uncertainty of the weather holds characteristics that are both imprecise (e.g. lack of knowledge) and random in nature (e.g. unpredictable). This leads to an argument that prediction performance of the short-term weather forecast models is dependent on i) how thoroughly a short-term forecast model captures significant dynamics of the weather and ii) how deliberate a short-term forecast model is able to cope with a sudden change of the weather.

In accordance with this argument, several research questions for short-term forecast models addressed in this work arise: "Does a short-term forecast model based on a collection of the past data have a sufficient potential to predict the future behavior that is inherently random?" and "If historical data are not available or only limited number of weather variables are available, what other alternatives would be possible and are they able to help refining an incomplete historical data-driven model?"

This study provides answers by testing short-term weather forecasts models in a worst-case weather scenario, i.e. a season when volatile weather conditions are frequent. The hypothesis is introduced that the use of online weather forecasts for model-based control applications will perform better in worst-case situations. Thus, online weather forecasts may replace or supplement the historical data-driven methods. Such online weather forecasts are made by using large-scale atmospheric models, satellite images,

multiple-points surface observations and massive computing power to predict the trend of climate changes (Zhang and Hanby 2007). The nature of data sources and composition principles of the online weather forecast are believed to support the hypothesis of this study.

A few examples exist of including online weather forecasts as weather inputs for model-based controls. However, these have not fully answered the above inquiries, nor have they satisfactorily credited the use of an online weather forecast for the model-based controls because of reasons caused by the limited functionality and applicability of the existing online forecasts. As an alternative approach, this study focuses on hourly reported weather forecast from the National Digital Forecast Database (the NDFD XML, http://www.weather.gov/ndfd). It is believed that this source of weather forecast will have the full capability to be used for model-based control applications.

5.2 Previous works

Prediction models in the literature are largely categorized into time series models (Seem and Braun 1991; Chen and Athienitis 1996; Henze, Felsmann et al. 2004) or neural network models (Kreider and Wang 1992; Dodier and Henze 2004). Both are based on the historical archive of weather variables of interest. Meanwhile a new hybrid direction, viz. utilizing online weather forecasts to modify or reduce a critical disparity of the archive from the actual observation, has demonstrated overall outstanding prediction performance. Among all other valuable studies a few milestone studies, particularly focusing on hybrid methods based on time series analysis are summarized as followings.

Chen and Athienitis (1996) developed a predictor model of ambient temperature and solar radiation, which is made by use of both historical observations and local weather forecasts. Online weather forecast modifies historic shape factors using look-up tables.

Ren and Wright (2002) presented historic time-series based prediction methods: a pure stochastic method (i.e. ARMA and ARMAX), a combined stochastic-deterministic method and a deterministic method (i.e. EWMA and sinusoidal function). For temperature prediction, the smallest prediction error was found in the combined stochastic-deterministic method, and so does the deterministic method for solar radiation prediction. Their contributions are re-examined and clarified by in-depth studies of Henze's group.

Henze et al. (2004) investigated impacts of both stochastic and deterministic short-term forecast models on predictive optimal control of active thermal energy system and passive building mass. The examined short-term forecast models include bin, unbiased random walk, and seasonal integrated ARMA predictors. The best prediction accuracy is found with the bin model that is developed from the previous 30 to 60 days of historic observations. Motivated by this result, Florita and Henze (2009) further investigated prediction accuracy of more short-term forecast models including moving average models with various enhancements and nonlinear autoregressive neural network model. Against a common belief that the neural network models are superior over traditional time series models, the simple time series models with deviation modifications outperformed even the most complicated NARX model for its use on the MPC applications. In this later work, the Exponentially Weighted Moving Average (EWMA) with absolute deviation modifications showed the best prediction performance in short-term predictions of dry-bulb temperature, global horizontal radiation and relative humidity.

Zhang and Hanby (2007) proposed a short-term forecast method using multiple on-line weather forecasts (e.g. Accuweather.com) with local observation data. Hourly ambient temperature is forecasted by a linear combination of the observation and directly forecasted temperatures from on-line sources. Hourly global solar radiation is also a result of the linear combination of those, but the solar radiation from each on-line source

is obtained through a stochastic conversion that interprets descriptive weather information into solar attenuation scales matching up with the observed solar radiation data.

In the literature, online weather forecasts are used to refine and enhance the data quality of weather files generated from a historic time series analysis. Specifically, they are used to rescale the profile of a weather variable, or to include extreme values that have been blunt off via sampling and/or averaging in the historical time series.

5.3 Challenges and motivations

The availability of weather forecast profiles tailored for an individual building is one of the biggest merits of historical data-driven methods. However, obtaining proprietary historical records is not an easy task for ordinary buildings, because individual and independent weather station and/or sensing and monitoring systems have to be installed and also the data should be collected for the period from which meaningful information can be derived, particularly for neural network models. In addition, maintaining a good quality of data requires extra efforts such as signal conditioning, data quality control, and persistent system maintenance.

With this circumstance and aware that concerns exist on the "incompleteness" of historical data-driven models due to a difficulty of getting quality data, using online weather forecasts has several merits such as:

a. Most of the required weather variables are directly forecasted from the online weather forecast service and
b. Its forecast accuracy has been validated during long period and officially announced by the provider, it is worthwhile to search for a direct use of the online weather forecast for model-based control applications.

However, some existing studies have raised objections against using online weather forecast as weather input sources for model-based control applications. Their arguments include

a. Some required weather variables in building simulations such as solar irradiation data are not directly reported
b. An increasing uncertainty when the forecast projection gets longer
c. Uncertainty due to the discrepancy between location of measurements and the site under interests
d. A risk of service interruption and resulting missing information
e. Reliability of external sources

The following sections discuss features of the NDFD XML that can be highlighted to overcome the known challenges of using online weather forecasts, eventually that illustrate how the NDFD XML leads to meet the goals of the study.

5.3.1 Missing critical weather variables such as hourly global horizontal radiation

This challenge has caused many previous studies to choose historical data-driven methods, instead of the online weather forecasts. However this challenge has motivated this study to search for a forecast method via first-hand weather information available in the NDFD XML. In case that is not possible it encourages this study to build a forecast model based on first-hand weather information.

A number of solar radiation modeling studies (Erbs, Klein et al. 1982; Reindl, Beckman et al. 1990; Alam, Saha et al. 2005; Ianetz, Lyubansky et al. 2007; Mondol, Yohanis et al. 2008), based on the empirical analysis have shown an outstanding prediction performance of global horizontal radiation models that are developed with a few critical ingredient weather factors. Those studies have emphasized impacts of local

cloud movements and cloud cover on estimating global horizontal radiation. As a functional component of the clear day index (Ianetz, Lyubansky et al. 2007) or the clearness index (Iqbal 1983), a local sky status takes a part of modeling an erratic change of solar surface insolation. A practice of The European Database of Daylight and Solar Radiation (Satel-Light project 1997) particularly motivated the use of sky condition information to develop an analytical method that forecasts hourly global horizontal solar radiation. In the meantime, the NDFD XML is able to provide those key weather factors including the status of hourly local sky condition (as of 7/8/2008).

5.3.2 Uncertainty from long forecast projections and positioning in grids

It is a natural characteristic of the forecast mechanism that a forecast with a longer projection imposes higher uncertainty. To minimize errors between the forecast and the reality, real time forecasts seem to be a resolution. Model-based control applications such as energy efficient controls - especially when the building mass plays a significant role – however do not necessarily require such type of real time forecasts due to its greater time constant. It would be more reasonable to find a length of forecast projection that is long enough to reflect a transition of significant behavior of building systems with a reasonable degree of accuracy.

Supportive to the above discussion, the NDFD XML equips with the capability to reduce such spatial and temporal uncertainty. For example, grids for the contiguous United States are available at 5 kilometer spatial resolution, and the NDFD is updated no more than one hour. Furthermore, a validation result of the NDFD (http://www.weather.gov/ndfd/verification/) shows that forecast errors for most of the required weather variables tend to be periodic, e.g. the forecast error at 3hr projection is almost similar to that at 24hr projection (Section 5.5). This implies the temporal uncertainty of the NDFD is not as large as it was thought to be.

5.3.3 Service stability and reliability

A study by (Zhang and Hanby 2007) tried to resolve issues of service quality by including multiple online weather sources. However, this service stability issue can happen to any system or model. Frequent break-downs of a national wide (or global wide) service should be treated as an "emergency" rather than "problematic" service quality issues. In this case a responsive back-up or a recovery plan should be put in place as general emergency management principle dictates.

In fact, the reliability issue can be more detrimental when only single source is used for the forecast. It is because it is hard to distinguish faulty information and correct information with single source. Two typical resolutions to resolve this issue include i) selective single source after a comparison with references, and ii) aggregated multi-sources. Both cases need multiple sources of weather forecasts, and a new way of interpreting multiple weather sources including the NDFD XML for model-based control applications is suggested in the discussion section.

Understanding practical limitations of the current practices to use short-term forecasts for control applications and known challenges of using online weather forecasts, potentials and merits of using the NDFD XML as a short-term forecast input for model-based control applications have motivated this study to aim for a few practical deliverables as followings

a. To suggest a short-term forecast method based on first-hand weather information from the NDFD XML
b. To propose a forecast model of hourly global solar radiation based on available first-hand NDFD XML information and theoretical modeling knowledge

c. To suggest a reasonable length of forecast projection of the NDFD XML that ensures a reasonable degree of accuracy and that also fits in model-based control applications
d. To demonstrate an exemplary application case of using the NDFD XML for widely used model-based control applications in real life and to inspect what the proper way of applying the short-term weather forecast models

5.4 Overview of the NDFD XML

National Digital Forecast Database (NDFD) Extensible Markup Language (XML) (http://www.nws.noaa.gov/xml) is a service providing the public, government agencies, and commercial enterprise with data from the National Weather Service's (NWS) digital forecast database (National Oceanic and Atmosphere Administrations 2010). This service enables users to request the NDFD data over the internet and to receive the requested information back in an XML format as featured in the Figure 5.1. The NDFD XML Simple Object Access Protocol (SOAP) makes this possible, and a procedure of requesting and receiving data is illustrated in the Figure 5.9.

NDFD XML contains weather forecasts for any combination of significant meteorological parameters including temperature, relative humidity, dew point, sky cover, snow amount, wind direction, wind gust, wind speed, weather description and etc. Along with its rich weather information, this study features merits of the NDFD XML service that are more appropriate as a weather forecast source for model-based control applications as follows.

a. Service quality control by the National NOAA
b. All meteorological elements are available for the contiguous United States
c. Useful and significant outlooks for control applications (e.g. One-month Avg. Temperature Above Normal) are being included

d. The NDFD is updated at every hour or less and it is on 24x7 basis

e. Grids for the contiguous United States are available at 5 kilometer spatial resolution

f. Multiple point forecast is available with zip code, city name and latitude and longitude pair searches

g. Forecast of most elements is projected either at every 6 hour out to 168 hours or at every 3 hour out to 72 hours

h. Free open source to the public

i. Convenient applicability features such as time-series data, and easy interface

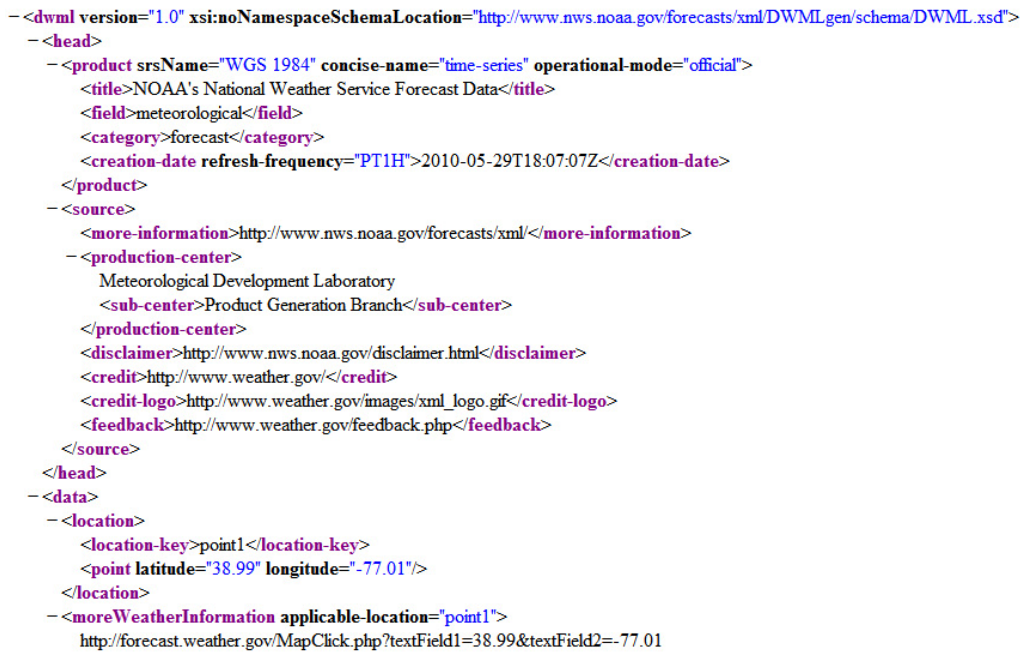

Figure 5.1 An exemplary code of the NDFD XML

5.5 Validation scores of the NDFD

The National Weather Service offers verifications for a few weather elements from the NDFD in terms of validation score. “Validation score” is statistical criteria for comparing between forecasted values and actual values, and a set of validation scores are

assessed for each weather variable (NOAA 2010). For example, validation scores for surface temperature and relative humidity include Mean absolute error (Equation 5.1) and bias (Equation 5.2), validation scores for sky cover include Fraction Correct (Equation 5.3) and Heidke Skill Scores (Equation 5.4).

$$MAE = \frac{1}{N}\sum_{i=1}^{N}|x_i - \hat{x}_i| \quad (5.1) \qquad Bias = \frac{1}{N}\sum_{i=1}^{N}(\hat{x}_i - x_i) \quad (5.2)$$

$$\text{Fraction Correct} = \frac{NC}{T} \quad (5.3) \qquad \text{Heidke skill score} = \frac{NC-E}{T-E} \quad (5.4)$$

where x stands for the observed variable; $\hat{x}$ stands for the estimated variable; NC equals to the number of times that the forecast and the observations match within the given threshold; T equals to the total number of forecasts; and E equals to the number of forecasts expected to verify based on chance.

They provide two types of validation scores each weather variable: one is for temporal validation (from 3hr projection to 168hr projection) of a weather variable, and the other is validation score distribution of a weather variable at 1394 stations in the U.S. continent at any projection hour.

A few findings from a close examination report: i) For any weather variable, a temporal validation along with the projection length shows a similar tendency over the year. This implies that there are only seasonal variations in forecasts, but forecast performance is stable over the year; ii) As expected, Mean absolute error, Fraction correct, and Heidke Skill Score tends to be worse as the projection hour is extended; and iii) Fluctuation frequency of MAE and bias is based on a regular interval (e.g. at every 24hr) for most weather variables.

A snapshot of MAE and Fraction Correct of three weather variables in February 2010 is taken as examples (NOAA 2010). In Figure 5.2 and 5.3 MAE tends to grows while fluctuating with a 24hr of the regular interval. Figure 5.4 shows that Fraction correct of the sky cover is almost stable with 0.4 until 24 projection hour. Although this tendency may vary per weather variable and per month, this observation presents an

important insight of selecting 24hr as an appropriate length of the forecast projection that is able to secure reasonable forecast accuracy compared with shorter projection hours.

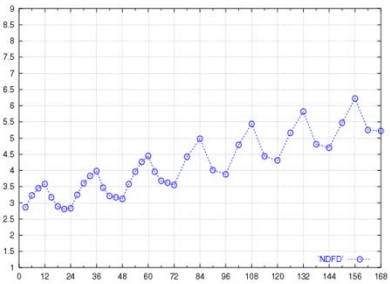

Figure 5.2 MAE of the surface temperature

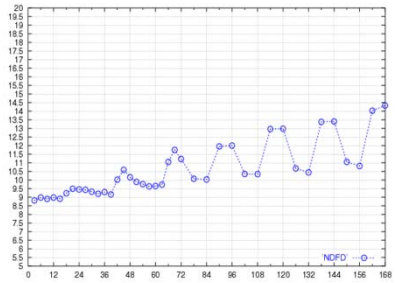

Figure 5.3 MAE of the relative humidity

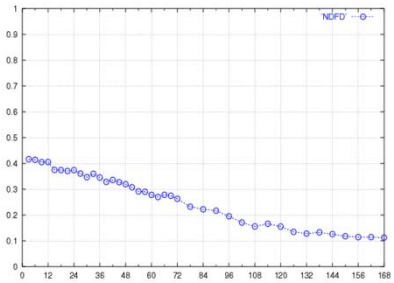

Figure 5.4 Fraction correct of the Sky cover

5.6 Modeling short-term weather forecasts using the NDFD XML

As previous studies reported (Ren and Wright 2002; Florita and Henze 2009), due to their prevalence as essential climate inputs for building simulations, three weather variables are selected and their hourly time-series data are forecasted through the NDFD XML. They include dry bulb temperature (Tamb), relative humidity (RH) and global horizontal radiation (Ih). However global horizontal radiation is not directly available with the NDFD XML, thus we develop a reliable model to estimate that.

5.6.1 Statistical criteria

Two standard statistical metrics evaluate both model accuracy and prediction accuracy of the forecasted weather variables. They are the coefficient-of-variation of the Root Mean Square Error (CV-RMSE) and the mean bias error (MBE), as shown in the following equations:

$$CV - RMSE = \frac{\sqrt{\frac{1}{N}\sum_{i=1}^{N}(x_i - \hat{x}_i)^2}}{\frac{1}{N}\sum_{i=1}^{N} x_i} \tag{5.5}$$

$$MBE = \frac{\frac{1}{N}\sum_{i=1}^{N}(x_i - \hat{x}_i)}{\frac{1}{N}\sum_{i=1}^{N} x_i} \quad (5.6)$$

where x stands for the observed variable; and $\hat{x}$ stands for the estimated variable.

CV-RMSE indicates the short-term deviation of a model allowing a term-by-term comparison, and it identifies how much the estimation is scattered with respect to the measurement. MBE indicates the long-term trend of a model, and it identifies how high or low the estimation is with respect to the measurement (i.e. average offset). A MBE of zero is possible, if over-estimation and under-estimation cancel each other. Therefore MBE should be looked at in conjunction with CV-RMSE to determine forecasting errors.

5.6.2 Estimation of hourly solar radiation and its validation

Local solar radiation does vary depending on its geographic location, temporal variation, and surroundings, for example, transient cloud movement, miscellaneous reflective objects around the measurement point, atmospheric turbidity and so forth.

Instead of a flawless prediction of the close-future weather that fully captures such highly transient local variety in atmospheric condition parameters, therefore, a reasonable and sound engineering estimation that captures a key phenomenon would result in better efficiency. This study chooses a decomposition model that is made up by a combination of significant subcomponents to estimate hourly global horizontal radiation based on theoretical models and critical weather variables forecasted by the NDFD XML.

To validate model accuracy of the estimation of hourly global horizontal radiation, two types of climates are investigated. Two U.S. sites with different cloud conditions, Acarta, CA (40.88°N, 124.08°W) and Las Vegas, NV (36.06°N, 115.08°W), are chosen. According to the NOAA fact sheet, Las Vegas is one of the least cloudy areas

(around 73 days per year) and Acarta is a considerably cloudy area (around 188 days per year) in the States.

Also the three-year actual measurements (from 2007 to 2009) of hourly global horizontal radiations in two sites are obtained for references through web open sources of the Measurement and Instrumentation Data Center (MIDC) of the National Renewable Energy Laboratory (NREL).

5.6.3 Modeling hourly global horizontal radiation (I_h)

A large number of models have been developed to describe transmitted solar radiation from the sky top and its loss on the way to the surface. In particular, clouds have the largest influence on atmospheric radiative transfer (Hammer, Heinemann et al. 2003). Thus a local cloud status must be included in predicting global horizontal radiation for higher accuracy. While the NDFD XML regularly reports current and future movement of clouds and status of local sky condition, this study suggests to use the knowledge on hourly reported sky condition status as well as to use established empirical models in order to obtain a high-fidelity global horizontal radiation estimation model. Some established concepts and terms are introduced as the below.

Cloud index (n): A cloud index (Fontoynont 1997; Fontoynont 1998) indicates a measure of the cloud cover. It varies between 0 (cloud free) and 1 (completely overcast), of which definition corresponds to the Sky cover in the NDFD XML matrix.

Clear sky index (k_C) : To relate the observed cloud state with an actual transmission loss due to clouds, the clear sky index is introduced. This describes cloud transmission as a ratio of the global horizontal radiation (G) to the clear sky global radiation (G_C) as defined,

$$k_C = \frac{G}{G_c} \tag{5.7}$$

If one can get hourly clear sky index and clear sky global radiation, the hourly global horizontal radiation at a site can be obtained via these equations. Within the Satel-Light project, a simple relationship with the Clear sky index and the Cloud index is derived (Fontoynont 1997; Fontoynont 1998). In this project an accurate cloud index n is calculated based on a relation of the albedo, the ground albedo and the cloud albedo that are read from a pixel in the satellite image. Replacing n directly with the Sky cover forecasted by the NDFD XML, however, results in a poor agreement with the actual global horizontal radiation.

To mitigate strong Cloud index n, a discount factor γ is introduced. After several adjustments, it is found that a simple linear relation works well with the three year of actual hourly global horizon radiations in both sites. It is defined as below:

$$k_C^* = 1 - \gamma n \qquad \text{where } 0 \le n \le 1 \text{ and } 0 \le \gamma \le 1 \tag{5.8}$$

For the hourly global horizontal radiation forecast model in this study, the γ value is optimized over the validation procedure through exhaustive searches. 0.55 is found optimal for Acarta, and 0.21 is found optimal for Las Vegas. As expected, this founding clearly indicates that the sky condition in the cloudy area is more sensitive in estimating the solar insolation accurately than it is in the sunnier area.

Clear sky global radiation (G_C): Key factors of the empirical correlation include site location and astronomical parameters such as the solar zenith angle, and these factors exclusively control accuracy of the global radiation model. Thus a clear sky global radiation model that was developed on the site having similar meteorological properties with the site under consideration would be best suited. Among many clear sky global radiation models (Haurwitz 1945; Haurwitz 1946; Adnot, Bourges et al. 1979; Berger

1979; Robledo and Soler 2000), Haurwitz's model (Equation 5.9) has shown a reasonably good agreement.

$$G_c = 1098 \cos\theta_z \; e^{-0.057/\cos\theta_z} \tag{5.9}$$

By use of Equation (5.7), (5.8) and (5.9), the hourly global horizontal radiation is obtained as Equation 5.10, where solar zenith angle θ_z is hourly updated by solar trajectory.

$$I_h = (1 - \gamma n) \cdot 1098 \cos\theta_z \; e^{-0.057/\cos\theta_z} \tag{5.10}$$

5.7 Model accuracy of hourly global solar radiation estimated with the NDFD XML

Figure 5.5 to 5.8 illustrate monthly CV-RMSEs and MBEs calculated based on both the observed and the estimated hourly global horizontal radiations. Variations of two statistical criteria indicate that estimations of the hourly global solar radiations have shown generally good agreement with three year's observations at both sites.

As previous studies on modeling solar insolation reported (Ianetz, Lyubansky et al. 2007), seasonal variations (warm season vs. cold season : the larger errors in cold season) and climate variations (cloudy and humid vs. sunny and arid : the smaller errors in sunny and arid climate) are observed.

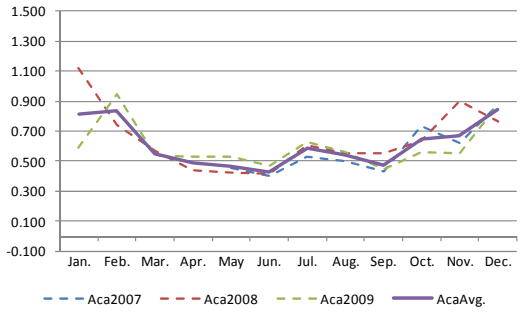

Figure 5.5 CV-RMSEsof the hourly global horizontal radiation in Arcarta from 2007 to 2009

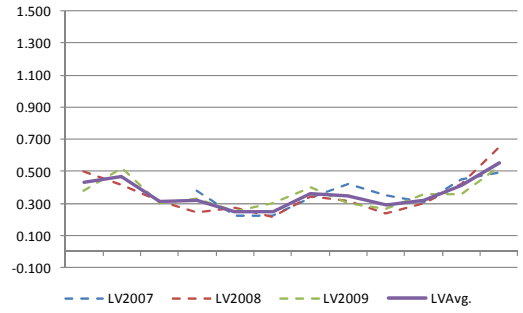

Figure 5.6 CV-RMSEs of the hourly global horizontal radiation in Las Vegas from 2007 to 2009

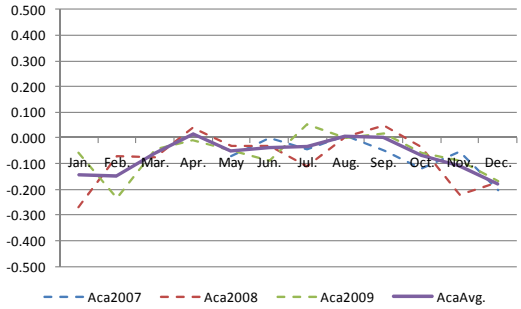

Figure 5.7 MBEs of the hourly global horizontal radiation in Arcarta from 2007 to 2009

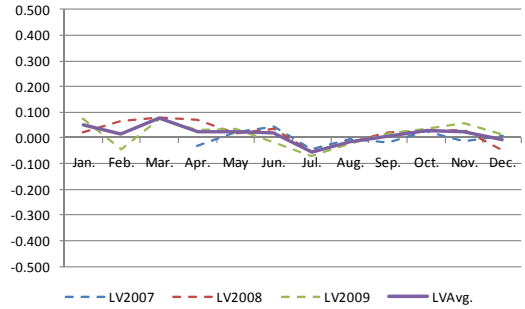

Figure 5.8 MBEs of the hourly global horizontal radiation in Las Vegas from 2007 to 2009

5.8 Prediction accuracy of the NDFD XML

In the previous section, the "model accuracy" of the proposed hourly global solar radiation estimation model is validated over three years of the observed data in two representative sites. As the sky cover critcially governs the model accuracy of the proposed model, indeed "prediction accuracy" of the sky cover forecated in the NDFD XML is a key factor for the proposed model to match the actual oservation of global horizontal radiation. Also we need to investigate prediction accruacy of temperature and relative humidity forecasted in the NDFD XML in order to form a complete set of the essential weather information.

To validate the prediction accuracy of three weather variables using the official validation data offered by the NDFD, firstly we need to select a right projection horizon that should be decided upon a choice of planning horizon (section 4.4.9) for model-based control applications. As a general guideline of using the NDFD XML for model-based control applications, this study suggests a 24hr planning horizon by two reasons: i) validation scores of temperature, relative humidity and sky cover in the NDFD at 24hr projection have reasonably good values compared to those at shorter projection horizons (section 5.5), and ii) daily (i.e. 24hr based) building load prediction is usually a basis to plan the operation of related HVAC&R components (Henze, Felsmann et al. 2004; Henze, Kalz et al. 2005; Henze 2008).

5.8.1 Annual prediction accuracy of the NDFD XML with 24hr projection

Table 5.1 and 5.2 list profiles of the monthly average ambient temperature, relative humidity and sky cover in 2009 for Arcata and Las Vegas, accompanied by MAEs, Bias and Fraction correct of the 24hr projection forecasts of each (NOAA 2010).

Similar to the previous findings in validating the model accuracy, the prediction accuracy of the three weather variables of Acarta (cloudy and humid) slightly underperforms those of Las Vegas (sunny and arid). However seasonal variations are not apparent. This implies that the NDFD XML guarantees stable forecast performances over the year.

Table 5.1 Monthly average temperature, RH and sky cover profiles of Arcata in 2009

	Jan	Feb	Mar	Apr	May	Jun	Jul	Aug	Sep	Oct	Nov	Dec
T_{suf}	45.5 °F	46.9 °F	46.0 °F	47.5 °F	51.6 °F	55.2 °F	54.4 °F	56.7 °F	57.1 °F	53.0 °F	49.1 °F	45.4 °F
MAE	[3, 5] °F	[3, 5] °F	[3, 5] °F	[3, 5] °F	[3, 5] °F	[3, 5] °F	[3, 5] °F	[3, 5] °F	[0, 3] °F	[3, 5] °F	[0, 3] °F	[0, 3] °F
Bias	[-3, 3] °F	[-3, 3] °F	[-3, 3] °F	[-3, 3] °F	[-3, 3] °F	[-3, 3] °F	[3, 5] °F	[-3, 3] °F	[-3, 3] °F	[3, 5] °F	[-3, 3] °F	[-3, 3] °F
RH	84.2 %	80.0 %	82.9 %	80.7 %	86.5 %	85.2 %	90.9 %	88.0 %	86.1 %	85.8 %	83.2 %	84.3 %
MAE	[10,20] %	[10,20] %	[10,20] %	[10,20] %	[10,20] %	[0,10] %	[0,10] %	[10,20] %	[10,20] %	[10,20] %	[10,20] %	[10,20] %
Bias	[-5,5] %	[-5,5] %	[-15,-5] %	[-15,-5] %	[-15,-5] %	[-5,5] %	[-5,5] %	[-5,5] %	[-15,-5] %	[-15,-5] %	[-15,-5] %	[-5,5] %
SC Frtn Crct	38.1 (0.2-0.4)	59.3 (0.4-0.6)	54.5 (0.2-0.4)	46.4 (0.2-0.4)	68.7 (0 - 0.2)	59.9 (0.2-0.4)	78.9 (0 - 0.2)	60.7 (0 - 0.2)	41.9 (0.2-0.4)	48.7 (0.2-0.4)	33.0 (0.4-0.6)	49.6 (0.2-0.4)

Table 5.2 Monthly average temperature, RH and sky cover profiles of Las Vegas in 2009

	Jan	Feb	Mar	Apr	May	Jun	Jul	Aug	Sep	Oct	Nov	Dec
T_{suf}	50.7 °F	56.1 °F	60.1 °F	66.5 °F	84.0 °F	83.9 °F	94.9 °F	91.2 °F	86.4 °F	67.3 °F	58.9 °F	45 °F
MAE	[0, 3] °F	[0, 3] °F	[3, 5] °F	[3, 5] °F	[0, 3] °F	[3, 5] °F	[3, 5] °F	[0, 3] °F	[0, 3] °F	[3, 5] °F	[0, 3] °F	[3, 5] °F
Bias	[-3, 3] °F	[-3, 3] °F	[-3, 3] °F	[-3, 3] °F	[-3, 3] °F	[-3, 3] °F	[-3, 3] °F	[-3, 3] °F	[-3, 3] °F	[-3, 3] °F	[-3, 3] °F	[-3, 3] °F
RH	37.5 %	32.2 %	21.6 %	21.2 %	14.9 %	19.0 %	18.0 %	14.9 %	17.4 %	21.3 %	23.4 %	40.8%
MAE	[10,20] %	[0,10] %	[0,10] %	[0,10] %	[0,10] %	[0,10] %	[0,10] %	[0,10] %	[0,10] %	[0,10] %	[0,10] %	[0,10] %
Bias	[-5,5] %	[-5,5] %	[-5,5] %	[-5,5] %	[-5,5] %	[-5,5] %	[-5,5] %	[-5,5] %	[-5,5] %	[-5,5] %	[-5,5] %	[-5,5] %
SC Frtn Crct	28.7 (0.2-0.4)	43.6 (0.2-0.4)	34.6 (0-0.2)	35.1 (0.2-0.4)	42.6 (0.2-0.4)	51.3 (0.2-0.4)	45.2 (0.2-0.4)	25.9 (0.2-0.4)	23.3 (0.4-0.6)	29.1 (0-0.2)	35.0 (0-0.2)	48.6 (0.2-0.4)

Although the above validation scores are officially published, their prediction accuracy still need to be compared with other benchmark forecast models using the same metric. Thus CV-RMSs and MBEs of the ambient temperature and the relative humidity of the NDFD of Acarta (of which prediction accuracy is expected lower than that of Las Vegas, thus worse case than Las Vegas) are calculated from MAEs and Bias reported in Table 5.1 and 5.2. Since it may have to impose too many assumptions to calculate CV-

RMSs and MBEs of the forecasted global horizontal radiation directly based on the reported Fraction Corrects of Sky cover, only CV-RMS and MBEs of those two weather variables are calculated. Results are shown in Table 5.3.

Compared to CV-RMSs and MBEs reported by benchmark forecast models, the NDFD has shown an affordable range of prediction accuracies for these two weather variables. The Hybrid method (Zhang and Hanby 2007) seems to outperform others. As the reported statistics are not analyzed based on the identical geographical locations and the seasonal conditions, however, it is hard to assert that one method is better than others with the limited information.

Table 5.3 Calculated CV-RMSs(upper) and MBEs(lower) of the 24hr projected NDFD and the CV-RMSs and MBEs reported by benchmark forecast models in the literature

	24hr proj. NDFD in Acarta, warm season (Mar-Aug)	24hr proj. NDFD in Acarta, cold season (Sep-Feb)	abs.dev.EWMA in 11 world-wide locations*	Hybrid method in Leicestershire, UK**	Sinusoidal in London and Garston, UK***
T_{suf} [°F]	0 – 0.11 0.05 - 0.09	0 – 0.11 -0.07 – 0.09	0.2 0.13	0.0061 0.00	0.0083 0.001
RH [%]	– 0.25 -0.19 – 0.06	0.12 – 0.25 -0.18 – 0.06	0.11 0.07	(not reported)	(not reported)

* Florita and Henze 2009 ** Zhang and Henby 2007 *** Ren and Wright 2002

5.9 Performance comparisons of short-term weather forecast models

Though the NDFD with 24hr projection has shown a reasonable range of prediction accuracy over the year in section 5.8.1, it is hard to declare the forecast performance of the NDFD XML is as good as, or even better than the existing forecast models by several reasons: i) comparisons are not done with the identical condition, ii) the important variable, global horizontal radiation is missing, and iii) a locality problem when it is applied to the actual site may happen.

Moreover as this study purposes to examine the NDFD XML as being capable to forecast erratic and sporadic characteristics of the weather, testing its robustness with a

sample of worst case weather scenarios would make more senses rather than taking tests for the whole year that may flatten the forecast performance. Hence actual NDFD XML forecasts are collected for a month from mid-February to mid-March in 2010. This period is chosen to represent a worst case weather scenario in Acarta in that i) the lowest overall accuracy of the proposed hourly global horizontal radiation forecast model is observed in Figure 5.5, which is supposedly due to highly erratic cloud movement and extended cloudy conditions, ii) higher MAEs and Bias of the temperature and the relative humidity (the shaded area in Table 5.1) is observed, and iii) a representative sample period of the cold season, i.e. Average diurnal temperature swing was around 14°F that is almost identical to the average diurnal temperature swing (15°F) during the cold season in 2009.

For a benchmark purpose we investigate several historical data-driven models in the literature. They include Exponentially Weighted Moving Average (Seem and Brown 1991, Ren and Wright 2002, Florita and Henze 2009), Autoregressive moving average, unbiased random walk, Sinusoidal functions (Ren and Wright 2002, Florita and Henze, 2009), Bin method, Like-yesterday model, Artificial neural network models. Since the EWMA and the Like-yesterday model have shown good prediction accuracy overall (Ren and Wright 2002, Florita and Henze 2009) in recent studies, we chose these two historic data-driven models.

5.9.1 EWMA with absolute deviation modification

An underlying idea of the EWMA is that recent observations in the historical data are more influential to the forecast. Thus weightings are exponentially decreasing when the older observations are involved in. A multiplication of the discount factor λ and its complement dampened over the duration make the older observations less influencing, according to the given equation

$$\hat{x}_t^w = \sum_{i=0}^{\infty} \lambda(1-\lambda)^i \, x_{t-24*i}^w \qquad 0< \lambda \leq 1 \text{ and } \sum_{i=0}^{\infty} \propto (1-\lambda)^i = 1 \qquad (5.11)$$

To account for a discrepancy of the forecast value from the observed value, adjusting the forecast value will provide better agreements. They suggested absolute and relative standard deviation modifications, and generally absolute deviation modification has shown better forecast accuracy (Florita and Henze, 2009). For a weather variable w, the deviation (δ_k^w) of the observed value (x_k^w) from its forecast value ($\hat{x}_k^w$) at time k is defined by the following equation,

$$\delta_k^x = x_k^x - \hat{x}_k^x \tag{5.12}$$

The deviation is calculated when the predictive control strategy starts being planned for the next control horizon, and then the calculated deviation at time pH_o is added to the forecast profile of weather variable w during pH_o between pH_n. It assumes that the deviation constantly persists for the control's execution horizon. The absolute deviation modification to the forecasted profile x of weather variable w is expressed in the following equation 5.13,

$$x'^w_t = \hat{x}^w_t + x^w_{pH_0} - \hat{x}^w_{pH_0} \qquad pH_o \le t \le pH_n \tag{5.13}$$

where $\hat{x}_t^w$ is the forecasted weather variable w during the planning horizon from pH_o to pH_n , and x'^w_t is the modified profile by the absolute deviation modification.

5.9.2 Like-yesterday method with absolute deviation modification

This method assumes today's weather profile would be identical with yesterday's profile (Equation 5.14). An adjustment is also added to compensate a discrepancy of the forecast value from the observed value (Equation 5.15).

$$\hat{x}^w_t = x^w_{t-24} \tag{5.14}$$

$$x'^w_t = \hat{x}^w_t + x^w_{pH_0} - \hat{x}^w_{pH_0} \qquad pH_o \le t \le pH_n \tag{5.15}$$

5.9.3 Comparisons of forecast performances

In the Table 5.4, prediction performances of three NDFD XML sets of hourly temperature (T_{amb}) and global horizontal radiation (I_h) during mid-February to mid-March in 2010 are statistically analyzed. Unfortunately the relative humidity measurements are not available for this period.

The first set consists of 6hr-projection forecast (e.g. retrieving the NDFD XML at every 4 hours to get the forecast during the next 6 hour; pH=6hr), the second set and the third set consists of 12hr-interval (pH =12hr) and 24hr-interval forecast (pH =24hr), respectively. Statistical analyses of the EWA with absolute deviation modification (abs.dev.EWMA) and Like-yesterday method (abs.dev.Like-yesterday) are compared for the same period. The abs.dev.EWMA triggers its modification at 6pm everyday is assumed since this moment is usually a beginning of the unoccupied hour.

Table 5.11 CV-RMSEs of three forecasts models for Acarta (upper) and La Vegas (lower)

	6hr projection NDFD XML	12hr projection NDFD XML	24hr projection NDFD XML	abs.dev.EWMA pH=24hr@1800	abs.dev. Like-yesterday
Temperature	0.08 0.07	0.10 0.07	0.09 0.08	0.09 0.07	0.12 0.09
Global horizontal radiation	0.71 0.41	0.76 0.42	0.78 0.43	0.97 0.50	1.29 0.57

Table 5.5 MBEs of three forecasts models for Acarta (upper) and Las Vegas (lower)

	6hr projection NDFD XML	12hr projection NDFD XML	24hr projection NDFD XML	abs.dev.EWMA pH=24hr@1800	abs.dev. Like-yesterday
Temperature	0.05 0.03	0.07 0.03	0.06 0.04	-0.01 0.01	-0.00 0.01
Global horizontal radiation	-0.05 0.03	-0.09 0.02	-0.09 0.03	0.06 0.07	0.03 0.01

Findings through observations during the worst-case scenario season and comparison results are summarized as the followings.

- In general shorter projections of the NDFD XML show better forecast performances. However the differences from 6hr projection through 24hr projection are small.
- CV-RMSEs and MBEs of two weather variables in Las Vegas are generally lower than those in Acarta. The different climate characteristics accounts for this result: Las Vegas has constantly hotter and sunnier climate year-around than Acarta.
- For both weather variables in both sites, CV-RMSEs of the NDFD XML are lower than those of two other methods. This observation indicates the NDFD XML is better at predicting more erratically scattered values.
- For predicting ambient temperature that possesses the stronger characteristic profile than global horizontal radiation, the abs.dev.EWMA appears to better perform.

5.10 An exemplary application case of using the NDFD XML

Short-term forecast weather profiles are able to replace legacy weather inputs for various resolutions of model-based building and HVAC control applications ranging from embedded local controllers to supervisory controls. Among all benefits of the short-term forecasts, this study highlights the potential of an improved daily thermal load profile prediction of a building particularly with the NDFD XML.

It is well-known that an accurate daily thermal load profile prediction is a prerequisite to compose a high performance control portfolio of a broad range of energy systems, e.g. from cooling towers to air terminal units. It is an intention of this study that, in particular, energy saving control applications taking advantages of thermal storage will take a large benefit of using the NDFD XML. It is because an accurate load profile prediction makes it possible i) to estimate the amount of total daily building energy consumption that could be saved by the thermal storage and ii) to compose an accurate

operation portfolio of subsidiary plants such as chillers. The combination of both eventually leads to energy and cost savings.

5.10.1 Process of including the NDFD XML in the BES

To replace conventional weather files in simulation with the NDFD XML, a series of weather variables written in the XML file firstly need to be parsed for the period of the forecast horizon. For this study, a Java XML DOM (The W3C Document Object Model) parser is employed and the parsed profiles are passed over to a suite of the simulation framework. Figure 5.9 describes the process of including the weather data originated from the NDFD.

The chosen BES tool, TRNSYS, facilitates this process by i) modularity to manipulate components one by one and ii) configurability with external programming and communication applications such as Java Runtime Environment and SOAP applications. After the parsed profiles is quality-controlled (e.g. cleaned and missing parts are filled), TRNSYS "Radiation Processor" and "Data Reader" components take the conditioned time series weather profiles, and then they format those profiles into hourly weather data such as insolations on an inclined surface.

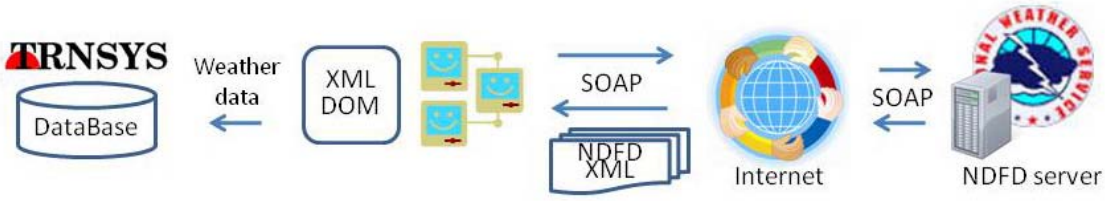

Figure 5.9 Process of including weather data originated from the NDFD server maintained by the NWS

5.10.2 Exemplary load profile predictions using forecast models and performance comparisons

During the same worst case scenario period (i.e. a month from mid. February to mid. March), heating load profile predictions using the Abs.Dev.EWMA and the NDFD

XML with 24hr projection are investigated. A large-sized sample office building ($4161m^2$) with twenty five thermal zones in Acrata is chosen as a test building. Average building mass that consists of exterior wall, interior wall, roof and floors is around 700 Kg/m^2. The occupancy profile and lighting schedule follow a typical office building profile (7am – 5pm with a 1 hour lunch break at noon) and peak building occupancy is 0.1 people per m^2. Occupants are assumed to be typical office workers (i.e. seated and light working), which corresponds to 120 W of heat gain. Computers are assumed to consume 140W and peak lighting density is 20 m^2 per square meter. Heating set point temperature is 20 °C during occupied hour and also has 18 °C of a set back during unoccupied hour.

Predicted heating load profiles by two methods are statistically compared with the heating load simulated with the actual weather observation. An interesting results is found that the heating load profile predicted with the Abs.Dev.EWMA has matched the simulated actual heating load profile slightly closer (with CV-RMSE 1.27) than that with the NDFD XML (with CV-RMSE 1.35) for this season, despite at least commensurable or better forecast performance in temperature and global horizontal radiation forecasts of the NDFD XML. Reasons for this and detailed analysis are discussed with examples of the following sample case study from Mar. 8th to Mar. 13th (Figure 5.10, 5.11 and 5.12).

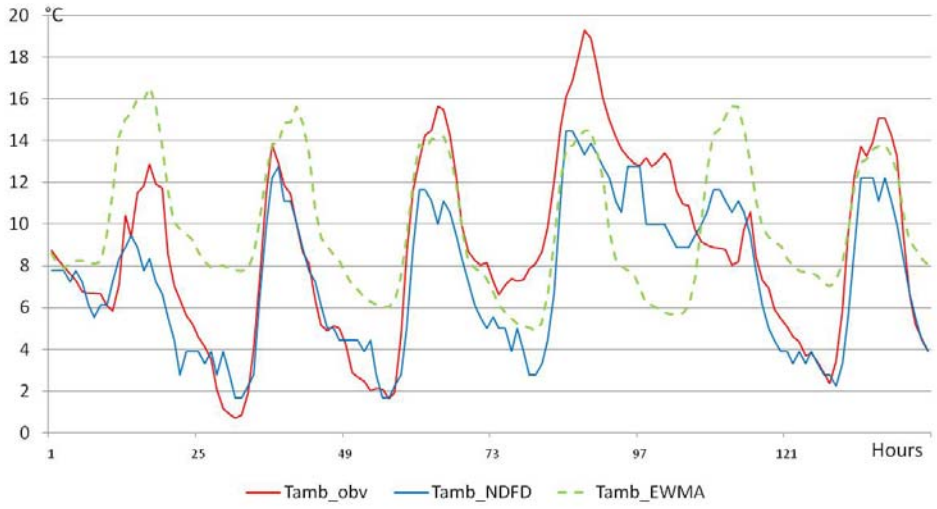

Figure 5.10 Comparisons of temperature profiles from Mar. 8th to Mar. 13th

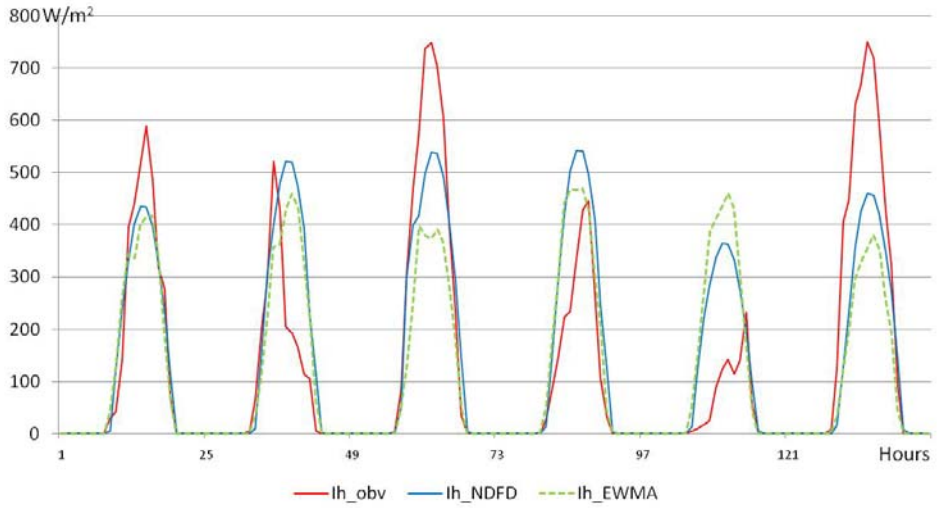

Figure 5.11 Comparisons of global horizontal radiation profiles from Mar. 8th to Mar. 13th

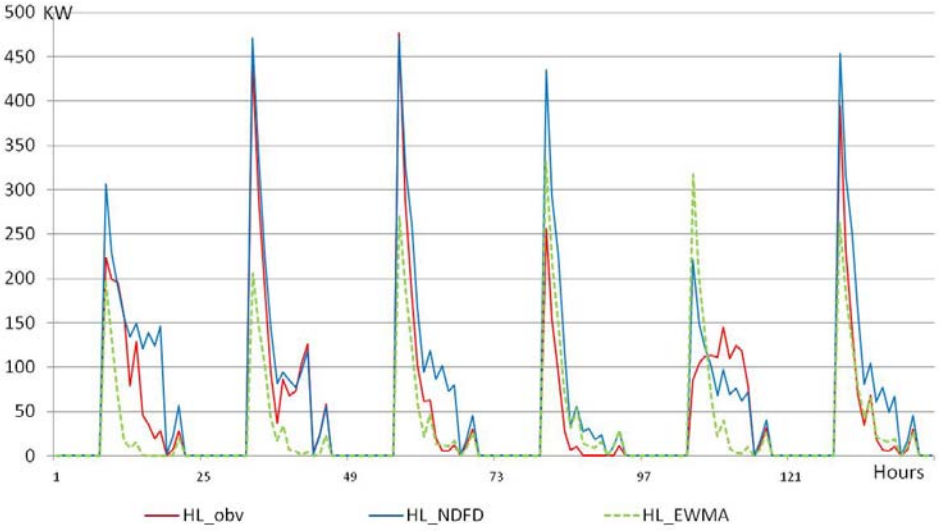

Figure 5.12 Comparisons of heating load profiles from Mar. 8th to Mar. 13th

- For global horizontal radiation prediction, as confirmed in the previous statistical analysis in section 5.9.3 a forecast by the NDFD XML is more prone to the actual observation than the abs.dev.EWMA is (Figure 5.11). This tendency apparently appears through the whole simulation period. As appeared in the Figure 5.11 and 5.12, however, the more accurate prediction of global horizontal radiation does not necessarily result in the more accurate prediction of the heating load profile. This is due to a relatively low contribution of the low global horizontal radiation

(109 W/m^2 on average) in Acarta during this season to the heating load. This observation indicates that i) during this season in Acarta, prediction accuracy of the ambient temperature is more sensitive to predict the heating load profile. This implies that ii) for summer or areas where solar radiation takes larger contribution of the heat gain, prediction accuracy of the global horizontal radiation would be more sensitive to predict the cooling load profile. In that case a forecast by the NDFD XML would result in a superior prediction performance of the cooling load profile.

- In predicting ambient temperature, it is found that any method that predicts closer to the actual extreme (i.e. highest and lowest) temperatures results in better prediction of the building load profile. (Figure 5.10 and 5.12).

- When the actual temperature profile is completely out of the shape and out of the range that cannot be bounded by the historical record, it is apparent that the forecast by the NDFD XML outperforms than the abs.dev.EWMA in catching up the actual sporadic temperature profile (March 11th and 12th in Figure 5.10).

5.11 Discussions

Statistical analyses and an application example of the building load profile predictions using three forecast methods have confirmed that short-term weather forecast using the NDFD XML is more capable of predicting erratic and sporadic characteristics of the weather compared to the other two historical archive based methods, in that

a. The proposed forecast method using the NDFD XML shows better performance in predicting global horizontal radiation despite its more erratic characteristics than ambient temperature, and

b. When ambient temperature behaves unexpectedly, the NDFD XML shows better performance than the historical archive based method.

To supplement the capability to predict erratic characteristics of the weather, in particular for the Moving Average method, previous studies have taken a superposition method that scales the (known) pattern to the extreme values provided from the online forecasts to account for "unexpected" characteristics of the weather (Seem and Braun 1991, Chen and Athienitis 1996, Florita and Henze 2009).

However such modification relying only on the online forecast still could be problematic. On March 10th in the Figure 5.10, for instance, the abs.dev.EWMA forecasts the daily high temperature almost closer to the actual, while the NDFD XML forecasts 4°C lower. If the forecasted profile of the abs.dev.EWMA is scaled according to the maximum temperature difference by the NDFD XML, the resulting predicted heating load would be higher than the actual.

As indicated in section 2.8.3.1 and section 2.9 when characterizing uncertainty sources according to the proposed frame, the randomness is more dominant and fatal to its uncertainty of the weather prediction. This is why it is recommended to represent the weather as a source of the scenario uncertainty if its prediction is used for any simulation or control applications.

As indicated in section 3.5.2 to capture both regular patterns and randomness of the scenario uncertainty, incorporating more data sources is recommended. Therefore when the short-term weather prediction is used, instead of a single source approach, a multi-source forecast method preferably including both the historical data-driven forecasts and the online forecasts is concluded to be an ideal solution.

5.12 Conclusions

This study has found that the short-term weather forecast capabilities of the NDFD XML allow it to be a valid replacement for the historic-data driven weather forecast methods. Its reliability (i.e. higher validation scores), availableness (i.e. almost at any location in the US continental with less than 1 hour interval updates), increasing functionalities (i.e. more and more significant weather variables and outlooks are added) and applicability (i.e. easy SOAP interface and time-series data) make itself more applicable to model-based control applications.

Also this study has shown that the short-term weather forecast of the NDFD XML is capable of predicting the erratic and sporadic characteristics of the weather with an increased accuracy compared to legacy historical data-driven forecast methods.

Since the weather is also one source of the scenario uncertainty, however, it still has strong random and discrete characteristics in nature despite its better prediction performance than others. To capture both regular patterns and randomness of the short-term weather, a multi-source forecast method including both the historical data-driven methods and the proposed online forecast method using the NDFD XML as independent events is concluded to be an ideal solution.

CHAPTER 6

CASE STUDY

6.1 Background and synopsis

This chapter introduces a case study of developing robust demand-side control strategies for both building thermal mass control and TES control. To highlight merits of the robust demand-side control strategy, a set of synopsis that could be an actual case is assumed.

Headquarter of Acme group, a nationally known IT consulting firm, is located in Atlanta, GA. The building is a large office with three stories built in 1970's. Due to increased energy price worldwide and an often overflowing peak power demands larger than its expected capacity during summer, Georgia power plans to launch a series of new utility plans that would have stronger rate incentives and penalties, e.g., higher on-peak and lower off-peak time-of-use (TOU) rates. Moreover, initiated by national movements it is heard that Georgia government considers The Carbon tax on an individual business unit, as such stiffly increasing operating cost seems to be unavoidable sooner or later. This tendency does not seem to be instantaneous but it will last in a stronger demand.

Thus board members of the Acme group ask Mr. Parker, an asset manager as well as a facility manager, to propose a resolution to avoid this increasing cost during cooling season or at least to compensate it by any means. Mr. Parker asks Green building technology group® (GBT) for a consultancy, who is a building energy consulting firm. The GBT comes up with two resolutions: the first one is demand-side controls both to reduce building net power demand and to increase the efficiency with given resources, and another measure is to install renewable energy sources additively to increase the supply, which will be eventually for the major self-supply.

Mr. Parker decides to choose the first choice by two reasons: i) demand-side control technologies can leverage utility incentives to the maximum, such that properly designed demand-side controls can compensate an increased on-peak rate more effectively. Even more this could lead to lower operating cost than current cost, thus finally demand-side controls will compensate first cost in the long run and ii) installing renewable energy systems may take more investment than the expected because a major renovation to the existing power supply stream and corresponding controls are required. Additionally either diminished power demand or shifted demand that a successful demand-side controls results in will increase an efficiency of renewable energy systems eventually when they are actually installed.

Upon the request of Mr. Parker, the GBT group proposes two demand-side control measures, a combination of building thermal mass control and use of active thermal energy storage (TES) systems, which is known to be the most effective demand-side controls. Also they suggest "robust supervisory MPC" as an operating control strategy. They have chosen this new control due to uncertainties around building and systems, thus the legacy deterministic optimal control, which is known to be the most advanced so far, may not be effective in some situations. Their reasoning includes i) this building is more than 35 year old and thus it is worn and leaky meanwhile experiencing numerous renovations, thus initial design condition may not be valid anymore. Therefore computational models of building and systems based on the design specifications would behave deviating from the actual physical behavior with a huge degree. ii) Due a nature of an IT consulting firm, occupancy level and the subsequent building usage schedule often tend to be off-the-typical. Moreover recent erratic weather conditions outlying from the typical weather observations add uncertainty.

The Acme group accepts this proposal and they decide to invest for TES systems, a dedicated TES chiller and auxiliary devices. And the GBT group undertakes developing robust demand-side supervisory control strategy that utilizes building thermal mass and

TES. Since renewable energy systems will not be installed yet, demand-side controls to be developed will pursue shedding and shifting of the demand first of all, which are primary objectives of general demand-side controls.

According to the proposed methodology of developing robust demand-side supervisory control strategy in chapter 4, next sections will describe key features of the Acme building and related HVAC&R systems first. After robust supervisory MPC strategy is developed, its control performance will be compared with conventional control strategies in varied and non-indigenous conditions to test their robustness.

6.2 Building descriptions

As shown in Figure 6.1 each floor consists of eight zones including a plenum, thus 24 zones in total. Each floor area is about 4161 m^2 in which core zone takes 2980 m^2 and perimeter zones take the rest of the area. Fenestration ratio is around 0.38 for each façade, and all glasses are double glazing filled with argon (4mm/16mm/4mm).

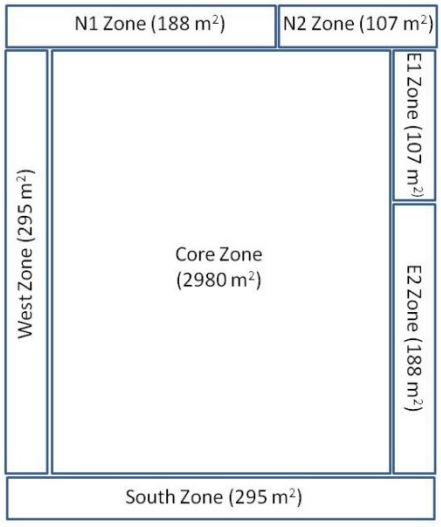

Figure 6.1 Typical floor plan of the Acme building

Constructions of structure are listed in the Table 6.1. Since a heavy building mass is prerequisite for a successful building thermal control, total density (i.e. total mass/total area) should be checked. Total density of this building is around 825.5 kg/m^2, which can be considered as a heavy mass.

Table 6.1 Constructions of building structure for the Acme building

Building structure	Construction layers (from outer to inner)
Exterior wall	AS01 (2mm steel siding); IN01 (8.2mm insulation); GP02 (16mm gypsum board)
Roof	AS01 (2mm steel siding); RF01 (141mm insulation); BR01 (10mm built-up roof)
Floor	CR01 (100mm concrete)
Ceiling	CL (Massless layer)
Slab floor	CR02 (203mm concrete); IN37 (110mm polystyrene)
Interior wall	GP06 (16mm gypsum sand aggregate); ST01 (89mm studs); GP06 (16mm gypsum sand aggregate)

6.2.1 Base case building usage scenario and utility rate plans

A typical office building usage scenario and lighting and equipment schedule have been surveyed as in Figure 6.2 and 6.3, and they will be used as a base case. Peak occupancy is 0.1 person/m^2. Each office occupant is thought to be a typical sedentary worker contributing 150 W of the internal gain, 50% of which is assumed to be sensible and the rest 50% is latent. Peak lighting density is 20 W/m^2 and peak equipment density is 12 W/m^2.

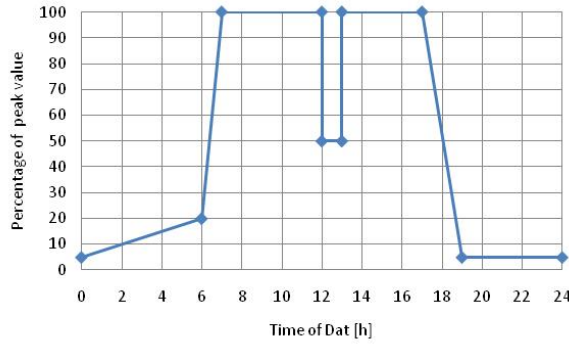

Figure 6.2 Weekday occuapncy schedule

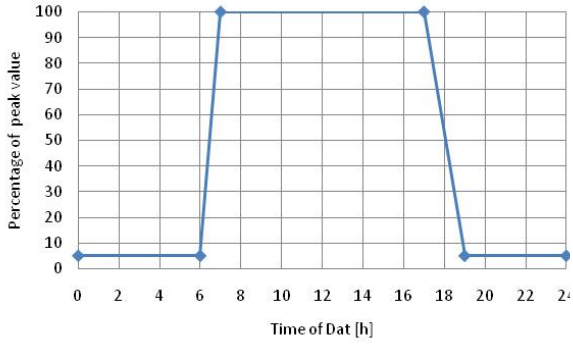

Figure 6.3 Weekday lihgting and equipment schedule

± 20% of variations in occupancy density is also observed due to nature of IT consulting company (e.g. most consultants are outsourced to client's offices except the supporting personnel). Hence occupancy level can be overestimated or underestimated

compared to the regular level from time to time. However it is not exactly known before it does happen, thus occupancy level is rather unpredictable.

Since Georgia power has not published future utility rate yet, robust MPC strategy will be developed under current rate plan. Current rate package is "Time of use – General service demand" (TOU-GSD-4) (Georgia Power 2010). It is composed of a base charge, TOU charge and demand charge combinations s of which seasonally vary. A sample rate of the TOU-GSD-4 is illustrated in Table 6.2 and Figure 6.4. Demand charge shall be levied to the highest 30-minute kW measurement during the specified period of each demand charge for the current month (Table 6.2).

Table 6.2 Summary of the rate structure in Georgia Power TOU-GSD-4

	June through September	October through May
Base charge	$181	$181
Energy charge (TOU)	On-peak (weekday 2-7pm) : 10.7639¢/kWh Shoulder (weekday 12-2pm and 7-9pm) : 5.1646¢/kWh Off-peak (except on-peak and shoulder) : 1.9393¢/kWh	1.9393¢/kWh
Demand charge	On-peak (weekday 2-7pm) : $12.93/kW Economy (except on-peak) : $4.32/kW	$4.32/kW

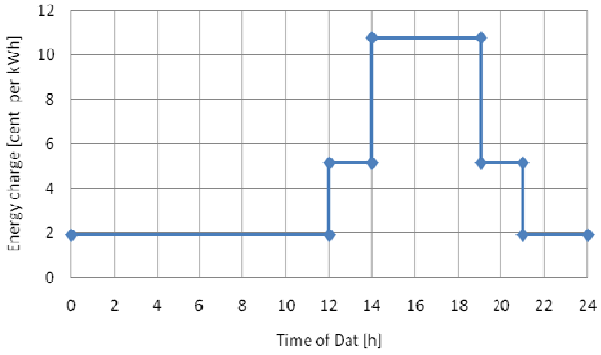

Figure 6.4 TOU rate from June to September

6.3 System descriptions

Fan coil units (FCU) with four pipes, i.e. a pair of supply and return pipes for chilled water and hot water, respectively, condition zones. Each zone has multiple FCUs and the number of FCUs is decided by design cooling load of each zone and capacity of a FCU. Figure 6.5 describes how FCU is controlled to meet the assigned zone set point temperature by means of manipulating fan speed and inlet water flow rate. Since a relatively small volume of local inlet air is conditioned through heat exchanger coils in terminal unit, FCU does not require colder or hotter supply water than generic central air handling unit (AHU) does, i.e. low heat system. Typically the required chilled water temperature is around 7-12°C, and the required hot water temperature is around 49-60°C. These "low heat" temperatures indicate that a chilled water storage system, outlet water temperature of which (4-7 °C) is typically higher than that of ice storage system would be able to provide a good performance with use of FCUs.

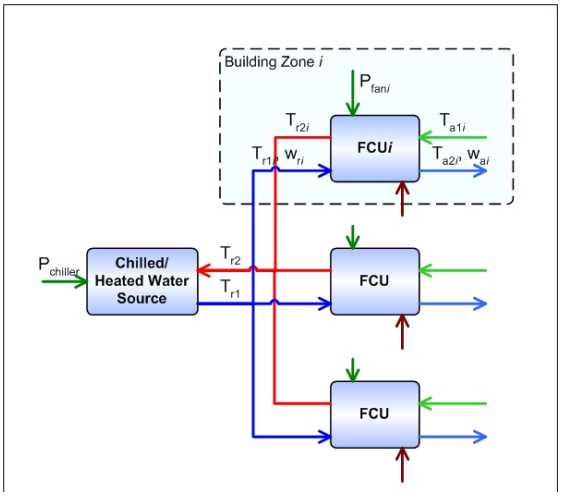

Figure 6.5 FCU conditions the inlet air with circulating chilled or hot water provided from central plants

Central plants, generally chillers and boilers, provide chilled and hot water. Figure 6.7 depicts only cooling plants in which this study is interested. Central cooling plants include the existing main chiller (nominal capacity = 500 kW), a new TES chiller (nominal capacity = 160 kW) and a new TES (nominal capacity = 1600 kWh). As shown

in Figure 6.7, the TES chiller is dedicated to the TES, and combinational operation between the main chiller and the TES serves building load. They are sized based on annual analysis that shows a building design cooling load of 440 kW (Figure 6.6), and it is assumed that 10 hour operation of TES (≈ 160kW*10hr) could cover 50% of the cooling load. Both chillers have a constant coefficient-of-performance (COP) of 3 that a bit exceeds the ASHRAE Standard 90.1-2004 minimum requirement of 2.80.

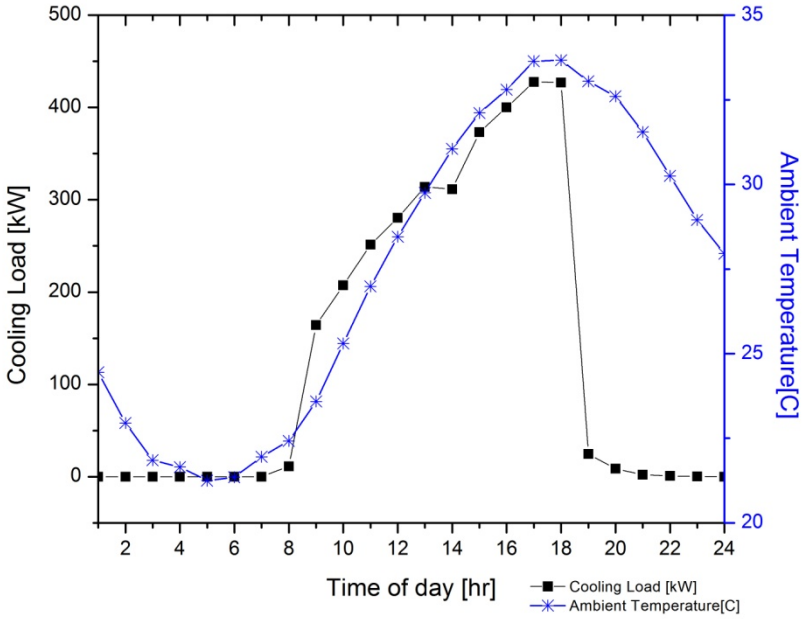

Figure 6.6 Building design cooling load on July 21st

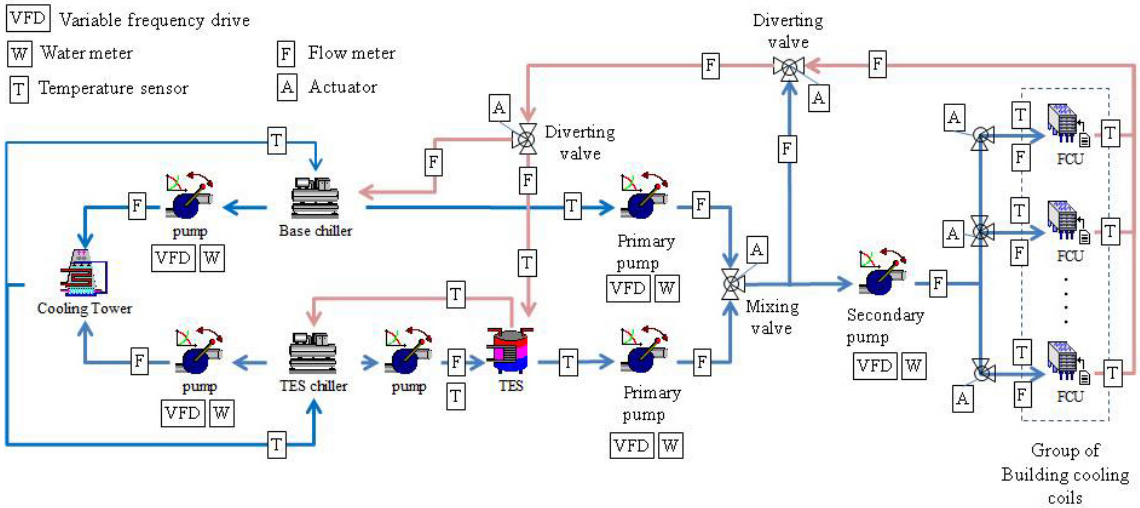

Figure 6.7 HVAC&R system schematic

6.4 Development of simulation and control models

The GBT develops simulations models of the Acme building and systems with the previously surveyed information. The simulation models, in particular, include models for controls of the building thermal mass and TES, and TRNSYS is used to model them. Herein the GBT firstly reviews physical modeling theories of TRNSYS component models in subsequent sections in order to seek for how control models can be efficiently developed in TRNSYS.

6.4.1 Modeling building

The GBT first models the Acme building in EnergyPlus and then they develop TRNSYS model to validate the TRNSYS model compared to the EnergyPlus model (Appendix A). The building model is built on with a typical multi-zone building component (Type 56). Detailed theories about Type 56 can be found in TRNSYS 16 document. Here a fundamental mathematical frame is summarized as described below in Figure 6.8 and a series of equations from (6.1) to (6.5).

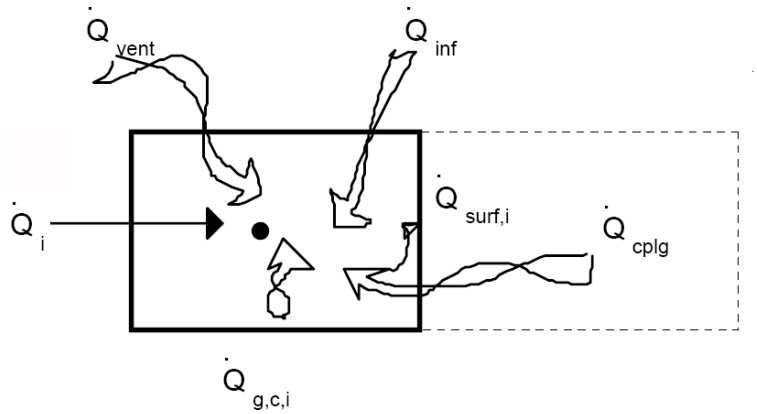

Figure 6.8 Heat balance on the zone air node

The rate of change of internal energy for thermal zone is equal to the net heat gain, therefore their relations are expressed by the following equations.

$$C_{zi}\frac{dT_i}{dt} = \dot{Q}_i \tag{6.1}$$

$$\dot{Q}_i = \dot{Q}_{surf,i} + \dot{Q}_{inf,i} + \dot{Q}_{vent,i} + \dot{Q}_{g.c,i} + \dot{Q}_{cplg,i} \tag{6.2}$$

where C_{zi} denotes the thermal capacitance of zone i; $\dot{Q}_{surf,i}$ denotes the transmission or delayed release of solar gains from all surfaces of zone i; $\dot{Q}_{inf,i}$ denotes the infiltration gains (air flow from outside only); $\dot{Q}_{vent,i}$ denotes the ventilation gains (the air flow from a user-defined sources like an HVAC system); $\dot{Q}_{g.c,i}$ denotes the internal convective gains (by people, equipment, illumination, and radiators etc.); and $\dot{Q}_{cplg,i}$ denotes the gains due to connective air flow from zone i or the boundary condition.

Equation (6.1) indicates that the net heat gain $\dot{Q}_i$ is a function of $T_i$and the temperature of all other zones adjacent to zone i (including exterior). Heat fluxes through current internal wall surfaces depend on a history of past inside and outside air and surface temperatures as well as inside and outside heat fluxes. Therefore transient response of the building envelope is typically modeled by transforming the heat diffusion equation:

$$\frac{\partial T_z}{\partial t} = \alpha\frac{\partial^2 T_z}{\partial x^2} \tag{6.3}$$

into a conduction transfer function, where the inside and the outside surface heat fluxes are determined with surface temperatures and coefficients of the time series (a,b,c, and d) as illustrated in Figure 6.9 and time series equations (6.4) and (6.5), where k refers to the term in the time series.

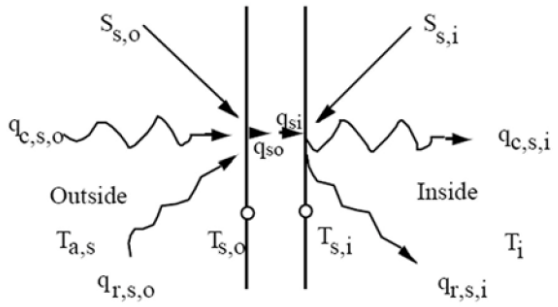

Figure 6.9 Surface heat fluxes and temperatures

$$\dot{q}_{s,i} = \sum_{k=0}^{n_{bs}} b_s^k \, T_{s,o}^k - \sum_{k=0}^{n_{cs}} c_s^k T_{s,i}^k - \sum_{k=1}^{n_{ds}} d_s^k \, q_{s,i}^k \tag{6.4}$$

$$\dot{q}_{s,o} = \sum_{k=0}^{n_{as}} a_s^k \, T_{s,o}^k - \sum_{k=0}^{n_{bs}} b_s^k T_{s,i}^k - \sum_{k=1}^{n_{ds}} d_s^k \, q_{s,o}^k \tag{6.5}$$

6.4.2 Passive building thermal mass control: zone temperature controls by modulating set-point temperature

Passive building thermal mass control modifies the power demand by means of modulating set-point temperature of zones. This modulation eventually determines the energy requirement for zones. The following paragraphs explain how this process is modeled and combined with the building model illustrated in Equation (6.1).

Heating or cooling energy flow is directly connected to zone air temperature node. Since terminal units (e.g. VAV box or FCU) typically supply heating or cooling energy, they can be coupled to zones as either internal convective gains or ventilation gains. Thus Equation (6.1) can be rewritten to include heating or cooling energy P as Equation (6.6),

$$C_i \frac{dT_i}{dt} = \dot{Q}_i - \ P_i \tag{6.6}$$

The temperature change of the zone air, when heating or cooling energy is supplied, is assumed to be linear over the time step. If enough energy is supplied to

maintain the final zone temperature at $T_{set,i}$, then the final and averaged zone temperatures are known. Assuming a constant power is supplied over the time step, this assumption leads Equation (6.6) to be discretized as the following Equation (6.7),

$$\frac{C_i}{\Delta t}\left(T_{set,i} - T_{\tau-\Delta t}\right) = \sum_j \dot{Q}_i^j - \bar{P}_i \tag{6.7}$$

where $\dot{Q}_i^j$ denotes a component of heat gains for zone i as in Equation (6.2); $T_{\tau-\Delta t}$ denotes the initial temperature when time τ starts.

For zone i that requires heating or cooling, the energy required to maintain the final zone temperature at the set-point temperature is determined. Thus if the required energy is less than the available maximum power of terminal unit, then the zone is considered to be "controlled" and terminal units no longer output heating or cooling power. Otherwise, terminal units output their maximum power in order to meet the required energy in the long run.

For Acme building case study, a design of the set-point temperature control follows the suggested building thermal mass control models (section 4.2). As illustrated in Figure 6.10, the exponentially decreasing set-point pre-cooling (EDPC) at mode 1 and the demand-limiting set-point release controls (DMR) at mode 3 are applied in each building mode identified by a combination of occupancy schedules and utility rate structure. At mode 2 and mode 4 constant set-point pre-cooling and constant set-point release are assumed, respectively.

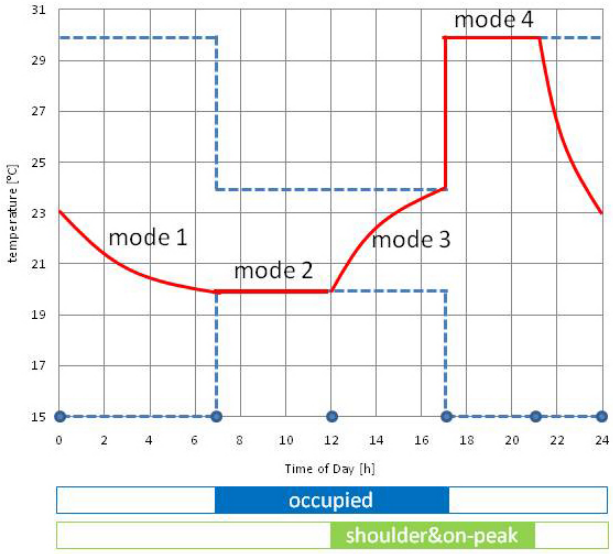

Figure 6.10 Set-point temperature controls per building mode

6.4.3 Modeling HVAC&R systems

As illustrated in Figure 6.7, main cooling plants include main chiller (Type 666), TES chiller (Type 666), TES (Type 533) and cooling tower (Type 51). Auxiliary systems include pumps (Type 742) and valves (Type 649), and FCUs are used as terminal units. FCUs and its local controller are developed based on manufacturer's specifications, while others are modeled using off-the-shelf library components of TRNSYS. Several important points and criteria of modeling three main components (i.e. FCU, chiller and TES) are briefly emphasized in following sections. More detailed engineering and mathematical principles can be found at TRNSYS reference documents.

6.4.3.1 Modeling FCU

Typically fan coil units are designed to satisfy the sensible thermal load only. Latent thermal load is satisfied by an air handler dedicated to supply ventilation air. This is to prevent condensation at the fan coil units and to avoid the complexities of installing a drain system. Sensible cooling capacity (Q_{td}) for a fan coil unit determined based on engineering fundamentals (ASHRAE, 2008) is given as:

$$Q_{td} = \dot{m}\, C_p\, (T_{in.air} - T_{in.water}) E_a \quad (6.8)$$

where $\dot{m}$, C_p, $T_{in.air}$, $T_{in.water}$, E_a denote the air flow rate, the specific heat of humid air, the coil entering air temperature, the coil entering water temperature and the air-side effectiveness for counter flow heat exchangers, respectively.

Based on the above model, there are 3 handles to change air temperature in a space: air flow rate (fan speed), water mass flow rate (valve position) and coil entering water temperature (supply water temperature). Typically these can be obtained from performance specification of a FCU.

The presented below is a snap shot of a FCU lookup table taken from cut sheets supplied by the manufacturer. Such lookup tables provide a convenient method to determine the performance of the fan coil units and hence the control action (fan speed, valve position and coil entering water temperature) required to provide a specific quantity of thermal energy. For example, to determine fan speed required to deliver 520W cooling energy, the supply water flow rate 200 kg/h at 16°C (non-condensing operation) requires fan speed 3 based on the lookup table for Size 630 in Figure 6.11.

Size 630 - 4-pipe-system - cooling and heating

n [-]	V [m³/h]	L_{A18} [dB(A)]	L_{wA} [dB(A)]	$Q_k/\Delta t$ [W/K]	Q_k^1 [W]	$Q_h/\Delta t$ [W/K]	$w_{ok}/\Delta p_w$ [kg/h]/[kPa]	$w_{oh}/\Delta p_w$ [kg/h]/[kPa]	P_{el} [W]
I	165	25	31	39	390	33	200/10	100/3,5	15
II	220	30	36	44	440	36			17
III	290	35	41	52	520	43			20
IV	350	39	45	58	580	47			22
V	410	45	51	66	660	52			27

Size 800 - 4-pipe-system - cooling and heating

n [-]	V [m³/h]	L_{A18} [dB(A)]	L_{wA} [dB(A)]	$Q_k/\Delta t$ [W/K]	Q_k^1 [W]	$Q_h/\Delta t$ [W/K]	$w_{ok}/\Delta p_w$ [kg/h]/[kPa]	$w_{oh}/\Delta p_w$ [kg/h]/[kPa]	P_{el} [W]
I	200	24	30	45	450	38	200/12	100/4	15
II	280	29	35	55	550	44			17
III	360	34	40	64	640	50			20
IV	430	39	45	71	710	57			22
V	510	45	51	80	800	62			27

Figure 6.11 An example of a look up table to determine the control actuation required for the fan coil units (LTG 2010)

6.4.3.2 Modeling chiller

A chiller model (e.g. Type 666) is a vapor compression style water cooled chiller. It relies on the catalog data that manufacturer provides to determine chiller performance. At a given time step, the chiller model first sends a call with the current cooling water temperature and the chilled water set point temperature, then it obtains in return the COP ratio and capacity ratio for those conditions. The chiller's nominal COP and the capacity at current conditions are calculated by multiplying each ratio with the rated value.

Operating the cooling equipment at part-load conditions is associated with an energy penalty that can be described by Fraction of full load power (FFLP):

$$P = \frac{Capacity}{COP} FFLP \tag{6.9}$$

FFLP is a typically quadratic function of the part-load ratio (PLR) as in Equation (6.10), and the value at current condition can be obtained from the manufacturer-provided data sheet in case of Type 666:

$$PLR = \frac{\dot{Q}_{load}}{Capacity} \tag{6.10}$$

where $\dot{Q}_{load}$ denotes the cooling load and Capacity denotes the chiller capacity.

6.4.3.3 Modeling TES

TES (Type 533) chosen for modeling the TES in Acme building is a fluid-filled and constant volume storage. The fluid in the storage tank interacts with outside environment (i.e. heat loss or gain) and with flow streams that pass into and out of the storage tank. The tank is divided into isothermal temperature nodes of equal volume to model stratification in storage tanks. Each thermal node interacts thermally with the nodes above and below through fluid conduction and fluid movement. The differential equations for the tank node j can be written as,

$$\frac{dT_{tank.j}}{dt} = \frac{(Q_{in.tank.j} - Q_{out.tank.j})}{C_{tank.j}} \tag{6.11}$$

where $Q_{in.tank.j}$ and $Q_{out.tank.j}$ denote the heat transfers at node j, respectively. And C is the thermal capacitance at node j.

Inlet flow and outlet flow can be placed in two nodes separately. At node j, therefore the heat gain and loss by inlet and outlet flows (driven by the charge and discharge flow rate C_k^u and D_k^u), auxiliary heat gains, losses to the environment, conduction loss and mixing gain/loss between nodes account for the heat transfer difference ($Q_{in.tank.j} - Q_{out.tank.j}$). This can be further described as a function of the ambient temperature, the inlet fluid conditions and flow rates. Equation (6.11) is then replaced with,

$$\frac{dT_{tank.j}}{dt} = aT_{tank.j} + b \tag{6.12}$$

where assuming that b is constant over the time step, $T_{tank.j}^{final}$ is defined by a function of $T_{tank.j}^{initial}$ and $T_{tank.j}^{avg}$. Then values of a and b change until two temperatures converge.

6.4.3.4 Active TES control: modulating charge flow rate and discharge flow rate of the TES

Recall section 4.3.4, controls for the TES through charge and discharge flow rate can have diverse design alternatives even with the same constraints. For example, both charge rate and discharge rate can be variable at every time step k, which indicates that the number of control variables u_k can be up to the number of control time steps within control horizons, e.g. 10hr of control horizon/0.5 hr of control time step = 20 sets of control variables, thus $\{u_1, u_2, \ldots, u_{20}\}$. A merit of this design is, of course, that it is closer to the mathematical optimum, whereas a drawback is that control problem

becomes more complex. A choice of control design, therefore, should depend on types and purposes of control applications and especially control efficiency.

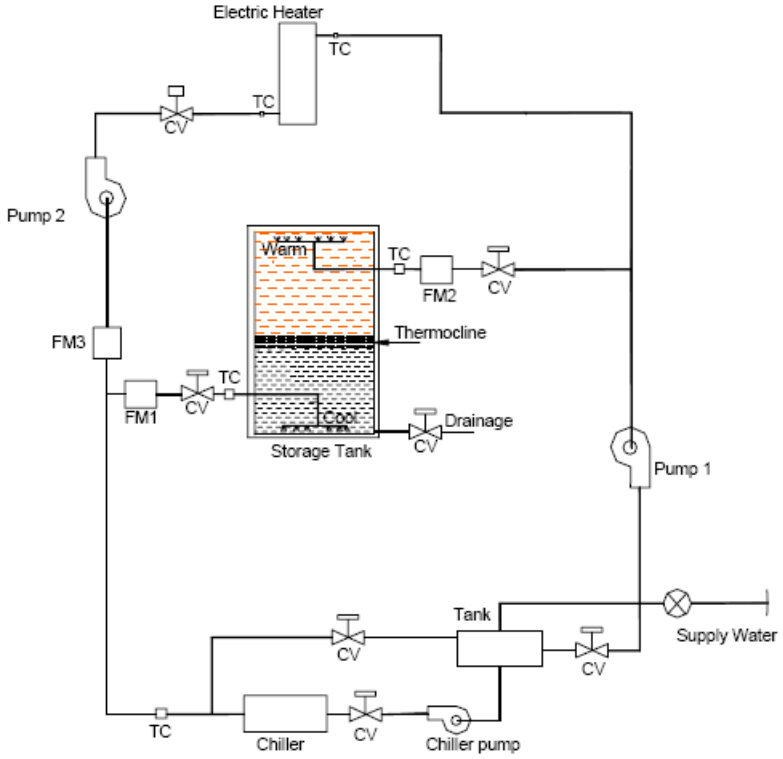

Figure 6.12 Charging and discharging operations of the TES (Karim 2011)

Heuristics of the GCT on TES operations has concluded several insights. Since the TES pursues load shifting under the TOU plan, an additional rule sets for variations of TES control strategies for each building control mode is employed as follows:

a. TES is charged only during off-peak period (i.e. mode 1 and 4)

b. TES is discharged only during on-peak period (i.e. mode 2 and 3)

This strategy leads to place C^u (Equation 4.4) at mode 1 and/or 2, and D^u (Equation 4.5) at mode 3.

As indicated in section 4.3.4 discharging cooling energy critically drives demand control performance of the TES, thus discharging control should be carefully designed in response to variations of cooling load and available inventory of TES. Then charging

control can be relatively relaxed than discharging control in order to reduce a complexity of controls. This strategy has resulted in the following designs for TES control actions.

a. Sub-control variables of D^u include a vector of discrete discharge flow rates at each time step k
b. Sub-control variables of C^u include start time or end time of charging and constant charge flow rate.

This design is subjected to the following constraints:

- Charge flow rate C_k^u is constant and positive real;
- Start time and end time of charging should range within the off-peak period;

  $t_{\text{off-peak.start}} \leq k \leq t_{\text{off-peak.end}}$ and $k_{\text{charge.start}} \leq k_{\text{charge.end}}$

- Discharge flow rate D_k^u is discrete per each time step k and positive real;
- Start time and end time of discharging should range within occupied and on-peak & shoulder periods;

  $k=k_{init} + \Delta t*j \leq k_{end}$ $j=\{0,1,\ldots, n\}$ where $k_{init} = \text{Max}(t_{occupied}, t_{shoulder})$ and $k_{end} = \text{Min}(t_{occupied}, t_{on\text{-}peak})$

- Sum of the charge flow rate should equal to sum of the discharge flow rate in order to avoid sparing more cooling energy than the required.

$$\sum_{k=charge.start}^{discharge.start} C_k^u = \sum_{k=discharge.start}^{discharge.end} D_k^u h \qquad (6.13)$$

6.4.4 Choice of planning horizon (pH) and execution horizon (eH)

According to step 7 for choosing adequate control horizons (Section 4.4.9), the GBT chooses 24hr for the planning horizon (pH) by several reasons: i) a series of studies by Henze's group (Henze, Felsmann et al. 2004; Henze, Kalz et al. 2005; Henze 2008) suggested a 24 hour of planning horizon for model-based control applications in which building mass is involved and ii) control profiles of both building thermal mass control and TES are developed for each building mode and an effective group of such building modes is decided based on an interval of 24hr.

Then the GBT has to decide the execution horizon and frequency of executions. A robust control strategy for the Acme building will be developed with a set of 24hr-ahead weather forecasts that have satisfactory accuracies (Section 5.9.3), highly feasible building usages scenarios and information of other uncertainties. Moreover robust control strategy will be designed such that its internal robust mechanism makes control performance stable despite uncertainties. Therefore control states that external scenarios, in particular, can change drastically may not need to be updated as frequent as real-time control applications do. The GBT made a decision that the execution horizon can be extended as long as the planning horizon (i.e. eH=24hr).

The energy management system (EMS) of the Acme building will execute the planned control strategy with a regular interval of 24hr at every 5pm when the control mode 4 starts. 5 pm of the day is chosen because the control mode 4 indicates when building is unoccupied but still in on-peak periods, thus set-point temperature must be released. In other words, no control action is required at the mode 4. Therefore it is a good time of the day to plan control strategies for next planning horizon and to execute the resulting control strategy without being strictly tied up with computation time.

6.4.5 Simulation process

The GBT develops a TRNSYS simulation model that contains the Acme building, related cooling plants, HVAC&R systems, and control systems based on the information

described in the previous sections. Figure 6.13 illustrates the overall simulation process that features i) optimizations of control variables (red letters) through the entire systems and their associations with their host components/systems and ii) processes that driving forces of a system (e.g., thermal loads) are delivered to subsequent processes or sub-components.

This simulation model is constructed with respect to the proposed framework of developing robust supervisory MPC. Here relevant uncertainty sources have been identified (Section 2.8 and Appendix B) and characterized according to three dimensions of uncertainty (Section 2.9). Then uncertainties are described and modeled in support of the SysML-TRNSYS transformation (Section 3.4, 3.5 and 3.6). Then the next step is to quantify uncertainties according to the proposed process (Section 3.7) that will be illustrated next.

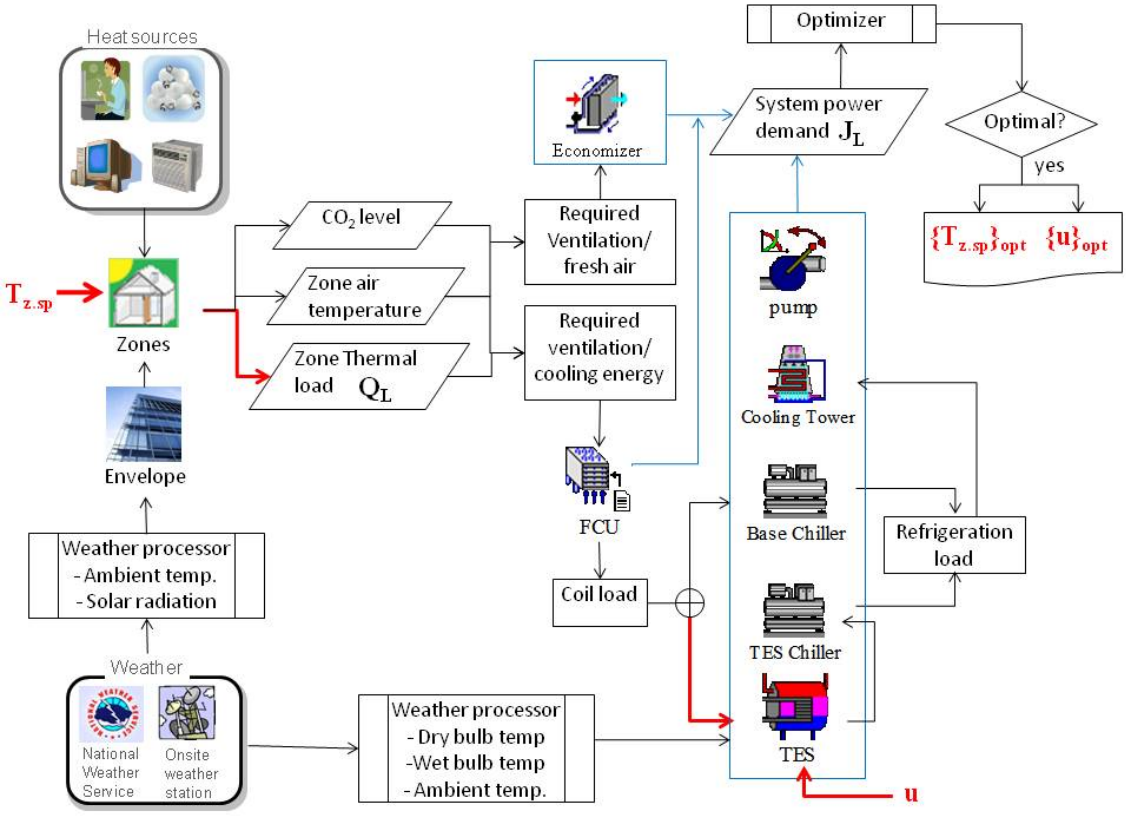

Figure 6.13 Simulation process highlighting controls and their flows

where $T_{z.sp}$ and u denote the zone set-point temperature and the charge/discharge flow rate of the TES, respectively

6.5 Quantifying uncertainty for the Acme building

Quantifying uncertainty within the TRNSYS model of the Acme building follows the process described in section 3.7. Three methods of quantifying uncertainties are recalled and summarized as below.

a. Latin hypercube sampling to quantify specification uncertainty
b. Scenario robust optimization to quantify scenario uncertainty
c. Bias and random noise filter components attached to system outputs of the TRNSYS model to quantify calibration uncertainty

6.5.1 Quantification of specification uncertainty

Detailed sources of specification uncertainty are subcategorized into four groups: building material properties (M), thermal zone properties (Z), built environment & external environment (E) and power efficiency & degradation of HVAC&R systems (S).

In addition, their uncertain ranges and base values are indicated. It is noted that these base values are set to estimate uncertain ranges, not in order to give a reference that a deterministic analysis could result in. The following tables (from Table 6.3 to 6.6) have listed identified uncertainty sources and related uncertain ranges, base values and referenced literature.

a. Uncertainties in building material properties (M)

Table 6.3 Uncertainties in building material properties and their range

	Uncertainty sources	Unit	Base	Min.	Max.	Ref.
M1	EXTWALL.AS01.conductivity	KJ/hr m K	162	153	170	McDonald 2002
M2	EXTWALL.AS01.capacity	KJ/kg K	0.4187	0.367	0.470	
M3	EXTWALL.AS01.density	kg/m^3	7688.9	7612	7765	
M4	EXTWALL.IN01.conductivity	KJ/hr m K	0.156	0.148	0.164	
M5	EXTWALL. IN01.capacity	KJ/kg K	0.837	0.734	0.940	
M6	EXTWALL. IN01.density	kg/m^3	96.1	95.1	97.1	
M7	EXTWALL.GP02.conductivity	KJ/hr m K	0.577	0.548	0.606	
M8	EXTWALL.GP02.capacity	KJ/kg K	0.8374	0.735	0.940	
M9	EXTWALL.GP02.density	kg/m^3	800.9	792	808	
M10	INTWALL.GP06.conductivity	KJ/hr m K	2.9508	2.803	3.098	
M11	INTWALL.GP06.capacity	KJ/kg K	0.8374	0.735	0.940	
M12	INTWALL.GP06.density	kg/m^3	1681.9	1665	1698	
M13	INTWALL.ST01.conductivity	KJ/hr m K	1.696	1.611	1.781	
M14	INTWALL. ST01.capacity	KJ/kg K	1.036	0.909	1.163	
M15	INTWALL. ST01.density	kg/m^3	49.1	48.6	49.6	
M16	FLOOR.CR01.conductivity	KJ/hr m K	6.2303	5.919	6.542	
M17	FLOOR. CR01.capacity	KJ/kg K	0.837	0.734	0.940	
M18	FLOOR. CR01.density	kg/m^3	2242.6	2220	2265	
M19	ROOF.RF01.conductivity	KJ/hr m K	0.156	0.148	0.164	
M20	ROOF. RF01.capacity	KJ/kg K	0.837	0.734	0.940	
M21	ROOF. RF01.density	kg/m^3	96.1	95.1	97.1	
M22	ROOF.BR01.conductivity	KJ/hr m K	5.8506	5.56	6.14	
M23	ROOF.BR01.capacity	KJ/kg K	1.4654	1.28	1.649	
M24	ROOF.BR01.density	kg/m^3	1121.3	1110	1132.5	
M25	SLABFLOOR.IN37.conductivity	KJ/hr m K	0.1246	0.118	0.131	
M26	SLABFLOOR.IN37.capacity	KJ/kg K	1.2142	1.065	1.363	
M27	SLABFLOOR.IN37.density	kg/m^3	28.8	28.5	29.1	
M28	SLABFLOOR.CR02.conductivity	KJ/hr m K	6.2303	5.919	6.542	
M29	SLABFLOOR. CR02.capacity	KJ/kg K	0.837	0.734	0.940	
M30	SLABFLOOR. CR02.density	kg/m^3	2242.6	2220	2265	
M31	CEILING.resistance	hr m^2 K/KJ	0.11	0.105	0.116	
M32	WINDOW.Glazing.U_value	W/m^2K	1.4	1.26	1.54	
M33	EXTWALL.Solar Absorptance	-	0.65	σ= 0.04	σ=0.04	
M34	ROOF.Solar Absorptance	-	0.6	σ= 0.04	σ=0.04	

b. Uncertainties in thermal zone properties (Z)

Table 6.4 Uncertainties in thermal zone properties and their range

	Uncertainty sources	Unit	Base	Min.	Max.	Ref.
Z1	Infiltration air change rate (perimeter)	ACH	0.3*	σ= 0.1	σ=0.1	Gowri, Winiarski et al. 2009 and McDonald 2002
	Capacitance:: ratio f	-	9**	3	16.02	Hu 2009 and TRNSYS manual
	Capacitance	kJ/K	12xVol	4.8xVol	20.4xVol	
Z2	ZoneF. Capacitance	kJ/K	9799.1	3919.6	16678.1	
Z3	ZoneB1.Capacitance	kJ/K	3559.0	1423.6	6057.5	
Z4	ZoneR1.Capacitance	kJ/K	6240.0	2496.0	10620.5	
Z5	ZoneR2.Capacitance	kJ/K	3559.0	1423.6	6057.5	
Z6	ZoneB2.Capacitance	kJ/K	6240.0	2496.0	10620.5	
Z7	ZoneL. Capacitance	kJ/K	9799.1	3919.6	16678.1	
Z8	ZoneI. Capacitance	kJ/K	98893.0	39557.4	168316.7	
Z9	ZonePNL. Capacitance	kJ/K	4586.1	1834.4	7805.6	
Z10	ZoneELV. Capacitance	kJ/K	29567.1	11826.8	50323.3	

* It is calculated using DOE-2 infiltration model (Gowri, Winiarski et al. 2009).
** It is chosen by performance benching marking of TRNSYS model compared to performance of EnergyPlus model (Appendix A).

c. Uncertainties in built environment & external environment (E)

Table 6.5 Uncertainties in built environment and external environment and their range

	Uncertainty sources	Unit	Base	Min.	Max.	Ref.
E1	External convective heat transfer coefficient (Palyvos's model)	%	0%	-20%	20%	Palyvos 2008
E2	Internal convective heat transfer coefficient (ceiling)	kJ/hr m^2K	1.8	1.08	2.88	de Wit 2001, Beausoleil-Morrison 1999
E3	Internal convective heat transfer coefficient (floor)	kJ/hr m^2K	10.8	10.8	18	
E4	Internal convective heat transfer coefficient (interior wall)	kJ/hr m^2K	9.0	5.72	14.7	
E5	Wind reduction factor :: constant K	-	0.35	0.35	0.43	Orme 1994, de Wit 2001 and Moon 2005
E6	Wind reduction factor :: exponent α	-	0.25	0.22	0.28	
E7	Ground albedo	-	0.17	0.15	0.3	de Wit 2001
E8	Soil density	kg/m^3	1700	1683	1717	McDonald 2002
E9	Soil conductivity	kJ/hr m K	6.3	5.99	6.62	
E10	Soil specific heat	KJ/kg K	1.705	1.50	1.91	

d. Uncertainties in power efficiency and degradation of HVAC&R systems (S)

Table 6.6 Uncertainties in power efficiency and degradation of HVAC&R systems and their range

	Uncertainty sources	Unit	Base	Min.	Max.	Ref.
S1	Primary chiller degradation coefficient	-	0.25	0.066	0.26	Goldschmidt 1980
S2	TES chiller degradation coefficient	-	0.25	0.066	0.26	Goldschmidt 1980
S3	Cooling tower fan efficiency	-	0.75	0.55	0.75	Monroe 1978
S4	FCU electricity consumption tolerance*	%	0%	-10%	+10%	Manufacture's specification
S5	TES heat loss coefficient	kJ/hr m^2K	1.19	0.155	1.58	Mather 2002, Wang 2009
S6	TES additional thermal conductivity	kJ/hr mK	0.9	0.83	0.97	Mather 2002
S7	Centrifugal Pump efficiency	-	0.85	0.60	0.85	DOE and Hydraulic Institute 1990
S8	Pipe heat loss coefficient	kJ/hr m^2K	15.8	15.0	16.6	McDonald 2002

* Typically manufacturers provide the performance testing guide-lines and specify the testing criteria for testing engineers.

6.5.2 Quantification of calibration uncertainty

In general uncertainty sources concerned in "port" properties are classified as calibration uncertainty. In the supervisory controls of building and HVAC&R systems, such uncertainty sources are quantified in either flow port or control port (Section 3.7.4).

A various sets of flow properties can define flow characteristics, however only calibration uncertainties that are relevant to the current system configuration of the Acme building and systems, and also quantifiable in the current simulation tool should be quantified. For example, the return chilled water from the Acme building has flow properties such as temperature, density, pressure, flow rate and etc. Since a chiller model is only interested in temperature and flow rate of the return chilled water, uncertainties about those two properties need to be quantified.

Control port largely includes sensor readings and control (or actuation) signals. Different from local controllers, control signals in supervisory controls refer to set-points

or operating sequences of devices. Therefore it is unlikely that uncertainties are observed in control signals of the supervisory controls. This study is more interested in uncertainties in sensors.

As shown in Table 6.7 four calibration uncertainty sources are identified for Acme building. It should be emphasized again that the range within which each source varies is still in the normal operating condition. In other words TAB (Testing and Balancing) validate each source and they are in the range of engineering tolerance. Refer to Appendix B for details.

Table 6.7 Calibration uncertainties and their range

	Uncertainty sources	Unit	Base	Min.	Max.	References
P1	Airflow rate of supply and return	m^3/h	0%	-10%	10%	PECI 2008
P2	Temperature	°C	0%	-1%	1%	PECI 2008
P3	Water flow rate of supply and return	m^3/h	0%	-10%	10%	PECI 2008
P4	Hysteresis in sensor reading	-	0%	-3%	3%	PECI 2008

6.5.3 Identification of daily external scenarios and quantification of scenario uncertainty

A typical summer day is chosen as the index day. Possible daily scenarios for the index day consist of i) daily occupancy profiles (Figure 6.14) and resulting lighting and equipment profiles and ii) daily weather forecast profiles for three important weather variables such temperature (Figure 6.15), solar irradiation and relative humidity.

Three daily occupancy profiles are surveyed from observations and facility managers' opinions. In Figure 6.16, the blue line refers to a regular profile (MO) while the red-dotted and the green-dotted refer to 20% more (HO) and 20% less (LO), respectively. Probabilities that each daily profile is observed are set to equal (i.e. 1/3).

Two weather forecasts are employed: the abs.dev.EWMA and the NDFD-XML (Chapter 5). Each forecast represents historical data based forecast and online weather forecast, respectively. For the index day, the abs.dev.EWMA projects a typical summer

day in Atlanta (W2: red-dotted), whereas the NDFD-XML projects higher max temperature (W1: sky-dotted).

Combinations of three building usage profiles {LO, MO, HO} and two weather profiles {W1, W2} result in total six scenarios that will be evaluated in the stochastic optimization:

$$\Sigma \in \{W1, W2\} \times \{LO, MO, HO\} \tag{6.17}$$

The W2MO is chosen for the reference scenario where comparison studies are necessary.

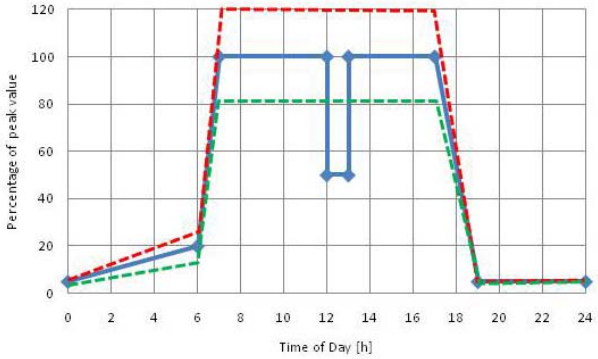

Figure 6.14 Three occupancy profiles identified on the index day: HO (higher occupancy), MO(medium occupancy) and LO(lower occupancy)

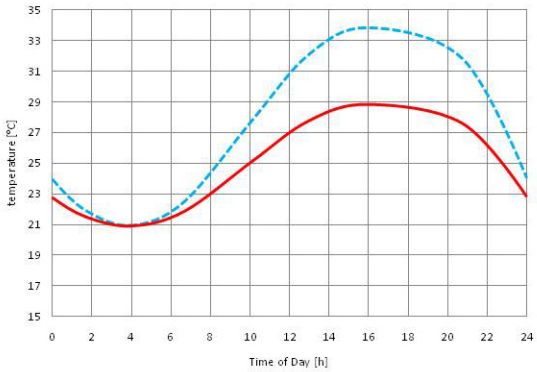

Figure 6.15 Two temperature profiles forecasted for the index day: W1 (higher max. tem) and W2 (lower max. tem)

6.6 Sensitivity analysis: parameter screening and a choice of the sample number to quantify specification uncertainty

6.6.1 Parameter screening

Total 82 design specification uncertainties are identified for the Acme building. As indicated in the previous section 4.4.8, it is not necessary to quantify all of 82 design specification uncertainties in order to get a near-optimal solution. As long as the same degree of sampling coverage can be fulfilled, the resulting solution should be closer enough to the optimal solution. The GBT performs the Morris method (Section 4.4.8.1)

to screen non-significant design specification parameters and they obtain 15 of dominant design specification uncertainty sources as in Table 6.8. Total 256 simulation runs are tested with the base case (i.e., regular building usage scenarios with the chiller priority control) during entire cooling season (From mid May to mid September).

Table 6.8 Top 15 dominant specification uncertainty sources with respect to the power consumptions of the Acme building

Rank	Index	Uncertainty sources	Type of pdf	Range of variation
1	Z1	Infiltration air change	Gaussian	μ=0.3 σ=0.1
2	S1	Primary chiller degradation coefficient	Uniform	[0.066, 0.26]
3	E7	Ground albedo	Uniform	[0.15, 0.3]
4	S7	Centrifugal Pump efficiency	Uniform	[0.60,0.85]
5	E3	Internal convective heat transfer coefficient (floor)	Uniform	[10.8, 18]
6	S4	FCU electricity consumption tolerance	Uniform	[-10%, 10%]
7	Z8	Zone I.Capacitance	Gaussian	μ=98893.0 σ=23141
8	Z4,Z6	Zone R1 and B2.Capacitance	Gaussian	μ=6240.0 σ=1462.2
9	Z3,Z5	Zone B1 and R2.Capacitance	Gaussian	μ=3559.0 σ=1249.3
10	E4	Internal convective heat transfer coefficient (interior wall)	Uniform	[5.72, 14.7]
11	M31	ROOF.Solar Absorptance	Gaussian	μ=0.6 σ=0.04
12	S2	TES chiller degradation coefficient	Uniform	[0.066, 0.26]
13	S5	TES heat loss coefficient	Uniform	[0.155, 1.58]
14	M30	EXTWALL.Solar Absorptance	Gaussian	μ=0.65 σ=0.04
15	E2	Internal convective heat transfer coefficient (ceiling)	Uniform	[1.08, 2.88]

It is observed that the set of 15 specification uncertainty sources accounts for 92.3% of variability with respect to a distribution of the sampled power consumptions. This is validated by means of comparing relative variability of two groups (S1: 15 dominant source control group vs. S2: complementary reference group) over the original

group (S) having all 82 uncertain sources. Detailed procedures can found at (de Wit 2001) and (Hu 2009).

$$\frac{Var\ (S1)}{Var\ (S)} = 0.923 \qquad (6.14) \qquad \frac{Var\ (S2)}{Var\ (S)} = 0.077 \qquad (6.15)$$

6.6.2 Choice of the sampling number to quantify specification uncertainty

The next step is to choose a rational number of Latin hypercube samplings. Coefficients of variation (CV) of samples from 4 to 256 sets are tested as shown in Figure 6.16. With the preset criteria (CV=0.05), most sampling numbers meet the requirement. However, the sample numbers under 12 show critical insecurities over 0.05 depending on sample populations. Therefore it is reasonable to choose 12 as the sampling number to quantify specification uncertainty. This analysis further signifies that 12 sampling sets is a manageable enough number to use a native form (Section 4.10.2) to evaluate the objective function in stochastic optimization.

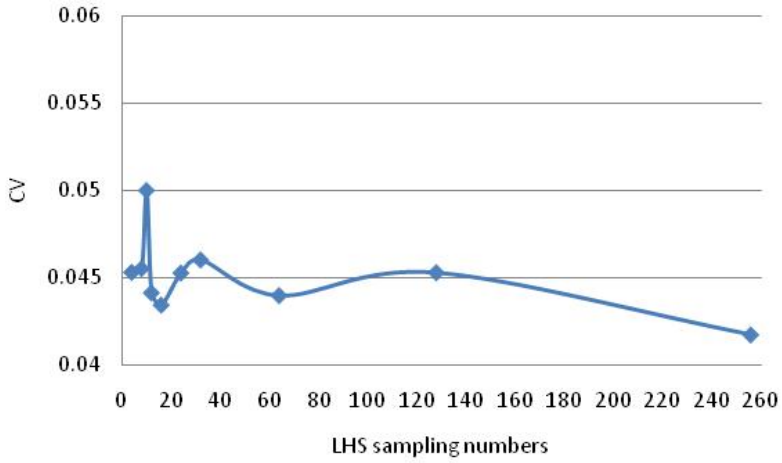

Figure 6.16 CV variations per number of LHS samples

6.7 Stochastic optimization and its preparation

6.7.1 Cost function and scenario-based demand charges

A cost function modified from a generic cost function of supervisory demand-side controls (Equation 4.18) is presented as in Equation (6.16). Natural gas related terms are eliminated since there is no plant consuming natural gas in the Acme building, and on-peak demand charges and economy demand charges are separately levied according to their schedule in Table 6.2.

$$\min_{\widehat{U}} E\{\ J(\ U, G, W)\ \}$$

$$\mathrm{J} = r_{base} + \sum_{k=1}^{N} {P_{ek}}^{\varsigma} r_{ek}{}^{\varsigma} \Delta t + \max_{1 \le \mathrm{k} \le \mathrm{M}} ({P_{ek}}^{\varsigma_\mathrm{h}}) * {r_{d.onpeak}}^{\varsigma} + \max_{1 \le \mathrm{k} \le \mathrm{L}} ({P_{ek}}^{\varsigma_\mathrm{h}}) * {r_{d.econ}}^{\varsigma}$$

$$\text{For all } \varsigma, \varsigma_\mathrm{h} \in \Sigma \qquad (6.16)$$

where Δt is the time interval; N is the number of time intervals in a billing period; M is the number of the time intervals of on-peak durations in a billing period; L is the number of the time intervals of economy-peak durations in a billing period, thus M+L = N; r_{base} is the base charge; r_{ek} is the energy cost per unit of electrical energy at the time interval k ($/kWh) from Table 6.2; P_{ek} is the total electrical power of the HVAC&R system at the time interval k (kW); $r_{d.onpeak}$ and $r_{d.econ}$ denote the on-peak demand charge and the economy demand charge, respectively. Two demand charges are calculated at the highest 30-minute kW measurement over each period ($/kW) in Table 6.2; and ς_h denotes the monthly highest cooling-load scenario.

6.7.1.1 Scenario-based demand charges

The cost function (Equation 6.16) finds the minimum operating cost over the billing period that is typically one month. This leads N to extend up to the number of time intervals over a month. Thus it will involve a large number of optimization variables, and this will increase a probability of finding local minima. For this case a decomposition suggested by (Henze et al. 2008) could be better approach, which is a monthly sequence

of optimal daily strategies minimizing the TOU plus monthly demand charges when actual demand is expected to be more than a "target demand limit" (ASHRAE 2007) pre-assigned by historical observations.

This case study basically accepts such daily decomposition approach. However a different analysis can be applied to levy monthly demand charges, which depends on scenarios.

Under the Georgia Power TOU-GSD-4, for instance a cooling load profile of the base case in the monthly highest cooling-load scenario (i.e., the scenario W2HO with the chiller priority control) illustrated in Figure 6.17 shows that economy-peak demand charge (the red star) and on-peak demand charge (the blue star) will be separately levied according to each schedule.

Since active TES control ultimately pursues no or little on-peak power demand during on-peak periods (i.e., in mode3), when robust controls for TES is applied instead of the chiller priority control, the robust controls will effectively take care of the on-peak demand.

Then the only control measure for economy-peak demand charge (mode 2) is passive thermal mass control. Since degree of the economy-peak power demand during mode 2 depends on degree of the peak building cooling load during mode 2, which is mainly decided by weather conditions and internal heat gains, whether monthly demand charge is levied or not depends on external scenarios composed of weather conditions and building usage scenarios.

Therefore it is more efficient to add two demand charge terms to Equation (6.16) only in case when "the monthly highest-cooling-load scenario" (i.e., the monthly highest temperature and occupancy level) is highly anticipated. Literally this occasion happens once in a month. However any combinations of weather combinations and building usage scenarios that are expected to be one of the feasible monthly highest cooling load

scenarios would have to include two demand charge terms into the daily cost function to hedge the risk of missing actual monthly highest-cooling-load scenario.

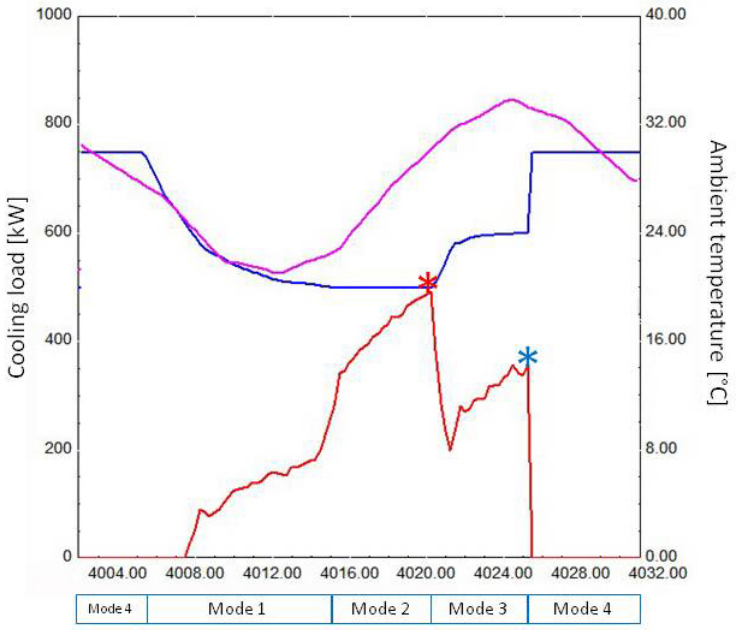

Figure 6.17 Economy-peak demand charge (the red star) and on-peak demand charge (the blue star) are indicated over cooling load profile (the red solid) of the base case in the monthly highest cooling-load scenario
;the blue solid denotes the set-point temperature and the purple solid denotes the ambient temperature

6.7.2 Optimization sequence and algorithm

This section introduces technical aspects of the optimization. Obviously a large number of technical methods are readily available for the same optimization problem. However a specific algorithm and procedures should be chosen considering their availability and applicability after that simulation models and supporting analysis packages are decided. The chosen algorithm and procedure should be compatible with traits of the chosen simulation tool and the characteristic of systems. Thus an appropriate algorithm and procedure will lead optimization problems to have simpler structures and will make the convergence faster.

6.7.2.1 Sequential optimization

Both thermal mass and TES controls pursue the minimum cost while TES control thrives to meet this goal in the basis of the lowest building load. Hence an optimization for building thermal mass control is performed first to make building load as low as possible, and then another optimization for TES control should be performed next. As illustrated in Figure 6.18, in the same scenario, the same quantified uncertainty and the same 24 hour prior thermal history, robust set-point temperature solutions {Tu}rbst that ensures the lowest building load is decided, and then the robust TES charge/discharge solutions {Cu, Du}rbst is calculated to minimize the daily operating cost.

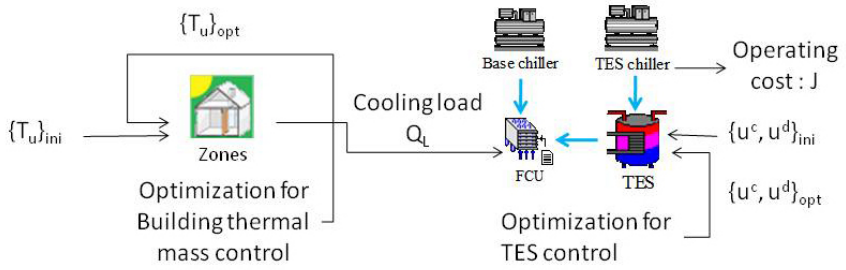

Figure 6.18 Sequential stochastic optimizations between building mass control and TES control

6.7.2.2 Sequential quadratic programming

The optimization of the cost function is accomplished using the Sequential quadratic programming (SQP, Bogg and Tolle 1996). It is developed based on the concept of:

- To directly solve the first-order necessary condition for the 2nd-order approximation of the Lagrangian function
- To find the solutions of first-order necessary conditioned equations using Newton's method (i.e. root finding)

Process of the SQP can be seen as finding search direction toward optimum sequentially through minimizing the quadratic approximation of the Lagrangian function

with the linear approximation. Consider a nonlinear programming problem (NLP) to be solved as:

$$\min_x f(x), \qquad \text{s.t. } h(x)\geq 0,\ g(x)=0 \tag{6.18}$$

This NLP can be converted into a Lagrangian function as:

$$L = f(x) + \lambda^T h(x) + \mu^T g(x) \tag{6.19}$$

where λ and μ are the Lagrangian multiplier vectors for the constraint h and g.

The corresponding sub-problem of quadratic programming is expressed as:

$$\min Q(s) = \min \nabla f^T s + \frac{1}{2} s^T (\nabla^2 L) s \quad \text{s.t. } \nabla h^T s + h \leq 0 \text{ and } \nabla g^T s + g = 0 \tag{6.20}$$

Through solving the above quadratic programming problem, the search direction s is found. Then the problem (Equation 6.20) becomes a one-dimensional search problem, which can be solved using exterior penalty function method as:

$$\min f(x) + \sum \lambda \max(0, h(x)) + \sum \mu |g(x)| \tag{6.21}$$

A number of optimization packages including Matlab contain the SQP as their base algorithm. The optimization package of the ModelCenter chosen for this case study also equips with the SQP as a standard Hessian-evaluating optimizer.

6.8 Robust solutions of two demand-side control measures

Based on the steps of developing robust supervisory demand-side control strategy and the given descriptions and uncertainty information about the Acme building, robust solutions of two demand-side control measures are obtained. As all of three types of uncertainties (Section 6.5) are quantified, each iteration of the stochastic optimization

evaluates all of twelve Latin hyper cube samples (LHS) in six scenarios as illustrated in Figure 6.19.

Although a significant sampling number of Latin hypercube that represents the actual cdf F(·) is calculated according to Billinton and Li (1994) and its stableness is verified in section 6.6.2, nine rounds of different combinations of the Latin hypercube samplings have been tested to ensure confidence. The next sections report robust solutions of two demand-side control measures and discuss observations and findings.

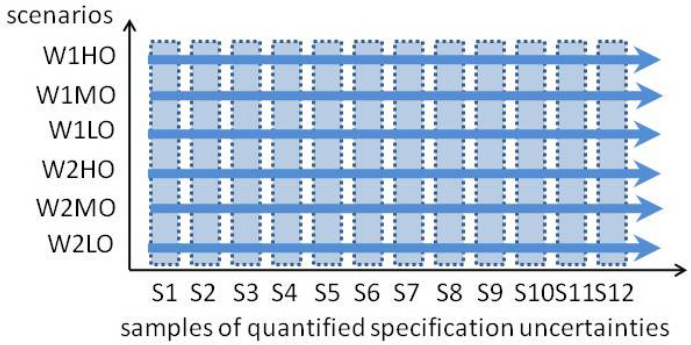

Figure 6.19 Twelve Latin Hypercube samples (LHS) in six scenarios per single round

6.8.1 Robust solutions of building thermal mass controls

As indicated in section 4.2, robust set-point temperature solutions $\{T_u\}_{rbst}$ consists of T_{float} (the floating temperature during mode 4), T_{pc} (the pre-cooling temperature during mode 1 and mode 2), t_{pc} (pre-cooling start time during mode 1 and mode 2) and tau (time constant). Figure 6.20 and Table 6.9 depict their profiles and numeric values of nine rounds, respectively.

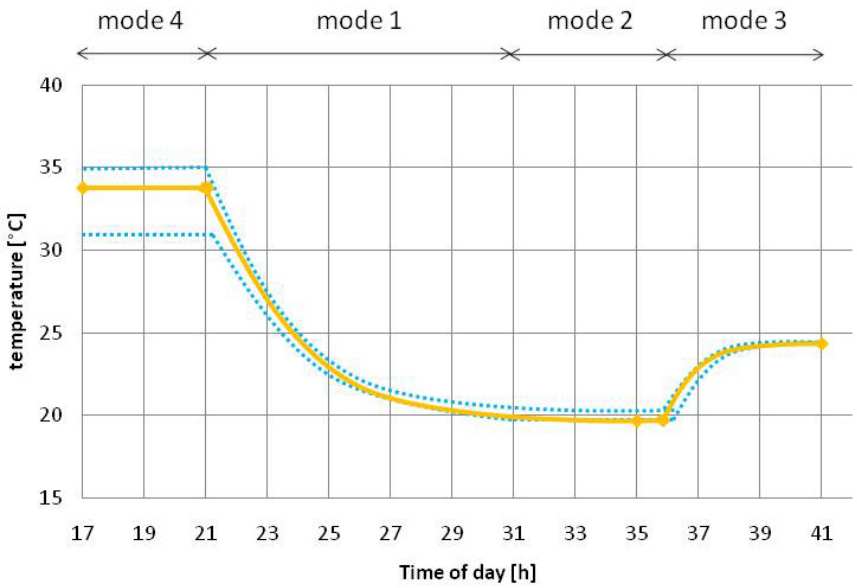

Figure 6.20 Range of nine rounds of LHSs of robust control solutions (the sky dotted) and their average (the orange solid) for the building thermal control

Table 6.9 Range of robust solutions per round and their average for building thermal controls

	R1	R2	R3	R4	R5	R6	R7	R8	R9	Avg.
T_{float}	34.9	33	32	35	35	30.9	34.9	34.5	35	33.9
t_{pc}	35.9	36	32	36	36	32	35.7	36	36	35.1
T_{pc}	19.9	19.8	20.1	19.7	19.8	20.4	20	20	19.8	19.9
tau(τ)	0.55	0.55	0.53	0.53	0.55	0.54	0.55	0.53	0.53	0.54

Nine rounds of LHSs of robust control solutions have not shown a critical difference among all sub-control variables. Compared to other sub-control variables, $T_{release}$ has a wider ranger. However, it is because $T_{release}$ is not sensitive in reducing cooling load. These results indicate that robust solutions for building thermal mass control are stable over different quantification sets of specification uncertainty.

To see a variation per scenario, robust set-point temperature control solutions for each scenario (i.e. horizontal arrows in Figure 6.19) are also compared as shown in Table 6.10. It is found that a robust set-point temperature solution for each scenario keeps

almost the same profile over all scenarios. This means that regardless of the degree of cooling load, which is highly dependent on occupancy levels and weather conditions (i.e., in different scenarios), robust set-point temperature control solution is consistent.

Table 6.10 Robust building thermal mass control solutions under each scenario

	W1HO	W1MO	W1LO	W2HO	W2MO	W2LO
T_{float}	34.7	34.9	36	36	36	36
t_{pc}	36	35.3	36	36	36	36
T_{pc}	19.8	20	19.8	19.8	19.8	20
tau(τ)	0.55	0.55	0.55	0.55	0.55	0.55

6.8.2 Robust solutions of TES control

As indicated section 6.4.3.4, robust TES control solutions $\{C^u,D^u\}_{rbst}$ consists of C^u (the relative constant charge rate during mode 2), $\{D_1^u, \ldots, D_5^u\}$ (the relative discharge rates at each time step k during mode 3) and $t_{ch.end}$ (the charging end time during mode 2). Figure 6.21 and Table 6.11 depict their profiles and numeric values, respectively.

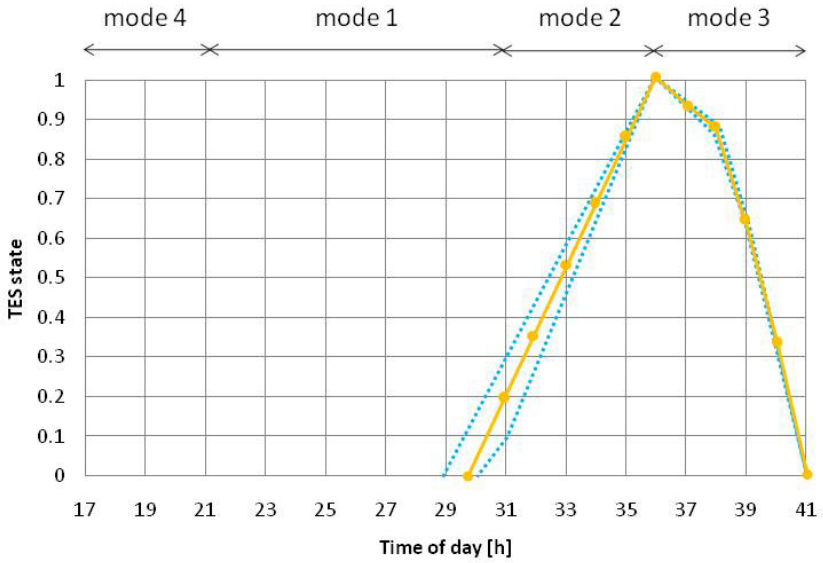

Figure 6.21 Range of nine rounds of LHSs of robust control solutions (the sky dotted) and their average (the orange solid) for the TES control

Table 6.11 Range of robust solutions per round and their average for TES controls

	R1	R2	R3	R4	R5	R6	R7	R8	R9	Avg.
C^u	0.148	0.172	0.145	0.17	0.155	0.18	0.175	0.165	0.16	0.163
$t_{ch.end}$	36	36	36	36	36	36	36	36	36	36
D_1^u	0.0675	0.0635	0.06	0.0555	0.062	0.061	0.056	0.054	0.055	0.060
D_2^u	0.0675	0.0635	0.06	0.0555	0.062	0.061	0.056	0.054	0.055	0.060
D_3^u	0.235	0.243	0.234	0.234	0.238	0.24	0.23	0.243	0.24	0.237
D_4^u	0.29	0.29	0.296	0.31	0.3	0.288	0.32	0.299	0.31	0.300
D_5^u	0.34	0.34	0.35	0.345	0.338	0.35	0.338	0.35	0.34	0.343

Comparisons show that nine rounds of robust control solutions are almost identical. Charge rates (C^u) in the robust solutions has a bit wider profile, but this is because it is not so critical in reducing operating cost. One eye-catching observation is that $t_{ch.end}$ of all solutions is almost always at 36h, i.e., at the boundary time between off-peak and shoulder period. This implies that the later charging of the TES is complete, the less the operating cost is. This can be explained by the fact that it is likely to lose the stored cooling energy if the steady state of the charged TES is exposed longer to the environment (i.e., more heat gain). Therefore a later charging of the TES right before need (when shoulder period starts) contains more cooling energy than earlier charging.

To examine variations of robust control solutions per scenario, robust TES control solutions for each scenario are analyzed as shown in Table 6.12. As each scenario imposes a different level of cooling load, robust TES control solutions vary upon scenario. As the righter sided scenario in Table 6.12 gives lower cooling load, the righter sided TES control solution needs less cooling medium, thus TES is less charged.

Table 6.12 Robust TES control solutions for each scenario

	W1HO	W1MO	W1LO	W2HO	W2MO	W2LO
C^u	0.195	0.186	0.165	0.145	0.132	0.11
$t_{ch.end}$	36	36	36	36	36	36
D_1^u	0.071	0.122	0.100	0.075	0.055	0.045
D_2^u	0.071	0.122	0.100	0.075	0.055	0.045
D_3^u	0.224	0.175	0.141	0.103	0.081	0.070
D_4^u	0.292	0.241	0.224	0.176	0.143	0.106
D_5^u	0.342	0.340	0.278	0.219	0.181	0.150
$\sum D^u$	1.00	1.00	0.84	0.65	0.52	0.42

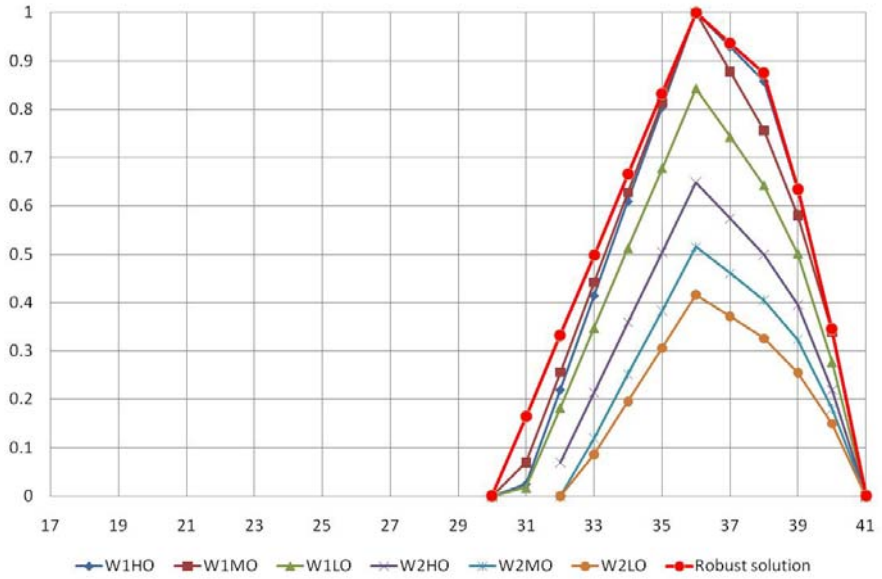

Figure 6.22 Robust TES control solutions for each scenario

An important finding from a comparison between Table 6.12 and Figure 6.22 is that an average of robust control solutions in Table 6.11 is very closer to the robust control solution for scenario W1HO, which is a scenario that results in the highest cooling load. Thus the robust control for scenario W1HO requires the largest amount of cooling medium for discharge. This can be explained that during stochastic optimization via the SAA, it is natural for the optimizer to take the "greediest" solution (i.e. the largest amount of cooling medium) as possible. It is because a penalty for the greediest solution is only the power consumption for charging the TES during off-peak period and the

resulting increased operating cost. But the increased operating cost for charging more than the required is relatively little compared to the saved operating cost benefitted by means of a large amount of discharging during on-peak.

This observation motivates a refutation about this robust control including all scenarios and also an incisive research question.

- Can we just assume the highest temperature and highest occupancy scenario, and then get a control solution for that? In that case, we don't need to take into account complex multiple scenarios. But still we can get an effective control solution paying a little bit more for the penalty.

This argument may look reasonable if all six scenarios equally happen for the day. However reality is that we don't know when one of six scenarios (or off-the-scenario) would be the case. Also if a less-cooling-load scenario is dominant for the day, a control solution derived for the most-cooling-load scenario is apparently an overflow.

Therefore a more reasonable approach would be a dynamic change of robust control solutions upon scenarios change. This motivation underlies the Multi-model predictive control (MMPC) that will be introduced in the chapter 7.

6.9 Benchmark and performance validation

Performance validations of the proposed robust control strategies compared to the benchmarks have two parts:

a. Robust building thermal mass control vs. Conventional setback set-point temperature control;
b. Robust demand-side control strategy vs. Deterministic demand-side control strategies including chiller priority control, storage priority control and optimal control

As discussed in the section 4.4.4, three main performance indices include:

a. $\tilde{P}_{onpeak}$: the mean on-peak power consumption,

b. $\tilde{P}_{daily}$: the mean power consumption and

c. $\tilde{C}_{daily}$: the mean operating cost with $\sigma_{C.daily}$ (the variance of operating cost) and $CV_{C.daily}$ (the coefficient of variation of operating cost)

Additionally validations evaluate performances of control strategies with subsidiary performance indices, i.e., the mean off-peak power consumption and the mean on-peak/off-peak operating cost, if necessary. A notation "on-peak" refers to the combined shoulder period and on-period specified in table 6.2 (i.e. weekday 12-9pm) while "off-peak" refers to the remaining period.

All performance validations are explored with the Monte Carlo samplings. The number of samples that quantify specification uncertainty is set to 256 for the case of single scenario, and 1526 (256 x 6) for the case of all six scenarios. This number of samples is sufficient enough to meet a critical sampling security (CV <0.05) as analyzed in section 6.6.2.

6.9.1 Performance validation of the robust building thermal mass control

6.9.1.1 Benchmark: setback set-point temperature control

Setback set-point temperature control is a conventional control strategy to save energy cost during unoccupied hours by means of pushing set-point temperature back to a release temperature. The dotted line in Figure 6.23 refers to the setback set-point temperature profile used in this comparison while the red solid line refers to the robust thermal mass control solution. During unoccupied hours (mode 4 and mode 1), set-back temperature is set to 28°C and during occupied hours (mode 2 and mode 3), set-point temperature is set to 24°C.

Figure 6.23 Set-point temperature profiles for the setback control (dotted) and the robust thermal mass control (solid)

6.9.1.2 Performance comparison

Since power consumptions and the resulting operating costs by variations of set-point temperature controls are compared, single main chiller (nominal capacity = 600 kW and COP=3) is considered as a main plant (i.e., no TES or TES chiller) while all other HVAC system setups are kept the same as previously described.

To see performance variations of both control strategies for different scenarios, in particular when more cooling load is anticipated than deterministic nominal condition, three scenarios {W2MO, W1MO, W1HO} (from the reference scenario towards higher-cooling-load scenarios) are considered and Monte Carlo analysis are performed (Figure 6.24 to Figure 6.29).

For all three scenarios in Table 6.13, the robust thermal mass control is superior to the setback SPT control showing i) 18-28.5% of reductions in the mean on-peak power consumptions and ii) 6.7-7.8% of reductions in the mean daily TOU operating costs. This is due to the reduced on-peak power consumption that is more expensive although mean daily power consumptions are increased.

A tendency is observed that moving toward higher-cooling-load scenarios (→), the reduction rate in mean on-peak power consumptions by the robust thermal mass control becomes smaller, thus the reduction rate in mean daily TOU operating costs also becomes smaller. However if demand charges that are levied once in a month is considered, it would make a big difference for monthly bills. Reasoning will be described next.

Table 6.13 Performance comparisons between setback control and robust thermal mass control for three scenarios

	W2MO Setback control	W2MO Robust control	W1MO Setback control	W1MO Robust control	W1HO Setback control	W1HO Robust control
$\tilde{P}_{daily}$ [kWh]	780 (100%)	869 (111.4%)	1226 (100%)	1258 (102.6%)	1354 (100%)	1368 (101%)
$\tilde{P}_{onpeak}$ [kWh]	487 (100%)	348 (71.5%)	705 (100%)	564 (80%)	768 (100%)	629 (81.9%)
$\tilde{C}_{dailyTOU}$ [$]	49.6 (100%)	45.3 (91.3%)	73.2 (100%)	68.2 (93.2%)	80.1 (100%)	74.7 (93.3%)
$\sigma_{C.daily}$ [$]	1.55	2.08	2.27	1.91	2.51	3.33
$CV_{C.daily}$	3.1%	4.6%	3.1%	2.8%	3.1%	4.5%
$\widetilde{DC}_{onpeak}$ [$]	-	-	-	-	180kW*x12.93$/kW = 2322(100%)	170kW*x12.93$/kW = 2198.1(94%)
$\widetilde{DC}_{econ}$ [$]	-	-	-	-	220kW**x4.32$/kW = 950.4(100%)	200kW**x4.32$/kW = 864(90%)

* Mean of on-peak power consumptions observed in the Monte Carlo samplings
** Mean of economy-peak power consumptions observed in the Monte Carlo samplings

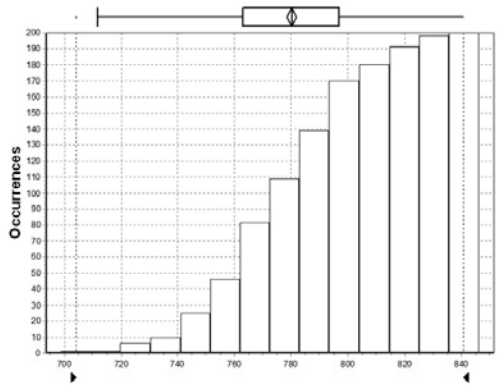

Figure 6.24 Occurrence of daily power consumptions [kWh] by setback control for scenario W2MO

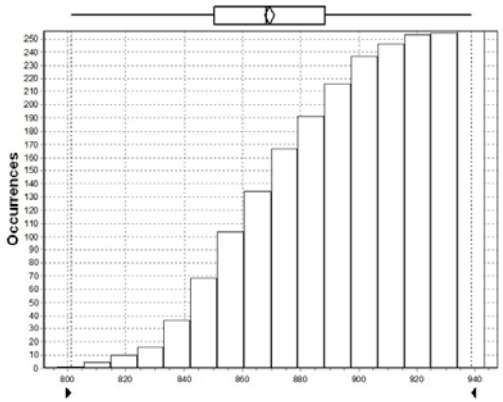

Figure 6.25 Occurrence of daily power consumptions [kWh] by robust thermal mass control for scenario W2MO

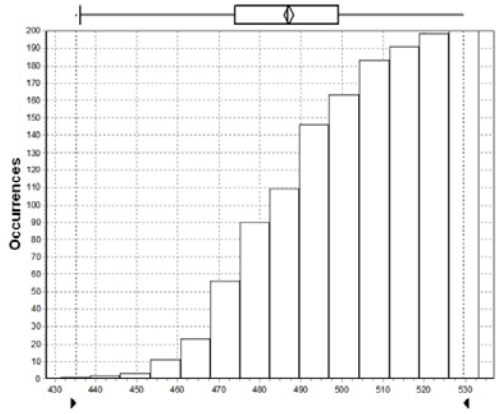

Figure 6.26 Occurrence of on-peak power consumptions [kWh] by setback control for scenario W2MO

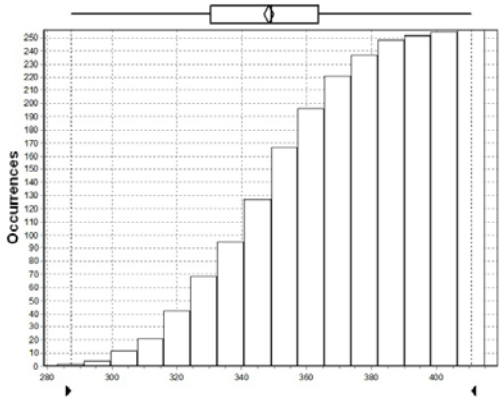

Figure 6.27 Occurrence of on-peak power consumptions [kWh] by robust thermal mass control for scenario W2MO

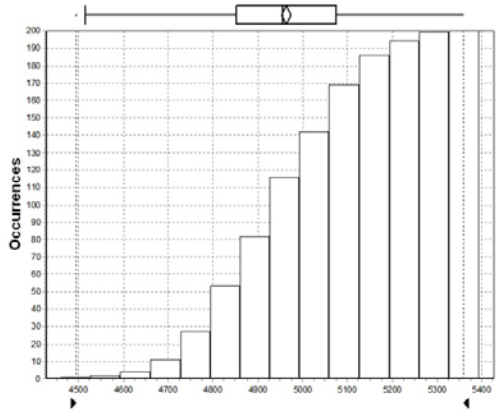

Figure 6.28 Occurrence of daily operating costs [cents] by setback control for scenario W2MO

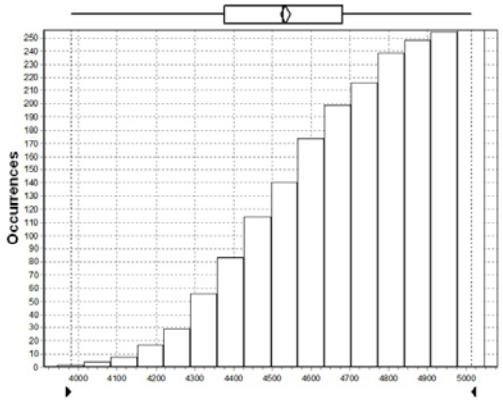

Figure 6.29 Occurrence of daily operating costs [cents] by robust thermal mass control for scenario W2MO

Demand charges are considered with an assumption that the scenario W1HO is expected to be the highest cooling load scenario for current month (Section 6.7.1.1). From table 6.13, it is observed that the mean on-peak demand charge and mean economy demand charge of the robust thermal control are approximately 6% and 10% lower than those of the setback SPT control, respectively.

As demand charges take a big portion of a monthly bill, a small reduction in the monthly highest on-peak and economy-peak power consumptions can save a big amount of the total operating cost. An example of this reduction can be found in exemplary power consumptions of a sample simulation set (Figure 6.30 and 6.31) as star marks highlight.

As featured in section 4.2.6, the exponentially decreasing set-point pre-cooling (EDPC) of the robust thermal mass control removes a spike in the economy-peak power consumption (the star mark in red profiles in Figure 6.31) compared to the setback SPT control (the star mark in red profiles in Figure 6.30), thus its economy demand charge cost turns lower.

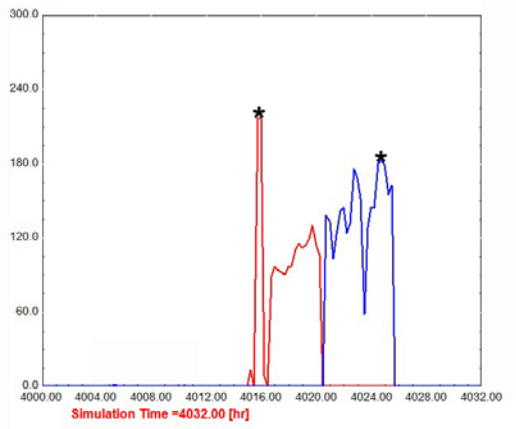

Figure 6.30 An example of power consumption [kW] profile by the setback SPT control for scenario W1HO

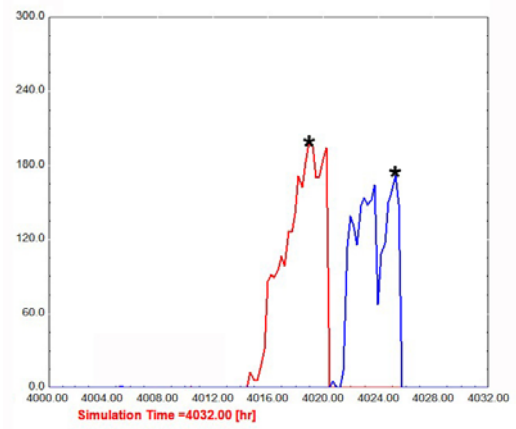

Figure 6.31 An example of power consumption [kW] profile by the robust thermal mass control for scenario W1HO

6.9.1.3 Summary of performance validation of the robust building thermal mass control

The robust thermal mass control solution outperforms the setback SPT control in (simulated) actual situations under uncertainty including varied external scenarios. For almost all scenarios, in particular, it reserves both lower mean on-peak power consumptions and lower mean daily TOU operating costs than the setback SPT control does. It also shows an outstanding control performance for demand charges when the monthly highest cooling-load scenario is expected.

6.9.2 Benchmark and performance validation of the robust TES control strategy

Although superior performance of the robust building thermal mass control is validated, a hypothesis of robust demand-side controls assumes a combinational operation of both building thermal mass control and mechanical TES control would result in an outstanding demand-side control performance than currently used control strategies.

Therefore a purpose of this section is to compare performances of the robust TES control strategy developed in uncertain configurations to those of various conventional TES control strategies developed in deterministic configuration. It is noted that both groups of control strategies are based on the robust building thermal mass control to clearly identify a superiority of the robust TES control strategy.

The deterministic configuration refers to the environment all simulation parameters are fixed (i.e. no uncertainty). And the deterministic control strategy is developed from such configuration for nominal single scenario. In this comparison case i) base parameters in from table 6.3 to table 6.7 and ii) the base scenario W2MO (i.e., weather forecast by the EWMA and medium occupancy level) become a set of deterministic parameters and the nominal scenario, respectively.

6.9.2.1 Benchmark: deterministic demand-side control strategies including chiller priority control, storage priority control and deterministic optimal control

Three legacy deterministic control strategies are compared. Two conventional strategies: chiller priority control and dynamic storage priority control are already introduced in section 4.3. Deterministic optimal control strategy introduced here pursues the minimum operating cost and offers a (near-)optimal control solution for the deterministic configuration and the preset nominal scenario W2MO.

a. Chiller priority control

Recall that with chiller priority control; main chiller fully operates to meet the building load at time k (Q_k^L) if the reduced cooling capacity ($Cap_{75\%}$) is sufficient (Equation 6.22-1). If the reduced chiller capacity (e.g. 75%) is not enough, then TES becomes active (Q_k^D >0) to meet the difference (Equation 6.22-2). Switching conditions and its control are described in the following Equation (6.22) and (6.23).

The simplicity of chiller priority control lies in that nonindigeous environment does not affect the chiller control. Since this control strategy favors the main chiller over the TES, however, it is not advantageous to maximize demand reduction that the TES results in.

$$Q_k^D \begin{cases} 0 & \text{if k is shoulder or on-peak and } Cap_{75\%} \geq Q_k^L \quad (6.22\text{-}1) \\ Q_k^L - Q^{chiller.75\%} & \text{if k is shoulder or on-peak and } Cap_{75\%} < Q_k^L \quad (6.22\text{-}2) \end{cases}$$

$$Q_k^C = Q_k^{C.max} \quad \text{If k is off-peak} \quad (6.23)$$

where Q_k^D and Q_k^C denote the discharged cooling energy from TES and the charged cooling energy to TES at time step k, respectively.

b. Storage priority control

Storage priority control discharges as much cooling medium as possible during shoulder and on-peak hours. Thus the main chiller operates at the predicted base load ($Q^{chil.base}$) during shoulder and on-peak hours and the TES serves the rest of the cooling

load. The predicted cooling load for the period, which the deterministic configuration and preset nominal scenario impose, determines $Q^{chil.base}$.

In Equation (6.25), N is the number of hours during next shoulder and on-peak period, and k' is the first hour therein. The first term ($\sum_{i=0}^{N-1} Q_{k'+i}^{pL}$) means the predicted cooling load for the next period viewed at the first hour and the second term ($\sum_{i=0}^{N-1} Q_{k'+i}^{pD}$) indicates the predicted discharged cooling energy by the TES. By this operation storage priority control meets its goal, i.e., to discharge as much cooling medium as possible while minimizing the main chiller operating. If the predicted cooling load profile is identical to the discharged cooling energy profile of the TES, the base load of the main chiller becomes none.

However if actual cooling loads become higher than the predicted, either the main chiller or the TES should take a responsibility for the increased cooling load. This case study takes the first approach (Equation 6.24) as an earlier depletion of the stored cooling medium may lead the main chiller to take the whole load later, which eventually may cause more operating cost in TOU and demand charge rate structure.

$$Q_k^{chiller} = Q_k^{L} - Q_k^{pD} \quad \text{if k is shoulder or} \quad (6.24)$$

$$Q_k^{chil.base} = Q_k^{pL} - Q_k^{pD} \text{ and } \sum_{i=0}^{N-1} Q_{k'+i}^{pL} = \sum_{i=0}^{N-1} Q_{k'+i}^{pD} \quad \text{on-peak} \quad (6.25)$$

$$Q_k^{C} = Q_k^{C.max} \quad \text{If k is off-peak} \quad (6.26)$$

where $Q_k^{chil.base}$ denotes the predicted base load at which the main chiller operates; Q_k^{pD} and Q_k^{pL} denote the predicted discharged energy and predicted building load to calculate Q_k^{pD}, respectively; $Q_k^{chiller}$ is the actual load at which the main chiller operates.

c. Deterministic optimal control

Illustrated in Equation (6.27), the deterministic optimal control decides (near-)optimal profiles of charging rate and discharging rate though minimizing the cost function J. Recall the Equation (6.16); two main differences of Equation (6.27) from Equation (6.16) include i) deterministic problem expression (i.e. no W and G terms thus no expected value E term) and ii) it only to consider the nominal scenario W2MO. As the

difference specifies, the deterministic optimal control solution guarantees the minimum operating cost in the deterministic configuration.

$$\min_{\hat{C},\hat{D}} J(C,D) = \min_{\hat{C},\hat{D}}[r_{base} + \sum_{k=1}^{N} {P_{ek}}^{W2MO} r_{ek}\Delta t + \max_{1\le k\le M}({P_{ek}}^{W2MO}) * r_{d.onpeak} + \max_{1\le k\le L}({P_{ek}}^{W2MO}) * r_{d.econ}] \quad (6.27)$$

6.9.2.2 Performance comparisons

Performance comparisons of robust demand-side control strategy against three legacy control strategies pursue validating its superior robustness when it is applied in possible actual uncertain situations. Actual situations lead to explore how extreme uncertainties from the nonindigeous environment would affect performances of deterministic control strategies. Eventually this analysis aims at letting people recognize that why approaches for robust controls are required.

For this purpose, two simulated validation cases will be firstly analyzed: i) a validation case where specification and calibration uncertainties quantified in the nominal scenario W2MO and ii) another validation case where all (identified) uncertainties quantified including six varied scenarios.

i) Simulated actual environment with specification and calibration uncertainties in the nominal scenario W2MO

Performances of four control strategies are compared in the simulated actual environment where specification and calibration uncertainties are quantified. It is assumed that there are no uncertain weather conditions and no uncertain occupancy profiles for the reference day, viz. the nominal scenario W2MO is presumed.

As expected and shown in Table 6.14, the chiller priority control consumes the most daily mean power, which causes the most expensive daily mean operating cost. Storage priority control and robust control consume more daily mean power than

deterministic optimal control does, however they consume far less on-peak mean power thus resulting in only 8% and 2% more of daily mean operating cost than that of deterministic optimal control, respectively.

Under the environment where the nominal scenario W2MO predominates, the deterministic optimal demand-side control strategy still outperforms the robust control by 2% less daily mean operating cost despite specification and calibration uncertainties. However if the rate incentive (i.e. on-peak rate over off-peak rate) grows, 2% is a low threshold that the robust control overcomes, thus the robust control is likely to outperform three deterministic control strategies.

Table 6.14 Performances of four demand-side control strategies with the simulated environment where specification uncertainties quantified in the preset scenario W2MO

	Chiller priority control	Storage priority control	Deterministic optimal control	Robust control
$\tilde{P}_{daily}$ [kWh]	867.6 (133%)	752 (116%)	650 (100%)	715 (110%)
$\tilde{P}_{onpeak}$ [kWh]	345 (575%)	52.9 (88%)	60 (100%)	39.8 (66%)
$\tilde{C}_{dailyTOU}$ [$]	45.1 (249%)	18.1 (108%)	16.7 (100%)	17 (102%)
$\sigma_{C.daily}$ [$]	2.18	0.79	1.14	0.48
$CV_{C.daily}$	4.8%	4.4%	6.8%	2.8%

ii) Simulated actual environment with all (identified) uncertainties including six varied scenarios

Performance superiority of the robust control becomes more apparent as shown in Table 6.15 when four control strategies are compared in the environment where all previously identified uncertainties (including six scenarios) are quantified. It should be noted that this simulated actual environment stands for an "average" scenario among six scenarios. In other word, all six scenarios have an equal probability of occurrence at each time step, i.e., 1/6. From a statistical perspective to obtain a mean value, this is a valid

expression to represent an "averaged" scenario. However this representation is hardly real. As each scenario causes very different profiles of cooling loads, daily power consumptions and operating costs resulted by each control strategy vary widely with an extraordinary degree as shown in CVs in Table 6.15.

Table 6.15 Performances of four demand-side control strategies with the simulated environment under all identified uncertainties quantified including scenario uncertainty

	Chiller priority control	Storage priority control	Deterministic optimal control	Robust control
$\tilde{P}_{daily}$ [kWh]	1036 (118%)	956 (109%)	875 (100%)	825 (94%)
$\tilde{P}_{onpeak}$ [kWh]	429 (219%)	169 (86%)	196 (100%)	73.7 (38%)
$\tilde{C}_{dailyTOU}$ [$]	53.8 (173%)	30.4 (98%)	31.1 (100%)	20.7 (67%)
$\sigma_{C.daily}$ [$]	10.8	12.6	14.2	4.8
$CV_{C.daily}$	21.4%	41.4%	45.7%	23.2%

A more realistic way of a validation is to analyze performances of demand-side control strategies scenario by scenario. From Table 6.16 to Table 6.19 presents comparative performances of demand-side control strategies for each scenario. For easier comparisons, performance indices of the deterministic optimal control are set to the reference (e.g. 100%). A few common patterns are observed as followings.

- As it has been repeatedly referred in literature (Henze, Felsmann et al. 2004), the chiller priority control strategy turns out to be mostly disadvantageous for demand-side control in all (indicated) circumstances.

- In scenarios resulting higher cooling loads than the reference scenario W2MO does (i.e. W1HO, W1MO and W2HO from Table 6.16 to Table 6.18), the storage priority control strategy has shown a slightly better performance than

deterministic optimal control in daily mean operating cost due to its lower mean on-peak power consumptions. In a lower-cooling-load scenario (W2LO at Table 6.19), the storage priority control strategy has not effectively leverage its smaller on-peak power consumption and the rate incentive, thus it results in 12% of more mean operating cost.

- In higher-cooling-load scenarios, the robust control outperforms all others in both mean on-peak power consumptions and daily mean operating costs with an outstanding degree. Only slightly underperformance (+2%) of the daily mean power consumption is observed under scenario W2HO. Likewise the storage priority control, however, in the lower-cooling-load scenario W2LO, it slightly underperforms the deterministic optimal control (around +9% of the daily cost and +14% of daily mean power consumption) despite far smaller mean on-peak power consumptions (-16%). This implies that the robust control consumes more power during off-peak to store more cooling energy into the TES.

Table 6.16 Performances of four demand-side control strategies in the simulated environment where specification and calibration uncertainties quantified and the higher-cooling-load scenario W1HO

	Chiller priority control	Storage priority control	Deterministic optimal control	Robust control
$\tilde{P}_{daily}$ [kWh]	1281.6 (107%)	1261 (105%)	1200 (100%)	1033.9 (86%)
$\tilde{P}_{onpeak}$ [kWh]	543 (139%)	355 (91%)	391 (100%)	150 (38%)
$\tilde{C}_{dailyTOU}$ [$]	65.7 (128%)	50 (97%)	51.5 (100%)	28.5 (55%)
$\sigma_{C.daily}$ [$]	1.3	4.6	3.3	1.8
$CV_{C.daily}$	2.0%	9.2%	6.4%	6.3%

Table 6.17 Performances of four demand-side control strategies in the simulated environment where specification and calibration uncertainties quantified and the higher-cooling-load scenario W1MO

	Chiller priority control	Storage priority control	Deterministic optimal control	Robust control
$\tilde{P}_{daily}$ [kWh]	1216.8 (106%)	1143 (105%)	1085 (100%)	963.8 (89%)
$\tilde{P}_{onpeak}$ [kWh]	522 (165%)	264 (83%)	316.4 (100%)	113.4 (36%)
$\tilde{C}_{dailyTOU}$ [$]	63.6 (145%)	40.5 (92%)	44 (100%)	25 (57%)
$\sigma_{C.daily}$ [$]	1.5	3.1	2.9	1.1
$CV_{C.daily}$	2.4%	7.6%	6.6%	4.4%

Table 6.18 Performances of four demand-side control strategies with the simulated environment where specification and calibration uncertainties quantified and the slightly higher-cooling-load scenario W2HO

	Chiller priority control	Storage priority control	Deterministic optimal control	Robust control
$\tilde{P}_{daily}$ [kWh]	969 (124%)	874 (112%)	781 (100%)	800.4 (102%)
$\tilde{P}_{onpeak}$ [kWh]	391.7 (408%)	96 (79%)	122 (100%)	53.1 (44%)
$\tilde{C}_{dailyTOU}$ [$]	50.3 (210%)	23.4 (98%)	23.9 (100%)	19.3 (81%)
$\sigma_{C.daily}$ [$]	1.6	1.8	2.3	0.7
$CV_{C.daily}$	3.2%	7.7%	9.7%	3.6%

Table 6.19 Performances of four demand-side control strategies with the simulated environment where specification and calibration uncertainties quantified and the lower-cooling-load scenario W2LO

	Chiller priority control	Storage priority control	Deterministic optimal control	Robust control
$\tilde{P}_{daily}$ [kWh]	721.6 (129%)	659 (118%)	559 (100%)	635.2 (114%)
$\tilde{P}_{onpeak}$ [kWh]	270 (982%)	34.6 (92%)	37.5 (100%)	31.4 (84%)
$\tilde{C}_{dailyTOU}$ [$]	36.6 (257%)	15.4 (112%)	13.7 (100%)	14.9 (109%)
$\sigma_{C.daily}$ [$]	1.8	0.5	0.6	0.4
$CV_{C.daily}$	4.9%	3.2%	4.3%	2.7%

6.9.2.3 Summary of performance validations of the robust TES control strategy

In general the robust demand-side control strategy outperforms conventional deterministic demand-side control strategies when higher cooling loads than the expected are observed. However when the scenario goes as predicted or when cooling loads actually turn lower than the expected, the robust control strategy slightly underperforms. At the same time, more expensive, mean on-peak power consumptions of the robust control in those two scenarios are still far below than mean on-peak power consumptions of legacy control strategies, particularly the deterministic optimal control. This implies that the robust demand-side control strategy would have a potential to outperform than convention deterministic control strategies if stronger rate incentives are applied.

6.10 Conclusion

As the GBT proposed, robust demand-side control strategy results in generally outstanding demand-side performance in varied and non-indigenous conditions compared with the existing control strategies. However distinct control profiles for each of varied scenarios motivate a further investigation for the demand-side control strategy to be adaptive and still robust for scenario uncertainties. Thereby the next chapter will introduce theories and applications of the Multiple model-based control (MMC) strategy of which different local models are chosen for varying scenarios and its performance will be also validated by comparisons of the existing control strategies.

CHAPTER 7

MULTIPLE MODEL-BASED CONTROL STRATEGY FOR ROBUST AND ADAPTIVE SUPERVISORY DEMAND-SIDE CONTROLS

7.1 Introduction

A case study for the Acme building has shown that the robust demand-side control strategy is capable of handling uncertain situations over conventional deterministic control strategies, which vary unexpectedly from the nominal.

While obtaining solutions of the robust demand-side control strategy, however, two significant findings are observed (section 6.8.2): i) a robust solution under all scenarios is the greediest solution which is very closer to the robust solution under the scenario resulting in the highest cooling load and ii) robust solutions under each scenario vary distinctly depending up to condition of each scenario. Eventually it motivates for a dynamic change of robust control solutions as scenarios change.

According to definition of the scenario and sources of the scenario uncertainty (section 2.5 and section 2.8), a change in weather conditions and building usage scenarios and the resulting internal gains drives change of scenarios. Therefore characteristics of uncertainty dominant in weather conditions and building usage scenarios would suggest a clue in choosing an appropriate robust control approach. As uncertainty sources of the weather and the internal building usage scenario are analyzed in section 2.8.3 and section 2.9, sporadic characteristics (i.e. unpredictable uncertainty) are more dominant in them.

The fact that scenarios are mainly driven by the unpredictable uncertainty poses two significant features of how the robust control solution should be. Firstly, to take a predictive control action for the unpredictable uncertainty is hardly feasible. In this case, a follow-up control action (i.e. reactive) that is taken promptly after an observation when a pattern of such uncertainty lasts would be an appropriate approach.

Second, as its literal meaning implies even capturing the unpredictable uncertainty as a follow-up control action is not easy. Therefore it is necessary to convert or transform such unpredictable uncertainty into less unpredictable, at least interpretable (or quantifiable) form such that it is readable as a control reference for the following-up control actions. From this sense, as it is discussed in the section about the representation of the scenario uncertainty (section 3.5.2), it is more appropriate to represent the scenario uncertainty in discretely distinguished profiles. This way would make the unpredictable uncertainty covered. This will be further explained via an example.

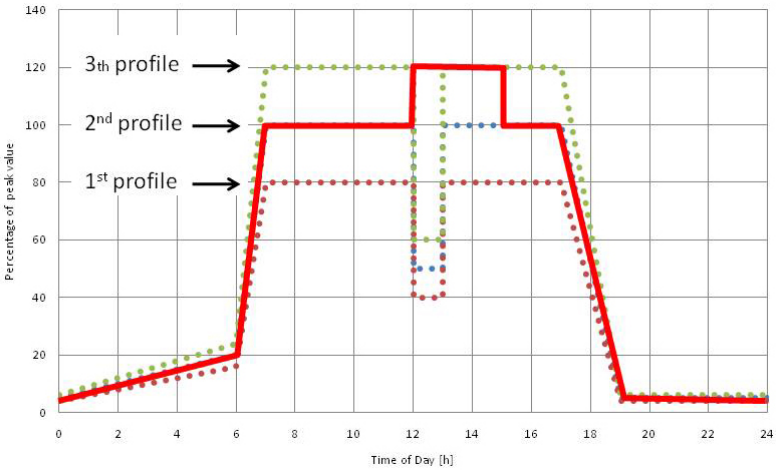

Figure 7.1 Occupancy level suddenly increases 20% at noon and back to the nominal in 3 hours

As illustrated in Figure 7.1, the daily occupancy profile was fixed as nominal (2nd profile). At noon, however, the occupancy level suddenly increases by 20% (3rd profile) due to an unforeseen gathering. Then it goes back to the nominal profile 3 hours later (2nd profile). In the mean time a coil load on FCUs to meet the specified room set-point temperature boosts up, consequently more cooling energy from the main plant (i.e., chiller or TES) is required.

Although it is an unexpected sudden change from a perspective of single scenario, however if a series of scenarios having higher occupancy level is assumed previously, this increase in occupancy level can be one of "expected" occupancy patterns. Then a

corresponding follow-up control strategy upon scenarios change can be readily obtainable.

7.1.1 A need for multiple robust control models

Recall section 6.8.2, the fact that different scenarios result in very different robust control solutions encourages a transfer over the spectrum of robust control strategies as scenarios change. Since a combination of different scenario elements (e.g. weather profiles, occupancy profiles) composes a distinctive scenario, multiple scenarios result in multiple operating regimes as many as the number of scenarios. Then one robust control solution profile can be developed for one operating regime, eventually resulting in multiple profiles of the robust control strategies of which each profile is distinct to each other.

Including multiple scenarios into a development process of the robust control strategy requires multiple instances of base robust control model. Here the base robust control model indicates a skeleton of the control model that can be instantiated in the modeling process by means of modifying values of model properties. Thus replacing the default scenario of the base robust control model by multiple scenarios leads to multiple instances of the base robust control model. The section about describing scenario uncertainty (section 3.6.3) well explains this.

A concept of multiple instances of the base robust control model coincides with the Multiple Model-based Control scheme (MMC, Murray-Smith and Johansen 1997) that is known as one practical approach for control of industrial high-dimensional and nonlinear processes. The detail about the MMC will be introduced next.

7.2 General problem statement of the MMC in the process control engineering

A number of real problems in modeling and control involve complex high-dimensional nonlinear systems. Superposed nonlinearity of such systems may lead the nonlinear model-based control performing more undesirably. In the literature of process control engineering, this underperformance can be attributed to the difficulties associated with: i) obtaining accurate nonlinear models (Morari and J.H.Lee 1999), ii) solving the complex resulting optimization problems (Albuquerque, Gopal et al. 1999), and iii) ensuring robustness with respect to uncertainties (Doyle, Packard et al. 1989). Briefly speaking uncertainty within and around the system causes these difficulties leading to the nonlinearity.

A general approach to complex problem solving is the divide-and-conquer strategy. The key to successful problem solving with this approach is to decompose the problem along a suitable axis. One engineering approach in the process control is namely "operating regime decomposition". The core of the operating regime approach is to make use of a partitioning of the system in order to solve modeling and control problems. This approach eventually leads to multiple model-based controls (MMC), where different local control models are applied under different operating condition (Figure 7.2).

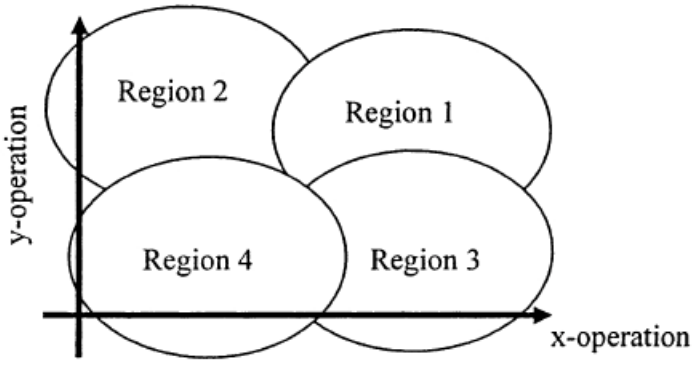

Figure 7.2 A global operating regime is decomposed into multiple local regimes

With this approach, multiple local control models representing each operating regime should be all "on-line". Also a supervisor needs to be involved to coordinate the

local controllers representing local control models as if it is a single controller (Figure 7.3). The next section will further review theoretical background and steps of the MMC commonly applied in the process engineering. It should be reminded again that its extended objective is to eventually find an application that specific for the robust supervisory demand-side controls for building and systems.

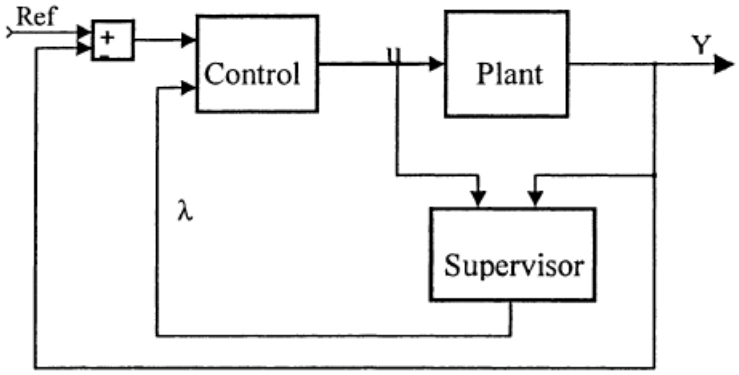

Figure 7.3 The supervisory controller coordinating local controllers works as a single controller (Rodriguez, Romagnoli et al. 2003)

7.2.1 Multiple model-based control theory and algorithm

In general the MMC typically constructs a set of linear local models at different operating regimes and it combines their outputs within the control frame. To do so, this approach requires a priori knowledge on the global range and behavior of a system and the coordination method between local models. This procedure can be summarized into a few steps to fully account for the requirement.

Step 1 : Decompose the system's full range of operation into multiple operating regimes

Step 2 : Select local model structures within each operating regime

Step 3 : Develop the two-level hierarchical structure that consists of the supervisor and local models and switching/synthesizing mechanisms in-between

7.2.1.1 Step 1: Decomposition of the full operation regimes

Any model or controller will have a limited range of operating conditions (Rodriguez et al., 2003). This is usually bounded by limitations such as modeling assumptions, stability constraints, modeling validity constraints when applied in various physical conditions. However, instead of a global control of "the big chunk", it is an argument of the MMC that it would be beneficial to split it into a (few) number of local controllers.

According to (Rodriguez et al., 2003), two insights make this idea practically possible. i) In most circumstances (including industrial applications) it is feasible to identify a "tangible set of phenomena" that can often be characterized into multiple operating regimes and ii) most industrial applications are inherently conceptualized in terms of "start-up and/or low-mid-high range" production and shutdown. Consequently clustering and linearization will often be sufficient to elaborate nonlinearity of the global system.

Then a key factor of clustering is to select a reasonable number of clusters of which union represents the full operating regime of the system. In addition to that, it is needed to choose the scope of each cluster, i.e. even or uneven resolution, in order to fully characterize a single region. Of course, the most desirable clustering strategy is the simplest, in other words, the smallest number of evenly scoped clusters while they meet the requirements. For this study, one solution to achieve this is the GK clustering algorithm (Gustafson and Kessel 1979) and the fuzzy satisfactory clustering (He, Cai et al. 2005).

Suppose a data set Z that is composed of the input-output data of the system and M local models can represent Z. M number of data subset Z_i ($1 \leq i \leq M$) exist and each subset data Z_i corresponds to i^{th} operating regime. For i^{th} subset Z_i ($1 \leq i \leq M$) defines a data pair $z_k = [\varphi_k, y_k]^T \in R^{d+1}$ ($1 \leq k \leq N_i$) where φ_k is the generalized input vector combining system inputs and past outputs, and y_k is the system output. Assume the i^{th} cluster C_i stands for the i^{th} subset Z_i, thus the i^{th} local model L_i is based on the data set of the cluster

C_i. GK clustering algorithm finds the partition matrix $U = [u_{ij}]_{MxN}$ and cluster centers $V=\{v_1, .., v_M\}$ by minimizing the objective function, i.e. RMSE.

Steps of algorithm to find the optimal cluster number are as followings.

Step 1: Set the initial cluster number as 2, i.e. M =2.

Step 2: With initial partition matrix, divide data set Z into M parts $\{A_1, \ldots, A_M\}$, where A_i stands for the i^{th} operating regime

Step 3: For each cluster, identify the local control model. The local control model L_i will be described as

L_i : if $(\varphi_k, y_k) \in A_i$ then $y_i = F_i(\varphi_k)$,

where F_i stands for the local model structure.

A number of local model structure formulations are possible from simple regression models to complex nonlinear models depending on the given problem. This will be further detailed in the next section.

Step 4: Compute the system output $\hat{y}$ corresponding to z_k,

$$\hat{y} = \sum_{i=1}^{M} u_{i,k}\, y_i / \sum_{i=1}^{M} u_{i,k} \qquad (7.1)$$

Step 5: Calculate root mean square error, RMSE= $\sqrt{\frac{1}{N_i}\sum_{k=1}^{N_i}(\widehat{y_k} - y_k)^2}$. If the RMSE is less than the pre-specified number (i.e. tolerance), the current cluster number M is satisfied. Otherwise, go to Step 6.

Step 6: Find a data pair from the given data set, which is the most different from the current cluster center $\{v_1, .., v_M\}$ and make it as a new center v_{M+1}. The index n of this pair is found by computing

$$n = \underset{n}{\operatorname{argmin}} \sum_{1 \le i,j \le c \; i \ne j} (u_{i,n} - u_{j,n})$$

.

Step 7: Let M = M+1. Formulate $\{v_1, .., v_{M+1}\}$ as the new initial cluster center, and update the initial partition matrix as below, go to Step 2.

For a new input φ, its partition ratio $u_i(\varphi)$ with respect to the i^{th} cluster is calculated by

$$u_i(\phi) = \frac{1}{\sum_{j=1}^{M} \left(\frac{D_{A_i^x}(\phi, v_i^x)}{D_{A_i^x}(\phi, v_j^x)}\right)^{\frac{2}{m-1}}} \tag{7.2}$$

where v_i^x denotes the projection of the i^{th} cluster center v_i onto generalized input space; $D_{A_i^x}(\varphi, v_i^x)$ denotes the distance between the new input φ and the projection of the cluster center v_i^x; m denotes a parameter that controls the fuzziness of clusters (m>1).

7.2.1.2 Step 2: Select local model structures within each operating regime and identify local controllers

Nonlinearity of the system which appears in the full operating regime can be fragmented (according to separated clusters), and this fragmentation is accomplished by incorporating the concept of time-dependent-functions. Thus these functions represent uncertainty, which is the main source of the nonlinearity.

Uncertainty is mainly divided into time-invariant parameters (approximately fixed) and time-varying parameters λ(t) that varies within a range $[\lambda_{min}, \lambda_{max}]$. This relation is defined as the state-space formulation (Equation 3.1) for the local model structure (M(λ) in Figure 7.4) and described as:

$$\begin{aligned} x(t+1) &= A\big(\lambda(t)\big)x(t) + B\big(\lambda(t)\big)u(t) \\ y(t) &= C\big(\lambda(t)\big)x(t) \end{aligned} \tag{7.3}$$

where λ(t) is a vector of time varying system parameters, and A(·), B(·), C(·) are fixed functions of λ.

This system is referred to as linear-parameter-varying (LPV) model. It implies an important feature of the LPV model that once the stability is verified for local models, the complete system in the whole operating regime could be stabilized through the use of a MMC controller (Rodriguez et al., 2003).

However the identification process of local model structure is not generic to all nonlinear process. Thus it is not always possible to develop a closed loop formation of the local model structure particularly when the nonlinearity of local model is quite complex. In this case, one option for the identification of each local operation is to generate it from a series of set-point and disturbance changes in open-loop (Rodriguez et al., 2003).

The next step is then to identify local controllers for the local model structure. In order to design a controller satisfying the feedback loop scheme, a state-space representation of the system (Equation 7.3) and controller must be obtained as depicted in Figure 7.4. Here M(λ) and C(λ) denote the local model structure and the local controller, respectively and both of them are LPV systems. A general expression of a local controller C(λ) then can be expressed as the following Equation 7.4. For further expansions and details, readers can refer to a comprehensive description of the algorithm given in (Banerjee, Arkun et al. 1997).

$$\begin{aligned} x_c(t+1) &= A_c(\lambda)x(t) + B_c(\lambda)e(t) \\ u(t) &= C_c(\lambda)x(t) + D_c(\lambda)e(t) \end{aligned} \tag{7.4}$$

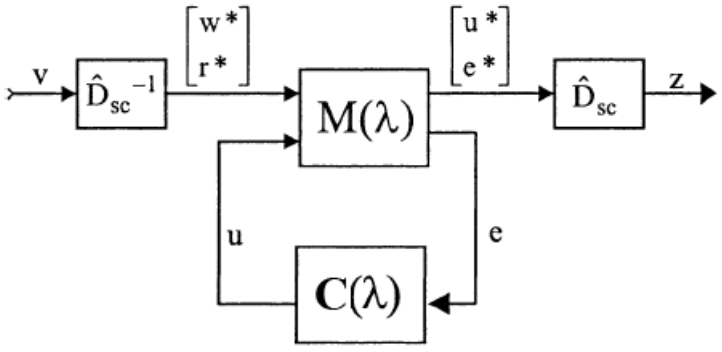

Figure 7.4 A general controller design scheme (Rodriguez et al., 2003)

7.2.1.3 Step 3: Develop the two-level hierarchical structure

The whole complex system is partitioned into a set of local subsystems. The global control strategy is then determined by integrating local controllers using certain rules. Among a number of integrating methods, fuzzy modeling technique where clusters are used to determine the number of fuzzy rules based on designers' experience, has certain advantages in forming multiple models since it results smooth behavior across all operating regions and can approximate arbitrary functions (Murray-Smith and Johansen 1997; Sousa and Kaymak 2002; Gustafson and Kessel 1979).

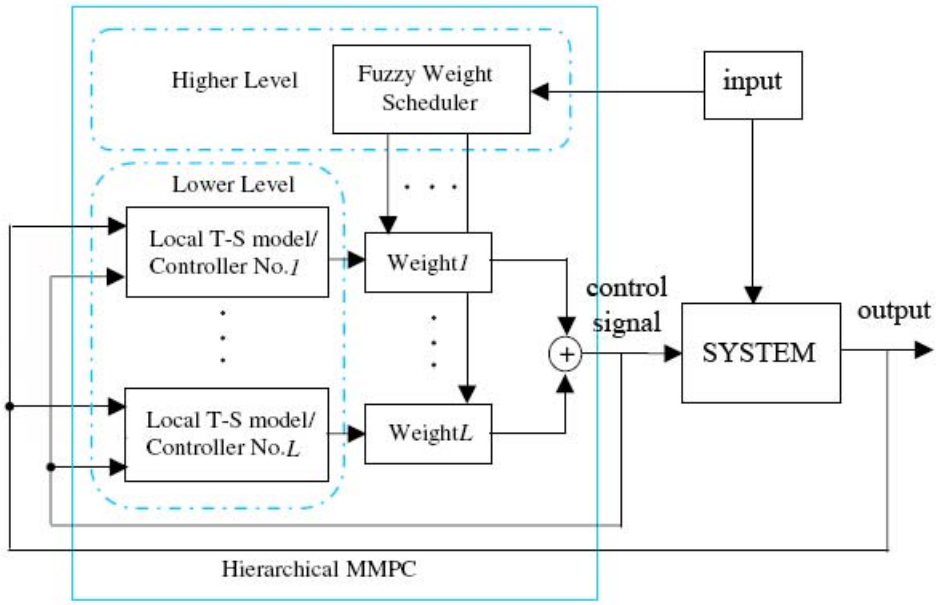

Figure 7.5 The two-level hierarchical structure of the MMC using fuzzy modeling technique

In this study, the two-level hierarchical MMC (Figure 7.5) consists of i) a set of local T-S models (Takagi and Sugeno 1985) (Figure 7.6) and ii) the overall system model constructed by fuzzy integration resulting in a linear-parameter-varying (LPV) model. As indicated previously, this LPV model enables the problem of rule-explosion (Raju, Zhou

et al. 1991) in fuzzy applications alleviated by dividing single high-dimensional fuzzy set into a collection of low-dimensional fuzzy system. Finally the global controller output is then aggregated through fuzzy weight scheduler (Figure 7.7) on the supervisory level. This process is summarized as the following algorithm.

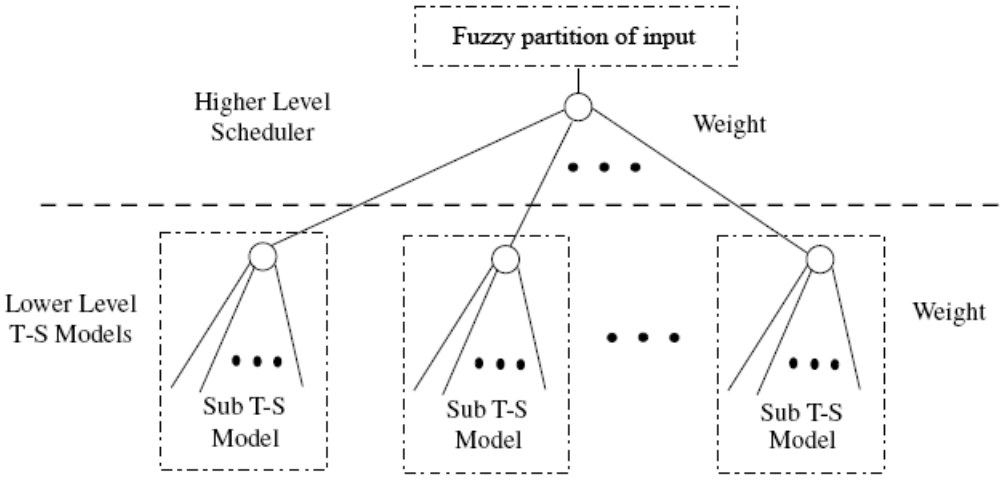

Figure 7.6 Hierarchical multiple sub T-S model structure

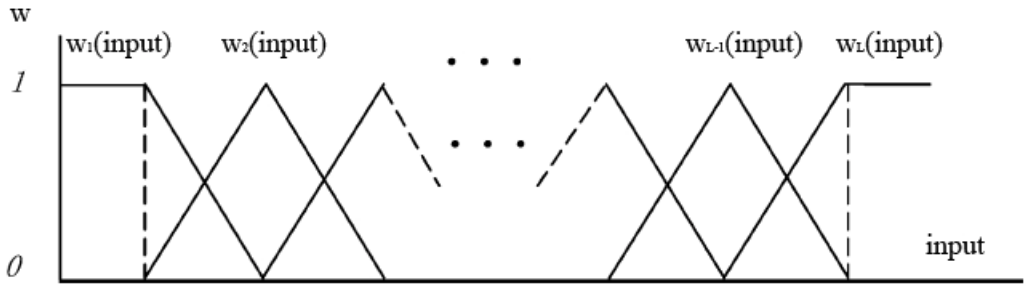

Figure 7.7 Membership function of the input

Steps of the algorithm to aggregate control outputs of individual local model are followings.

Step 1: Develop the data set $z_k = [\varphi_k, y_k]^T$ composed by the input-output data of the system

Step 2: Using the clustering algorithm, divide the whole system into M number of T-S models based on the fuzzy partition of varying input φ_k on its operation range

Step 3: Identify local controllers for each local T-S model as indicated in Section 7.2.1.2

Step 4: Measure the actual input-output values and determine fuzzy weights w_j, j=1, …, M of local T-S models.

Step 5: Compute the control signal Δu_j of each local T-S model and aggregate it through the fuzzy weight w_j to calculate the whole incremental control Δu signal as specified by Equation 7.5.

$$\Delta u = \frac{\sum_{j=1}^{L} w_j \Delta u_j}{\sum_{j=1}^{L} w_j} \tag{7.5}$$

Step 6: Compute the system control output u = u + Δu. Go back to Step 4 if the system operation is still in process.

7.3 The MMC framework tailored for robust supervisory demand-side controls

7.3.1 Application of the MMC framework to robust supervisory demand-side controls

The MMC framework for supervisory demand-side control strategy generally can follow the steps of the general MMC framework described in section 7.2.1. There are, however, a few distinguished points that require a customization of the standard procedure for domain-specific applications.

a. As identified, the uncertainty within and around the system is a main source to cause nonlinearity response of the system. Since scenario uncertainty is the major uncertainty type that causes very distinct profiles of robust solutions per scenario, a set of operation regimes from which distinct robust control profiles are developed accounts for the full operation regime where the robust control solution eventually explores. Therefore distinct scenarios are likely to determine operation regimes.

b. In the general MMC framework, a trigger to transfer from one cluster (i.e. operation regime) to another cluster is a variation of the input value that is sensitive enough to do this role. Therefore the corresponding trigger in the MMC framework for the supervisory demand-side control is a variation of the building load since it is a directly indicator that is dependent on current scenario.

In addition, a value of the current building load does not necessarily 100% match for specific scenario. It is because the fuzzy weight scheduler of the global controller calculates percentages of the contribution of each scenario that causes the value of the current building load, thus the resulting control strategy is an aggregated profile based on multiple control profiles of all associated scenarios taking account of contributions of individual scenarios. For instance, a value of the current building load happens to be in the middle of two load profiles which two scenarios resulted in. Then the value of the control input u_{new} is composed of 50% of the control input u_{sce1} (by the first scenario) and 50% of the control input u_{sce2} (by the second scenario).

In general the first-hand indicator of the building load for a building is the coil load imposed on the main plant. In case of the Acme building, however the coil load on the FCUs can be a direct indicator of current building load.

7.3.2 Flows of the MMC framework for robust supervisory demand-side controls

Based on the steps of the general MMC framework and the customization needs for the demand-side supervisory controls, a flow of necessary works is arranged and described in the following steps.

Step 1: Identify a set of feasible scenarios. Each scenario should be enough distinct from another scenario.

Step 2: Develop the base robust control model that is composed of static sub-components and scenario-dependent sub-components (section 3.6.3), and under each scenario prepare multiple instances of the base robust control model by means of quantifying specification and calibration uncertainties.

Step 3: Under each scenario develop a profile of the robust control strategy via the stochastic optimization.

Step 4: Under each scenario run Monte Carlo simulations with the robust control strategy developed in Step 3 to populate the building load profiles at each time step. Refer to Figure 7.8 for an example.

Step 5: Determine clusters of the building load at each time step considering scenarios and the clustering algorithm at Section 7.2.1.1. As indicated the above, clusters of the full operation regime are likely to be determined by a set of distinct scenarios.

And determine fuzzy weights w_j, j=1, …, M of clusters based on the membership function. Refer to Figure 7.9 for an example.

Step 6: Compute the control signal Δu_j of each cluster and aggregate it through the fuzzy weight w_j to calculate the whole incremental control Δu signal by the Equation (7.5)

Step 7: Compute the system control output $u = u + \Delta u$.

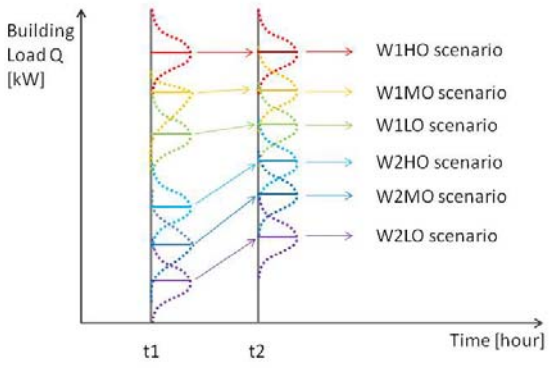

Figure 7.8 Six scenarios compose six clusters of distinct building load profiles.

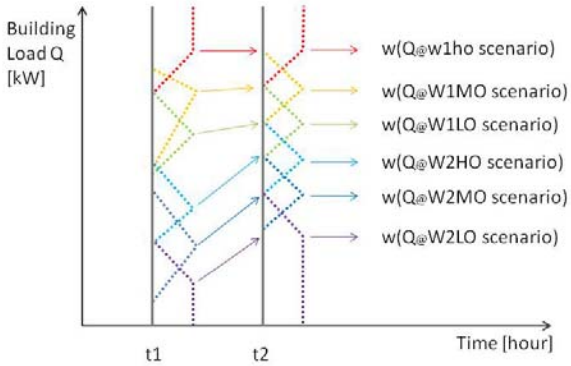

Figure 7.9 Building loads distributions at the time step t1 and t2 (Figure 7.8) calculates profiles of fuzzy weights of each building load profile.

7.4 Performance verification with the Acme building case

The MMC approach for the demand-side supervisory controls is applied to the Acme building introduced at the case study (chapter 6). This section pursues to validate how effectively and efficiently the multi-model based robust control strategy can select the most relevant scenario(s) and provide a proper control solution for such highly uncertain conditions.

Therein this validation will demonstrate that a "dynamic" robust solution upon a change of uncertain conditions, which has an outstanding merit in coping with unpredictable uncertainties over the existing "static" robust demand-side control solutions presented in chapter 6.

These case studies test performance of the multi-model based robust control strategy (the MMC robust control) in uncertain situations including i) under indentified possible scenarios, ii) under extreme load scenarios and iii) under varying occupancy scenarios where unpredictable characteristics of uncertainty give highly risk on the building load prediction.

7.4.1 Simulated actual environment with specification and calibration uncertainties in the known possible scenarios

7.4.1.1 In the expected nominal scenario (W2MO) and lower-cooling-load scenario (W2LO)

In the previous validation at chapter 6, the static robust control slightly underperforms the deterministic optimal control in two scenarios: the expected nominal scenario (W2MO) and the lower-cooling-load scenario (W2LO).

As seen in Table 7.1 and Table 7.2, however, the MMC robust control slightly outperforms the deterministic optimal control in daily mean operating cost and daily

power consumption. Its seemingly small improvement, in fact, implies substantial underlying enhancements.

Mean on-peak power consumption of the MMC robust control is still far less (in W2MO) or almost at the same level (in W2LO) with that of the deterministic control, and also mean daily power consumption is slightly lower in both scenarios. An implication is that the mean off-peak power consumption has not increased as against the static robust control does. In other words, the MMC robust control stores only a necessary amount of the cooling energy in the TES during off-peak hours, therefore it results in higher efficiency of using the stored cooling potential that eventually leads to lower daily mean operating costs.

Table 7.1 Performances of three demand-side control strategies in the simulated environment where specification and calibration uncertainties quantified and the nominal scenario W2MO

	Deterministic optimal control	(Static) Robust Control	MMC robust control
$\tilde{P}_{daily}$ [kWh]	650 (100%)	715 (110%)	638 (98%)
$\tilde{P}_{onpeak}$ [kWh]	60 (100%)	39.8 (66%)	42.9 (72%)
$\tilde{C}_{dailyTOU}$ [$]	16.7 (100%)	17 (102%)	15.9 (95%)
$\sigma_{C.daily}$ [$]	1.14	0.48	0.7
$CV_{C.daily}$	6.8%	2.8%	4.4%

Table 7.2 Performances of three demand-side control strategies in the simulated environment where specification and calibration uncertainties quantified and the scenario W2LO

	Deterministic optimal control	(Static) Robust Control	MMC robust control
$\tilde{P}_{daily}$ [kWh]	559 (100%)	635.2 (114%)	539 (96%)
$\tilde{P}_{onpeak}$ [kWh]	37.5 (100%)	31.4 (84%)	38 (101%)
$\tilde{C}_{dailyTOU}$ [$]	13.7 (100%)	14.9 (109%)	13.6 (99%)
$\sigma_{C.daily}$ [$]	0.6	0.4	0.9
$CV_{C.daily}$	4.3%	2.7%	6.6%

A decrease in mean daily power consumption of the MMC robust control under the environment where all uncertainties quantified (Table 7.3) confirms its enhanced performance that the MMC robust control stores only necessary amount of the cooling energy during off-peak hours. Finally it demonstrates the least daily operation cost among three strategies.

Table 7.3 Performances of three demand-side control strategies with the simulated environment under all identified uncertainties quantified including scenario uncertainty

	Deterministic optimal control	(Static) Robust Control	MMPC robust control
$\tilde{P}_{daily}$ [kWh]	875 (100%)	825 (94%)	786 (89%)
$\tilde{P}_{onpeak}$ [kWh]	196 (100%)	73.7 (38%)	74 (38%)
$\tilde{C}_{dailyTOU}$ [$]	31.1 (100%)	20.7 (67%)	20.3 (65%)
$\sigma_{C.daily}$ [$]	14.2	4.8	4.9
$CV_{C.daily}$	45.7%	23.2%	24.1%

7.4.1.2 In higher-cooling-load scenarios W1HO, W1MO and W2HO

In higher-cooling-load scenarios in the Table 7.4, demand-side control performance of the MMC control is outstanding (the shaded cells). As the static robust

control performs better when higher cooling load is anticipated (←), the MMC control also shows the same tendency with a slight better performance than the static robust control does.

In particular under the scenario W2HO that imposes a slightly higher cooling load than the nominal scenario W2MO, the MMC control outperforms the deterministic optimal control resulting that the daily mean power consumption becomes the lowest among three control strategies (95%), whereas the static robust control slightly underperforms the deterministic optimal control (102%).

Table 7.4 Performances of three demand-side control strategies with the simulated environment where specification and calibration uncertainties quantified under the higher-cooling-load scenarios W1HO, W1MO and W2HO

	W1HO Det.optimal control	W1HO Stat.Robust Control	W1HO MMC control	W1MO Det.optimal control	W1MO Stat.Robust control	W1MO MMC control	W2HO Det.optimal control	W2HO Stat.Robust Control	W2HO MMC control
$\tilde{P}_{daily}$ [kWh]	1200 (100%)	1033.9 (86%)	1007 (84%)	1085 (100%)	963.8 (89%)	929 (86%)	781 (100%)	800.4 (102%)	744 (95%)
$\tilde{P}_{onpeak}$ [kWh]	391 (100%)	150 (38%)	137 (35%)	316.4 (100%)	113.4 (36%)	97.4 (31%)	122 (100%)	53.1 (44%)	57.8 (47%)
$\tilde{C}_{dailyTOU}$ [$]	51.5 (100%)	28.5 (55%)	27.4 (53%)	44 (100%)	25 (57%)	24 (55%)	23.9 (100%)	19.3 (81%)	19.1 (80%)
$\sigma_{C.daily}$ [$]	3.3	1.8	1.8	2.9	1.1	1.5	2.3	0.7	1.6
$CV_{C.daily}$	6.4%	6.3%	6.6%	6.6%	4.4%	6.3%	9.7%	3.6%	9.4%

7.4.2 Simulated actual environment with specification and calibration uncertainties in extreme load scenarios

A merit of the MMC control is its dynamic reactions upon scenarios change. This feature is highlighted when current scenario turns unexpectedly, for instance when extremely higher or lower cooling load scenario far outranges from the six possible scenarios. The extreme high scenario (Ext. HL) assumes the max temperature 4°C higher and 30% more of internal heat gains than the W1HO, and the extreme low scenario (Ext. LL) assumes the max temperature 4°C lower and 30% less of internal heat gains than the W2LO.

As comparison results show in Table 7.5, the MMC control outperforms other two strategies. The lowest daily mean power consumption and daily mean operating cost well accounts for an enhanced control flexibility of the MMC control in both extreme conditions. An apex capability of the MMC control is observed, specially, when it faces an extreme lower cooling situation (Ext. LL). That is, while the static robust control eventually fails to move lower than its lowest limit of both mean on-peak and off-peak power consumptions, the MMC control transforms into an adequate strategy for the extreme low scenario. Finally it achieves better demand-side control performance than the deterministic control in terms of all of three performance criteria.

Table 7.5 Performances of three demand-side control strategies with the simulated environment where specification and calibration uncertainties quantified in extreme-higher- and lower-cooling-load scenarios (Ext. HL and Ext. LL, respectively)

	Ext. HL Deterministic optimal control	Ext. HL Static Robust Control	Ext. HL MMC control	Ext. LL Deterministic optimal control	Ext. LL Static Robust Control	Ext. LL MMC control
$\tilde{P}_{daily}$ [kWh]	1506 (100%)	1300 (86%)	1239 (82%)	378 (100%)	407 (108%)	361 (96%)
$\tilde{P}_{onpeak}$ [kWh]	638 (100%)	368 (58%)	319 (50%)	16.2 (100%)	17.5 (108%)	16.1 (99%)
$\tilde{C}_{dailyTOU}$ [$]	73.2 (100%)	47.4 (65%)	41.3 (56%)	8.7 (100%)	9.4 (108%)	8.4 (97%)
$\sigma_{C.daily}$ [$]	2.8	2.7	2.4	0.3	0.4	0.3
$CV_{C.daily}$	3.8%	5.7%	5.8%	3.5%	4.3%	3.6%

7.4.3 Simulated actual environment with specification and calibration uncertainties in varying occupancy scenarios

Focusing on testing control flexibility, as shown in Figure 7.10 this test case presumes unexpected situations when occupancy level suddenly increases in the afternoon. Demand-side control performances of three control strategies are compared in two scenarios (W1VO and W2VO) that have two types of weather conditions as described in Table 7.6. For all three performance indices, the MMC demonstrates superior control flexibility than the deterministic optimal control and the static robust control.

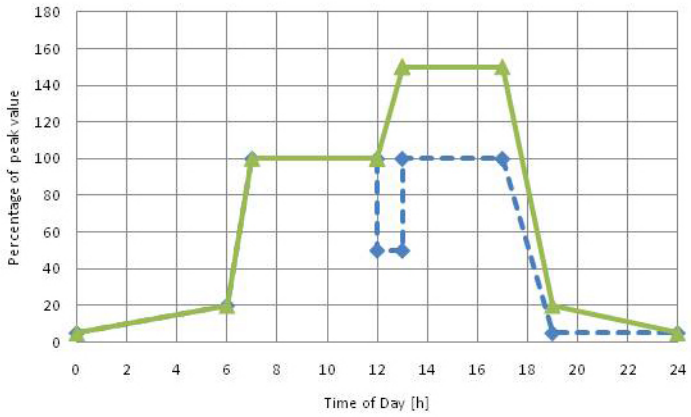

Figure 7.10 Regular medium level occupancy (MO : the sky dashed) and an abruptly increased occupancy in the afternoon (VO: the green solid)

Table 7.6 Performances of three demand-side control strategies with the simulated environment where specification and calibration uncertainties quantified in varying occupancy scenarios W1VO and W2VO

	W1VO Deterministic optimal control	W1VO Static Robust Control	W1VO MMC control	W2VO Deterministic optimal control	W2VO Static Robust Control	W2VO MMC control
$\tilde{P}_{daily}$ [kWh]	1240 (100%)	1044 (84%)	1013 (82%)	840 (100%)	815 (97%)	740 (88%)
$\tilde{P}_{onpeak}$ [kWh]	451 (100%)	188 (42%)	162 (36%)	193 (100%)	81 (42%)	71 (37%)
$\tilde{C}_{dailyTOU}$ [$]	56.9 (100%)	30.7 (54%)	28.6 (50%)	30.5 (100%)	20.7 (68%)	20 (66%)
$\sigma_{C.daily}$ [$]	3.0	2.4	1.8	2.0	0.8	1.5
$CV_{C.daily}$	5.3%	7.8%	6.3%	6.6%	3.9%	7.5%

Spectrum analyses, which represent how much portion of the control signal profile developed in each scenario contributes on formulating final control input u of the robust MMC at each time step, indicates how flexible the MMC robust control transits control profiles when unpredictable scenario uncertainty is observed. From Figure 7.11 to Figure 7.16, the purple line (in Figure 7.13 and 7.14) and the yellow line (in Figure 7.15 and 7.16) indicate control signal profiles developed in higher-cooling-load scenarios than W2MO, which are W2HO and W1LO, respectively.

- In Figure 7.11, 7.13 and 7.15 (the first column), when actual scenario is W2MO frequencies of the control signal profiles developed in higher-cooling-load scenarios become less.
- In side-by-side comparisons in each row, when the abrupt occupancy increase is observed in the afternoon (i.e., the actual scenario is W2VO) frequencies of the control signal profiles developed in higher-cooling-load scenarios (Figure 7.14 and Figure 7.16) become more frequent.

These spectrum analyses clearly verify that the robust MMC choose the most appropriate control signal profile as closest to actual scenario as possible.

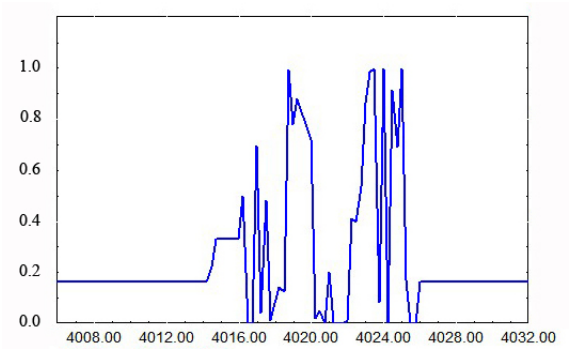

Figure 7.11 The reference case I with the contribution of the control signal profile W2MO in the scenario W2MO.

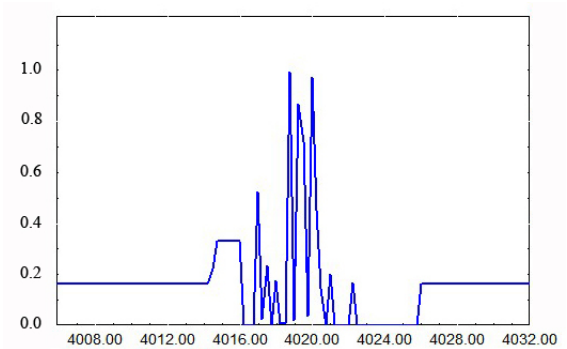

Figure 7.12 Compared to the reference case I in Figure 7.11, the control signal profile of the scenario W2MO tends to be less frequent when the abrupt occupancy increase is observed (the scenario W2VO).

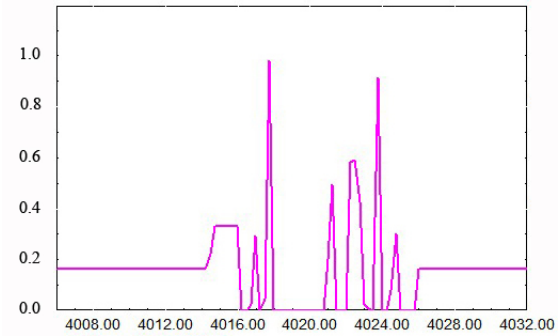

Figure 7.13 The reference case II with the contribution of the control signal profile W2HO in the scenario W2MO.

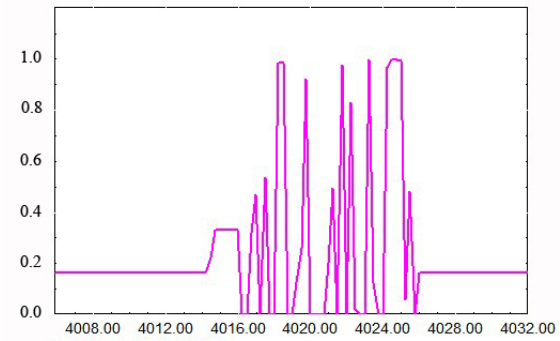

Figure 7.14 Compared to the reference case II in Figure 7.13, the control signal profile of the scenario W2HO tends to be more frequent when the abrupt occupancy increase is observed (the scenario W2VO).

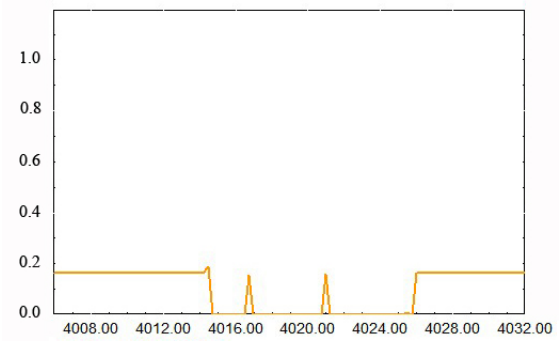

Figure 7.15 The reference case III with the contribution of the control signal profile W1LO in the scenario W2MO.

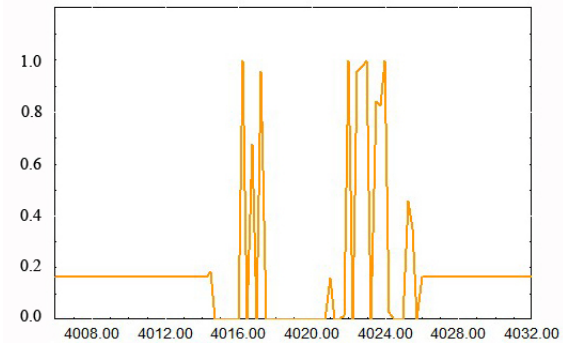

Figure 7.16 Compared to the reference case II in Figure 7.15, the control signal profile of the scenario W1LO tends to be more frequent when the abrupt occupancy increase is observed (the scenario W2VO).

In section 6.9.1.2, the robust thermal mass control proves its capabilities of reducing the monthly highest on-peak and economy-peak power consumptions that take a substantial cost impact on the total operating cost. The robust thermal mass control as a sub-control measure of the robust MMC still makes a significant control effort for avoiding demand charges getting higher. It is found in case of the scenario W1VO. As indicated in section 6.7, if the W1 is the monthly highest cooling load weather condition, it is likely that the on-peak demand charge would be levied when occupancy level increases in the afternoon (in the sky blue area from time step 4022 to 4027 in Figure 7.18). In such scenario, the robust MMC thrives to reduce the on-peak demand charge as much as possible as illustrated next.

The robust MMC reserves the stored cooling energy before on-peak hours and then uses it during on-peak hours to make the on-peak demand charge as small as possible. In Figure 7.17, it is clearly shown that the discharge (the brown solid) holds still before on-peak hours (until time step 4022), and finally it discharges when on-peak hours starts (after the time step 4022). Meanwhile the main chiller (the sky solid) provides the chilled water to meet the required by FCUs (the navy solid) till the time step 4022, and after that operation the main chiller almost freezes during between time step 4022 and 4027.

In Figure 7.18, the MMC control avoids the on-peak power consumption getting higher in the sky area by means of shifting the peak power consumption back right before the on-peak (the spike right before the time step 4022), which is still in the shoulder period. Since the economy demand charge (the red start point) is already in its highest pitch, this spike would not make the economy demand charge higher. Instead the saved cooling energy that could have been consumed (In Figure 7.17 the lower brown line still lies almost zero during between the time step 4021 to 4022) is used to provide more cooling energy during on-peak hours in order to make the on-peak power consumption as

evener and smaller as possible. Eventually the on-peak demand charge is levied at the blue star point while the economy demand charge is levied at the red star point.

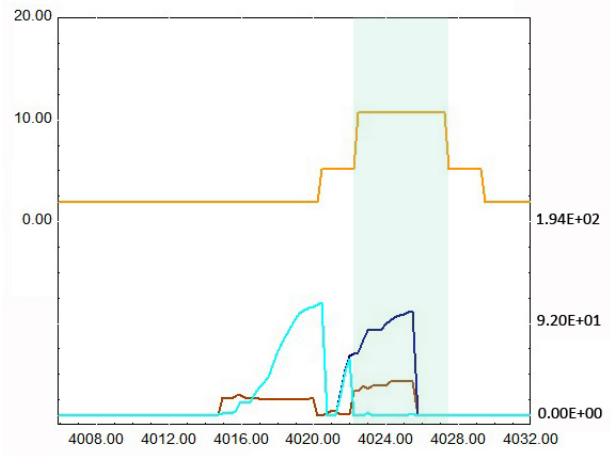

Figure 7.17 TOU rate (yellow), the chilled water required by main chiller (lower sky), the chilled water required by FCUs (lower navy) and the charged/discharged chilled water of the TES (lower brown) by the robust MMC in the scenario W1VO
All are in relative terms except the TOU rate.

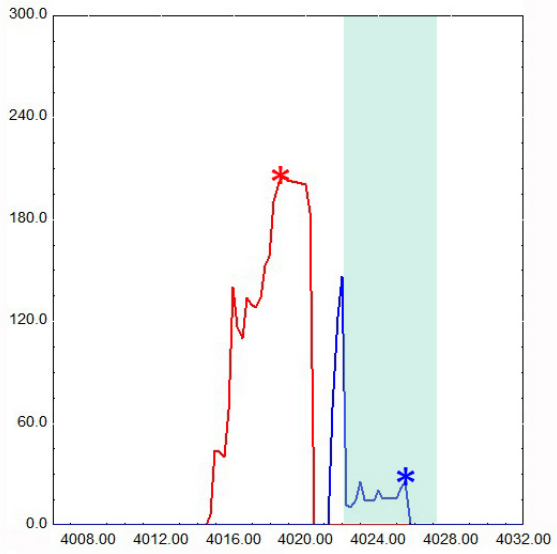

Figure 7.18 Power consumption [kW] profile by the MMC control in the W1VO

7.5 Summary and conclusions

In the previous case study, it has been validated that the static robust demand-side control strategy overall outperforms the conventional deterministic control strategies particularly in highly uncertain conditions such as the higher-cooling-load scenarios. This is because the static robust control solution has been developed based on the "greedy" mechanism of the robust control, i.e. regardless of which scenario imposes how much of the cooling load, it holds as much cooling energy as possible for discharge during expensive on-peak hours since a penalty (charging during inexpensive off-peak hours) is comparatively negligible.

The building load is mainly dependent on a combination of weather conditions and internal heat gains that are dependent on building usage scenarios. Therefore multiple

scenarios of such combinations result in multiple profiles of the building loads, thus the corresponding multiple profiles of the robust control strategies are favored. This fact naturally leads to consider a specific profile of the control strategy reactive for current scenario at each time, rather than an "average" control solution over multiple scenarios as the static robust control suggested.

The robust MMC control has shown outstanding credits in all three performance criteria of the demand-side controls and in uncertain conditions such as i) in the known possible scenarios, ii) in extreme load scenarios and iii) in abruptly varying occupancy scenarios.

Along with its superiority in the higher-cooling-load scenarios, when i) the actual cooling load is not much different from the expected and ii) in the lower-cooling-load scenarios, in which the static robust control slightly underperforms the deterministic optimal control in the previous cases, the robust MMC control is fairly flexible and more sensitive, thus resulting outstanding control performances.

Additionally the MMC control equips with controllability to avoid demand charges that getting higher when the monthly highest-cooling-load scenario is anticipated, thus it demonstrates an excellent control performance in any scenario.

CHAPTER 8

DISCUSSIONS AND REMARKS

This chapter is composed of discussions and reviews of the material from the preceding chapters. The first part highlights the main contributions and implications of the presented methodology to develop robust demand-side control strategies. The second part states limitations of the presented methodology and looks outward and to the future. Also this part reviews emerging research questions and needs for the related future works from a perspective of improving the proposed control strategy, which focuses on engineering aspects, to a broader perspective of extended uses of the presented methodology for building and HVAC&R systems.

8.1 Summary of contributions and benefits

This research demonstrates importance of the demand-side control for a building in the global carbon economy, and a value of the development methodology of the robust demand-side controls under uncertainty to attain the maximum benefit in both theoretical and practical perspectives. They are summarized in the following subsections.

8.1.1 This study reminds rudimental and core objectives of the demand-side controls

Chapter 1 reviews that the very fundamental objective of the demand-side control is to increase an effectiveness of an erratic supply of renewable energy sources that are alternatives of existing fossil-fuel based energy sources. It is a rudimental goal to reduce Carbon emission of both at an individual building level and at the grid level.

This study underlines this fundamental objective of the demand-side control, which have been often disregarded and overridden by the effort toward reducing operating cost in the existing demand-side control paradigm. Obviously, however, the least operating cost is not a negligible objective of the demand-side control. Rather this study emphasizes that one should employ multiple aspects of the demand-side control

performance mandated by its multiple goals to develop and evaluate demand-side control strategies.

According to basic objectives of the demand-side control, those include i) reducing the net demand (i.e. load shedding) and ii) load shifting (i.e. peak clipping and load building), Chapter 4 suggests three performance criteria. The case study illustrated in Chapter 6 and 7 has proven that the robust demand-side control strategies developed according to the proposed framework eventually outperform the existing legacy control strategies in all three performance indices when various types of uncertainties in certain operating conditions in the field exist.

8.1.2 This study asks for recognizing potentially detrimental impacts of uncertainty on the performance of the demand-side controls and more attentions for fundamental studies about the uncertainty

Existing researches proposing model-based optimal controls has assumptions that either (or both) i) pre-fixed deterministic conditions are justified for the purpose of engineering efficiency (e.g. an assumption of single nominal condition) or iii) uncertainty issues can be somehow (or have been already) cleared by internal robust mechanism of their engineering measures.

However we often observe certain operating conditions where a critical disparity between the predicted and the actual performance is found when deterministic optimal controls are actually applied. This is primarily due to various degrees of uncertainties ranging from non-linearity and time-varying characteristics of HVAC&R Systems to external prediction uncertainties such as weather forecasts. Chapter 1 illustrates examples where unexpected uncertainty may cause detrimental impacts on the performance of the demand-side controls.

Thereby capturing uncertainty as accurate as possible is the most fundamental resolution for the demand-side controls especially implemented based on the model-based control (MPC) theory. This is, however, not always feasible since uncertainty holds characteristics that are both ad-hoc in nature (e.g. unpredictable) and imprecise (e.g. lack of knowledge). In particular scenario uncertainty that originates primarily from weather, building usage scenarios and/or utility rate structure has not been seriously taken account for the simulation despite its critical impacts on building energy performance. Previous practices either have treated the scenario uncertainty as a single flat assumption or have not fully recognized its strong sporadic characteristics than other types of uncertainties.

Also different dimensions of uncertainties initiate issues such as whether uncertainties are identifiable, whether and/or how strongly they influence the performance of the demand-side controls, how feasible to capture and represent them, how they can be associated with the development process of the demand-side controls and how to make the demand-side control robust against them.

By these reasons, a fundamental investigation on uncertainty and an identification of systemic approaches of the uncertainty analysis with respect to development process of the robust demand-side control solution are in utmost needs. Chapter 2 scrutinizes fundamentals and sources of uncertainty, and it delivers a matrix frame to classify uncertainty sources according to the proposed three dimensions. Chapter 3 proposes a modeling method of the identified uncertainty for the robust model-based predictive controls according to the three dimensions. Both chapters take an approach to review general theories first and to analyze them in domain-specific aspects and applications next.

8.1.3 This study proposes the robust supervisory demand-side controls as a better solution to cope with a variety of dimensions of uncertainties

Chapter 4 introduces two representative demand-side control measures and a step-by-step methodology to develop robust supervisory demand side control strategies. Chapter 6 contains the case study with namely, the static single model-based robust controls considering all scenarios and this chapter verifies its performance against legacy control strategies including the deterministic optimal control.

This study proposes two new perspectives to improve performance of the static single model-based robust controls. Chapter 5 reports how a use of single source, which is based on the historical archive to forecast short-term weather condition, could cause underperforming demand-side controls. This chapter emphasizes a need that the short-term weather forecast should be based on multiple sources of both historical archive and online forecasts. In accordance with issues of the scenario uncertainty, chapter 7 introduces the Multiple model-based controls (MMC) to mitigate detrimental impacts of sporadically varying scenario uncertainty. This chapter verifies its performance against the static single model-based robust controls and the deterministic optimal controls.

The proposed robust supervisory demand-side control strategy based on the uncertainty analysis shows distinguished features with the existing control strategies including deterministic optimal controls in that:

a. It meets the very fundamental objective of the demand-side controls.
b. It reduces the variability of performance under varied conditions, and thus will avoid the “worst” case scenario.
c. It is not overly conservative in the “good” and “best” scenarios in deciding demand-side control portfolios, thus it will pursue the maximum value in terms of energy efficiency, mechanical serviceability, thermal comfort, and economy.
d. It is adaptive and reactive in cases of critical “discrepancy”, thus it makes prompt online control decisions for hedging risks by means of eliminating or reducing the expected loss so as to gain more value.

This study also proposes a management method for users to model uncertainty, implement and deploy uncertainty analysis, and develop the robust demand-side controls in a faster and systemic fashion. Since a difficulty of such implementation and deployment lies in the quality and volume of uncertainty data, an issue with a large volume of data and the resulting prolonged processing time would hinder its widespread applications in building automation industry where feasibility and fast turn-around are virtues. The proposed method is based on the Systems Modeling Language (SysML) and exploits the advanced cloud computing environment. Chapter 3 and 4 introduce theories and feasible applications of such.

8.1.4 Lessons learnt and implications

This study reviews fundamentals of uncertainty, identifies sources of uncertainty relevant to the demand-side controls and then characterizes them according to three dimensions of uncertainty. Characterizing uncertainty eventually purposes to divide the identified uncertainties into heuristic and physical uncertainties. While the heuristic uncertainty should be prevented through clear guidelines, normative procedures or use of standard tools in the process of model preparation and development, the physical uncertainty preliminarily residing in model inputs and parameters should be quantified into the model and modeling process.

Most of the existing studies concerning uncertainty emphasize an importance of the physical uncertainty in model data. Basically this study agrees with them, but also this study emphasizes that heuristic uncertainties can be origins of such physical uncertainties.

Criticality of the physical uncertainty for better control performance has motivated a direction of researches toward mitigating the physical uncertainty. Two recognized approaches to deal with the physical uncertainty in general engineering

modeling theories are “refinement” and “relaxation”. The first approach improves an accuracy of the model data in pursuit of making the model behaves as real as possible. The latter approach admits actually possible variations of properties of the model and thus includes those variations in the model and modeling process in order to make the model less sensitive to uncertainty. Therein the latter approach pursues overall “robust” performance of the model in reality.

This study takes the latter approach. However it premises and clearly understands that the well performing robust controls should be based on a good quality of the model data, and this objective can be met firstly through the refinement approach.

Recognition of uncertainty in building and systems modeling, BES and building operations indeed requires a switchover of the existing deterministic analysis to a stochastic analysis. Inherently this movement initiates further investigations about characteristics of the physical uncertainty that have not been seriously emphasized yet in terms of properties, features and dynamics of the physical uncertainty, which require very different treatments in modeling, simulation and building operations. These investigations can be backed up by more field and data-oriented studies. Eventually they will call for richer research topics in handy data acquisition, efficient management of extensive volume of data, databases, innovative data analysis methods and new modeling approaches mainly based on data mining and gray-box models.

8.2 Onward and outward

Although this study contains several major contributions in the demand-side controls, there are still significant opportunities for future works in demand-side controls, robust supervisory controls, and the general area of building simulations under uncertainty.

Some opportunities are based on improvements and extensions beyond limitations of the proposed methodology for developing the demand-side controls and the robust supervisory model-based predictive control (MPC). Others opportunities concern many applications for the proposed uncertainty modeling and the robust MPCs beyond the scope of this thesis. The following sub-sections explore two primary opportunities.

8.2.1 Arising research questions and future works based on the limitation

8.2.1.1 More case studies of the demand-side controls

A highlight of the proposed robust demand-side control strategy is its adaptability when degree of uncertainty is beyond the tolerance range that typical robust controls can hold. Such types of uncertainty are characterized as unpredictable uncertainty, a dominant feature of the scenario uncertainty (section 2.5).

Chapter 7 proposes the Multiple model-based robust controls (MMC) as an adequate solution for handling such scenario uncertainty. An idea of risk control capability of the MMC, which is based on reactive and manifold approaches, is shown and verified in additional case studies of the Acme building. However cases studies with more dynamic and highly uncertain situations will further demonstrate its superiority distinguished from existing control strategies. Three plausible cases that require new robust control strategies are presented as in below sub-sections.

In each case, sources of the scenario uncertainty to be analyzed include all of the three uncertainty sources of the external scenario (section 2.8.3). Thus three cases demonstrate how unpredictable uncertainty caused from an independent or a synergy of three scenario uncertainty sources can degrade performance of the planned control strategy. Finally three cases motivate more diversified aspects and expanded dimensions of adaptive control strategies in order to handle the scenario uncertainty.

a. Case studies of load shaping when renewable energy sources and battery are employed

When renewable energy sources are employed to individual building, a new criterion to evaluate the performance of the demand-side controls is evitable. It is load shaping that pursues synchronizing both demand and supply profiles in terms of frequency and magnitude. Therefore the well-provisioned load shaping supports the base for a net zero-energy building (ZEB) (Torcellini, Pless et al. 2006).

Distinguished from a concept of an off-grid building, the net zero-energy building typically uses the grid power when the on-site generation is not sufficient. Vice versa when the on-site generation is greater than the building demand, excess electricity is exported to the grid. However in high market penetration scenarios the grid may not always need the excess energy, thus on-site energy storage (e.g. battery) would become necessary.

Two situations with or without auxiliary storage are possible.

i) **Without auxiliary storage for the on-site generation**: The demand-side controls thrive to make a full use of the on-site supply as much as possible. Then the surplus power typically far cheaper than the grid power is used to spare more cooling (or heating) energy if active demand-side control measures such as TES are available. If not, the surplus power is exported to the grid while expecting cheaper or even free on-peak power draw.

If no storage is available for both demand and supply, and no grid connection, as there is no controlling mechanism the on-site energy production must be oversized to take advantages of the renewable energy from design and sizing perspectives. Then investment/design issues (such as higher first cost vs. compensation by reduced operating cost or a choice of criteria for optimal design

and efficiency issues caused by the fact that excess generated energy cannot be used) are emphasized.

ii) **With batteries to store the on-site generated power**: If demand-side control measures are not available, the supply-side control is able to do the same objectives of the demand-side control.

If both demand-side and supply-side controls are possible, control problems becomes more complex: synchronization of two profiles is the first objective of the control, however, it should be achieved through altering two profiles as flat as possible as shown in Figure 8.1. It is because lower and flatter profiles of both power demand and supply cause less issues of using the onsite renewable power generation (Section 1.1.2) meanwhile taking the most advantage of benefits of the demand-side controls (Section 1.2).

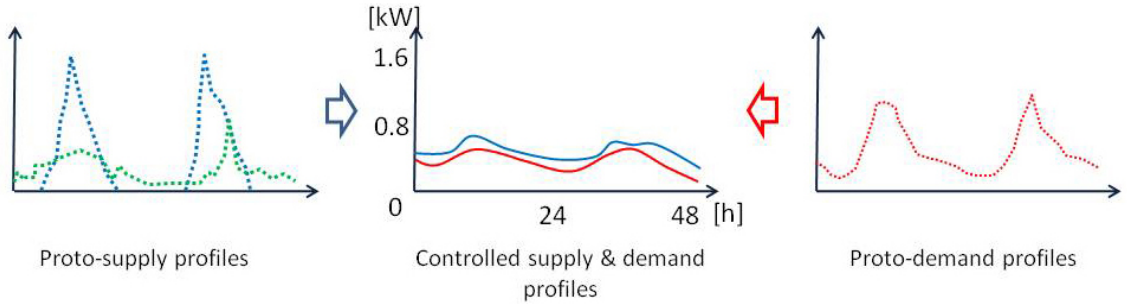

Figure 8.1 The supply-side and demand-side controls alter the proto-supply profiles (the blue and the green dotted denote the PV supply and the wind turbine supply respectively) and the proto-demand profiles (red dotted), and pursue higher synchronization of two controlled profiles.

In any case whether control is put on to the demand-side, the supply-side or both, using "storage" would be a prerequisite to ensure well-performing control strategies when renewable energy sources are employed. As indicated in section 1.4 the model-based predictive control (MPC) is known to be the most suitable control solution for such storages. In nature, then, uncertainty issues are not avoidable.

For both controls, the external scenario makes a vast influence on formulating control strategies and modifying the control strategy during operation; i) short-term weather prediction directly participates in setting up control strategies for the renewable energy supply and ii) Both weather and occupancy predictions are the most impacting uncertainty sources to the demand-side control performance. It is believed that the proposed robust MMC is fully capable of handling these issues and would produce superior robust control strategies.

b. Case studies with the Real-time pricing (RTP) rate

Along with the combination of the Time-of-use (TOU) and demand charges, the Real-time pricing (RTP) is another commonly considered and commercially available utility structure, which is known as one of the greenest guidelines since it reduces a variance of the grid level demands (Holland, Mansur et al. 2007). Also as the Smart grid is being promoted with the growth of extensive digital communication networks an idea that utility cost reflects the real-time power supply market, thus customers change their use of energy as prices enforces them to reduce energy use during high peak demand, becomes technically tangible.

Several control studies to leverage extreme cost incentives of the RTP to reduce the operating cost of a building have shown, however, their limitations in taking into account uncertainty of the RTP.

Henze (2003) concluded that the RTPs do not imperil superior cost-saving benefits of cool-storages operated with the deterministic optimal controls when compared to the chiller-priority or storage-priority controls. In general U.S. utility providers offer two types of RTPs: an-hour-ahead RTP and a-day-ahead RTP. As the utility provider informs the an-hour-ahead RTP only an hour ago its uncertainty becomes more detrimental in formulating predictive control strategies. Henze used a Bin model (Henze, Dodier and Krarti 1997) to predict the hour-ahead RTP of which external sub-variables

include historically analyzed ambient conditions and cooling loads/non-cooling demands (Figure 8.2).

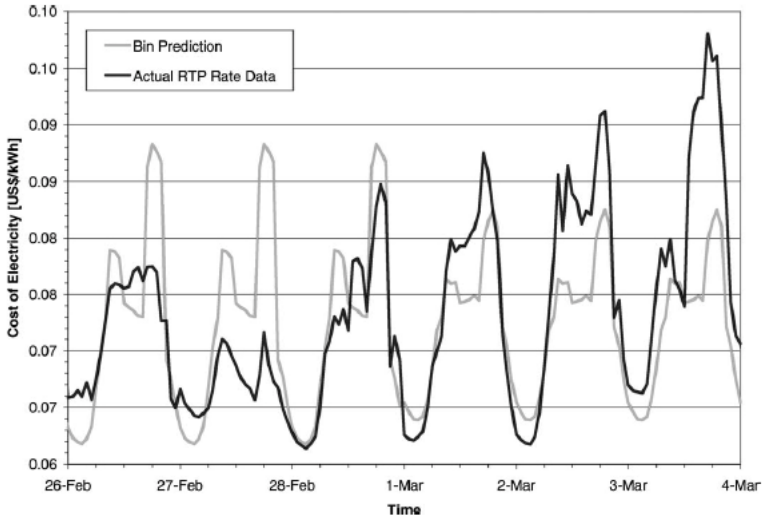

Figure 8.2 An hour-ahead RTP profiles on the West Coast (Henze 2003)

However this Bin model still possesses scenario uncertainty. As discussed about accuracies of the short-term weather forecasts in chapter 5, other types of models (i.e., not based on historical archive) that take heterogeneous model structures, internal/external data sources or temporal resolutions, such as models based on online weather forecasts, may output other patterns of the an-hour-ahead RTP. However they may turn out to perform better or may be not due to strong unpredictable uncertainty of the an-hour-ahead RTP. Therefore it is recommended to a mixed-use of two different types of weather forecast sources.

Braun (2007) proposed a near-optimal control strategy that swings between the chiller-priority and the storage priority controls depending on effective on-peak and off-peak durations when the RTP is chosen. To calculate two durations, he used daily building load forecasts His conclusion is that despite much simpler control mechanism and lighter modeling preparations and less instrumentations, the near-optimal control only slightly underperforms the deterministic optimal control in terms of operating cost. However he assumes perfect knowledge of both utility rates and building loads when

developing control strategies and evaluating them. Therefore his method would not be free from the concerns caused by the scenario uncertainty of the RTP.

As discussed about representing the scenario uncertainty in section 3.5.2, a multiple and heterogeneous source prone approach should be more adequate to comprehend strong unpredictable characteristic of the scenario uncertainty. As complementing to the historical archive-based prediction method, this study suggests use of the time-varying RTP model (Sun, Temple et al. 2006) that depends on time of day and maximum temperature for the day (Figure 2.13). Likewise other prediction models for the RTP, this model may not be representing the complete knowledge about the relationship between the function of time, the maximum temperature and the RTP. With a conjunction to the online weather forecast, however, it is believed that it provides affluent RTP profiles to represent the scenario uncertainty of the RTP. Then the suggested robust MMC would result in superior control performance than other control strategies under the RTP.

c. Case studies when occupants feel thermal discomfort

A case that occupants request for changing their thermal environment is one of representative unpredictable uncertainties that the building control system would encounter. This request indicates that mechanical systems do not provide enough cooling energy to meet the set-point temperature, thus actual zone temperature is above the set-point temperature (mode 2 and mode 3 in Figure 8.3). Or the current occupants are not satisfied with current thermal criteria although they are still within the comfort range, therefore the upper comfort bound temperature (T_{up} in Equation 4.1) needs to be lowered down. This will result in modifying the control strategy for the building thermal mass (section 4.2).

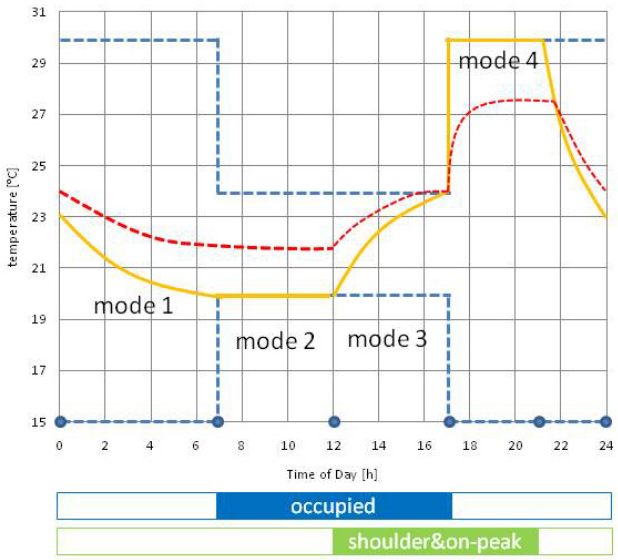

Figure 8.3 If internal heat gain is more than the expected, the actual indoor temperature (red dotted) can be above the set-point temperature (orange solid). The blue dotted denotes the bound for thermal comfort.

Both cases require extra cooling energy and corresponding tunings of the supervisory control for mechanical systems (Hu 2009), in particular tunings of the planned control strategy for the TES. Several situations ask for different tuning options as below.

At mode 2 the grid supply covers the extra cooling energy since it is still before the shoulder & on-peak period. If unexpected external scenarios such as higher ambient temperature or higher internal heat gains cause such demand for the extra cooling energy, however, the charge rate C_k^u (Equation 4.4) of the TES should increase in order to spare more cooling energy as more demand in the afternoon is expected.

At mode 3 instead of expensive on-peak grid power, the reserved cooling energy supply from the TES covers the extra cooling. Therefore the discharge rate D_k^u (Equation 4.5) of the TES is altered. A point of making control decisions to modify the current

discharge rate depends on how efficiently inventory of the TES (x_k in Equation 4.7) can be used for the remaining hours. For instance, if the moment to alter the planned control strategy passes the moment of daily peak load (e.g. by highest daily temperature) the remaining inventory could be consumed faster. Vice versa if it is still before daily peak load the inventory should be consumed carefully.

At mode 3 a trade-off between thermal comfort and operating cost can be an option for the control strategy. If occupants are willing to put up with thermal discomfort for a limited time and thus the TES runs as planned despite the higher demand for extra cooling energy, the operating cost and the on-peak power consumption would not make a surprise. Typically this situation could be when extremely high operating cost such as a levy of demand charges or real-time pricing is anticipated. Distinguished from the value-based approach, as Hu (2009) suggested, this option is a risk-based approach thus its preconditions include defining risk criteria, preferences and their parameters.

In three situations where the unpredictable characteristic of all uncertainty sources of the external scenario leads to alter the current control strategy, the scenario uncertainty strongly governs how the control strategy should be altered. Likewise the above two cases where a criticality of the scenario uncertainty is highlighted, the robust MMC would be a feasible control solution for this case as well.

8.2.1.2 Robust stability of the robust MPCs

With an importance of the performance of a control system, stability is an important criterion and is generally a safety issue in the engineering of a system. The stability of a system relates to its inputs or disturbances. A system that remains in a constant state unless affected by an external action and which returns to a constant state when the external action is removed can be considered to be stable.

Knowing that the system is stable is not generally sufficient for the requirements of control system designs. The stability analysis is necessary to determine how close the system is to instability, how much margin when disturbances are present and when the gain is adjusted. The objectives of stability analysis is to determine the following

a. Degree or extent of system stability;
b. The steady state performance;
c. The transient response.

The robust stability of the robust MPC introduces uncertainty notions with a relaxation factor on the objectives of control stability. When we say that a control system is robust we mean that robust stability is maintained and that the performance specifications are met for a specified range of model variations and uncertainty range, i.e. stability in the presence of uncertainty.

The various design procedures of the model-based predictive controls achieve the robust stability in two different ways (Bemporad and Morari 1999): i) indirectly by specifying the performance objectives and uncertainty descriptions in such a way that the optimal control leads to robust stability (Min-Max performance optimization) and ii) directly by enforcing a contraction constraint which guarantees that the state will shrink for all plants in uncertainty set (Robust contraction constraint).

Zheng (1995) demonstrated that the Min-Max performance optimization (Equation 3.9) alone does not guarantee robust stability by a proof with a counterexample. Therefore to ensure robust stability the uncertainty must be assumed to be time varying.

For stable plants, Badgwell (1997) proposes a robust MPC algorithm for stable, constrained, linear plants that is a direct generalization of the nominally stabilizing regulator presented by Rawlings and Muske (1993). By using Lyapunov arguments, robust stability can be proved when the following stability constraint is imposed.

$$J(U, x(t), \Sigma_i) \leq J(U_1^*, x(t), \Sigma_i) \quad (8.1)$$

This can be seen as a special case of the contraction constraint. This constraint can always be met for some control variable U, where $J(U, x(t), \Sigma_i)$ is the cost associated with the system prediction model for a pair of the planned horizon and control horizon, and $U_1^* \cong \{u^*(t|t-1), \ldots, u^*(t-1+N_m|t-1), 0\}$ (N_m denotes the length of the control horizon) is the shifted optimal sequence computed at time t-1.

As this constraint implies, it may add prohibitive conservativeness to control applications. Therefore a careful consideration of taking this approach is required for developing an efficient robust MPC for building and HVAC systems.

8.2.1.3 Extension to the Modelica platform and Algebraic modeling language (AML)

The robust supervisory controls seek for the best performance of the entire system taking into consideration of the system level characteristics and interactions among all components and their associated values, and they eventually deliver a composite of i) operation modes, ii) operation sequences and iii) set-points of individual components as the resulting control strategy.

The supervisory control strategies are typically made at the level of the system architecture where system topology and related properties are described. Mathematically they are obtained through a large scale global optimization of control variables related the devices defined in the system architecture. Different types of supervisory control variables, for instance on/off operation of devices vs. continuous set-point profiles of devices, therefore choose an appropriate mathematical program.

Many existing studies about developing supervisory control strategies including this study have chosen domain-specific, de-facto simulation tools (such as TRNSYS) and their popular partner optimization algorithms (such as Sequential quadratic programming). These tools are chosen because developers judge that these tools are

suitable representations for the given architecture model and these mathematical programs are proper optimization algorithms for both the given control model and the use of the resulting control strategy. However most existing studies are yet limited to only a few kinds and/or partial scopes of supervisory control problems. Several existing and emerging needs for new simulation and optimization platforms on which supervisory control strategies are developed include as below.

a. Open architecture that enables a concurrent use of different types of discretization methods: For example Integer programming for an optimization of operation sequences and Quadratic programming for optimization of set-points of devices
b. Variable time steps to properly represent a stiff system and to reject the disturbance (Wetter and Haugstetter 2006)
c. Use of purely algebraic equation-based system models but that capture significant behaviors in order to expedite the global optimization
d. Hierarchical modeling with reusable model library
e. Interoperability with external tools/environment such as Java and .net

Fortunately proven features of a general modeling language Modelica and its advanced solver would be able to support the above issues (Wetter, Haves et al. 2008; Wetter 2009). From a perspective of constructing supervisory control models using Modelica, however, a new usage of Modelica for dynamic optimization may require new constructs at the language level (i.e. Algebraic modeling language) in order to enable modeling specific needs of the robust supervisory controls.

Most of the required needs are related to numerical aspects of the extended optimization except the last two points. The design of numerical scheme of the optimization to discretize the control and state variables often strongly influences the properties of the resulting solutions. The choice of discretization also affects the

optimization execution for solving the problem. Also as the last two requirements indicate, the users' needs to model the optimization problem both in terms of const functions and constraints conveniently by taking advantages of high-level block descriptions draw a careful attention.

For constructing efficient supervisory control models and extended optimizations this study suggests an extension of the Modelica, namely Optimica, which takes advantages of modularity features of Modelica as well as reinforces the needs of the transcription dynamic optimization. The Optimica enables compact and intuitive formulations of both static/dynamic optimization problems based on Modelica models. It is indeed a recent development to the research community of the Systems modeling, therein new prototypes and applications are being actively published (www .jmodelica.org as of 2011). Readers can refer to Åkesson (2008) where a good overview about the Optimica is introduced.

8.2.2 Potential areas for future applications in building and system controls

The next sections briefly introduce feasible applications of the proposed robust model-based predictive controls (MPC). The emphasis is on blind spots where the existing works in general building and system controls may have passed by since impacts due to uncertainty is overlooked, critical characteristics of uncertainty are under recognition or handling of uncertainty is not appropriate for the given control problem. Then it will be shown how the proposed method is able to suggest constructive directions for the blind spot.

8.2.2.1 Robust model-based predictive controls (MPC) for the state-of-art control applications

This study demonstrates superiority of the proposed robust demand-side controls under uncertain conditions. One of main contributors for this success would be the MPC

of both thermal “storages” to regulate the demand profile. As already stated, it is because control performance of the storage (technically speaking, capacitance) relies on the accuracy of the forecasting behavior of the system and external forces, thus the proposed robust MPC that is i) less sensitive to statistical uncertainty and also ii) adaptive to a wider degree of scenario uncertainty should result in overall good outputs. This mechanism of the robust MPC would result in outstanding performance for any MPC applications, in particular, utilizing storages.

Apart from specific device controls, the principle of general building and HVAC&R controls is to manage, command, direct or regulate the behavior of building components (e.g. thermal mass or windows) or mechanical devices to meet certain goals. The required work to meet certain goals in building service then becomes load. Either it is a mechanical load to meet the set-point or an effort to reduce the mechanical load through getting more heat gains in winter or heat losses in summer, forecasting the building load underlies the basis for making such control decisions. Therefore a state-of-art and sophisticated building and HVAC&R controls that pursue distinguished building services should take into account uncertainty as very sensitive issue to overcome. Then the proposed robust MPC methodology would be a good candidate to develop such high-end control applications.

8.2.2.2 New framework for model calibration according to multiple operation regimes

Model calibration in order to obtain more realistic input data for simulation is another recognized engineering approach to deal with uncertainty. “Being calibrated”, however, does not mean no or negligible uncertainty (section 1.6.2). It is because calibration typically aims at not removing imprecision uncertainty but reducing it, therefore it is more appropriate to state that proper model calibrations result in less imprecision uncertainty.

In addition to that, unpredictable uncertainty cannot be calibrated in nature and even impacts of the less imprecise uncertainty after calibration can be augmented detrimentally with which unpredictable uncertainty is overlaid. In case of calibrating multiple components via the system identification, an observation of (Buswell and Wright 2004) supports this argument: the data available from HVAC systems for model calibration are not typically from the range of operation, thus if the calibrated model is used out of the calibration range, it may behavior in an unexpected manner.

A primary factor that makes the operation regimes of building and systems outbound the calibration range is the unpredictable uncertainty of external scenarios. It implies that if model calibrations take place in multiple domain models per scenario, then the resultant multiple profiles of the calibrated data would achieve more credentials. The concept of the Multiple-model controls (MMC) introduced in chapter 7 would provide technical backgrounds for implementing this idea.

APPENDIX A

VERIFICATIONS OF TRNSYS MODEL COMPARED TO ENERGYPLUS MODEL

Thermal performance of a TRNSYS model of the Acme building in the case study (Section 6.2) is verified compared to an EnergyPlus model. A purpose of verifications is to validate a creditability of the TRNSYS model by means of adjusting base values of the model parameters default assumptions of which may cause the TRNSYS model behave diverging from what the reference EnergyPlus model does. An example of model parameters that require this adjustment includes base values for thermal capacitances of each zone, which is supposed to be explicitly written in the TRNSYS model, but internally assumed in the EnergyPlus model.

Two simulations are tested under the same conditions as described in the case study. Tests ran during July 20h to July 26th under the setback temperature control that maintains the indoor temperature 23°C from 8 am to 8 pm. In this comparative study i) temperature variations of two conditioned zones (south and core zones) and one unconditioned zone (Plenum space) and ii) cooling load variations of three zones (south, west and core zones) are drawn as samples.

Figure A.1 illustrates results of indoor temperature variations of two simulation models. A slightly higher temperature profile of south and core zones is observed in the EnergyPlus model. This results in slightly higher cooling load of the same zones as shown in Figure A.2 and A.4. However their profiles are almost synchronized while they match peaks.

One interesting phenomenon is also observed that the core zone shows a slower thermal response, which can be typically characterized through movement of indoor temperature. When the set-point temperature is released after 8 pm, indoor temperature

floats slowly. When the set-point temperature turns back on after 8am, indoor temperature resumes slowly. This is due to a heavier internal active thermal mass of the core zone (i.e., higher capacitance) than that of the south zone.

In conclusion, model parameters of the TRNSYS model are well tuned and then the resulting TRNSYS model demonstrates satisfactory thermal performances of each single zone, compared to the reference EnergyPlus model.

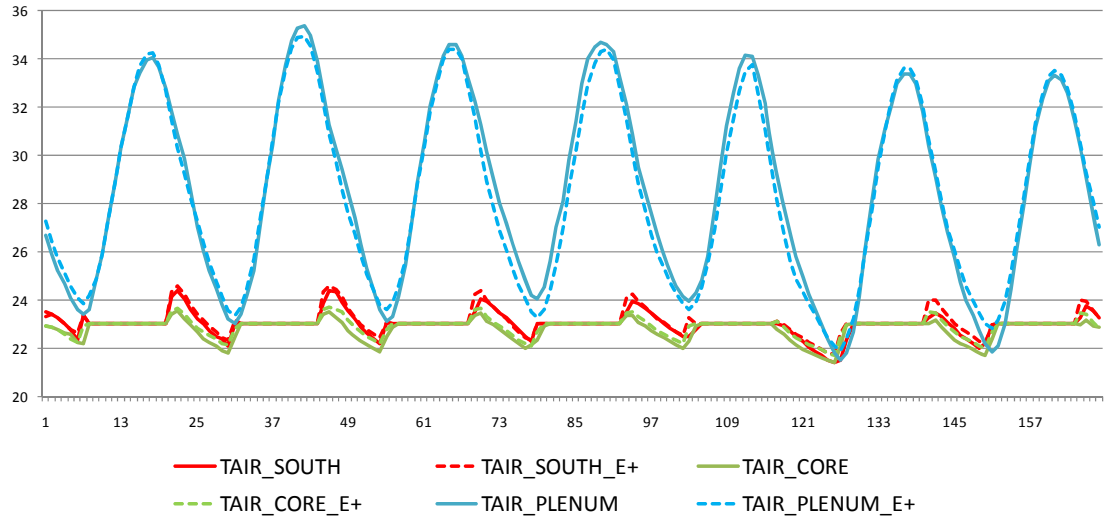

Figure A.1 Temperature [°C] variations of south, core and plenum zones simulated using TRNSYS (the solid) and EnergyPlus (the dotted)

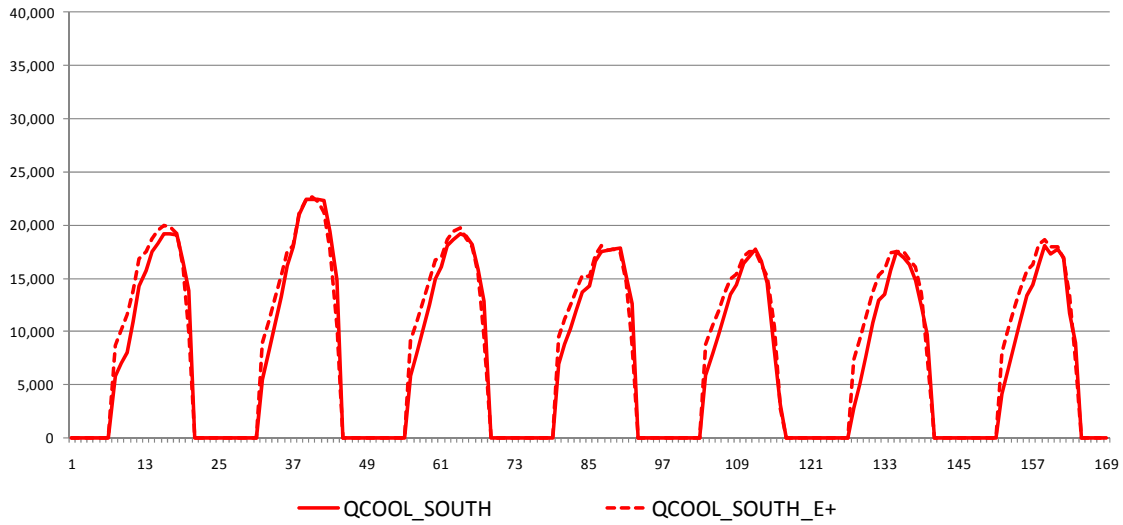

Figure A.2 Cooling load [W] variations of south zone simulated using TRNSYS (the solid) and EnergyPlus (the dotted)

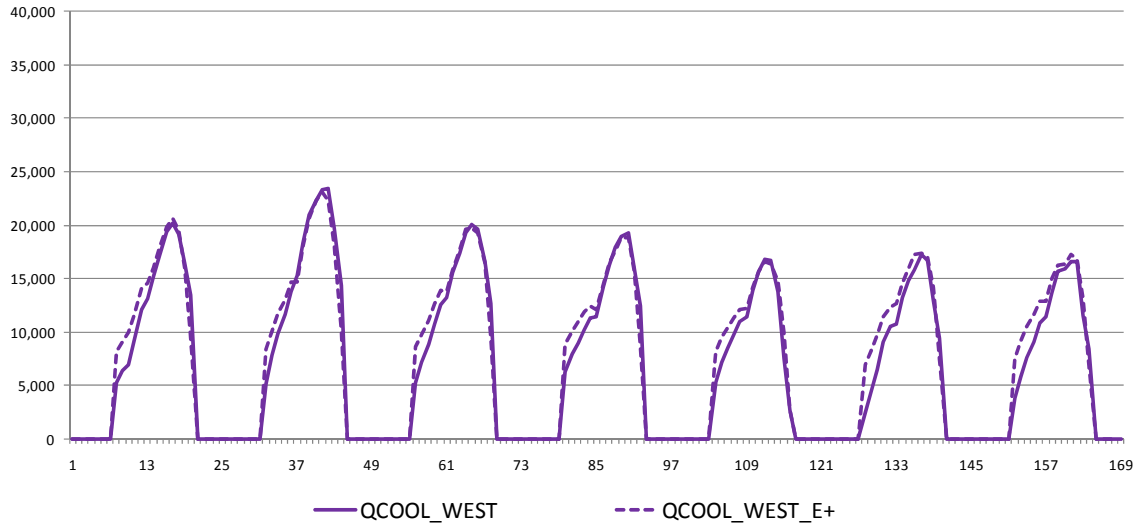

Figure A.3 Cooling load [W] variations of west zone simulated using TRNSYS (the solid) and EnergyPlus (the dotted)

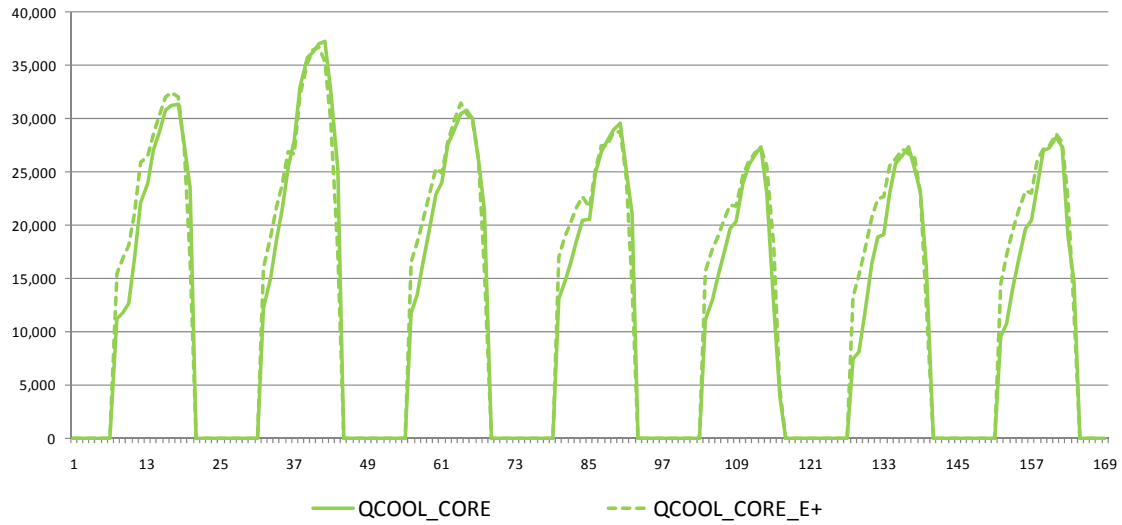

Figure A.4 Cooling load [W] variations of core zone simulated using TRNSYS (the solid) and EnergyPlus (the dotted)

APPENDIX B

VERIFICATIONS OF TRNSYS MODEL COMPARED TO ENERGYPLUS MODEL

This section introduces uncertainty sources in building and system description of Acme building to develop supervisory robust demand-side control strategy. Uncertainty sources and their ranges are obtained through an extensive literature review. They are briefly described and more focus on factors causing the uncertainty. Readers who want more details can refer to the main reference literature indicated in each section.

B1. Thermophysical properties in building material properties

Uncertainty in thermophysical properties in building material properties is typically caused by a discrepancy between product specifications based on testing conditions and actual behavior in operating conditions.

Degree of uncertainty is often documented in product specifications as confidence limits provided by manufacturer (Hu 2009). This is because the normal distribution function is one of the most commonly to represent uncertainty associated with material properties according to the central limit theorem (Spiegel 1975). Macdonald (2002) investigated ranges of uncertainty for three critical factors of thermophysical properties in building material properties as in Table B.1. Also base values and their standard deviations of surface thermophysical properties of unpainted materials are indicated in the Table B.2 to suggest a reference of how standard deviation can be calculated (Macdonald 2002).

Table B.1 Uncertainty range of three critical thermophysical properties of impermeable materials

Material thermophysical property	Uncertainty range
Conductivity	5%
Density	1%
Specific heat	12.25%

Table B.2 Base value and standard deviation of surface thermophysical properties of unpainted materials

	Absorptivity	Std. dev	Emissivity	Std. dev
Metals polished	0.32	0.07	0.05	0.01
Metals	0.56	0.12	0.24	0.06
Brick (light)	0.49	0.04	0.90	0.02
Brick (dark)	0.76	0.04	0.90	0.02
Stone (natural)	0.63	0.10	0.91	0.02
Plaster	0.40	0.03	0.90	0.02
Concrete	0.68	0.04	0.90	0.02

More references: Macdonald 2002

B2. Zone thermal capacitance

Zone capacitance indicates a degree of internal active thermal mass that typically consists of interior partitions and furniture. Along with a building structure thermal mass, internal thermal mass plays a critical role to introduce beneficial time lag (i.e. load shifting), especially for passive demand-side control strategies by building thermal mass. For instance in summer internal thermal mass absorbs some portion of the penetrating solar radiation and slowly releases it later on when the cooling demand is smaller.

The literature to seek for main contributors of controlling thermal mass and to suggest reasonable numerical models have been found. Balaras (1996) described that main factors to control the performance of thermal mass include material thermophysical properties, thermal mass location and distribution. Therefore internal thermal mass of a building is largely determined by i) characteristics of the building exterior envelop, ii) interior structural partitions and iii) furniture.

Antonopoulos and Koronaki (1998) have summarized the methods to estimate thermal mass such as direct measurement procedures, thermal network models, or a set of differential equations that describe the transient thermal behavior. Barakat and Sander estimated thermal capacitances of various types of residential buildings using thermal response factor program (1982). As Hu (2009) expressed, however, there is no explicit description whether they have included important factors of internal thermal mass such as partitions and furniture. Comprehending all sources and resulting single value for the thermal capacitance is not an easy task.

In trials of suggesting reasonable thermal mass model in single value, Hu (2009) suggested Equation (B.1) showing the relationship of total internal thermal mass and air mass of the space.

$$\text{Total interior thermal mass} = (1+f)\text{x Air\_Mass} \qquad \text{(B.1)}$$

where Air_Mass denotes the total thermal capacity of indoor air ($=\rho_{air}V_{room}C_{p,air}$); f denotes the ratio of the total internal thermal capacities from furniture and interior partitions and the thermal capacity of indoor air.

A wide spectrum of f has been found in the literature. Industry practices show that the typical extra thermal mass from furniture and interior partitions is five times the thermal mass from indoor air for residential buildings and three times of those for office buildings, i.e. foffice = 3 (Hu 2009). Barakat and Sander (1982) set 810KJ/K·m2of floor area for very heavy office buildings, i.e. foffice = 186.5 when ceiling height is 3.6m. TRNSYS manual sets its default value as 1.2 x V_{room}, i.e. foffice = 0 (TRNSYS 2010). However the manual recommends that users can adjust it if necessary. This wide spectrum is caused by the fact that people may have different life styles leading to different levels of internal thermal mass, thus it is building-specific.

To represent this uncertainty of internal thermal capacitance, this study takes the most recent and relevant approach indicated by (Hu 2009), which is used for testing

power reliability of an off-grid house. She assumed that f follows a normal distribution with mean and standard deviation as 26% of the mean. Instead of taking a value from the above mentioned range for the mean that is not supported by a strong scientific reasoning, and thus may cause non-realistic results, alternatively the mean is chosen via varying the value of f and picking up the best matching one during comparing resulting varied thermal performances of TRNSYS model to the reference model (e.g. EnergyPlus) that contains the same thermophysical environment.

More references: Hu 2009

B3. Infiltration

Conjunction with ventilation typically determined by building usage scenario, infiltration is highly correlated to building construction quality and building use. In particular the construction quality will affect the unintended leakage of air through the building structure and possibly may cause HVAC system errors. The weather and local micro climate also affect the infiltration rate.

Two main methods to measure building infiltration are available in energy simulation studies: effective leakage area (ELA) and air exchange rate per hour (ACH). Since TRNSYS sets the latter as its standard, this study more focuses on representing the infiltration with the ACH method.

There are various literatures concerning average air change rate of office buildings in different countries (Macdonald 2002, DOE bench mark, ASHRAE Standard 90.1-1989, DOE-2 infiltration methodology, BLAST infiltration methodology and ASHRAE 90.1-2004) as listed in the Table B.3. This spectrum of infiltration rate confirms that ACH varies per individual building rather than choosing one representative value for all. Therefore a deviation from the mean value that is specific to each building actually indicates a plausible uncertain range of infiltration rate for individual building.

To calculate this mean value, this study takes DOE-2 methodology as recommended by Infiltration modeling guidelines for commercial building energy analysis (PNNL 2009).

To investigate a deviation, Macdonald (2002) calculated frequencies of Air change rates based on his samples and (CIBSE 2001) by using an air flow network simulation. And he concluded that the distributions are approximately normal and standard deviation would be from 1/3 to 1/2 of the mean. This study takes more conservative value, which is 1/3 of the mean.

Table B.3 Infiltration flow rate input for all zones assuming the building level air change is distributed equally in all zones from various references

References	Infiltration rate basis
Air change rate of *standard* construction based on ASHRAE fundamental 1989 in UK (Macdonald 2002)	Mean: 0.33 ACH Max: 0.81 ACH Std. deviation: 0.102 ACH
Air change rate of *tight* construction based on ASHRAE fundamental 1989 in UK (Macdonald 2002)	Mean: 0.21 ACH Max: 0.50 ACH Std. deviation: 0.061 ACH
DOE benchmark (PNNL 2009)	0.3 ACH perimeter 0.15 ACH core
ASHRAE Standard 90.1-1989 (PNNL 2009)	0.038 cfm/sf of exterior wall area
DOE-2 methodology (PNNL 2009)	1.8 cfm/sf of above grade envelope area@0.3 in w.c.(75Pa)
BLAST methodology (PNNL 2009)	1.8 cfm/sf of above grade envelope area@0.3 in w.c.(75Pa)

More references: Macdonald 2002, PNNL 2009, DOE Commercial benchmark building models (http://www1.eere.energy.gov/buildings/commercial_initiative)

B4. Convective heat transfer coefficient

Both external and internal convective heat transfers have been regarded as critical uncertainty sources, as they are thermophysical phenomenon occurring at the boundaries, i.e. between spaces and solid enclosures for the external and between interior surfaces and indoor air for the internal.

For internal convective heat transfer, Awbi's chamber test (1988) shows that the internal convective heat transfer coefficient for floors varies mostly as a function of the temperature difference between surface temperature and air temperature. de Wit (2001) summaries that it ranges from 1.57 – 3.21 W/m^2K when the indoor-outdoor temperature difference equals to 2 °C. de Wit's and Beausoleil-Morrison's surveys are chosen for this study as an uncertain range of the internal convective heat transfer.

External convective heat transfer is mostly dominated by forced convection caused by wind, thus it varies more rapidly with a variation of wind condition and surface roughness. A choice of convective heat transfer modeling algorithm strongly influences the building energy performance and a difference of 20-40% in energy consumption predictions is observed due to different convective heat transfer models (Beausoleil-Morrison 1999).

To represent uncertainty of external convective heat transfer, this study takes relatively recently published convective heat transfer model - Palyvo's linear model (2008). Palyvo concluded that in many cases the linear regression equations are equally in agreement with experimental data although fundamental heat transfer theory predicts a power law relationship between external convective heat transfer coefficient and wind speed. When wind speed is within the range 0-4.5 m/s, the maximum deviation of the external connective heat transfer coefficient for windward cases (Equation B.2) averaged to ±18% and the one for leeward cases (Equation B.3) averaged to ±22%. Therefore the uncertainty can be represented as a uniform distribution ranging between the lowest and

highest deviations from the base value in each case. The base value is calculated from (B.2) or (B.3):

$$h_f = 7.4 + 4.0\ V_\beta \text{ (windward)} \quad \text{(B.2)}$$

$$h_f = 7.4 + 4.0\ V_\beta \text{ (leeward)} \quad \text{(B.3)}$$

where V_β denotes free stream wind speed (~10m above roof) in m/s.

More references: Hu 2009, De Wit 2001, Palyvo 2008, Beausoleil-Morrison 1999

B5. Wind reduction factor

The fact that actual local wind speed differs from that from a meteorological station is a serious uncertainty source for building energy performance prediction. Their systemic relationship can be described by the wind reduction factor. It is the ratio of onsite local wind speed and the potential wind speed measured at a meteorological station at 10m above ground level. In general it is used to estimate local wind speed based on wind speed in TMY weather data in building simulations. Equation (B.4) defines the wind reduction factor (ASHRAE 2001).

$$\gamma = \frac{V_{local}}{V_{pot}} = \left(\frac{\delta_{pot}}{H_{pot}}\right)^{\alpha_{pot}} \left(\frac{H}{\delta}\right)^{\alpha} \quad \text{(B.4)}$$

where V_{local} and V_{pot} denote the hourly local wind speed at height H and the wind speed measured at the reference height respectively. δ denotes the wind boundary layer thickness, α denotes the wind exponent and H is the height of location of interest.

Orme et al. (1994) transformed Equation (B.4) into a simpler form as in Equation (B.5) that consists of constant K and height H. This simplified equation is chosen for a majority of uncertainty analysis literature.

$$\gamma = \frac{V_{local}}{V_{pot}} = KH^{\alpha} \quad \text{(B.5)}$$

$$K = \left(\frac{\delta_{pot}}{H_{pot}}\right)^{\alpha_{pot}} \left(\frac{1}{\delta}\right)^{\alpha}$$

de Wit (2001) and Moon (2005) surveyed uncertain ranges of the constant K and exponent α as illustrated in Table B.4. The uncertainty in wind reduction factor K and α can be represented as an uniform distribution that varies between the range according to its terrain type.

Table B.4 Uncertain ranges of the constant K and exponent according to types of terrain

Terrain	Description	Constant K	Exponent α
1	Large city centers, in which at least 50% of buildings are higher than 21m, over a distance of at least 0.8 km or 10 times the height of the structure upwind, whichever is greater	0.14 – 0.21	0.33 – 0.4
2	Urban and suburban areas, wooded area, or other terrain with numerous closely spaced obstructions having the size of single-family dwellings or larger, over a distance of at least 460m or 10 times the height of the structure upwind, whichever is greater	0.35 – 0.43	0.22 – 0.28
3	Open terrain with scattered obstructions having heights generally less than 9.1m, including flat open country typical of meteorological station surroundings	0.52 – 0.72	0.14 – 0.2
4	Flat, unobstructed areas exposed to wind flowing over water for at least 1.6km, over a distance of 460m or 10 times the height of the structure inland, whichever is greater	0.68 – 0.93	0.10 – 0.17

More references: De Wit 2001, Moon 2005

B6. Degradation in chiller performance

The mechanical work is required when a chiller transfers thermal energy from a lower-temperature medium to a higher-temperature medium. Thus performance of a chiller is typically described with Coefficient of Performance (COP) by dividing thermal energy (Q_c) by the mechanical work (W) as in Equation (B.6).

$$COP = \frac{Q_C}{W} \tag{B.6}$$

COP of a commercial chiller tested in a lab environment usually ranges from 3 to 5.However COP tested in the field is often lower than the specification due to various non-indigenous factors from the lab condition such as operating conditions, thermostat settings, cycling of the equipment on/off, and the system frosting and defrosting.

Another source of significant efficiency degradation is cyclic effect (Goldschmidt 1980). The steady state COP is measured at full capacity and under actual operating conditions it is common that the chiller works at part load condition. When it operates under part load condition, the compressor of a chiller has to switch between on and off more often in order to respond to the dynamics especially when there is a narrow thermostat dead band. The extra cost of energy is called cyclic effect. The cyclic effect can be taken into account by a degradation coefficient in building simulation.

Equation (B.7) explains the relationship between actual COP after considering cyclic effects (COP_{cyclic}) and the steady state COP ($COP_{steady-state}$) with part load factor (PLF) as in Equation (B.8).

$$COP_{cyclic} = COP_{steady-state} \times PLF \tag{B.7}$$

$$PLF = 1 - C_d \times (1 - PLR) \quad \text{(B.8)}$$

where PLF denotes part load factor; C_d denotes degradation coefficient and PLR denotes partial load ratio that is calculated as the ratio of the building requirement supplied by the plant to the maximum energy that could be supplied by the same plant if it continues to work at full capacity.

Hu (2009) reviewed the literature concerning degradation coefficient for air-source heat pumps and summarized its uncertain range uniformly varies from 0.066 to 0.26 when it runs on cooling mode.

More references : Hu 2009, Goldschmidt 1980

B7. Thermal energy storage (TES) heat loss

Thermal energy storage of interest in this study stores the sensible energy, i.e. stratified chilled water. "Stratified chilled water" is often represented by a one-dimensional and multi-node model. Here a 'node' refers to a horizontal layer of water, modeled as isothermal at its nodal temperature (Mather 2002).

Since its operation principle is to store the energy and stand-by, and then to use it, thermal characteristics of TES are largely dependent on heat conduction between adjacent nodes and heat losses through tank walls.

The heat conduction model uses Fourier's law of heat conduction. However, rather than using the thermal conductivity k of water, attaching additional conductivity parameter Δk, i.e. k+ Δk, is an empirical correction to account for the circulation induced because the tank wall temperature is different from the water temperature. Newton et al. (1995) recommended using experimental data to select a value of Δk appropriate for the tank of interest.

They also recommended experiments to determine the heat loss coefficients UA_i (at node i) governing the heat transfer from the different nodes to the room in which the tank sits. Due to the above mentioned circulation, these heat loss coefficients are different than the coefficients using standard heat transfer theory.

Mather (2000) reported a range of Δk and UA_i by observing the temperature decay of thermocouples located at various point of the tank. Δk was found to be 0.25±0.02 W/mK and UA_i to be 0.043-0.44 W/K.

More references : Mather 2000, Mather 2002

B8. Efficiency degradation in cooling tower fan

The cooling tower cools a liquid stream by evaporating water from the outside of coils containing the working fluid. The basic premise that the saturated air temperature is the temperature at the air-water interface and it is also the temperature of the outlet fluid. Thus the more air flow rate induces the more evaporation cooling. The power consumption of the cooling tower is, therefore, dominant by the power drawn by the fan given in the Equation (B.9) and (B.10), where coefficients are fan efficiency parameters and γ_{air} denotes a ratio of the air flow rate to the design air flow rate.

$$\dot{P}_{fan} = \dot{P}_{fan,rated}\left[a_0 + a_1(\gamma_{air}) + a_2(\gamma_{air})^2 + \ldots\right] \quad \text{(B.9)}$$

$$\gamma_{air} = \frac{\dot{m}_{air}}{\dot{m}_{air,design}} \quad \text{(B.10)}$$

As a result of good aerodynamic design and minimized losses, total efficiencies are generally in the 75 to 85% range (Hydraulic Institute 1990). From experience with many full-scale fan tests, it is rare that ‘real life’ performance exceeds 55 to 75% total efficiency (Monroe 1978).

More references: Monroe 1978

B9. Efficiency degradation in cooling tower fan

Calibration uncertainty is a natural variation of readings and actuations of properly working devices. It is generally dealt in functional testing of building system as one standard criterion. Calibration and Leak-by test procedure (PECI 2006) specifies the guideline of calibration method. All field-installed temperature, relative humidity, CO, CO2 and pressure sensors and gages, and all actuators (dampers and valves) on all equipment shall be calibrated using the suggested methods.

Calibration methods are available for sensor calibration, valve and damper stroke setup and check, coil valve leak check and isolation valve or system valve leak check. In particular this guideline provides ranges of required tolerance per individual flow and signal property during calibration as Table B.5. This required tolerance of each flow and signal property can be used as calibration uncertainty range.

Table B.5 The required tolerance of flow and signal properties specified by (PECI 2006)

Flow and signal properties	Required Tolerance (+/-)	Flow and signal properties	Required Tolerance (+/-)
Cooling coil, chilled and condenser water temps	0.4F	Flow rates, water Relative humidity	4% of design 4% of design
AHU wet bulb or dew point	2.0F	Combustion flue temps	5.0F
Hot water coil and boiler water temp	1.5F	(monitored) Oxygen or CO_2	0.1 % pts
Outside air, space air, duct air temps	0.4F	(monitored)CO	0.01 % pts
Watthour, voltage & amperage	1% of design	Natural gas and oil flow rate	1% of design
Pressures, air, water and gas	3% of design	Steam flow rate	3% of design
Flow rates, air	10% of design	Barometric pressure	0.1 in. of Hg

More references: PECI (2006)

REFERENCES

Abushakra, B. (2001). Short-term Monitoring Long-term Prediction of Energy Use in Commercial and Institutional Buildings: the SMLP Method, Texas A&M University. A Ph.D. dissertation.

Adnot, J., B. Bourges, et al. (1979). Utilisation des courbes de frequence cumulees pour le calcul des. Analise Statistique des Processus Meteorologiques Appliquee al'Energie Solaire, Paris, CNRS.

Åkesson, J. (2008). Optimica---An Extension of Modelica Supporting Dynamic Optimization [Elektronisk resurs].

Alam, M. S., S. K. Saha, et al. (2005). "Simulation of Solar Radiation System." American Journal of Applied Science 2(4): 751-758.

Albuquerque, J., V. Gopal, et al. (1999). "Interior point SQP strategies for large-scale, structured process optimization problems." Computers & Chemical Engineering 23: 543-554.

Alcamo, J. and J. Bartnicki (1987). "A framework for error analysis of a long-range transport model with emphasis on parameter uncertainty." Atmospheric Environment 21(10): 2121-2131.

Antonopoulos, K. A. and E. Koronaki (1998). "Apparent and effective thermal capacitance of buildings." Energy 23(3): 183-192.

ASHRAE (1989). Energy efficient design of new building except low-rise residential buildings. Atlanta, GA, ASHRAE Inc.

ASHRAE (1995). Handbook of Fundamentals. Atlanta, GA, ASHRAE Inc.

ASHRAE (2001). 2001 AHSHRAE Handbook-fundamentals. Atlanta, ASHRAE.

ASHRAE (2002). ASHRAE Guideline 14, Measurement of Energy and Demand Savings, ASHRAE Standards Committee.

ASHRAE (2007). Evaluation of building thermal mass savings. Atlanta, ASHRAE. RP-1313 Final report.

ASHRAE (2008). 2008 AHSHRAE Handbook-fundamentals. Atlanta, ASHRAE.

Aughenbaugh, J. M. (2006). Managing Uncertainty in Engineering Design Using Imprecise Probabilities and Principles of Information Economics, Georgia Institute of Technology. Ph.D. Thesis.

Awbi, H. B. (1998). "Caculation of convective heat transfer coefficients of room surfaces for natural convection." Energy & Buildings 28(2): 219-227.

Badgwell, T. A. (1997). "Robust model predictive control of stable linear systems." International journal of control 68(4): 797-818.

Baird, S. (1993). "Energy Fact Sheet: Hydro Electric Power." Retrieved 2/24/2011, from http://www.physics.ohio-state.edu/~kagan/phy367/P367_articles/HydroElectric/hydroelectric.html.

Balaras, C. A. (1996). "The role of thermal mass on the cooling load of buildings: An overview of computational methods." Energy and Buildings 24(1): 1-20.

Banerjee, A., Y. Arkun, et al. (1997). "Estimation of nonlinear systems using linear multiple models." AIChE J May. 43: 5.

Barakat, S. A. and D. M. Sander (1982). Utilization of solar gain through windows for heatinf houses. D. o. b. research. Ottawa, Canada, National Research Council of Canada.

Beausoleil-Morrison, I. (1999). Modelling mixed convection heat transfer at internal building surfaces.

Beck, M. B. (1987). "Water quality modelling: a review of the analysis of uncertainty." Water resource research 23(8): 1393-1442.

Bemporad, A. and M. Morari (1999). Robust Model Predictive control : A survey. Robustness in identification and control.

Bemporad, A. and M. Morari (1999). Robust model predictive control: A survey. Robustness in identification and control. A. Garulli and A. Tesi, Springer Berlin / Heidelberg. 245: 207-226.

Bemporad, A. and E. Mosca (1998). "Fulfilling hard constraints in uncertain linear systems by reference managing." Automatica 34(4): 451-461.

Berger, X. (1979). Etude du Clima en Region Nicoise en vue d'Applications a l'Habitat Solaire. Paris, CNRS.

Billinton, R. and W. Li (1994). Reliability assessmnet of electric power systems using Monte Carlo methods, New York: Plenum Press.

Bogg, P. T. and J. W. Tolle (1996). "Sequential Quadratic Programming." Acta Numerica: 1-52.

Born, F. J. (2001). Aiding renewable energy integration through complimentray demand-supply matching. Energy Systems Research Unit, University of Strathclyde. PhD Dissertation.

Box, G. E. P. and K. B. Wilson (1951). "On the experimental attainment of optimum conditions." Journal of the Royal Statistical Society 13(1): 1-45.

Braun, J. (1990). "Reducing energy costs and peak electrical demand through optimal control of building thermal storage." ASHRAE Transactions.

Braun, J. E. (2007). A Near-Optimal Control Strategy for Cool Storage Systems with Dynamic Electric Rates (RP-1252). HVAC&R Research, American Society of Heating, Refrigerating & Air-Conditioning Engineers, Inc. 13: 557-580.

Braun, J. E. and K. H. Lee (2006). "Assessment of Demand Limiting Using Building Thermal Mass in Small Commercial Buildings." ASHRAE Transactions 112(1): 547-558.

Braun, J. E., J. W. Mitchell, et al. (1987). "Performance and control characteristics of a large cooling system." ASHRAE Transactions 93(1): 1830-1852.

Braun, J. E., K. W. Montgomery, et al. (2001). "Evaluating the performance of building thermal mass control strategies." HVAC&R Research 7(4): 403-428.

Busch, J. F. and J. Eto (1996). "Estimation of avoided costs for electric utility demand-side planning." Energy Sources 18: 473-499.

Buswell, R. A. and J. A. Wright (2004). "Uncertainty in model-based condition monitoring." Building Services Engineering Research and Technology 25(1): 65-75.

Campolongo, F., J. Cariboni, et al. (2007). "An effective screening design for sensitivity anlalysis of large models." Environmental modelling and software 22(10): 1509-1518.

Charnes, A. and W. W. Cooper (1959). "Chance-Constrained Programming." Management Science 6(1): 73-79.

Chen, T. Y. and A. K. Athienitis (1996). "Ambient temperature and solar radiation prediction for predictive control of HVAC systems and a methodology for optimal building heating dynamic operation." ASHRAE Transactions 9102(1): 26-35.

CIBSE (2001). Ventilation and air conditioning, CIBSE Guide B2. London, Chartered Institution of Building Services Engineers.

City_of_Boulder (2006). "Boulder voters pass first energy tax in the nation." Retrieved 5/20/2009, from http://www.bouldercolorado.gov/index.php?option=com_content&task=view&id=6136&Itemid=169.

Coffey, B., F. Haghighat, et al. (2010). "A Software Framework for Model Predictive Control with GenOpt." Energy and Buildings 42.

Conniff, J. P. (1991). "Strategies for reducing peak air conditioning loads by using heat storage in the building structure." ASHRAE Transactions 97: 704-709.

Dantzig, G. B. (1955). "Linear programming under uncertainty." Management Science 1: 197-206.

Davis, P. K. and R. Hillestad (2000). Exploratory analysis for strategy problesm with massive uncertainty. Santa Monica, CA, RAND.

de Wilde, P., Y. Rafiq, et al. (2008). Uncertainties in predicting the impact of climate change on thermal performance of domestic buildings in the UK. Building Services Engineering Research & Technology, Sage Publications, Ltd. 29: 7-26.

de Wit, M. S. (2001). Uncertainty in predictions of thermal comfort in buildings. Delft, TU Delft. Ph.D.

Department_of_Trade_and_Industry (2000). "New & renewable energy prospects for the 21st Century." Retrieved 2/24/2011, from http://webarchive.nationalarchives.gov.uk/+/http://www.berr.gov.uk/files/file21097.pdf.

Dodier, R. H. and G. P. Henze (2004). "Statisitical analysis of neural networks as applied to building energy prediction." Journal of Solar Energy Engineering 126(1): 592-600.

DOE_bench_mark. "Commercial Building Initiative." Retrieved 4/5/2010, from http://www1.eere.energy.gov/buildings/commercial_initiative/index.html.

Doyle, F. J., A. K. Packard, et al. (1989). "Robust controller design for a nonlinear CSTR." Chemical Engineering Science 44(9): 1929-1947.

Drees, K. H. and J. E. Braun (1995). Modeling of area-constrained ice storage tanks. HVAC&R Research. 1: 143-159.

Egorov, I., G. Kretinin, et al. (2002). How to execute robust design optimization. 8th AIAA/USAF/NASA/ISSMO Symposium on Multidisciplinary Analysis and Optimization, Atlanta, GA, American Institute of Aeronautics and Astronautics (AIAA)

Ellis, P. G., P. A. Torcellini, et al. (2007). Simulation of Energy Management Systems in EnergyPlus. Building Simulation '2007 10th International IBPSA Conference Beijing, China.

Energy_Information_Administration (2000). "U.S. Electric Utility Demand-side Management: Trends and Analysis." Retrieved 2/20/2011, from http://www.eia.doe.gov/cneaf/pubs_html/feat_dsm_conents.html.

Environmental_Resources (1985). Handling uncertainty in environmental impact assessment. London, Environmental Resources.

EPA (1992). Guidelines for exposure assessment.

EPA (2000). Proposed guideline on cummulative risk assessment of pesticide chemicals that have a common mechanism of toxicity, Office of Pesticide Programs.

Erbs, D. G., S. A. Klein, et al. (1982). "Estimation of the diffuse radiation fraction for hourly, daily and mohtly-average global radiation." Solar Energy 28(4): 293-302.

Fisher, J. (1998). "Model-based systems engineering: A new paradigm." INCOSE Insight 1(3): 3-16.

Florita, A. R. and G. P. Henze (2009). "Comparison of Short-Term Weather Forecasting Models for Model Predictive Control." HVAC&R Research 15(5): 835-853.

Fontoynont, M., Dumortier, D., Heinemann, D., Hammer, A., Olseth, J., Skartveit, A., Ineichen, P., Reise, C., Page, J., Roche, L., & Beyer, H. G., Wald, L. (1997). SATELLIGHT—processing of METEOSAT data for the production of high quality daylight and solar radiation available on a world wide web internet server. mid-term progress report. jor3-ct9-0041. Tech. rep.

Fontoynont, M., Dumortier, D., Heinemann, D., Hammer, A., Olseth, J., Skartveit, A., Ineichen, P., Reise, C., Page, J., Roche, L., & Beyer, H. G., Wald, L. (1998). Satellite: A WWW server which provides high quality daylight and solar radiation data for Western and Central Europe. 9th conference on satellite meteorology and oceanography. Paris: 434–437.

Funtowicz, S. O. and J. R. Ravetz (1990). Uncertainty and quality in science for policy. Dordrecht, Kluwer Academic Publishers.

Gartner.com (2010). "Gartner Says Cloud Computing Will Be As Influential As E-business." Retrieved 8/22/2010, from http://www.gartner.com/it/page.jsp?id=707508.

Georgia_Power (2010). "Tme of use - General service demand schedule: "TOU-GSD-4"." Retrieved 5/11/2010, from http://www.georgiapower.com/pricing.

Gero, J. S. and E. E. Dudnik (1978). "Uncertainty and the design of building subsystems--A dynamic programming approach." Building and Environment 13(3): 147-152.

Goldschmidt, V. W., G. H. Hart, et al. (1980). "A note on the transient performance and degradation coefficient of a field tested heat pump-cooling and heating mode." ASHRAE Transactions 86(2): 368-375.

Gorissen, D., I. Couckuyt, et al. (2010). "A Surrogate Modeling and Adaptive Sampling Toolbox for Computer Based Design." Journal of Machine Learning Research 11: 2051-2055.

Gowri, K., D. Winiarski, et al. (2009). Infiltration modeling guidelines for commercial building energy analysis.

Green, M. and D. Limebeer (1995). Linear robust control. Englewood Cliffs, N.J., Prentice Hall.

Gustafson, D. E. and W. C. Kessel (1979). Fuzzy clustering with fuzzy covariance matrix. Proc. IEEE CDC.

Gwerder, M. and J. Tödtli (2005). Predictive Control for Integrated Room Automation. Clima 2005, Lausanne, Switzerland.

Hammer, A., D. Heinemann, et al. (2003). "Solar energy assessment using remote sensing technologies." Remote Sensing of Environment 86(3): 423-432.

Haurwitz, B. (1945). "Insolation in relation to cloudiness and cloud density." Journal of Meteorology 2: 154-166.

Haurwitz, B. (1946). "Insolation in relation to cloud type." Journal of Meteorology 3: 123-124.

He, M., W.-J. Cai, et al. (2005). "Multiple fuzzy model-based temperature predictive control for HVAC systems." Information Sciences 169(1-2): 155-174.

Henze, G. P. (2003). "Impact of real-time pricing rate uncertainty on the annual performance of cool storage systems." Energy and Buildings 35(3): 313-325.

Henze, G. P., B. Biffar, et al. (2008). "Optimization of Building Thermal Mass Control in the Presence of Energy and Demand Charges." ASHRAE Transactions 114(2): 75-84.

Henze, G. P., M. J. Brandemuehl, et al. (2007). Final Project Report for ASHRAE Research Project 1313-RP: Evaluation of Building Thermal Mass Savings. R. American Society of Heating, and Air-Conditioning Engineers. Atlanta, GA.

Henze, G. P., R. H. Dodier, et al. (1997). Development of a predictive optimal controller for thermal energy storage systems. International Journal of HVAC&R Research. 3: 233 - 264.

Henze, G. P., C. Felsmann, et al. (2004). Impact of Forecasting Accuracy on Predictive Optimal Control of Active and Passive Building Thermal Storage Inventory. HVAC&R Research, American Society of Heating, Refrigerating & Air-Conditioning Engineers, Inc. 10: 153-178.

Henze, G. P., C. Felsmann, et al. (2004). "Evaluation of optimal control for active and passive building thermal storage." International Journal of Thermal Sciences 43(2): 173-183.

Henze, G. P., D. E. Kalz, et al. (2005). Experimental Analysis of Model-Based Predictive Optimal Control for Active and Passive Building Thermal Storage Inventory. HVAC&R Research, American Society of Heating, Refrigerating & Air-Conditioning Engineers, Inc. 11: 189-213.

Henze, G. P. and M. Krarti (1999). "The impact of forecasting uncertainty on the performance of a predictive optimal controller for thermal energy storage systems." ASHRAE Transactions 105(1): 553–561.

Henze, G. P. and M. Krarti (2005). Predictive Optimal Control of Active and Passive Building Thermal Storage Inventory, US Dept. of Energy National Energy Technology Laboratory.

Henze, G. P., M. Krarti, et al. (2003). "Guidelines for improved performance of ice storage systems." Energy and Buildings 35(2): 111-127.

Hodges, J. S. (1987). "Uncertainty, policy analysis and statistics." Statistical science 2(3): 259-291.

Holland, S. P., E. Mansur, et al. (2007). Is real-time pricing green? the environmental impacts of electricity demand variance. NBER working paper series working paper 13508. Cambridge, MA, National Bureau of Economic Research.

Holland, S. P. and E. T. Mansur (2007). Is Real-Time Pricing Green? The Environmental Impacts of Electricity Demand Variance.

Hu, H. (2009). Risk-conscious design of off-grid solar energy houses. College of Architecture. Atlanta, Georgia Institute of Technology. Doctor of Philosophy.

Huang, Y. (1999). Uncertainty assessment methodology and applications for HVAC systems, University of Iowa. M.S.

Hyun, S.-H. and C.-S. Park (2007). Natural Ventilation in Residential Dwellings under Uncertainty. ASHRAE Transactions, American Society of Heating, Refrigerating and Air-Conditioning Engineers, Inc. 113: 173-181.

Hyun, S. H., C. S. Park, et al. (2008). Analysis of uncertainty in natural ventilation predictions of high-rise apartment buildings. Building Services Engineering Research & Technology, Sage Publications, Ltd. 29: 311-326.

Ianetz, A., V. Lyubansky, et al. (2007). "Inter-comparison of different models for estimating clear sky solar global radiation for the Negev region of Israel." Energy Conversion and Management 48(1): 259-268.

Iman and Helton (1985). A Comparison of Uncertainty and Sensitivity Analysis Techniques for Computer Models. Albuquerque, New Mexico, Sandia National Laboratories.

INCOSE (2004). "Model Based Systems Engineering." Retrieved 11/5/2010, from http://mbse.gfse.de/.

Iqbal, M. (1983). An introduction to solar radiation. Canada, Academic Press.

Jenkins, N., R. Allan, et al. (2000). Embedded Generation, The Institution of Engineering and Technology.

Jiang, W., T. A. Reddy, et al. (2007). "General Methodology Combining Engineering Optimization of Primary HVAC and R Plants with Decision Analysis Methods--Part II: Uncertainty and Decision Analysis." HVAC & R Research 13(1): 119-140.

Johnson, C. D. (2002). Process Control Instrumentation Technology, Prentice Hall.

Jones, D. R. (2001). "A taxonomy of global optimization methods based on response surfaces." Journal of Global Optimization 21: 345-383.

Karim, M. A. (2011). "Performance evaluation of a stratified chilled-water thermal storage system." International journal of Aerospace and Mechanical Engineering 5(1): 18-26.

Keeney, K. R. and J. E. Braun (1996). "A Simplified Method for Determining Optimal Cooling Control Strategies for Thermal Storage in Building Mass." HVAC&R Research 2(1): 59-78.

Klein, S. A., J. A. Duffie, et al. (1976). "TRNSYS - A transient simulation program." ASHRAE Transactions 82(1): 623-633.

Kleywegt , A. and A. Shapiro (2000). Stochastic Optimization, SISE Gerogia Institute of Technology.

Kothare, M. V., V. Balakrishnan, et al. (1996). "Robust constrained model predictive control using linear matrix inequalities." Automatica 32(10): 1361-1379.

Kreider, J. F. and X. A. Wang (1992). Improved artificial neural networks for commercial building energy use prediction. Solar Engineering: Proceedings of Annual ASME International Solar Energy Conference, Maui, HI.

Lee, B. (2010). SysML-TRNSYS transformation. Atlanta, Georgia Institute of Technology.

Lee, J. M. and J. H. Lee (2008). "Value function-based approach to the scheduling of multiple controllers." Journal of Process Control 18(6): 533-542.

Lee, K.-h. and J. E. Braun (2008). "Model-based demand-limiting control of building thermal mass." Building and Environment 43(10): 1633-1646.

Lee, Y. T. (1999). Information modeling:From design to implementation, NIST.

LTG (2010, 4/5/2010). "Fan coil unit type VKB." from http://www.ltg-ag.de.

Macdonald, I. and P. Strachan (2001). "Practical application of uncertainty analysis." Energy and Buildings 33(3): 219-227.

Macdonald, I. A. (2002). Quantifying the Effects on Uncertainty in Building Simulation, University of Strathclyde. Ph.D. Thesis.

Mahdavi, A. (2001). "Simulation-based control of building systems operation." Building and Environment 36: 789-796.

Mahdavi, A. and C. Pröglhöf (2009). User behavior and energy performance in buildings. IEWT 2009.

Martin, R., C. Federspiel, et al. (2002). Supervisory control for energy savings and thermal comfort in commercial building HVAC systems. AAAI Technical Report SS-02-03 American Association for Artificial Intelligence.

Mather, D. W. (2000). Modular Stratified Thermal Energy Storage for Solar Heating Systems. Department of Mechanical Engineering. Waterloo, Ontario, Canada, University of Waterloo. MASc thesis.

Mather, D. W., K. G. T. Hollands, et al. (2002). "Single- and multi-tank energy storage for solar heating systems: fundamentals." Solar Energy 73(1): 3-13.

McAllister, C. D. and T. W. Simpson (2003). "Multidisciplinary Robust Design Optimization of an Internal Combustion Engine." Journal of Mechanical Design 125(1): 124-130.

Modelica_Association (2010) Modelica language specification Ver. 3.2.

Mondol, J. D., Y. G. Yohanis, et al. (2008). "Solar radiation modelling for the simulation of photovoltaic systems." Renewable Energy 33(5): 1109-1120.

Monroe, R. C. (1978). Improving cooling tower fan system efficiencies. Combustion magazine. 50.

Moon, H. J. (2005). Assesing Mold Risks in Buildings under Uncertainty. College of Architecture. Atlanta, GA, Georgia Institute of Technology. PhD.

Morari, M. and J.H.Lee (1999). "Model predictive control: pat, present and future." Computers & Chemical Engineering 23: 667-682.

Morgan, M. G. and M. Henrion (1990). Uncertainty: a guide to dealing with uncertainty in quantitative risk and policy analysis. Cambridge, Cambridge university press.

Morris, F. B., J. E. Braun, et al. (1994). "Experimental and simulated performance of optimal control of building thermal storage." ASHRAE Transactions 100(1): 402-414.

Morris, M. D. (1991). "Factorial sampling plans for preliminary computational experiments." Technometrics 33(2): 14.

Mulvey, S. M. and R. J. Vanderbei (1995). Robust optimization of large-scale systems. Operations Research, INFORMS: Institute for Operations Research. 43: 264.

Murray-Smith, R. and T. A. Johansen (1997). Multiple Model Approaches to Modelling and Control. London, Taylor and Francis.

Newton, B. J., M. Schmid, et al. (1995). Storage tank models. ASME/JSME/JSME International Solar Energy Conference, New York.

Nikolaidis, E., D. M. Ghiocel, et al. (2005). Engineering design reliability handbook. New York, CRC Press.

NOAA (2010). "NDFD SOAP Web Service." Retrieved 6/21, 2010, from http://www.weather.gov/xml/.

NOAA (2010). "NDFD Verification." Retrieved 6/25, 2010, from http://www.weather.gov/ndfd/verification/.

Oldbach, R. (1994). Embedded electricity generation, Strathclyde University. Msc Thesis.

Olson, R. (1987). Optimal allocation of building cooling loads to chilled water temperature, UIUC. PhD thesis.

Orme, M., M.W.Liddament, et al. (1994). Numerical data for air infiltration & natural ventilation calculations. Great Britain, Air Infiltration and Ventilation Center.

Page, J., D. Robinson, et al. (2008). "A generalised stochastic model for the simulation of occupant presence." Energy and Buildings 40(2): 83-98.

Palyvos, J. A. (2008). "A survey of wind convection coefficient correlations for building envelope energy systems' modeling." Applied Thermal Engineering 28(8-9): 801-808.

Paredis, C. J., Y. Bernard, et al. (2010). An overview of the SysML-Modelica transformation specification. Proceedings of the 2010 INCOSE International Symposium, Chicago, IL.

Paredis, C. J. and T. Johnson (2008). Using OMG's SysML to support simulation, Proceedings of the 2008 Winter Simulation Conference.

PECI (2008). "Functional Testing and Design Guides." 6/15/2010, from http://www.peci.org/ftguide/ftg/index.htm.

Pehnt, M. (2006). "Dynamic life cycle assessment (LCA) of renewable energy technologies." Renewable Energy 31(1): 55-71.

Pheonix_Integration (2005) Accelerating product development through grid computing. CenterLink Technical white paper

Phoenix_Integration (2010). "Phoenix CenterLink." Retrieved 8/20/2010, from http://www.phoenix-int.com/software/phx_centerlink.php.

Pistikopoulos, E. N. and M. G. Ierapetritou (1995). "Novel approach for optimal process design under uncertainty." Computers & Chemical Engineering 19(10): 1089-1110.

Raju, G. V. S., J. Zhou, et al. (1991). "Hierarchical fuzzy control." International Journal of Control 54(5): 1201-1216.

Rawlings, J. B. and K. R. Muske (1993). "The stability of constrained receding-horizon control: applications to industrial processes." Automatica 14(5).

Reindl, D. T., W. A. Beckman, et al. (1990). "Diffuse fraction correlations." Solar Energy 45(1): 1-7.

Ren, M. J. and J. A. Wright (2002). "Adaptive diurnal prediction of ambient dry-bulb temperature and solar radiation." HVAC&R Research 8(4): 383-402.

Robledo, L. and A. Soler (2000). "Luminious efficacy of global solar radiation for clear skies." Energy Conversion and Management 41: 1769-1779.

Rodriguez, J. A., J. A. Romagnoli, et al. (2003). "Supervisory multiple regime control." Journal of Process Control 13(2): 177-191.

Rowe, W. D. (1994). "Understanding uncertainty." Risk analysis 14(5): 743-750.

Ruud, M. D., J. W. Mitchell, et al. (1990). "Use of building thermal mass to offset cooling loads." ASHRAE Transactions 96(2): 820-829.

Samson, S., J. A. Reneke, et al. (2009). "A review of different perspectives on uncertainty and risk and an alternative modeling paradigm." Reliability Engineering & System Safety 94(2): 558-567.

Schlesinger, J. R. (1996). Organizational structures and planning. Santa Monica, CA, RAND.

Seem, J. E. and J. E. Braun (1991). "Adaptive methods for real-time forecasting of building electrical demand." ASHRAE Transactions 97(1): 710-721.

Shrader-Frechette, K. (1996). Methodological rules for four classes of uncertainty. Cambridge, Blackwell Science.

Simeng, L. and G. P. Henze (2004). Impact of Modeling Accuracy on Predictive Optimal Control of Active and Passive Building Thermal Storage Inventory. ASHRAE Transactions, American Society of Heating, Refrigerating and Air-Conditioning Engineers, Inc. 110: 151-163.

Solar_Energy_Laboratory, TRANSSOLAR, et al. (2010). Multizone building modeling with Type56 and TRNBuild.

Sousa, J. M. and U. Kaymak (2002). Fuzzy Decision Making in Modeling and Control.

Spiegel, M. R. (1975). Schaum's outline of theory and problems of probability and statistics. New York, McGraw-Hill.

Sun, C., K. Temple, et al. (2006). Interaction Between Dynamic Electric Rates and Thermal Energy Storage Control. Final report for RP-1252. Atlanta GA, ASHRAE.

SysML_Forum (2009). "SysML FAQ." Retrieved 11/10/2010, from http://www.sysmlforum.com/FAQ.htm.

Takagi, T. and M. Sugeno (1985). "Fuzzy identification of systems and its application to modeling and control." IEEE Trans. Syst. Man Cybernet 15(1): 116-132.

Thomas, C. (1996). Renewable Generation: The British Experience, WREC.

Tintner, G. (1955). Stochastic linear programming with application to agricultural economics, Proceedings of the Second Symposium in Linear Programming.

Torcellini, P., S. Pless, et al. (2006). Zero Energy Buildings: A Critical Look at the Definition; Preprint.

Underwood, C. P. (2000). Robust Control of HVAC Plant I: Modeling, Proceeding of CIBSE.

Underwood, C. P. (2000). Robust Control of HVAC Plant II: Controller Design, Proceeding of CIBSE.

USGBC (2007). "Building Design Leaders Collaborating on Carbon-Neutral Buildings by 2030." Retrieved 5/20/2009, from http://www.usgbc.org/News/PressReleaseDetails.aspx?ID=3124.

Van_Asselt, M. B. A. (2000). Perspectives on uncertainty and risk. Dordrecht, Kluwer Academic Publishers.

Van_Asselt, M. B. A. and J. Rotmans (2002). "Uncertainty in integrated assessment modelling: from Positivism to Pluralism." Climate Change 54: 75-105.

Van_der_Heijden, K. (1996). Scenarios: The art of strategic conversation. Chichester, Wiley.

Van_der_Sluis, J. P. (1997). Anchoring amid uncertainty: on the management of uncertainties in risk assessment of anthropogenic climate change, University of Utrecht, Netherlands. Ph.D. dissertation.

Vose, D. (1996). Quantitative risk analysis:A guide to Monte Carlo Simulation. West Sussex, England, John Wiley&Sons Ltd.

Walawalkar, R. (2004). Financing Demand Side Management Initiatives, American Public Power Association.

Walker, W. E., P. Harremoes, et al. (2003). "Defining Uncertainty: A Conceptual Basis for Uncertainty Management in Model-Based Decision Support." Integrated Assessment 4(1): 5-17.

Walley, P. (1999). Towards a unified theory of imprecise probability. 1st International Symposium on Imprecise Probabilities and their applications, Ghent, Belgium.

Wang, S. W. and Z. J. Ma (2008). "Supervisory and Optimal Control of Building HVAC Systems: A Review." HVAC&R Research 14(1): 3-32.

Weisemoller, I., F. Klar, et al. (2009). Development of tool extensions with MOFLON Heidelberg, Springer Verlag.

Wetter, M. (2009). "Modelica-based Modeling and Simulation to Support Research and Development in Building Energy and Control Systems." Journal Name: Journal of Building Performance Simulation; Journal Volume: 2; Journal Issue: 2; Related Information: Journal Publication Date: June 2009: Medium: ED.

Wetter, M. and C. Haugstetter (2006). Modelica versus TRNSYS - A Comparison Between an Equation-Based and a Procedural Modeling Language for Building Energy Simulation. Proc. of the 2nd SimBuild Conference. Cambridge, USA.

Wetter, M., P. Haves, et al. (2008). Using SPARK as a Solver for Modelica.

Wikipedia (2010). "Grid computing." Retrieved 9/10/2010, from http://en.wikipedia.org/wiki/Grid_computing.

Wikipedia (2010). "Sustainable energy." Retrieved 2/24/2011, from http://en.wikipedia.org/wiki/Sustainable_energy.

Wyss, G. D. and K. H. Jorgensen (1998) A user's guide to LHS: Sandia's Latin hypercube sampling software.

Zhang, Y. and V. I. Hanby (2007). Short term prediction of weather parameters using online weather forecasts. Building simulation 2007.

Zheng, Z. Q. (1995). Robust control of systems subject to constraints. Pasadena, CA, California Institute of Technology. Doctor of Philosophy.

VITA

SEAN HAY KIM

Sean Hay Kim came from Korea. She received a B.A. and M.S. in Architectural engineering from Yonsei University in 1998 and 2000, respectively. She joined to LG EDS in 2000 as a computer systems engineer before coming to the U.S. She received a M.S. in building performance and diagnostics from Carnegie Mellon University, Pittsburgh PA in 2006. Then she obtained Ph.D. in building technology from Georgia Tech in 2011.

She worked for many research projects such as WorkPlace 20•20/National Environment Assessment Toolkit funded by General Service Administration (GSA), Healthcare Design Web funded by Center for Healthcare Design (CHD), BIM-Enabled Design Guides funded by GSA, and UAACE (Stand-alone micro power grid for army base) funded by U.S. Department of Defense and United Technologies Research Center (UTRC). She is interested in building performance analysis taking advantage of computer-aided modeling and simulations, and their applications in real life.

She enjoys her time with her husband and son, Edmund Yoon Jin Lee.